FORMULATION AND EVALUATION OF VAGINAL DRUG DELIVERY SYSTEM OF TENOFOVIR: AN EXPERIMENTAL STUDY

Thesis submitted to

THE KLE ACADEMY OF HIGHER EDUCATION AND RESEARCH, BELAGAVI

(KLE DEEMED UNIVERSITY)

[Declared as Deemed-to-be-University u/s 3 of the UGC Act, 1956 vide Govt. of India Notification No. F.9-19/2000-U.3 (A)]

(Re-Accredited 'A^{+}' Grade by NAAC) (3rd Cycle)

[Placed in Category 'A' by MHRD (GoI)]

For the award of the degree of

Doctor of Philosophy in the Faculty of Pharmacy

By

Dhruti Avlani

(Registration No.: KLEU/Ph.D./19-20/DO1219011)

Under the guidance of

Prof. (Dr.) H.N.Shivakumar

Vice-Principal & Head,

Department of Pharmaceutics,

KLE College of Pharmacy, Bengaluru

July 2024

UNDERTAKING

I, Dhruti Avlani hereby declare that the information and the data mentioned in my thesis entitled *"Formulation and Evaluation of Vaginal Drug Delivery System of Tenofovir: An Experimental Study"* belongs to me and is original.

I am aware of definition of plagiarism as detailed below:

- An act or instance of using or closely imitating the language and thoughts of another author without authorization and the representation of that author's work as one's own, as by not crediting the original author.
- A piece of writing or other work reflecting such unauthorized use or imitation.
- The deliberate or reckless representation of another's words, thoughts or ideas as one's own without attribution in connection with submission of academic work, whether graded or otherwise.

I hereby declare that the thesis prepared by me is original-one and does not involve plagiarism anywhere. In case at a later stage, it is found that I have indulged in plagiarism, then I am solely responsible for the same and the Institution is at liberty to take any disciplinary action against me including cancellation of dissertation or any other penalties imposed by the University.

Dhruti Avlani
Ph.D. Research Scholar
KLE College of Pharmacy, Bengaluru

Date:

Place: Bengaluru

PLAGIARISM REPORT

Ref. No. KAHER/AA/24-25/D-145 12th June 2024

Madam,

The soft copy of Ph.D. research thesis of **Ms. Dhruti Avlani, Faculty of Pharmacy, KAHER,** has been submitted for anti-plagiarism check at the office of the undersigned through "Turn-it-in" package. The scan has been carried out and the scanned output reveals a match percentage of **5%** which is within the acceptable limit of 10%.

To obtain the comprehensive report of the plagiarism test, research scholar can send a mail to **diracademic@kledeemeduniversity.edu.in** along with the Registration Number, Name of the Scholar, Name of Guide/Co-guide and title of the thesis.

DIRECTOR * ACADEMIC AFFAIRS * Deemed-to-be University

Dr.(Mrs.) Roopa M. Bellad
Director, Academic Affairs

To,
Ms. Dhruti Avlani
Full-Time Research Scholar
2019-20 Batch, Faculty of Pharmacy,
KLE College of Pharmacy,
KAHER, **Bengaluru.**

Cc to :
1. The Principal, KLE College of Pharmacy, Bengaluru
2. Dr. H. N. Shivakumar, Professor, KLE College of Pharmacy, Bengaluru- **Guide**

KLE ACADEMY OF HIGHER EDUCATION AND RESEARCH

(Deemed-to-be-University)

[Declared as Deemed-to-be-University u/s 3 of the UGC Act, 1956 vide Govt. of India Notification No.F.9-19/2000-U.3 (A)]

(Re-Accredited 'A^{+}' Grade by NAAC) (3rd Cycle)

[Placed in Category 'A' by MHRD (GoI)]

BELAGAVI

COPYRIGHT DECLARATION

We hereby declare that **KLE ACADEMY OF HIGHER EDUCATION AND RESEARCH, BELAGAVI, KARNATAKA,** *shall have the rights to preserve, use and disseminate this thesis in print or electronic format for academic/research purpose.*

Dhruti Avlani
Ph.D. Research Scholar
KLE College of Pharmacy,
Bengaluru - 560010

Prof. (Dr.) H.N. Shivakumar
Vice-Principal & Head
Department of Pharmaceutics
KLE College of Pharmacy,
Bengaluru - 560010

Place: Bengaluru
Date:

KLE ACADEMY OF HIGHER EDUCATION AND RESEARCH

(Deemed-to-be-University)

[Declared as Deemed-to-be-University u/s 3 of the UGC Act, 1956 vide Govt. of India Notification No.F.9-19/2000-U.3 (A)]

(Re-Accredited 'A^{+}' Grade by NAAC) (3rd Cycle)

[Placed in Category 'A' by MHRD (GoI)]

BELAGAVI

DECLARATION

I hereby declare that the thesis entitled "Formulation and Evaluation of Vaginal Drug Delivery System of Tenofovir: An Experimental Study" is a bonafide and original research carried out by me under the guidance of Dr. H.N. Shivakumar, Vice-Principal & Head, Department of Pharmaceutics, KLE College of Pharmacy, Bengaluru. The thesis or any part thereof has not formed the basis for the award of any degree/fellowship or similar title to any candidate of any University.

Place: Bengaluru
Date:

Dhruti Avlani
Ph.D. Research Scholar
KLE College of Pharmacy,
Bengaluru - 560010

KLE ACADEMY OF HIGHER EDUCATION AND RESEARCH

(Deemed-to-be-University)

[Declared as Deemed-to-be-University u/s 3 of the UGC Act, 1956 vide Govt. of India Notification No.F.9-19/2000-U.3 (A)]

(Re-Accredited 'A^{+}' Grade by NAAC) (3rd Cycle)

[Placed in Category 'A' by MHRD (GoI)]

BELAGAVI

CERTIFICATE

This is to certify that the thesis entitled "Formulation and Evaluation of Vaginal Drug Delivery System of Tenofovir: An Experimental Study" is a bonafide and genuine research carried out by Dhruti Avlani under the guidance of Dr. H.N. Shivakumar, Vice-Principal & Head, Department of Pharmaceutics, KLE College of Pharmacy, Bengaluru.

Place: Bengaluru
Date:

Dr. Kalpana Patil
Dean, Faculty of Pharmacy
KAHER, Belagavi

KLE ACADEMY OF HIGHER EDUCATION AND RESEARCH

(Deemed-to-be-University)

[Declared as Deemed-to-be-University u/s 3 of the UGC Act, 1956 vide Govt. of India Notification No.F.9-19/2000-U.3 (A)]

(Re-Accredited 'A^{+}' Grade by NAAC) (3rd Cycle)

[Placed in Category 'A' by MHRD (GoI)]

BELAGAVI

CERTIFICATE

This is to certify that the thesis entitled "Formulation and Evaluation of Vaginal Drug Delivery System of Tenofovir: An Experimental Study" is a bonafide record of original research carried out by Dhruti Avlani for the award of degree of DOCTOR OF PHILOSOPHY IN FACULTY OF PHARMACY under my supervision and guidance.

Place: Bengaluru
Date:

Prof. (Dr.) H.N. Shivakumar
Vice-Principal & Head
KLE College of Pharmacy,
Bengaluru - 560010

KLE ACADEMY OF HIGHER EDUCATION AND RESEARCH

(Deemed-to-be-University)

[Declared as Deemed-to-be-University u/s 3 of the UGC Act, 1956 vide Govt. of India Notification No.F.9-19/2000-U.3 (A)]

(Re-Accredited 'A^{+}' Grade by NAAC) (3rd Cycle)

[Placed in Category 'A' by MHRD (GoI)]

BELAGAVI

CERTIFICATE

This is to certify that the thesis entitled "Formulation and Evaluation of Vaginal Drug Delivery System of Tenofovir: An Experimental Study" is a bonafide record of original research carried out by Dhruti Avlani for the award of degree of DOCTOR OF PHILOSOPHY IN FACULTY OF PHARMACY under the guidance of Dr. H.N. Shivakumar, Vice-Principal & Head, Department of Pharmaceutics, KLE College of Pharmacy, Bengaluru.

_____

Place: Bengaluru
Date:

Prof. (Dr.) Rajamma AJ
Principal
KLE College of Pharmacy,
Bengaluru

ACKNOWLEDGEMENT

The successful completion of this research project was made possible through extensive guidance and support, for which I am deeply fortunate. I am profoundly grateful to everyone who has supported and mentored me throughout this doctoral journey. This thesis represents the culmination of years of dedication, perseverance, and invaluable contributions from countless individuals and institutions. Their steadfast encouragement, constructive feedback, and unwavering confidence in my abilities have played a pivotal role in shaping this work.

First and foremost, I express my heartfelt gratitude to my guide, ***Prof. (Dr.) H.N. Shivakumar, Vice-Principal and Head of Department of Pharmaceutics, KLE College of Pharmacy, Bengaluru*** for his unwavering guidance, patience, and insightful suggestions and feedback. His innovative ideas, expertise, and mentorship have been invaluable in shaping the direction of this research and nurturing my growth as a scholar.

I am deeply grateful to ***Prof. (Dr.) Rajamma AJ, Principal, KLE College of Pharmacy, Bengaluru***, for her continuous support and understanding during my PhD journey. Her guidance has been invaluable in navigating challenges and overcoming obstacles and her unwavering support shaped my academic journey significantly.

I want to express my deepest appreciation to ***Dr. Subhas S. Karki*** and all the ***PhD committee members***, for their constructive criticism, encouragement, and valuable suggestions that have enriched the content and quality of this thesis.

My sincere appreciation extends to all the faculties of the ***Department of Pharmaceutics of KLE College of Pharmacy, Bengaluru***, where I have found a

supportive academic community. The intellectual exchange and collaborative spirit within the department have significantly contributed to my academic development.

I am thankful to ***Vision Group on Science and Technology, Bengaluru, Karnataka, India*** for their financial support through GRD No. 747 of CISEE, for providing the necessary resources to conduct this research.

In addition, I would also like to extend my thanks to all the ***library staff, laboratory technicians, and attenders*** for their invaluable assistance throughout the project, providing me with all the basic necessary requirements for my work.

A special thanks to my ***colleagues and fellow researchers***, for their support, stimulating discussions, and shared experiences that have broadened my understanding and enriched the academic discourse surrounding my research.

I extend my deepest gratitude to my ***parents*** for their unwavering love, encouragement, and sacrifices throughout my academic journey. Their belief in me has been my source of strength.

This thesis is a testament to the collective efforts and support of all those mentioned above and many more who have touched my life in meaningful ways. I am profoundly grateful for each contribution, however small, that has culminated in this significant milestone.

_____

Dhruti Avlani

Date: Ph.D. Research Scholar

Place: Bengaluru

TABLE OF CONTENTS

LIST OF ABBREVIATIONS

Sl. No.	Abbreviation	Full Form of Abbreviation
1	%EE	Drug Entrapment Efficiency
2	%yield	Practical yield
3	AEs	Adverse events
4	AIDS	Acquired Immunodeficiency Syndrome
5	AntiRV	Antiretrovirals
6	AUC	Area under the curve
7	BCS	Biopharmaceutical classification system
8	BMI	Body Mass Index
9	$CaCl_2$	Calcium chloride
10	CM	Chitosan microparticles
11	C_{max}	Maximum VF concentration
12	DLSA	Dynamic laser scattering analysis
13	DNA	Deoxyribonucleic acid
14	DSC	Differential Scanning Calorimetry
15	DT	Disintegration time
16	DT	Dispersible vaginal tablet
17	DT-T-CM	T-CM (ECH-4) loaded dispersible tablets
18	EVG	Elvitegravir
19	f_1	Difference factor
20	f_2	Similarity factor
21	FC	Formulation code
22	FC	Formulation code

23	FTIR	Fourier Transform Infrared Spectrometry
24	HAART	Highly Active Antiretroviral Therapy
25	HIV	Human Immunodeficiency Virus
26	HPMC	Hydroxy propyl methyl cellulose
27	IC_{50}	Half-maximal inhibitory concentration
28	IP	Indian Pharmacopoeia
29	IR	Infrared
30	IS	Internal standard
31	IVDR	*In-vitro* drug release
32	LA-ARTs	Long-acting AntiRV therapies
33	LC-MS	Liquid Chromatography-Mass Spectroscopy
34	LC-MS/MS	Liquid Chromatography Mass Spectroscopy/Mass Spectroscopy
35	LLP	Light liquid paraffin
36	MAP	Microneedle array patches
37	MT	Marketed TDF Oral Tablet
38	NRTI	Nucleoside reverse transcriptase inhibitor
39	NT	Normal Control
40	PBMCs	Peripheral blood mononuclear cells
41	PrEP	Pre-exposure prophylaxis
42	PT	TDF Vaginal Pessary
43	P-XRD	Powder X-ray Diffractometry
44	RDC	Relative degree of crystallinity
45	RH	Relative Humidity

46	S-Alg	Sodium alginate
47	S-CMC	Sodium carboxymethyl cellulose
48	SD	Standard deviations
49	SEM	Scanning electron microscopy
50	SVF	Simulated vaginal fluid (pH 4.5)
51	TAF	Tenofovir Alafenamide
52	T-AM	TDF-loaded bio-adhesive sodium alginate microspheres
53	T-CM	TDF-loaded bio-adhesive chitosan microparticles
54	TD	Tenofovir disoproxil
55	TDEMs	Tenofovir disoproxil-loaded enteric-microparticles
56	TDF	Tenofovir Disoproxil Fumarate
57	TFV	Tenofovir
58	TFV-DP	Tenofovir diphosphate
59	TM	Tamarind mucilage
60	T_{max}	Time to reach the maximum VF concentration
61	TPP	Sodium tripolyphosphate
62	TT	TDF Vaginal Tablets
63	USFDA	United States Food and Drug Administration
64	USP	United States Pharmacopoeia
65	UV-S	UV-VIS spectrophotometer
66	VF	Vaginal fluid

67	VF	Vaginal fluid
68	w/o	Water-in-oil
69	X_c	Degree of crystallinity
70	ΔH_f	Enthalpy of fusion

LIST OF TABLES

LIST OF FIGURES

ABSTRACT

Background: Human Immunodeficiency Virus (HIV) and Acquired Immunodeficiency Syndrome (AIDS) pose significant worldwide challenges. Low oral bioavailability of antiretrovirals (AntiRV), hinders their effectiveness in reaching infection sites and increasing the risk of relapse. Preventative measures like topical vaginal pre-exposure-prophylaxis (PrEP) are crucial in reducing HIV transmission for HIV-negative individuals to lower their virus contraction risk during intercourse.

Objectives: The first part of the project aimed to design and develop novel PrEP sispersible vaginal tablets (DT) composed of tenofovir disoproxil fumarate (TDF)-loaded bio-adhesive chitosan microparticles (T-CM). The second part focused on formulating pessaries with TDF-loaded bio-adhesive sodium alginate (S-Alg) microspheres (T-AM) for intra-vaginal administration to address the shortcomings associated with conventional oral dosage forms.

Methodology & Results:

Part 1: DT composed of T-CM

T-CM were formulated by emulsification-internal-gelation technique by varying the drug-to-polymer ratio and quantity of cross-linking agent. Among various batches of T-CM, ECH-4 demonstrated high entrapment efficiency (%EE) (68.93±1.76%) and sustained TDF release for 24h (88.05±0.38%). *Ex-vivo* studies of ECH-4 using rabbit vaginal mucosa (substrate) in modified USP disintegration apparatus indicated good bio-adhesion for 24h. Scanning electron microscopy (SEM) demonstrated the spherical shape of T-CM. Dynamic laser scattering analysis (DLSA) indicated that

ECH-4 displayed a mean diameter of Dv(90) of 193.42±3.70µm. Fourier Transform Infrared Spectrometry (FTIR) ruled out any possible chemical interaction between TDF and other excipients. Solid-state characterization employing Differential Scanning Calorimetry (DSC) and Powder X-ray Diffractometry (P-XRD) revealed that TDF existed in an amorphous state in chitosan matrix. The batch ECH-4 was eventually incorporated into DT for intra-vaginal insertion. DT (F3) were found to readily disperse (31.33±4.63s) and release 89.98±1.61% of TDF over 24 h in simulated vaginal fluid (pH 4.5) (SVF).

Part 2: Pessaries composed of T-AM

T-AM were formulated employing emulsification-internal-gelation technique by varying the drug-alginate ratio. The drug-alginate ratios and polymer incorporated influenced the particle size, %EE, and *in-vitro* drug release (IVDR). Batch EH-8, with a 1:4 drug-to-polymer ratio and equal parts S-Alg and HPMC K100M, exhibited optimal %EE (62.09±1.34%) and controlled TDF release (97.02±4.54%) for 12h. EH-8 displayed good mucoadhesion on rabbit vaginal mucosa for over 12h. SEM demonstrated the spherical shape of T-AM. DLSA of EH-8 indicated a Dv(90) of 68.68±0.91µm. FTIR analysis proved the chemical integrity of the TDF in T-AM. Solid-state characterization using DSC and P-XRD revealed amorphization of drug in the polymer matrix. EH-8 loaded novel meltable pessaries were found to melt at 35.33±0.58°C and exhibited a sustained TDF release of 95.31±1.37% over 12h in SVF.

To ascertain the biodistribution of the TDF in vagina, the intra-vaginal tablets and pessaries developed were compared to the marketed oral formulation in rabbits. *In-*

vivo experiments identified that pessaries displayed a significantly higher TDF concentration (C_{max}) (P<0.005) in VF with a lower T_{max} (P<0.0001) compared to oral and intra-vaginal tablets. The pessaries efficiently maintained inhibitory concentrations in the critical early hours of insertion, which may be quite crucial in offering adequate protection against HIV transmission during sexual intercourse.

Conclusion: The smaller size and higher surface-to-volume ratio of bio-adhesive microparticulate systems were found to enhance vaginal drug delivery by improving residence time, and prolonging TDF release. This makes the bio-adhesive microparticles ideal carriers for retention in vaginal mucosa, facilitating the regional concentration and biodistribution. As the focus in HIV prevention shifts towards long-acting systemic formulations, intra-vaginal inserts like tablets and pessaries provide a novel on-demand option for HIV-negative individuals.

Keywords: Intra-vaginal; tenofovir; chitosan; sodium alginate; microparticles; vaginal tablet; pessaries; mucoadhesion.

GRAPHICAL ABSTRACT

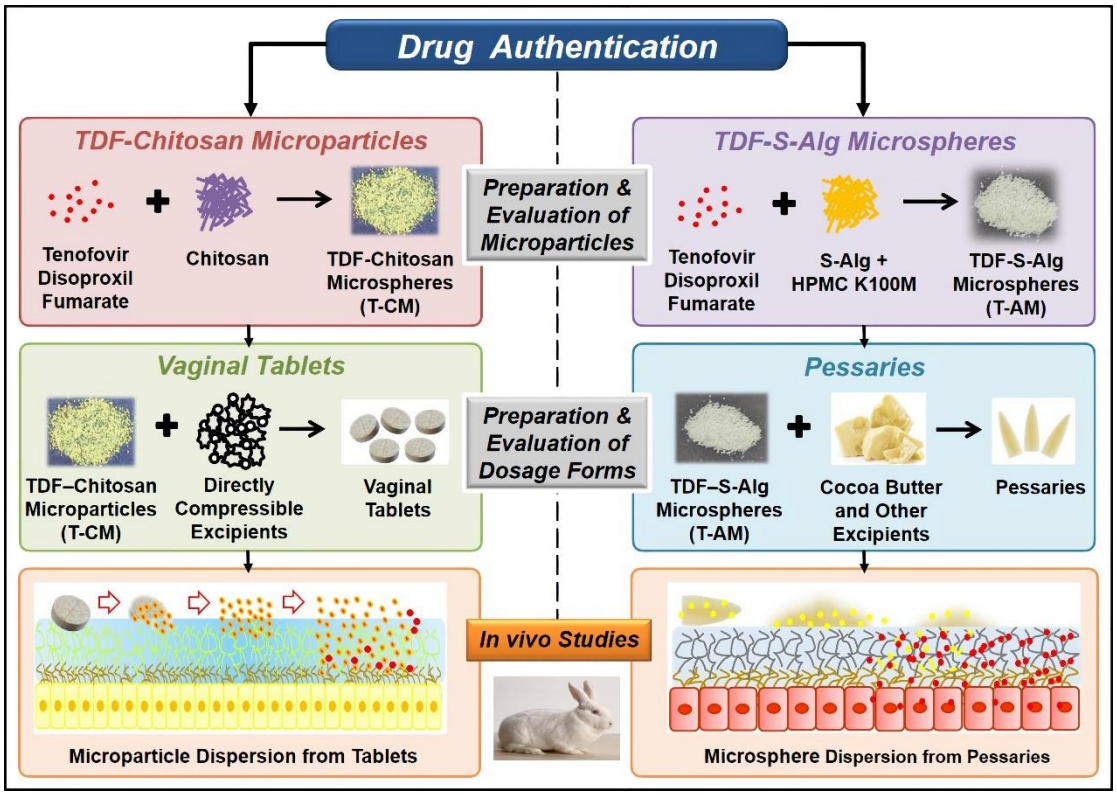

INTRODUCTION

1. INTRODUCTION

1.1. Background.

HIV (Human Immunodeficiency Virus) targets and causes the destruction of specifically CD4 cells, which are crucial for a healthy immune response against infections. This targeted attack gradually undermines the immune system's ability to defend the body, ultimately progressing to Acquired Immunodeficiency Syndrome (AIDS), if left untreated.[1] This process highlights the insidious nature of HIV as it systematically dismantles the body's defence, making it increasingly susceptible to opportunistic infections characteristic of AIDS.[2]

HIV/AIDS has presented substantial challenges to worldwide health, society, and economies for a lengthy period, impacting not only individuals but also communities and nations at large. Despite developments and advancements in healthcare, awareness, and treatment availability, these diseases persist as significant global health concerns. In 2023, the World Health Organization estimated globally 39 million people were living with HIV by the end of 2022. This figure reflects the ongoing challenge of managing and preventing the spread of the virus. Additionally, there were 1.5 million new HIV infections in 2022, indicating that efforts to control the spread of the virus continue to remain critical. Furthermore, approximately 650,000 deaths were attributed to HIV/AIDS in 2022, underscoring the significant impact and severity of the disease on a global scale.[1,2]

The Centers for Disease Control and Prevention states that most HIV infections are transmitted through vaginal or anal sexual intercourse, as well as through the sharing of needles/syringes. In industrialized nations, the implementation of Highly Active

AntiRV Therapy (HAART) has led to substantial decreases in both the incidence of illness (morbidity) and death-rates (mortality) associated with HIV infection. However, a significant number of AntiRV drugs used in HAART exhibit low oral bioavailability, primarily due to challenges such as poor solubility or restricted ability to penetrate cell membranes effectively. Consequently, the inadequate targeting of AntiRVs to dormant infection sites within the body remains a major factor contributing to the recurrence of HIV and the need for additional treatment interventions.[3-5]

In this instance, preventive strategies involving pre-exposure prophylaxis (PrEP) are crucial for reducing HIV transmission, with Truvada® and Descovy® being the only USFDA-approved AntiRV drugs for daily oral administration as PrEP; which involves HIV-negative individuals taking these drugs regularly to lower their probability of contracting the viral infection.[6] Truvada®, despite its effectiveness, is not commonly prescribed in the United States because of its prohibitively high price, kidney toxicity, and low adherence from patients. It can impact kidney function and bone density, and its effectiveness depends greatly on how consistently it is taken. Additionally, it can interact with other medications, lowering their efficacy or increasing the risk of adverse effects. Descovy®, approved in 2019 by USFDA as an alternative for HIV PrEP, has a better safety profile, particularly concerning kidney and bone density issues. However, both formulations necessitate strict adherence for successful outcomes, as non-adherence can lead to drug resistance and reduced effectiveness.[7-11]

Topical intra-vaginal PrEP, along with additional strategies, holds substantial promise in halting new/fresh HIV-1 infections in HIV-negative women, offering a novel strategy to lower the disproportionate risk of viral transmission during intercourse.

The concept behind topical PrEP method is to prevent HIV-1 infection at the mucosal level by using compounds with specific antiviral activity in medically designed products applied to the vagina/rectum, to halt viral transmission during the sexual intercourse. This strategy involves directly applying AntiRV medications to the vaginal mucosa using various intra-vaginal dosage forms, namely, tablets, gels, pessaries, and vaginal rings. By creating a protective barrier at the site of potential HIV exposure, topical PrEP effectively prevents the virus from infecting susceptible cells in HIV-negative individuals.[12-13]

Unlike the conventional oral drug delivery route, vaginal administration bypasses the gastro-intestinal and hepatic first-pass effects, allowing drug delivery directly into the systemic circulation. This not only reduces the required dose but also lowers the incidence of side effects. Direct application of AntiRV medications to the vaginal mucosa promotes localized defence against HIV viral transmission via enhancement of drug absorption in the vaginal mucosa because of the dense network of blood vessels and extensive surface area, leading to improved regional bioavailability at the intended site of operation. Furthermore, vaginal formulations can minimize off-target systemic adverse/side effects due to the limited absorption of drug substances into the bloodstream, while also exhibiting relatively low enzymatic activity, thereby allowing self-administration and prolonged release of drug. Formulations for intra-vaginal administration elicit the therapeutic concentrations at the targeted application site; deliver discreet and user-controlled protection, allowing informed decisions and reducing the vulnerability to developing HIV.[14-15]

Topical inserts designed for vaginal drug delivery involving films, rings, gels, suppositories, and tablets appear to be a potential strategy to address PrEP.[4,5]

Traditional vaginal inserts namely gels, creams, suppositories, or douches containing AntiRVs are reported as prospective dosage forms for on-demand PrEP. Vaginal films have certain constraints such as the inability to achieve sustained release, potential for local irritation, and the lack of mass production feasibility due to underdeveloped production resources. Additionally, films are limited in their drug content uniformity, typically comprising less than half of the total weight of the formulation, due to their small size and lightweight nature. The disintegration and drug release of vaginal films is influenced by the varying and limited volume of vaginal fluid (VF), which can differ widely among women and at different times, making drug release unpredictable. Additionally, the films begin disintegrating as quickly as they come into contact with VF, complicating administration. Furthermore, there are no standardized regulations for the manufacture and characterization of these films.[15]

Vaginal rings offer several advantages over other forms of drug delivery. One key benefit is their ability to provide sustained release of the drug, which can lead to improved patient adherence and efficacy of the treatment. Moreover, compared to other dosage forms, vaginal rings typically require fewer applications, which can enhance convenience and patient compliance. Furthermore, the mass production of vaginal rings has become more advanced, leading to increased availability and accessibility of this dosage form. However, vaginal rings also have some disadvantages that need to be considered. One drawback is that they require a higher financial investment compared to some other forms of drug delivery. This can be a barrier to access for some patients, especially in resource-limited settings. The manufacturing cost of vaginal rings is also higher, which can impact their affordability and availability, particularly in low-income countries. Another potential

disadvantage of vaginal rings is their possible influence on sexual intercourse. Some individuals may find the presence of the ring uncomfortable or may experience changes in sexual sensation or lubrication, which can affect sexual activity.[15]

Vaginal gels pose numerous challenges. Firstly, adherence to therapy can be problematic, with users struggling to consistently follow the prescribed regimen. Additionally, these gels are prone to dissipation and may not be retained effectively over time, limiting their ability to deliver the intended dose and therapeutic effects. The application of gels to the vagina requires the use of an applicator, which may be inconvenient for some individuals. There is also a risk of experiencing local irritation and leakage, potentially causing discomfort or affecting their overall effectiveness. Moreover, vaginal gels may lack stability in adverse environmental conditions, such as temperature, humidity, or exposure to certain substances, which can compromise their reliability. The tenofovir 1% gel, which initially appeared effective in the CAPRISA 004 trial, did not demonstrate consistent efficacy in subsequent Phase IIb/III trials. This was likely due to inconsistent and insufficient use by young, at-risk women in different dosing regimens. Overall, conventional formulations used for PrEP have shown poor adherence and compliance issues.[12-15]

Recognizing and considering the cons of conventional intra-vaginal formulations, we intend to develop a dispersible vaginal tablet (DT) and pessary comprising of mucoadhesive microparticulate system of tenofovir disoproxil fumarate (TDF) to further improve regional drug retention and delivery. Therefore, by broadening options for prevention, PrEP aids in worldwide attempts to combat HIV/AIDS.

Tenofovir ($C_9H_{14}N_5O_4P$), a nucleoside reverse transcriptase inhibitor (NRTI) (BCS Class III drug), used to treat HIV infection has been extensively studied as a prophylactic treatment. To improve its permeability, a prodrug called TDF ($C_{23}H_{34}N_5O_{14}P$) has been developed, which functions by inhibiting reverse transcription, a crucial step in the HIV replication process. Specifically, it causes chain termination during the DNA extension phase conducted by HIV Reverse Transcriptase. This interruption prevents the synthesis of viral DNA, thereby hindering the replication and spread of the virus within the host cells.[12,16] The oral bioavailability of TDF is low (25% in the fed state) due to intestinal degradation and efflux transport, highlighting the need for a vaginal dosage form.[17] TDF leads to a 1000-fold increase in the intracellular concentration of tenofovir-diphosphate compared to the tenofovir base. Moreover, TDF has a 100-fold lower IC_{50} than the tenofovir base, indicating better permeability.[18,19] TDF has an extended half-life (12-15h) and a favorable efficacy and safety profile, making it an ideal topical microbicide for preventing the sexual transmission of HIV.[5,20,21]

Achieving effective prophylactic prevention must ensure the drug reaches adequate therapeutic levels at the potential site of infection. Vaginal inserts are designed to achieve this goal by delivering the drug locally to target cells/tissues in the vaginal lumen. This delivery mechanism is based on the physicochemical characteristics and mechanism of action of the ingredients used in the inserts. Bio-adhesive vaginal dosage forms, in particular, are capable of delivering actives over a prolonged period. They achieve this by adhering to the vaginal mucosa and ensuring controlled and sustained release of the drug into the surrounding cervicovaginal fluid and tissue. This

sustained release is crucial for maintaining effective drug concentrations at the site of potential infection, enhancing the effectiveness of the prophylactic treatment.[18,22]

The small size of the bio-adhesive microparticulate system, along with its high surface-to-volume ratio, has a notable impact on biodistribution, retention, and cellular uptake. These microparticles can be modified to improve their ability to penetrate mucus barriers and epithelial layers, enhancing their efficacy. Unlike unit dosage forms, they are less likely to be expelled, ensuring a more sustained presence at the site of action. Moreover, these microparticles offer versatility in drug delivery, allowing for sustained/controlled release by incorporating mucoadhesive polymers such as sodium alginate (S-Alg), sodium carboxymethyl cellulose (S-CMC), hydroxy propyl methyl cellulose (HPMC), guar gum, carbopol, among others. Recent advancements suggest that using multifunctional polymers like poly (acrylates), chitosan, and their thiolated derivatives could further enhance mucoadhesion, penetration, and enzyme-inhibiting properties. These polymers are thought to interact with the vaginal surface through specific functional groups, ensuring the formulation remains adhered to the mucosa while releasing the drug. This interaction is vital for the success of the formulation. Additionally, the gelation of these polymers upon contact with aqueous media can help to control drug release through diffusion.[20,22,23]

Chitosan, derived from natural sources, is a hydrophilic and positively charged mucopolysaccharide. It boasts excellent biodegradability and biocompatibility. [24,25] Its flexibility is akin to that of natural tissues, and it is abundantly accessible, positioning it as an eco-friendly biomaterial ideal for healthcare product development and tissue engineering applications.[26] Chitosan's ability to adhere to mucus stems from its positively charged nature. The mucous membrane is composed of mucin

glycoproteins, which contain negatively charged sialic acid and sulfonic acid groups. The cationic groups in chitosan interact with these anionic acids, forming ionic bonds. This interaction gives chitosan its mucoadhesive properties, allowing it to effectively adhere to mucus. The release of drugs from chitosan microparticles (CM) is controlled by several mechanisms: polymer swelling, drug absorption, drug diffusion, polymer erosion or degradation, and a combination of both erosion and degradation. Each of these processes contributes to the overall rate and efficiency of drug delivery from the microparticles.[14,25,27]

S-Alg is a natural, biocompatible, and biodegradable biomacromolecule used for delivering microencapsulated actives.[28] It can be combined with hydrophilic polymers such as chitosan, HPMC, and S-CMC to enhance drug absorption. As a monovalent, water-soluble polysaccharide, S-Alg forms a gel when exposed to divalent ions like calcium. In its solid state, alginate shows strong mucoadhesion through hydrogen bonding, hydration, and polymer gelation.[29,30]

Dispersible vaginal tablets are compact, unit systems designed for vaginal insertion, aiming to deliver active ingredients immediately or over a sustained period. They offer several advantages over traditional vaginal forms, including more precise dosing, better stability, and lower production costs. These tablets can be customized for sustained or controlled drug delivery by including mucoadhesive polymers like S-Alg, HPMC, chitosan, S-CMC, and a few more as key primary components.

These polymers bind to the vaginal surface through specific functional groups present in both the polymers and biological tissues. This interaction aids the formulation in adhering to the vaginal mucosa while facilitating drug release. This adherence is

crucial for the tablet's effectiveness. When these polymers gel upon contact with moisture, they can further regulate drug release by allowing the drug to diffuse through the gel layer. DTs that use multi-particulate systems are favored over single-unit forms because they provide more consistent retention within the vaginal mucosa (Figure 1). Consequently, the risk of failure for these specialized tablets is minimal.[4,15,22,31]

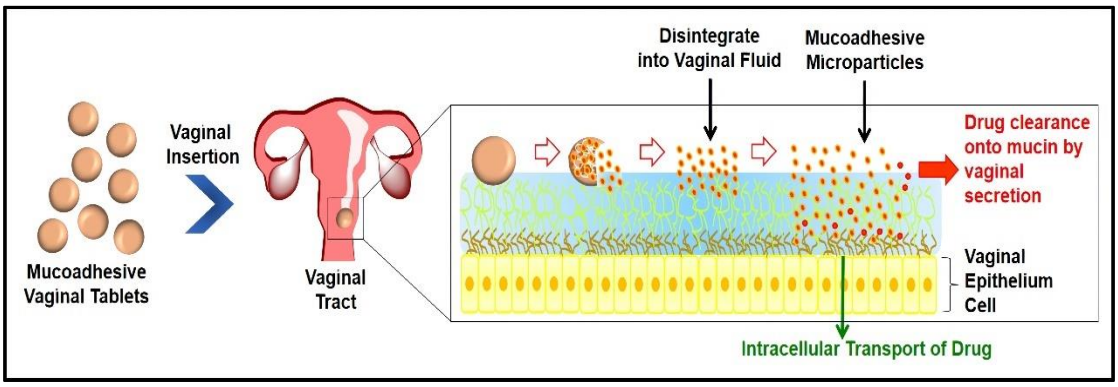

Figure 1: The bio-distribution of TDF administered via DT embedded with bio-adhesive microparticles.

Pessaries are excellent intra-vaginal forms capable of accommodating materials with varying polarities. TDF, with its extended half-life and low IC_{50}, shows promise as a microbicide for prophylactic pessaries. S-Alg was chosen as the bio-adhesive polymer for microsphere fabrication. Cocoa butter is specifically selected as the base material for the pessaries to prevent the water-soluble TDF from dissipating into the base. Unlike traditional single-unit intra-vaginal forms, these innovative microsphere-laden pessaries are less likely to be expelled. They melt to release the drug-loaded bio-adhesive microspheres, which are then retained on the vaginal mucosa, ensuring controlled drug release (Figure 2).[32]

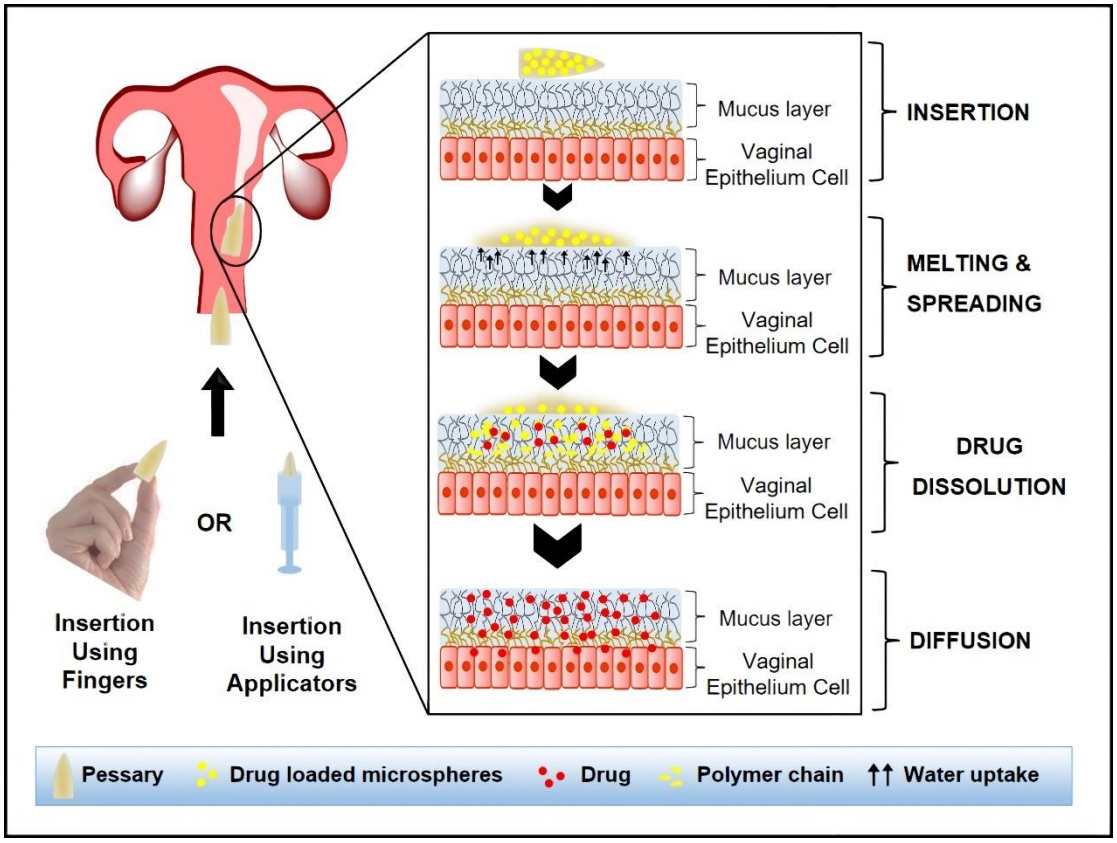

Figure 2: The bio-distribution of TDF administered via pessaries embedded with bio-adhesive microparticles.

1.2. Literature Review

Xu *et al.*, (2023) reported that drug resistance due to continuous viral mutation, poor adherence to long-term regimens, problems targeting difficult viral components, and latent reservoirs complicate the discovery of effective anti-HIV drugs. However, advances such as long-acting regimens, structured drug design, high-quality compound libraries, new strategies such as covalent inhibitors and PROTACs, and cutting-edge technologies such as gene editing and CAR-T therapy are accelerating the development of new HIV drugs.[33]

Gatto *et al.*, (2022) reported that administering AntiRVs for HIV PrEP is very effective and may be enhanced by new long-acting drug delivery methods. The study describes a subcutaneous reservoir implant for the delivery of tenofovir alafenamide (TAF) and evaluates its clinical safety in New Zealand white rabbits (3 groups of 5), beagles (2 groups of 6), and rhesus-macaques and evaluates the pharmacokinetics in details. Macaque monkeys (2 groups of 3 animals). Placebo implants were used in rabbits (n=10) and dogs (n=12). Parameters such as TAF morphology, choice of excipients, and PCL formulation are important for determining the activity of tenofovir diphosphate (TFV-DP), an active TAF anabolic, in peripheral blood mononuclear cells (PBMCs) and mucosal tissues associated with HIV infection. Achieving the target concentration of stable TFV-DP concentrations >100 fmol/10^6 cells was observed in PBMCs in all animal species, indicating effective delivery of TAF for 3-6 months. However, unlike placebo implants, all active implants cause local adverse events (AEs) such as skin inflammation and necrosis. Despite these AEs, the implant maintained the drug release profile, supporting further development of this drug delivery platform.[34]

Paredes *et al.*, (2022) developed a novel formulation for administering AntiRV drugs using microneedle array patches (MAPs), which offer a user-friendly option for painlessly self-applied to the skin and deliver drugs systemically. Implantable MAPs loaded with TAF have been developed to release the drug into the body. These MAPs were strong enough to pierce full-thickness pig skin to create drug stores. *In-vitro* drug release (IVDR) experiments showed rapid drug delivery, while Franz cell experiments showed that dissolved and implantable MAP deposited 47.87 ± 16.33 μg and 1208.04 ± 417.9 μg of TAF into the skin within 24 h. Pharmacokinetic studies in rats demonstrated rapid conversion of TAF to tenofovir with subsequent rapid elimination from plasma. These MAPs could serve as an alternative to existing oral HIV treatment.[35]

Sankaraiah *et al*., (2022) formulated a bi-layer tablet has been developed as a multidrug regimen to treat HIV infections, combining the effects of Brand SUSTIVA® (efavirenz600 mg), EPIVER® (lamivudine300 mg), and VIREAD® (tenofovir disoproxil300 mg). The tablet consists of two layers: layer-I with efavirenz, created using a wet granulation process, and layer-II with lamivudine and TDF, developed by rolling. Both layers were then compressed and coated with a film. Different concentrations of diluents, surfactants and disintegrants were used to enhance the solubility of efavirenz and improve the fluidity and uniformity of layer II. The optimal formulation was tested for *in-vitro* dissolution against each branded drug. A three-drug mixture under 50°C/75% RH conditions was found to increase tenofovir impurities and decrease the tenofovir assay in the presence of efavirenz. Sodium lauryl sulfate was critical for increasing the solubility of efavirenz and influencing drug dissolution. Microcrystalline and croscarmellose sodium affected tenofovir

dissolution and friability, while powdered cellulose improved lamivudine layer uniformity and dissolution. P-XRD confirmed no polymorphic changes and no interactions between the three active substances. The optimized formulation provided consistent IVDR comparable to each branded drug, proving robust and scalable for further development.[36]

Sneller *et al.*, (2022) investigated developing effective alternatives using long-acting antivirals to combat viral replication. A two-part clinical trial reported the results of passive transfer of two HIV-specific broadly neutralizing monoclonal antibodies, 3BNC117 and 10-1074. Part I, a double-blind, placebo-controlled study, included participants who started AntiRV therapy during acute/early HIV infection. The second open-label study included patients with controlled viremia receiving AntiRV therapy for the first time. Up to eight infusions of 3BNC117 and 1074-10 over 24 weeks were well tolerated, with no serious infusion-related adverse events. Compared with placebo, the antibody combination maintained complete suppression of plasma viremia after discontinuation of treatment (up to 43 weeks), unless antibody-resistant HIV was present at baseline. Similarly, strong HIV suppression was observed in viremic participants with susceptible virus. These data suggest that combination therapy with a neutralizing monoclonal antibody can achieve long-term viral suppression without AntiRV therapy and suggest future trials with long-acting antibodies.[37]

Cobb *et al.*, (2021) developed nanocrystals by transforming tenofovir (TFV) by converting it to blue prodrug nanocrystals (NM1TFV and NM2TFV) formed with long-acting surfactants. In Sprague Dawley rats, an intramuscular injection of NM1TFV, NM2TFV, or nanoformulated TAF at a dose equivalent to 75 mg/kg TFV reduced the level of activated TFV-DP by 94%. Effective dose 2 months. NM1TFV,

NM2TFV, and NTAF induced TFV-DP levels of 11276, 1651, and 397 fmol/g in rectal tissue, respectively. These findings represent important progress toward long-acting TFV ProTide.[38]

Godela *et al.*, (2021) developed and validated a reverse phase high-performance-liquid chromatography method for the simultaneous estimation of lamivudine, efavirenz, and TDF in pure and combined tablet formulations. Separation was efficiently achieved using a Zorbax eclipse XDB-Phenyl column, with a mobile phase of methanol and buffer (0.1%v/v formic acid in water) in a 73:27v/v ratio at a flowrate of 1mL/min with isocratic elution, and detection at260nm. Acetonitrile and equal parts water were used as diluents. Retention times for lamivudine, TDF, and efavirenz were ~2,4, and 5 minutes, respectively. The method showed linear responses for lamivudine and TDF (15–45 μg/mL) and for efavirenz (20–60 μg/mL). This method successfully separated the three drugs in both powder and tablet forms, and was capable of separating degradants produced under stress conditions with high resolution and sensitivity, indicating its stability-indicating property. The study suggests that this method could be useful for adoption in the pharmaceutical industry.[39]

Thoueille *et al.*, (2021) reviewed that USFDA has approved a long-acting AntiRV combination of cabotegravir and rilpivirine, which reduces the daily pill burden for HIV patients to just six intramuscular injections per year. Another promising development is letravir, a nucleoside reverse transcriptase translocation inhibitor intended to be formulated as an implant with dosing intervals of 1 year or longer. Currently, long-acting AntiRV therapies (LA-ARTs) are administered at fixed standard doses, regardless of patient weight, BMI, or other factors that may affect

drug disposition. However, this 'one-size-fits-all' approach does not take into account the significant inter-individual variability in LA-ART pharmacokinetics. Therapeutic drug monitoring is crucial for precision medicine and can provide clinicians with valuable information about actual drug exposure, leading to improved patient management in real-life situations.[40]

Lee *et al.*, (2021) conducted a study to assess the pharmacokinetcs and safety of tenofovir disoproxil phosphate to TDF in healthy male subjects. It was an open-label, randomized, crossover study involving 37 volunteers. The results showed that tenofovir disoproxil phosphate (292 mg) was bioequivalent to TDF (300mg), as the GMR and 90% CIs fell within the bioequivalence range (0.8–1.25). Both forms of were well-tolerated, demonstrating similar safety profiles.[41]

Jhunjhunwala *et al.*, (2021) investigated the development of suppositories containing combination of TFV and, elvitegravir (EVG) in different suppository bases. *In-vivo* pharmacokinetic studies in macaques showed similar drug release profiles for both bases, with TFV and EVG levels in rectal fluids exceeding levels associated with high-efficacy against rectal simian-HIV exposure. Based on this, a lower-dose combination of TAF and EVG was developed and achieved similar rectal-drug exposures in maecaques.[42]

Pashayan *et al.*, (2021) formulated bifunctional suppositories with antifungal and probiotic properties to treat vulvovaginal candidasis and promoting colonization of vaginal cavity by beneficial *lactobacilli*. The suppositories contained freeze-dried *Lactobacillus delbrueckii* MH10, known for producing H_2O_2, along with terconazole. Adhesion to mucosa and release rates varied among the bases, with Suppocire AP showing the highest adhesion and longest shelf life. L. delbrueckii MH10 exhibited strong antagonistic effects against Candida albicans, with more than 90% population

reduction during joint cultivation. The study concluded that Suppocire AP was the preferred base to prepare vaginal suppositories.[43]

Osmalek *et al.*, (2021) reviewed the potential of drug administration through the vagina, focusing on current vaginal formulations made of natural or synthetic polymers with various functions. While the vagina is commonly studied for topically acting drugs, its anatomical and physiological characteristics also support systemic drug absorption. The article outlines recent research directions and challenges in vaginal drug administration.[44]

Sailaja *et al.*, (2021) reviewed the current HIV-AIDS treatment landscape includes various antiviral drugs that help manage the condition and improve survival rates. However, these drugs have limitations such as low bioavailability/permeability, and shorter half-lives. Higher dosages can lead to toxicity and increased drug resistance, while lower doses with nanocarriers can target specific areas more effectively. Nanotechnology-based drug delivery systems have emerged as a promising solution to overcome these challenges. Nanocarriers like liposomes, dendrimers, nanoparticles, polymeric micelles, and nanoemulsions can enhance drug delivery to target tissues, revolutionizing pharmaceutics and pharmacokinetics. Studies suggest that nanotechnology-based AntiRV drug delivery can improve efficiency and reduce adverse effects in controlling HIV. Integrating other available HIV drugs into nanotechnology-based formulations could further enhance drug delivery effectiveness.[45]

Patel *et al.*, (2020) formulated thermosensitive mucoadhesive in-situ vaginal gel of TDF for HIV pre-exposure prophylaxis, providing effective spreading and coating of

the vagina for extended effects. The gel, made with poloxamer 407 and carbopol 934, was prepared using a cold method. Formulation F2 was identified as the most suitable based on evaluation parameters, demonstrating the desired properties. The mucoadhesive performance, measured by work of adhesion values, was 0.324 ± 0.036 N, indicating strong adhesion to vaginal mucosa. Hen'sEgg Test-Chorioallantoic Membrane test confirmed the formulation as non-irritating to vaginal mucosa. F2 remained stable throughout the study period.[46]

Kim *et al.*, (2020) formulated and evaluated tenofovir disoproxil (TD)-loaded enteric-microparticles (TDEMs) were developed for enhanced delivery to the duodenum. The study included dissolution tests with varying pH to simulate conditions in the gastrointestinal tract. The encapsulation efficiency (EE%) of TD in TDEMs was found to be >90%, indicating effective loading of the drug. The combination of EL and EC provided better enteric properties to the TDEMs compared to using either polymer alone. The optimized TDEM formulation (TD/EL/EC = 0.2//1/1, w/w/w ratio) exhibited a mean dissolution rate of <10% in 1 h at pH1.2, indicative of enteric protection. However, at pH 6.5, the microparticles showed rapid and complete dissolution, with more than 85% of the drug released within 1 hour. This suggests that TDEMs could be a promising formulation for targeted delivery of TD to the duodenum.[47]

Rao *et al.*, (2020) formulated microsponges loaded with TDF using quasi emulsion solvent diffusion with varying proportions of polymers Eudragit RS100 and Ethyl cellulose. SEM showed that the microsponges were spherical with pores, and their size decreased with an increase in the drug and polymer ratio, while %EE and production yield increased with this ratio. Different kinetic models were used for the

release study, and formulation F8, which showed 90.22% drug release in 15 hours, was considered the optimized formulation. The IVDR data fitted well with the zero-order release model, indicating a constant release rate over time. Overall, the study concluded that microsponge-based TDF gel could be a promising alternative to traditional therapy for HIV.[48]

Fernandes *et al.*, (2020) reviewed and reported HAART effectively suppresses the HIV replication but does not provide a cure and can lead to various health issues. The virus can persist in latent reservoirs, increasing the risk of viral rebound. Immunoengineering, which uses bioengineering to enhance the immune system's ability to fight HIV, is gaining attention in cure research. Nanoparticle-based immunoengineering is particularly promising, improving drug delivery and function. These approaches aim to enhance HAART, reverse latency, develop vaccines, target viral fusion, improve gene editing, and boost immune-cell mediated reservoir clearance. While still in preclinical stages, these approaches show great potential for an HIV cure.[49]

Gada *et al.*, (2019) investigated the potential of microspheres, loaded with lamivudine, S-Alg and tamarind mucilage (TM) via the ionic-gelation-technique. The microspheres (769.22 to 978.56 μm) were free-flowing, %EE ranged from 65.28% to 92.33%, and the percentage of drug released after 12h ranged from 85±1.51% to 97±1.44%. *In-vitro* wash-off studies demonstrated strong mucoadhesivity, with 20% of the microspheres adhering after 6h. These findings suggest that the formulation could be effectively prepared, offering a promising method for controlled drug release and enhanced bioavailability.[50]

1.3. Justification

The current social scenario and decline in moral and human values have led to an alarming increase in the risk of HIV/AIDS among the young population.[1] It is crucial to educate individuals about the consequences of unhealthy lifestyles. As pharmacists and health professionals, we have a responsibility to protect the younger generation from the severe consequences and mortality associated with HIV/AIDS. While long-acting systemic formulations are currently favored for HIV prevention, vaginal inserts offer an on-demand option for HIV-negative individuals.[4]

TDF, classified as a NRTI, works by interrupting the reverse transcription process carried out by the enzyme HIV Reverse Transcriptase, leading to chain termination during DNA chain extension in the HIV cycle. Despite its effectiveness, TDF has poor oral bioavailability due to pre-systemic elimination, primarily caused by the hepatic first-pass effect or p-glycoprotein efflux.[12,14] The low oral bioavailability of TDF, especially in the fed state (~25%), is attributed to intestinal degradation and efflux transport mechanisms. This limitation underscores the importance of developing a vaginal dosage form for TDF.[15-20]

The project aims to address the increasing risk of HIV among the youth by developing a novel, economically feasible PrEP DT, and pessaries containing bio-adhesive particulate systems of TDF for vaginal delivery. These formulations aim to overcome the limitations of conventional dosage forms and provide a viable alternative to oral and parenteral PrEP. DT containing multi-particulate systems offer advantages over single-unit vaginal dosage forms, providing more reliable retention time on the vaginal mucosa. These tablets have several benefits over traditional vaginal dosage

forms, including more precise dosing, greater stability, and lower manufacturing costs. Additionally, they are versatile and can be adjusted to achieve sustained/controlled drug delivery by incorporating mucoadhesive polymers. Pessaries are well-suited intra-vaginal forms that can accommodate materials with varying polarities. TDF's longer half-life (12-15h) and lower IC_{50} make it an appealing candidate for developing prophylactic pessaries as a topical microbicide.

The proposed bio-adhesive vaginal inserts are expected to deliver a higher therapeutic concentration of TDF at the site of transmission, potentially exceeding the IC_{50} for TDF. As no similar product is currently available in the Indian market, this project has significant potential to save lives and reduce HIV infections, particularly among females who account for nearly half of the HIV-infected population and mostly acquire the infection through sexual intercourse. The project utilizes techniques that are industrially feasible, easily scalable, and have high translational potential, making it a promising approach to HIV prevention.

1.4. Aim and Objectives

Aim:

To formulate and evaluate vaginal drug delivery system of Tenofovir to overcome the limitations of the conventional dosage forms.

Objectives:

Primary Objective

- To develop bio-adhesive particulate system of Tenofovir and characterize the same for particle size, bio-adhesion, drug loading, entrapment efficiency and *in-vitro* drug release.

Secondary Objectives

- To incorporate the developed particles into suitable dosage forms.
- To carry out *in-vitro* release studies of Tenofovir from the dosage forms.
- To carry out *in-vivo* studies of Tenofovir from the dosage forms.

MATERIALS AND METHODS

2. MATERIALS AND METHODS

2.1. Materials

2.1.1. Chemicals

Drug:

TDF was received as a gift sample from Aurobindo Pharma, Hyderabad, India.

Polymers:

Chitosan was received as a gift sample from the Central Institute of Fisheries Technology, Kochi, Kerala, India. **S-Alg** (Protanal LFR 5/60 USP NF; M/G = 30/70%) was received as a gift sample from FMC BioPolymers, USA. **HPMC K4M** (Methocel) and **HPMC K-100M** (Benecel) were received as a gift sample from The Dow Chemical Company, USA.

Other Chemicals:

Sodium Tripolyphosphate Anhydrous (TPP) (extra pure) was purchased from Sisco Research Laboratories Pvt. Ltd., Maharashtra, India. **Cocoa butter** was procured from SK Organics, Anand, Gujarat, India.

S-CMC, light liquid paraffin (LLP), span 80, calcium chloride ($CaCl_2$), acetic acid, petroleum ether, tween 60, beeswax, potassium hydroxide, sodium chloride, calcium hydroxide, glycerol, lactic acid, glycerol, glucose, and urea were purchased from S.D. Fine Chemicals Ltd., India.

All the reagents/chemicals used for the research project were of analytical grade.

2.1.2. Instruments/Equipments

The list of all the instruments/equipments utilized for the research work is tabulated in Table 1.

Table 1: List of instruments/equipments.

Sl. No.	Name of the Instrument/Equipment	Make & Model of the Instrument/Equipment
1	Analytical Balance	Shimadzu, BL-220H
2	Centrifuge	PR 24, Remi World, Mumbai, India
3	Differential Scanning Calorimeter	NETZSCH, STA 449 F5 Jupiter thermal analyzer, Germany
4	Friabilator	Roche Friabilator
5	FTIR Spectrometer	Jasco, 460 Plus, Jasco Inc., United States
6	Hardness Tester	Pfizer Hardness Tester
7	Homogeniser	T18 digital Ultra Turrax®, IKA®, Ultra Instruments, Bengaluru, India
8	Magnetic Stirrer	Remi Instruments Ltd.
9	Mechanical Stirrer	Remi Instruments Ltd.
10	Optical Microscope	Labomed, LB-200
11	Particle Size Analyser	Malvern Mastersizer -v3.62 (Malvern Instruments Ltd., UK
12	Powder X-ray Diffractometer	Bruker D8 ADVANCE X-ray Diffractometer, United States

13	Scanning Electron Microscope	TESCAN-VEGA3 LMU
14	Sonicator	2.5L GT-Sonic Ultrasonic bath sonicator
15	Tablet Rotary Press	Model RSB-4, Rimek mini press
16	USP Disintegration Apparatus	Electrolab, ED-2L
17	USP IV Flow Through Dissolution Apparatus	Electrolab, Model No. EFT-01
18	UV-VIS Spectrophotometer	Shimadzu UV-Vis Spectrophotometer 1900i, Shimadzu Corporation, Japan
19	Vernier Calliper	Mitutoyo Corporation, Tokyo, Japan
20	Liquid Chromatography Mass Spectroscopy/ Mass Spectroscopy	Sciex, API-4000, Shimadzu

2.2. Methods

2.2.1. Authentication of Drug

2.2.1.1. DSC Analysis

The thermal response of TDF was recorded using a DSC thermal analyzer system. Samples were analyzed at a heating rate of 30°C/10.0K/min over a temperature range of 20-300°C to enable data acquisition.[51,52]

2.2.1.2. Mass Spectroscopy

The drug sample was sent for Liquid Chromatography-Mass Spectroscopy (LC-MS) studies conducted at Acquity Labs Pvt. Ltd., Bengaluru, Karnataka.[53,54]

2.2.1.3. FTIR Spectroscopy

FTIR spectrometry is an appropriate analytical method for characterizing TDF. To prepare the samples, they were finely grounded using a glass mortar-pestle with potassium bromide, which helps to reduce IR scattering on the particle surface. The prepared sample was placed in the sample holder and analyzed using an FTIR spectrometer within the range of 4000 cm^{-1} to 1000 cm^{-1}. This technique allows for the detailed examination of the chemical bonds present in the sample, aiding in its identification and characterization.[51]

2.2.1.4. UV-VIS Spectrophotometry

Preparation of Simulated Vaginal Fluid of pH 4.5 (SVF): SVF was prepared using 3.51 g/L sodium chloride, 1.40 g/L potassium hydroxide, 0.22 g/L calcium hydroxide, 1.00 g/L acetic acid, 2.00 g/L lactic acid, 0.16 g/L glycerol, 5.00 g/L glucose, and 0.40 g/L urea. The pH of the fluid was adjusted to 4.5 with hydrochloric acid or sodium hydroxide.[55]

Determination of λ_{max}: A primary stock solution of concentration 1000 µg/mL was prepared by accurately weighing 10 mg of TDF and dissolving it in 100 mL of SVF. A secondary stock solution with a concentration 100 µg/mL was prepared from the primary stock solution. Subsequently, a dilution of 20 µg/mL was made from the secondary stock solution and scanned in UV-VIS spectrophotometer (UV-S) over the range of 200-400 nm against SVF (blank).

Preparation of Calibration Curve: Aliquots of 0.5-4.0 mL were taken from the secondary stock solution to produce concentrations of 5-40 µg/mL. The absorbance of the resulting solutions was measured at 259 nm against SVF using UV-S.[56,57]

2.2.2. Pre-formulation Studies

2.2.2.1. Solubility Studies

The solubility of TDF was determined in triplicate in 0.1 (N) HCl (pH 1.2), SVF, distilled water (pH 7.0), and phosphate buffer (pH 7.4). In a glass vial, an excess amount of drug was added to the predetermined volume of the above solvents and equilibrated for 24-48 h at room temperature with intermittent shaking. The resultant dispersion was subjected to cold centrifugation at 3000 rpm (10 mins) at 25°C. The solubility of TDF was determined spectrophotometrically at 259 nm following suitable dilutions.[58]

2.2.2.2. Drug-Excipient Compatibility Studies

FTIR spectroscopy is frequently used to analyze potential chemical interactions between drugs and polymers intended for formulation. This technique is valuable for screening and selecting appropriate polymers for formulation development. To minimize IR scattering on the particle surface, the samples were prepared by

uniformly mixing with potassium bromide. The resulting mixture was loaded into the diffuse reflectance sample holder and analyzed using an FTIR spectrometer. The analysis was conducted within the wavelength range of 4000 cm^{-1} to 1000 cm^{-1}, with a scanning speed of 2 mm/sec.[51,52,59]

2.2.3. Preparation of TDF Loaded Chitosan Microparticles (T-CM)

The emulsification-internal-gelation technique was adopted to develop TDF-loaded microparticles with chitosan as the bio-adhesive polymer as represented in Figure 3.

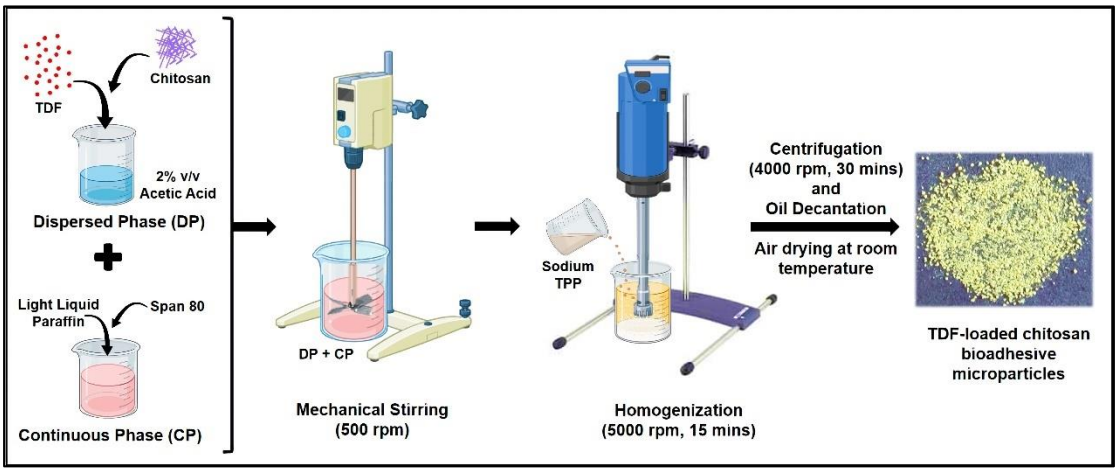

Figure 3: Development of T-CM.

Specified amounts of TDF and chitosan, at various concentrations, were dissolved in 2% v/v acetic acid to achieve a homogeneous solution.[60,61] Approximately 20 ml of this solution was then added to 60 ml of light liquid paraffin (LLP) containing 1.5% v/v Span 80, which served as the continuous phase.[46] By introducing the dispersed phase into the continuous phase while maintaining a constant mechanical stirring at 500 rpm, a water-in-oil (w/o) emulsion was formed and subsequently homogenized at 5000 rpm for 15 mins. Continuous stirring was maintained as sodium tripolyphosphate (TPP) solution was added, resulting in the formation of rigid, discrete microparticles. These microparticles were then separated through

centrifugation at 4000 × g for 30 mins, washed multiple times with petroleum ether to remove any traces of oil adhering to the microparticles and dried at room temperature.[46,61] The compositions of different batches of T-CM are indicated in Table 2.

Table 2: Composition of T-CM.

Formulation Code (FC)	Drug (%w/v)	Chitosan (%w/v)	TPP (%w/v)
EC-1	1.0	1.0	5.0
EC-2	1.0	2.0	5.0
EC-3	1.0	3.0	5.0
EC-4	1.0	4.0	5.0
ECH – 1	1.0	1.0	10.0
ECH – 2	1.0	2.0	10.0
ECH – 3	1.0	3.0	10.0
ECH – 4	1.0	4.0	10.0

2.2.4. Evaluation of T-CM

2.2.4.1. Practical Yield and Drug Entrapment Efficiency

The practical yield (%yield) of each batch of T-CM was calculated from the proportions of the total raw materials used in the formulation of T-CM, using equation (1) to evaluate the mass balance. To determine the percentage encapsulation efficiency (%EE) of TDF, an accurately weighed quantity of T-CM were pulverized and digested

in 5 mL of SVF in a screw-cap vial on a bath sonicator to extract the entrapped TDF. The resulting dispersion was centrifuged at 10,000 × g for 5 mins.[55] The amount of TDF in the supernatant was assayed using a UV-S at 259nm, following appropriate dilution. The %EE was determined in triplicate for all batches using equations (2), (3), and (4).[61-63]

$$\%\ Practical\ Yield = \frac{Weight\ of\ microparticles}{Weight\ of\ drug + Weight\ of\ polymers}\ X\ 100 \quad ..(1)$$

$$\%\ Theoretical\ Drug\ Loading\ (DL) = \frac{Weight\ of\ drug\ taken}{Weight\ of\ drug\ taken + Weight\ of\ polymers\ taken}\ X\ 100 \quad ..(2)$$

$$\%\ Practical\ Drug\ Loading\ (DL) = \frac{Weight\ of\ drug\ loaded\ into\ microparticles}{Weight\ of\ microparticles}\ X\ 100 \quad ..(3)$$

$$\%\ EE = \frac{\%\ Practical\ DL}{\%\ Theoretical\ DL}\ X\ 100 \quad ..(4)$$

2.2.4.2. Surface Morphology

The surface morphology and topography of the T-CM were analyzed using SEM. The microparticles were mounted on an SEM sample holder with adhesive tape and then coated with a thin layer of gold (~200 nm) via ion sputtering at reduced pressure for 5 mins. This gold coating helps to enhance the resolution and contrast of the SEM images by increasing the conductivity of the microparticles. The gold-coated samples were then scanned to capture photomicrographs at appropriate magnifications.[64,65]

2.2.4.3. Particle Size Analysis

The DLSA technique was employed to determine the size of the microparticles by Malvern Mastersizer. The microparticles were dispersed in propanol and subjected to sonication with a 600W probe for 10 mins before measurement in order to

deaggregate the microparticles to enable clear detection. The volume-surface mean diameter was calculated using equation (5).[51,66-68]

$$Volume - Surface\ Mean\ Diameter\ (d_{vs}) = \frac{\Sigma nd^3}{\Sigma nd^2} \quad ..(5)$$

where, n is the number of particles in each size range, and d is the mean of size range in μm.

2.2.4.4. FTIR Spectroscopic Analysis

FTIR spectrometry is an appropriate and effective analytical technique for characterizing TDF, polymer, physical mixture, and formulations. The samples were prepared by finely grinding them with potassium bromide in a glass mortar and pestle to minimize IR scattering on the particle surface. The prepared sample was placed in the sample holder and observed in the FTIR spectrometer in the range of 4000 cm^{-1} – 1000 cm^{-1}.[51,52,59]

2.2.4.5. DSC Analysis

DSC has been an extensively used calorimetric technique to characterize the solid state of the drug-in-polymer. The thermal response of TDF, polymer, physical mixture, and formulation was recorded using a DSC thermal analyzer system. Samples were analyzed at a heating rate of 30°C/10.0 K/min over a temperature range of 20 – 300 °C to enable data acquisition.[51,52,69]

2.2.4.6. P-XRD Analysis

P-XRD techniques are widely used to characterize the solid state of drugs-in-polymers. The diffraction studies of TDF, polymer, physical mixture, and formulation were conducted using a P-XRD. The operating conditions included a 2.2 kW X-ray

source with a Cu anode and a fine focus ceramic X-ray tube, operating at 40 kV and 40 mA, with a power of 1.6 kW. Data were recorded between 5° and 40° 2θ values and collected using a LYNXEYE high-speed SSD160-2 detector with a 500 µm sensor.[51,70]

2.2.4.7. *In-vitro* Drug Release

The *in-vitro* dissolution studies of T-CM were conducted in triplicate for all batches using a USP IV flow-through-cell dissolution apparatus as represented in Figure 4. Approximately 150 mg of T-CM were confined in the sample holder. Glass beads were loaded into the flow-through cell to ensure a laminar flow of the media (SVF), maintained at 37±0.5°C. A flow rate of 16 mL/min was maintained in a closed-loop system to facilitate the disaggregation of the particles, enhancing dissolution. TDF has good aqueous solubility, allowing the 900 mL of media to easily maintain sink conditions. Thus, the study was conducted in a closed-loop configuration, which indicated recirculation of the fixed volume of media similar to USP Apparatus I and II.[71-73] Aliquots were withdrawn at predetermined intervals up to 24 hours and analyzed spectrophotometrically at 259 nm to measure the released TDF.

Figure 4: USP (Type IV) flow through cell dissolution apparatus.

The obtained IVDR data were fitted to four different kinetic mathematical model-dependent methods – zero order, first order, Higuchi and Korsmeyer-Peppas release equations as presented in Table 3.[74,64,61]

Table 3: Mathematical models used to describe IVDR curves.

Model	Equation
Zero Order	$Q_t = Q_0 + K_0t$
First Order	$\text{Log } Q_t = \text{Log } Q_0 + K_1t$
Higuchi Model	$Q = K_H * \sqrt{t}$
Korsmeyer-Peppas	$F = (Q_t/Q) = K_K * t^n$

where, t = Time in hours, Q_0 = Initial amount of drug, Q_t = Cumulative amount of drug release at time (t), K_0, K_1, K_H, K_K = Zero order, First order, Higuchi and Korsmeyer-Peppas release constant respectively, F = Fraction of drug released at time (t), Q_t = Amount of drug released at time (t), Q = Total amount of drug in dosage form, n = Diffusion or release exponent which explains different mechanisms of drug transport from polymeric drug delivery systems.

2.2.4.8. *Ex-vivo* Mucoadhesion Study

The mucoadhesive properties of T-CM were evaluated using a modified USP disintegration apparatus. A freshly excised piece of rabbit vagina (5x1 cm) was used as a substrate and mounted on a glass slide with glue. Approximately 200 microparticles were uniformly sprinkled over the substrate, and the glass slide was suspended on the arm of the disintegration apparatus with appropriate support. When the disintegration apparatus was operated, the tissue specimen underwent a slow, regular up and down movement in SVF, maintained at 37 ± 0.5 °C for a duration of

24 h. At predetermined time intervals, the apparatus was stopped and the number of particles adhering to the mucosal tissue were counted using a microscope in triplicates and percentage mucoadhesion was calculated using equation (6).[64,75]

$$\%\ Mucoadhesion = \frac{No.of\ microparticles\ adhered}{Initial\ no.of\ microparticles}\ X\ 100 \quad ..(6)$$

2.2.5. Preparation of Vaginal Tablets

The optimized T-CM formulation ECH-4 was incorporated into DT (DT-T-CM) using the conventional direct compression technique. T-CM (ECH-4), containing 15 mg of TDF, was geometrically dry blended with croscarmellose sodium, polyvinylpyrrolidone K-30, and microcrystalline cellulose (pH 102) in varying ratios, then passed through a 120 μm sieve. The sieved blend was lubricated with magnesium stearate and talc for a few mins. The lubricated blend was compressed into flat-faced bevel-edge tablets, each weighing 300 mg, on a rotary tablet press using tablet B tooling of 8.75 mm diameter. The batch size for each tablet composition was 30 tablets. Three different batches of DT containing ECH-4 (coded as F1-F3) and one batch of DT containing TDF (coded as F4) were produced by varying the blend composition as tabulated in Table 4.[76,77]

Table 4: Composition of vaginal tablets.

Ingredients	Quantity (mg)			
	F1	F2	F3	F4
TDF	-	-	-	15
ECH-4	150	150	150	-
Avicel (pH 102)	120	120	120	75

Polyvinyl pyrrolidine K-30	9	12	15	5
Croscarmellose sodium	15	12	9	3
Magnesium stearate	3	3	3	1
Talc	3	3	3	1
Weight of each tablet	**300 mg**			**100 mg**

*150 ECH-4 contains 15 mg of TDF

2.2.6. Evaluation of Vaginal Tablets

2.2.6.1. Physical Characterization of Vaginal Tablets

The prepared materials were evaluated for quality control tests like organoleptic properties, tablet thickness and diameter, weight variation, hardness, friability, and content uniformity tests following the official procedures.[78]

i. **Organoleptic properties:** The tablets were inspected visually for shape and color.

ii. **Weight variation:** Twenty tablets were randomly selected and weighed individually. The average weight and percentage deviation from the average weight were calculated.

iii. **Tablet thickness and diameter:** Uniformity in tablet thickness and diameter of tablets ensures uniformity of tablet size which is essential during packaging. Ten tablets were examined for their thickness and diameter using a vernier caliper and the mean thickness and diameter value along with SD were calculated.

iv. **Hardness:** The resistance of a tablet to shipping or breakage, conditions of storage, transportation, and handling, before usage, depends on its hardness.

Ten tablets were randomly selected and the hardness of each tablet was measured using Pfizer hardness tester.

v. **Friability:** Friability is a measure of tablet strength. Twenty-two tablets were accurately weighed and placed in the Roche friability chamber, which revolves at 25 rpm for 4 mins, dropping the tablets through a distance of 6 inches with each resolution. After 100 revolutions, the tablets were reweighed, and the percentage loss in tablet weight was determined following equation (7).

$$\%\ Friability = \frac{Initial\ weight\ of\ tablets - Final\ weight\ of\ tablets}{Initial\ weight\ of\ tablets}\ X\ 100 \quad ..(7)$$

vi. **Content uniformity:** The TDF content in ten randomly selected tablets from each batch was determined spectrophotometrically at 259nm.

vii. ***In-vitro*** **disintegration test:** Disintegration time (DT) for six DT was determined using the disintegration test apparatus in SVF maintained at 37±0.5 °C. The time point at which the tablets completely disintegrated was recorded as the disintegration time.

2.2.6.2. *In-vitro* Dissolution Study

The IVDR of TDF from the DT-T-CM tablets for all batches was performed in triplicate using a USP IV flow-through cell dissolution apparatus. The USP apparatus IV addresses various issues encountered with USP Apparatus 1 and 2, such as tablet sticking, floating, coning, dead zones, and problems related to sampling and sample introduction effects. By using USP apparatus IV, these challenges are likely to be eliminated, ensuring more accurate and reliable dissolution testing. The study was conducted using a closed-loop flow-through method in SVF, maintained at 37 ±0.5 °C

for 24 h. The tablet was placed in the sample holder in such a way that the medium flow was always perpendicular to the disintegrated particles of the tablet. A flow rate of 16mL/min was maintained throughout the 24 h period. Aliquots were withdrawn at predetermined time intervals, filtered, and analyzed by UV-S at 259 nm to measure the released TDF.[71,73]

A model-dependent method was followed to compare the dissolution profile of TDF tablets and T-CM tablets by determining the difference factor (f_1) and similarity factor (f_2) using equations (8) and (9).

$$Difference\ Factor\ (f_1) = \frac{\sum_{t=1}^{n}(R_t - T_t)}{\sum_{t=1}^{n} R_t}\ X\ 100 \quad ..(8)$$

$$Similarity\ Factor\ (f_2) = 50\ X \log\{\sqrt{\left[1 + \frac{1}{n}\sum_{t=1}^{n}(R_t - T_t)^2\right]}\ X\ 100\} \quad ..(9)$$

where, 'n' is the number of dissolution time points; R_t is the dissolution value of the reference drug product at time t; and T_t is the dissolution value of the test drug product at time t.

In the range of 0-100, the dissolution profile of the test sample is considered to be identical to that of the reference sample if f_2 ranges from 50≤100 and f_1 ranges from 0≤15.[79,80]

The obtained IVDR data from DT-T-CM were subjected to fitting to four different kinetic mathematical model-dependent methods – zero order, first order, Higuchi and Korsmeyer-Peppas release equations as presented in Table 2.[60,74,81]

2.2.6.3. *In-vivo* Study

The bio-distribution of TDF in the vagina was assessed by comparing intra-vaginal TDF concentrations, vaginal tissue concentrations, and histopathology results between

the formulated DT-T-CM for vaginal delivery and an oral marketed formulation in rabbits. Detailed methodology and results are provided in sections 2.2.11 and 3.1.11, respectively.

2.2.7. Preparation of TDF Loaded S-Alg Microspheres (T-AM)

The emulsification-internal-gelation technique, as illustrated in Figure 5, was used to prepare T-AM using S-Alg as a bio-adhesive polymer alone and in combination with various polymers (Table 5).[82]

A homogeneous aqueous dispersion (2% w/v) of TDF and polymers was added to the continuous phase, which consisted of 60 mL of LLP and 1.5% v/v Span 80 while maintaining constant mechanical stirring at 500 rpm.[83] The resulting homogeneous water-in-oil emulsion was then homogenized at 5000 rpm for 15 mins.

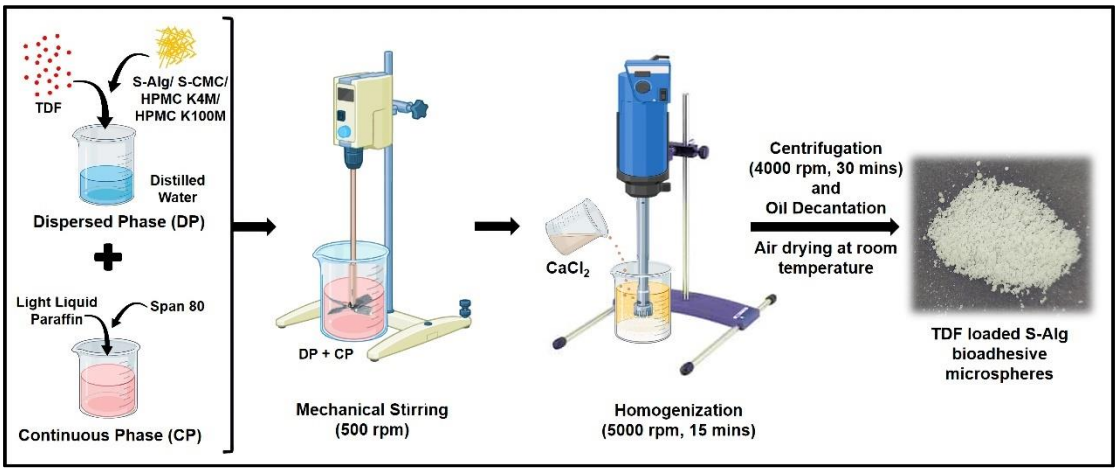

Figure 5: Preparation of T-AM.

While stirring continuously, a 10% w/v calcium chloride ($CaCl_2$) solution was added to form rigid, discrete particles.[84] The microspheres obtained were separated by centrifugation at 4000 × g for 30 mins, washed several times with petroleum ether to remove any residual oil remnants, and air-dried at room temperature.[62,63]

Table 5: Formulation of different batches of T-AM.

FC	Drug (%w/v)	Na-Alg (%w/v)	Na-CMC (%w/v)	HPMC K4M (%w/v)	HPMC K100M (%w/v)	$CaCl_2$ (%w/v)
EH – 1	1.0	2.0	-	-	-	10.0
EH – 2	1.0	1.0	1.0	-	-	10.0
EH – 3	1.0	1.0	-	1.0	-	10.0
EH – 4	1.0	1.0	-	-	1.0	10.0
EH – 5	1.0	4.0	-	-	-	10.0
EH – 6	1.0	2.0	2.0	-	-	10.0
EH - 7	1.0	2.0	-	2.0	-	10.0
EH – 8	1.0	2.0	-	-	2.0	10.0
EH – 9	1.0	9.0	-	-	-	10.0
EH – 10	1.0	4.5	4.5	-	-	10.0
EH – 11	1.0	4.5	-	4.5	-	10.0
EH – 12	1.0	4.5	-	-	4.5	10.0

2.2.8. Evaluation of T-AM

2.2.8.1. Practical Yield and Drug Entrapment Efficiency

The procedure for determining % yield and %EE of T-AM was conducted according to the methodology outlined in section 2.2.4.1.

2.2.8.2. Surface Morphology

The procedure for investigating the surface morphology of T-AM was conducted according to the methodology outlined in section 2.2.4.2.

2.2.8.3. Particle Size Analysis

The procedure for determining the particle size of T-AM was conducted according to the methodology outlined in section 2.2.4.3.

2.2.8.4. FTIR Spectroscopic Analysis

The procedure for characterizing the drug, polymers, physical mixture, and optimized formulation (T-AM) was conducted according to the methodology outlined in section 2.2.4.4.

2.2.8.5. DSC Analysis

The procedure to analyze the thermal behaviour of drug, polymers, physical mixture, and optimized formulation (T-AM) was conducted according to the methodology outlined in section 2.2.4.5. The degree of crystallinity (X_c) of T-AM was also calculated using equation (10).[85]

$$X_c = \frac{\Delta H_m}{(1-w)\times \Delta H_m^0} \times 100 \quad ..(10)$$

Where, ΔH_m is the measured heat of fusion, ΔH^0_m is the heat of fusion of 100% crystalline sample, and 'w' is the weight fraction of TDF in the polymer matrix.

2.2.8.6. P-XRD Analysis

The procedure to characterize the solid state of the drug and obtain diffraction patterns of the drug, polymers, physical mixture, and optimized formulation (T-AM) was conducted according to the methodology outlined in section 2.2.4.6. The relative degree of crystallinity (RDC) was determined by comparing some representative peak heights in the diffraction patterns of the formulation with those of the drug, using equation (11).[86]

$$RDC = \frac{I_{sample}}{I_{reference}} \quad ..(11)$$

where, I_{sample} is the characteristic peak height of the optimized formulation and $I_{reference}$ is the characteristic peak height at the same angle for the drug with the highest intensity.

2.2.8.7. *In-vitro* Drug Release

The IVDR studies of various batches of T-AM were conducted according to the methodology outlined in section 2.2.4.7.

2.2.8.8. *Ex-vivo* Mucoadhesion Studies

The *ex-vivo* mucoadhesion studies of the optimized microspheres were conducted according to the methodology outlined in section 2.2.4.8.

2.2.9. Preparation of Pessaries

The optimized T-AM formulation was incorporated into pessaries using the conventional fusion molding technique with pessary molds, as represented in Figure 6. Drug-loaded pessaries were prepared using cocoa butter, beeswax, and Tween 60 according to the formula in Table 6.

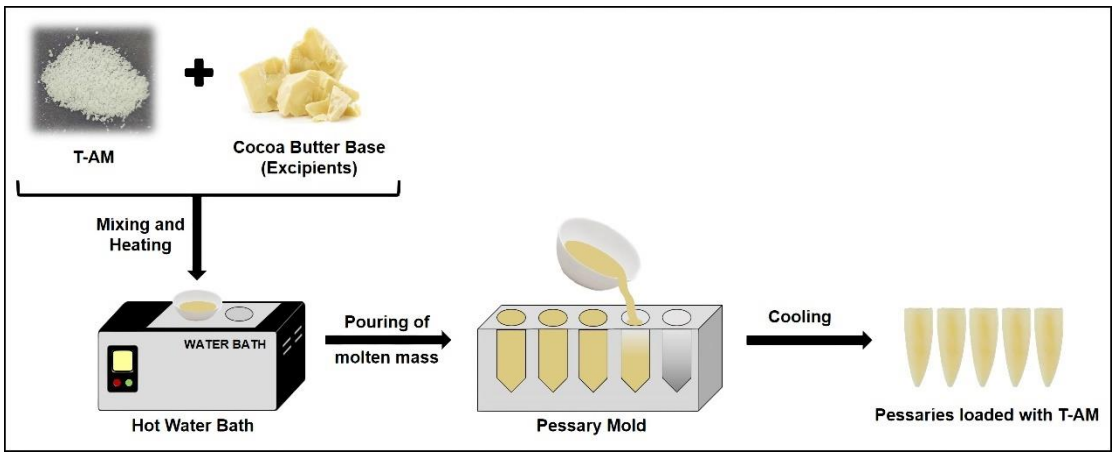

Figure 6: Preparation of T-AM loaded pessaries.

Cocoa butter served as the pessary base and was melted in a porcelain dish on a heated water bath at approximately 40°C. Beeswax, Tween 60, and T-AM were added to the melt in small portions to prevent the formation of aggregates. The base-microsphere mixture was thoroughly dispersed, and once uniformity was achieved, the molten mass was poured into previously calibrated stainless steel pessary molds (0.9–1.0 g). The pessaries were allowed to cool in a refrigerator maintained at 2-8°C until they were completely solidified.[87,88]

Table 6: Composition of pessaries.

Ingredients	Quantity (%)		
	F1	**F2**	**F3**
Drug (T-AM EH-8)	17	17	17
Cocoa Butter	65	62	60
Beeswax	10	15	17
Tween 60	8	6	6

2.2.10. Evaluation of Pessaries

2.2.10.1. Physical Characterization of Pessaries

The formulated pessaries of each batch were subjected to quality control checks following the official procedures as mentioned in the Indian pharmacopoeia 2018 (IP).

i. **Organoleptic Properties:** Ten randomly selected pessaries from each batch were visually inspected to examine the color and surface texture of the pessaries for possible cracks/pits potentially caused by air entrapment.

ii. **Weight uniformity:** Twenty pessaries from each batch were randomly selected and weighed individually in an analytical balance. The average weight and percentage deviation from the average weight were calculated to assess the weight uniformity.[89]

iii. **Melting point:** The melting points of three batches of pessaries were determined using the ascending melting point method. In this method, capillary tubes, measuring 10 cm in length were sealed at one end and were filled with the pessary formulation to a height of ~1 cm. This filling procedure was carried out while the capillaries were in an ice bath to prevent the pessary from melting during handling. Subsequently, these tubes were immersed in an electro-thermal thermometer with heat gradually increasing, and the temperature at which the pessaries melted was noted.

iv. **Content uniformity:** Ten pessaries were randomly selected from each batch and tested for content uniformity. Each pessary was allowed to melt in SVF maintained at 40°C and sonicated to extract the drug. The drug content was quantified spectrophotometrically on suitable dilution at 259 nm.[89-91]

v. ***In-vitro*** **disintegration time:** DT of six pessaries from each batch was determined using the disintegration tester apparatus in SVF (500 mL) maintained at 37 ± 0.5°C. The time point at which the fat-soluble-based pessaries melted to release the constituent T-AM was recorded as the DT.[89]

2.2.10.2. *In-vitro* Dissolution Study

The IVDR of TDF from pessaries was evaluated over a 12 h period following the methodology detailed in section 2.2.6.2.[73,92]

2.2.10.3. *In-vivo Studies*

The bio-distribution of TDF in the vagina was assessed by comparing intra-vaginal TDF concentrations, vaginal tissue concentrations, and histopathology results between the formulated pessaries for vaginal delivery and an oral marketed formulation in rabbits. Detailed methodology and results are provided in sections 2.2.11 and 3.1.11, respectively.

2.2.11. *In-vivo* Studies

Experimental Design: The *in-vivo* experimental protocol was approved by the Institutional Animal Ethical Committee (No.05/HNSK/2021) and conducted at KLE College of Pharmacy, Bengaluru. For the animal studies, a total of three treatment groups with six animals in each group were assigned. Twenty-four female adult New Zealand rabbits, aged 10-12 months and weighing 2.0±0.2kg, were selected as the *in-vivo* model for the pharmacokinetic studies and grouped as detailed in Table 7.

Table 7: Experimental design of *in-vivo* study.

Group No.	Treatment Group	No. of Animals
G–I	Normal Control (NT)	6
G–II	Treated with Marketed TDF Oral Tablet (MT)	6
G–III	Treated with TDF Vaginal Tablets (TT)	6
G–IV	Treated with TDF Vaginal Pessary (PT)	6

Pharmacokinetic Studies: To commence the studies, the rabbits were anesthetized with Isoflurane (0.1-0.2 mL/kg) before drug administration.[93] Animals in G-I were treated with an intra-vaginal dispersion of 1 mL of placebo microspheres, serving as the control. A dose of 7.5mg/kg body weight was orally administered to animals in G-

II, while those in G-III and G-IV were treated intra-vaginally with formulated DT and pessaries, respectively with the help of a catheter as demonstrated in Figure 7. Vaginal secretions/fluids, measuring 4-5 mL, were withdrawn at predetermined time intervals of 1, 2, 4, 6, 12, and 24 h using a catheter and syringe following the flush technique, in addition to the sample drawn at time zero, which served as the baseline value.[94,95] The samples were then subjected to cold centrifugation (10,000 rpm, 10 mins) and analyzed chromatographically using Liquid Chromatography-Mass Spectroscopy/Mass Spectroscopy (LC-MS/MS).[95,96,13]

Figure 7: *In-vivo* studies in rabbit model.

Analytical Method: The extraction solution was prepared by combining 200 mL of acetonitrile, 200 µL of 100% formic acid, and 40 µL of Verapamil used as an internal standard (IS) (250 µg/mL), followed by vortexing for 2 mins. The standard stock solution was prepared with 1 mg of TDF standard and 1 mL of methanol to achieve a concentration of 1 mg/mL. The working solutions for the calibration curve were in the concentration range of 12.5–20,000 ng/mL. In the processing method, 22.5 µL of VF was taken and placed in a centrifuge tube. Subsequently, 2.5 µL of calibrant or QC working solutions and 1 mL of internal standard extraction solutions were added to the labeled tubes. After vigorous vortexing for 10 mins at 1200 rpm, the samples were centrifuged for 15 mins at 15,000 rpm. Finally, 100 µL of the resulting supernatant was collected and subjected to analysis using LC-MS/MS.

The pharmacokinetic parameters, including the maximum VF concentration (C_{max}) and the time to reach the maximum VF concentration (T_{max}), as well as the area under the curve (AUC) of TDF concentration in the VF as a function of time, were computed for all the groups from the plot of VF concentration versus time profiles. These parameters were calculated using the pkSolver software.

Tissue Concentration Studies: Following the 24 h study period, the animals were euthanized using an overdose of Isoflurane, and vaginal tissue samples were collected from each rabbit. The cranial and caudal parts of the vagina were separated and placed into cryovials. The tissues were rapidly frozen and stored at -80°C until further analysis for tissue concentration studies, which were conducted following the procedure reported by Clark et al., 2012.[95]

Histopathology: The tissues intended for histopathology studies were preserved in formalin. They were then stained with hematoxylin and eosin and examined

microscopically to evaluate the overall morphological state of the cervicovaginal mucosa. A scoring system, as outlined by Clark et al., 2012, was utilized to evaluate cervicovaginal tissue damage.[77,95]

DATA ANALYSIS PLAN

3. DATA ANALYSIS PLAN

3.1. Statistical Analysis for Evaluation of Formulations

All formulation studies were performed in triplicate, and the mean values were presented along with their standard deviations (mean ± SD). Microsoft Excel® was used for calibration and dissolution studies, while FTIR, DSC, and P-XRD graphs were analyzed with Origin85® software.

3.2. Statistical Analysis for Evaluation of *In-vivo* Studies

Pharmacokinetic parameters were estimated by applying the pkSolver® software. The results from *in-vivo* studies were statistically compared to determine the level of significance using GraphPad Prism 5.0® (GraphPad Inc., CA, USA), and the mean values were reported with their standard deviations. A paired t-test (two-tailed) was used to compare different groups, with a P-value of <0.05 considered statistically significant.

RESULTS

4. RESULTS

4.1. Authentication of Drug

4.1.1. Melting Point

The DSC curve of TDF is represented in Figure 8.

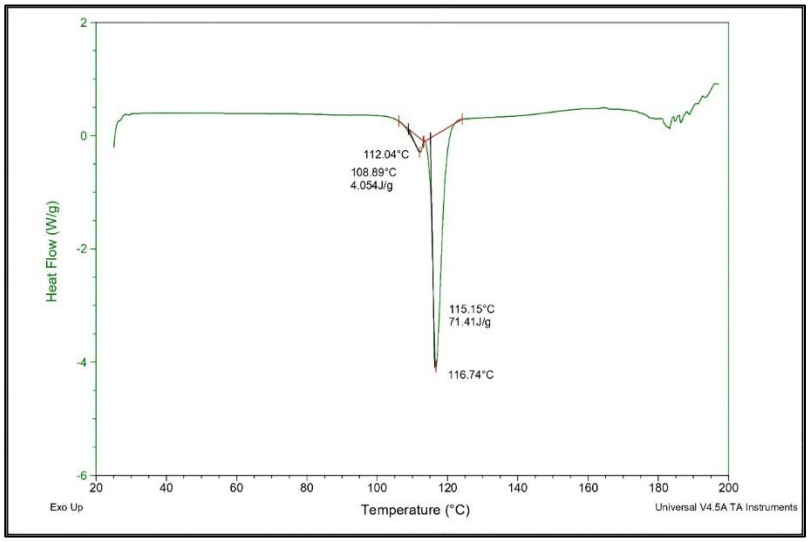

Figure 8: DSC curve of TDF.

4.1.2. Mass Spectroscopy

The LC-MS spectrum of TDF in positive mode is represented in Figure 9.

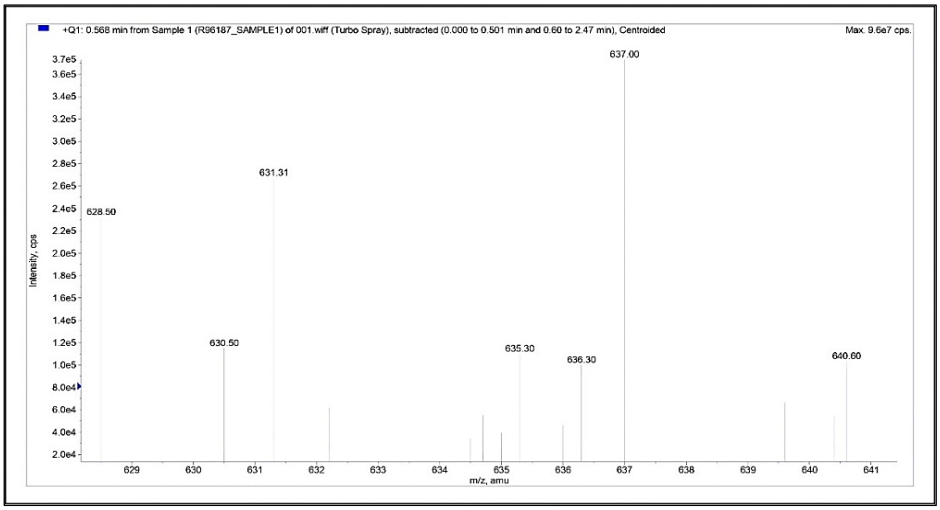

Figure 9: LC-MS spectrum of TDF in positive mode.

4.1.3. FTIR Spectroscopy

The FTIR spectrum of TDF is presented in Figure 10 and its corresponding interpretation for the identification of functional groups and bonds is given in Table 8.[43,44]

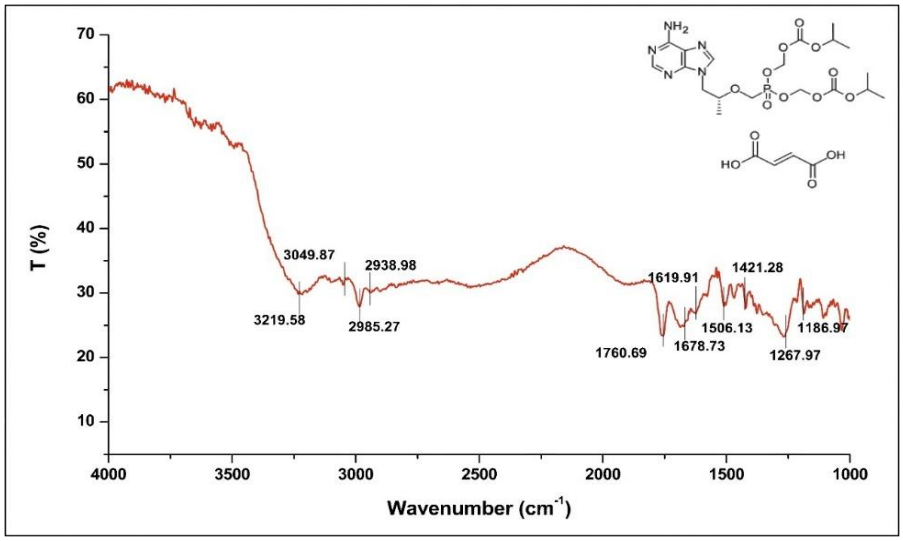

Figure 10: FTIR spectrum of TDF.

Table 8: Interpretation of FTIR spectrum of TDF.

Wavenumber (cm^{-1})	Functional Group
3219.58	–N-H stretching/ –OH stretching
3049.87	Aromatic –CH stretching
2985.27	Aliphatic –CH stretching
2938.98	Aliphatic –CH stretching
1760.69	–C=O stretching
1678.73	–C=O stretching
1619.91	–C=C– stretching
1506.13	$–NH_2$ scissoring band
1421.28	Aromatic –C-C stretching

1267.97	–P=O stretching
1186.97	Aliphatic –CN stretching

4.1.4. UV-VIS Spectrophotometry

The absorbance maxima of TDF is represented in Figure 11. The calibration curve of TDF in SVF is tabulated in Table 9 and depicted in Figure 12.

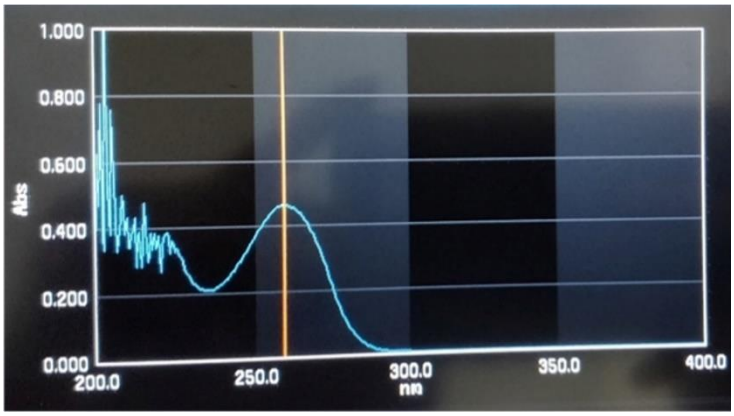

Figure 11: UV spectrum of TDF.

Table 9: Calibration of TDF in SVF.

Concentration (µg/mL)	Absorbance at 259 nm
0	0
5	0.127 ± 0.007
10	0.236 ± 0.011
15	0.348 ± 0.004
20	0.468 ± 0.006
25	0.574 ± 0.011
30	0.696 ± 0.011
35	0.827 ± 0.014
40	0.924 ± 0.012

*Data shows mean ± SD (n=3)

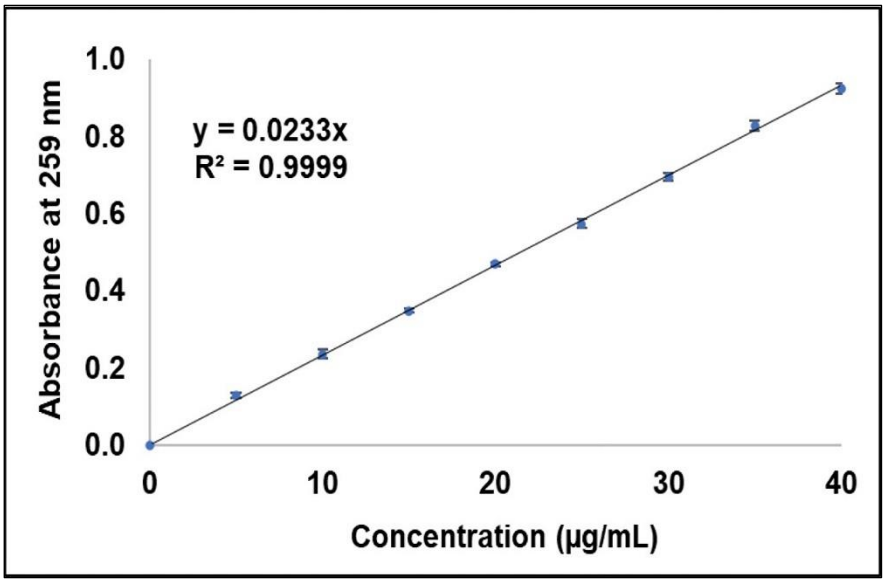

Figure 12: Calibration curve of TDF in SVF.

4.2. Pre-formulation Studies

4.2.1. Solubility Studies

The solubility profile of TDF in various mediums of varying pH is represented in Figure 13.

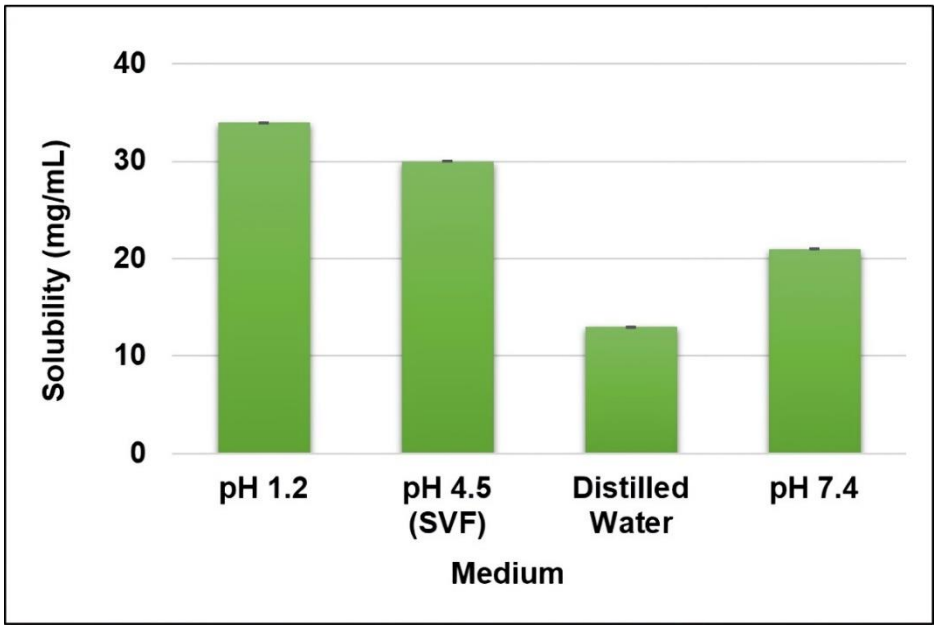

Figure 13: Solubility profile of TDF in various mediums of varying pH.

4.2.2. Drug-Excipient Compatibility Studies

The FTIR spectra of TDF along with various polymers is represented in Figure 14.

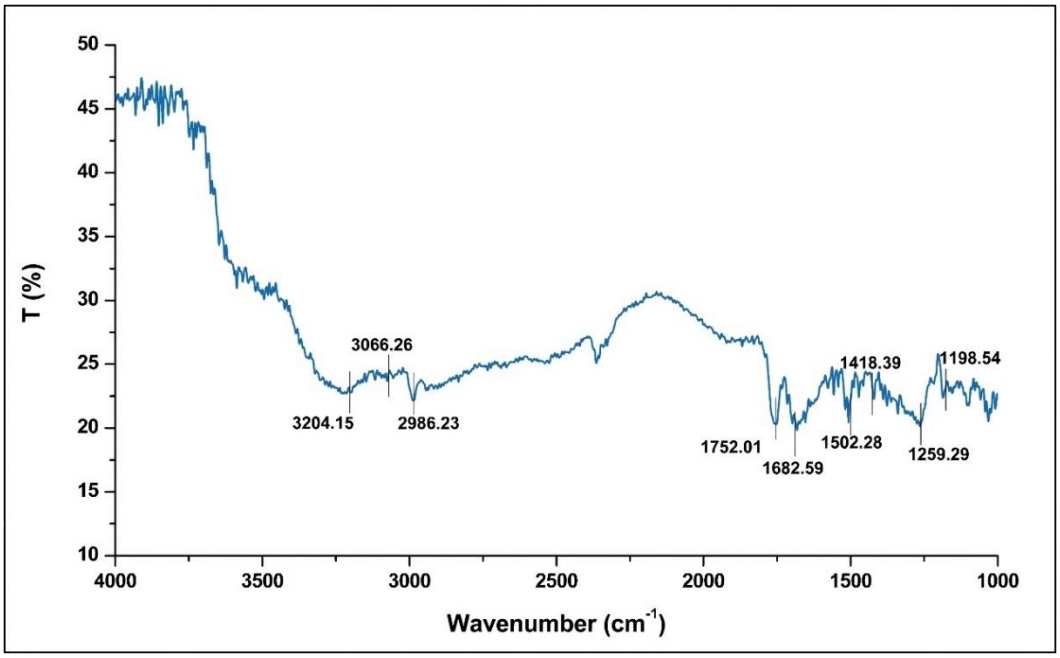

(A)

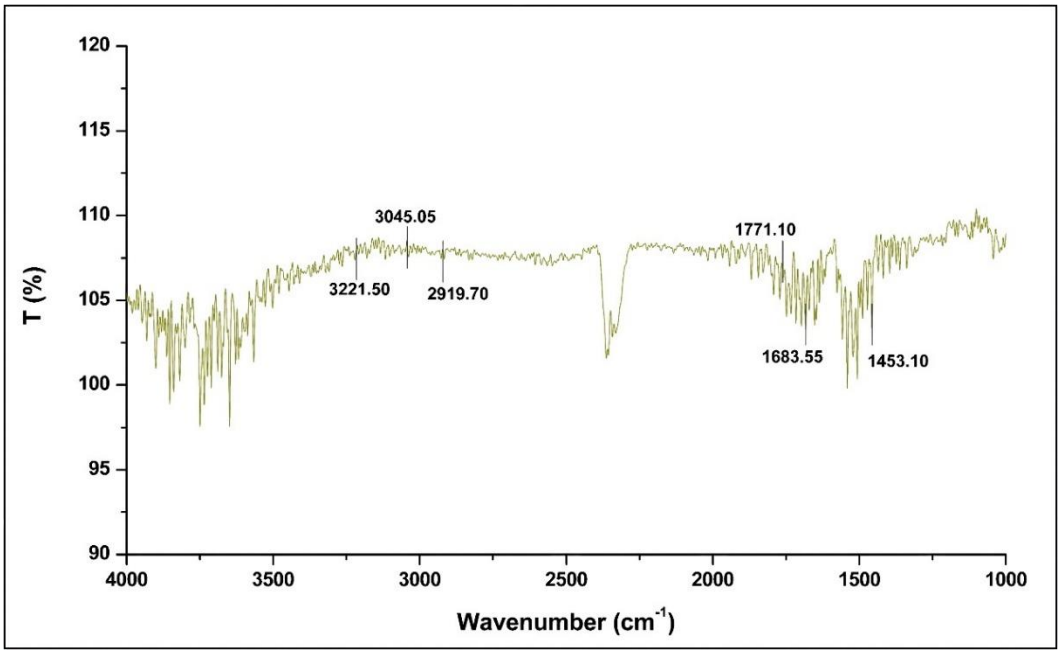

(B)

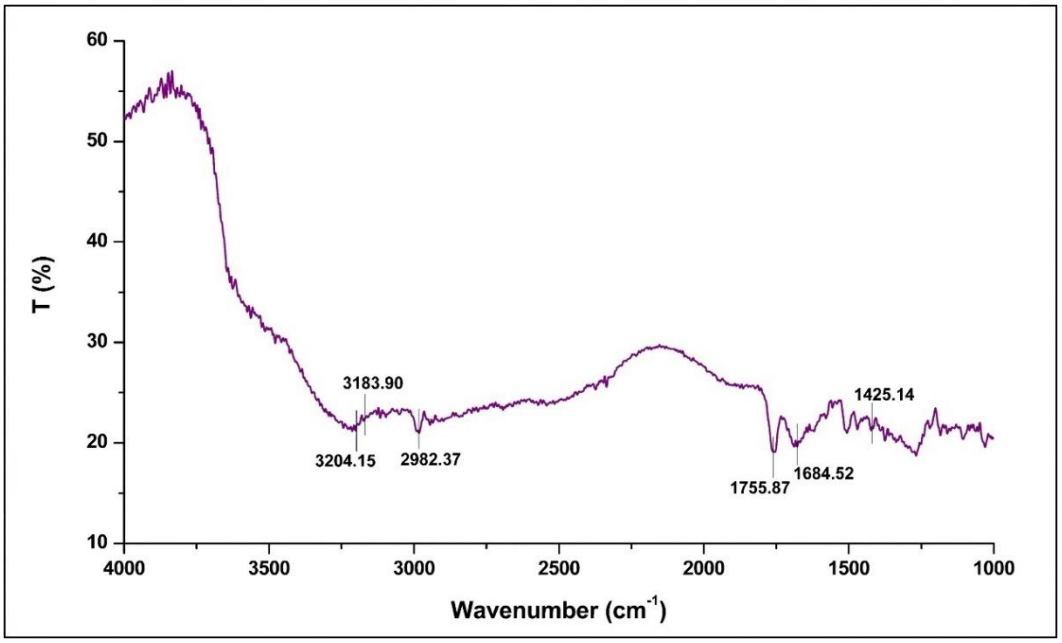
T (%)
Wavenumber (cm-1)
3183.90
3204.15
2982.37
1755.87
1684.52
1425.14

(C)

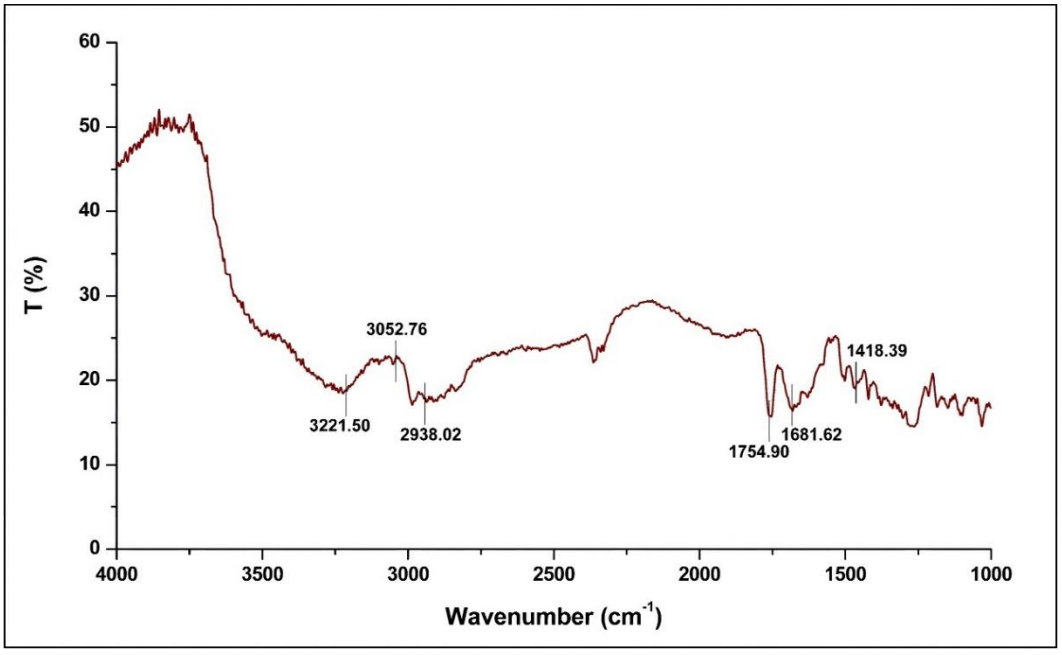
T (%)
Wavenumber (cm-1)
3052.76
3221.50
2938.02
1754.90
1681.62
1418.39

(D)

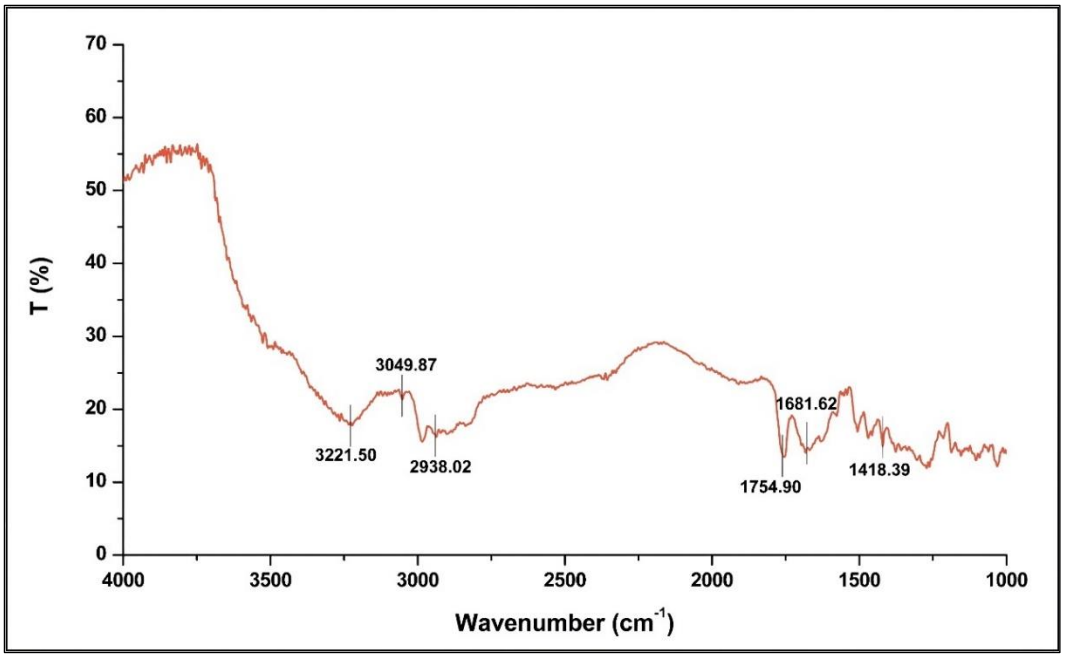

(E)

Figure 14: FTIR spectra of TDF along with (A) chitosan, (B) S-Alg, (C) S-CMC, (D) HPMC K4M and (E) HPMC K100M.

4.3. Preparation of T-CM

The formulated T-CM is represented in Figure 15.

Figure 15: T-CM.

4.4. Evaluation of T-CM

4.4.1. Practical Yield and Drug Entrapment Efficiency

The %yield of T-CM increased from 30.50 ± 5.32% to 61.23 ± 2.61% for EC-1 to EC-4, and from 48.75 ± 0.50% to 90.80 ± 2.31% for ECH-1 to ECH-4, with an increase in chitosan concentration as represented in Figure 16.

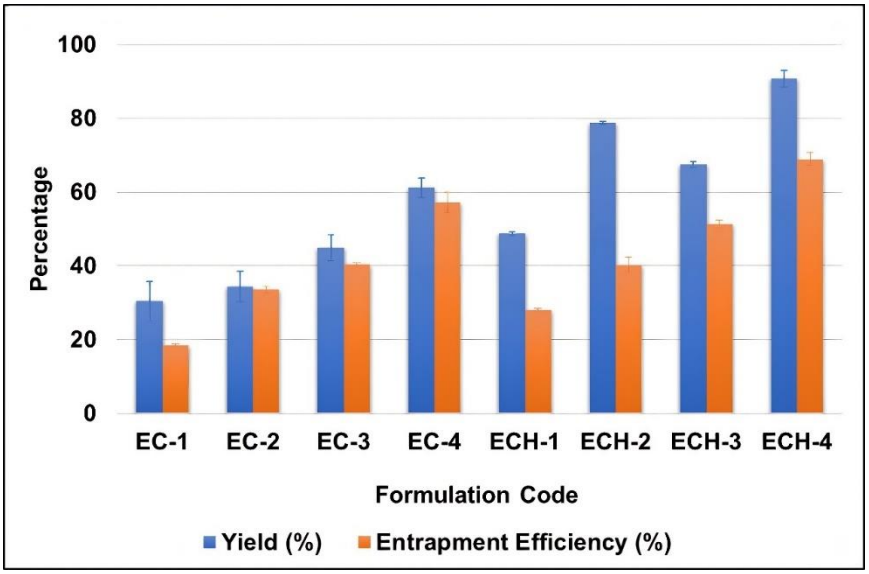

Figure 16: The %yield and %EE of T-CM.

The %EE for EC-1 to EC-4, produced with 5% TPP, ranged from 18.55 ± 0.41% to 57.24 ± 2.73%. When the TPP concentration was increased to 10% for ECH-1 to ECH-4, there was an increase in %EE ranging from 27.97 ± 0.60% to 68.93 ± 1.76%, as shown in Figure 16

4.4.2. Surface Morphology

The photomicrograph of ECH-4 (T-CM) under a magnification of 20k× is represented in Figure 17.

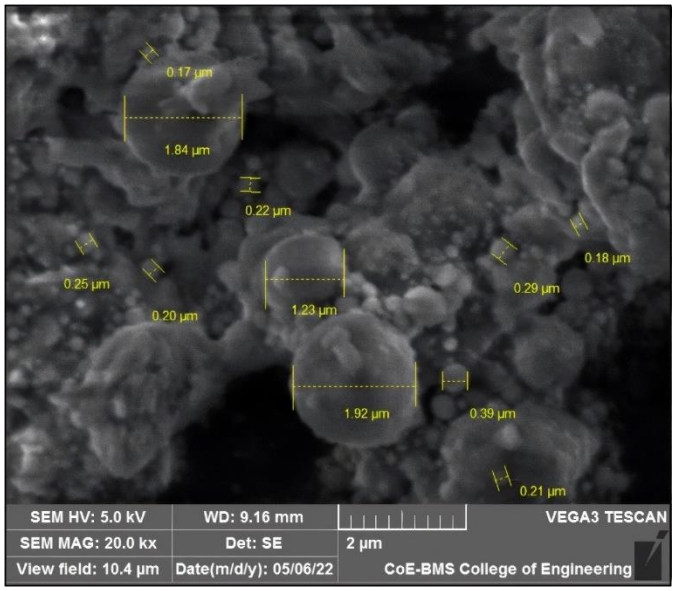

Figure 17: Photomicrographs of T-CM of formulation ECH-4 on a scanning electron microscope under a magnification of 20 k×.

4.4.3. Particle Size Analysis

The particle size-volume distribution curve of ECH-4 (Figure 18) indicates a size range from 0.52 ± 0.00 µm to 284.79 ± 21.41µm. The volume-surface-mean diameter of ECH-4 was calculated to be 204.42 ± 0.13 µm. Approximately 50% of the microparticles in ECH-4 were around 58.014 ± 1.037 µm in size, while 90% were ~193.42 ± 3.70 µm.

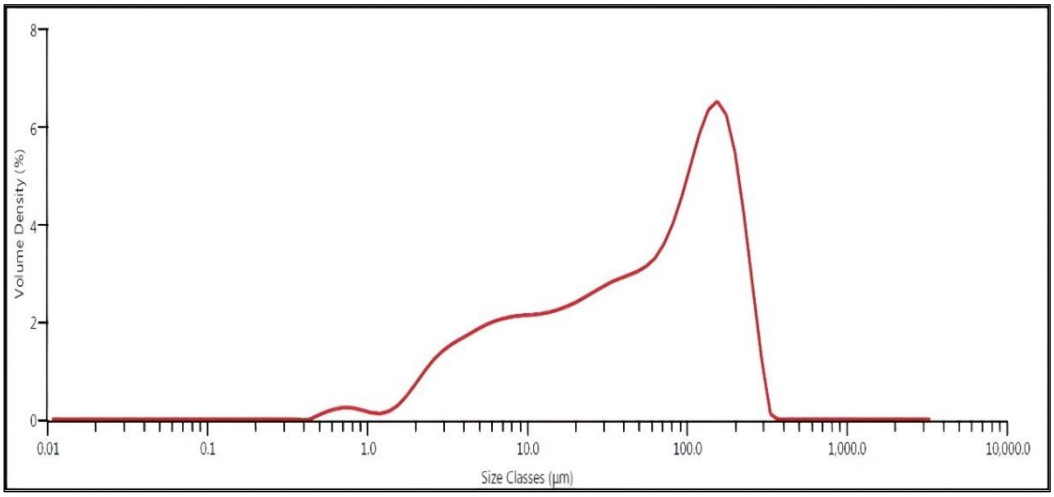

Figure 18: Particle size distribution of T-CM formulation ECH-4.

4.4.4. FTIR Spectroscopic Analysis

An overlay of the FTIR spectra of TDF, chitosan, physical mixture, and the kneaded product (ECH-4) are displayed in Figure 19 and Table 10.

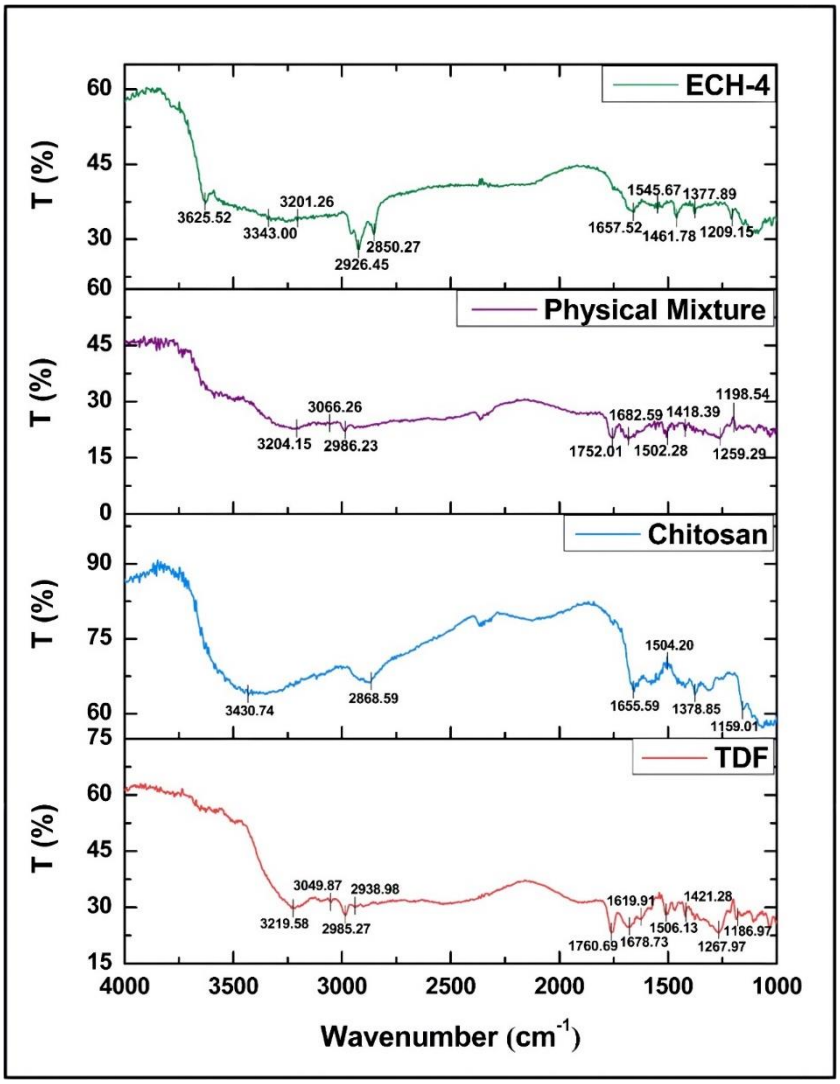

Figure 19: FTIR spectra of TDF, chitosan, physical mixture, and kneaded product (ECH-4).

Table 10: Peaks observed in the FTIR spectra of (a) TDF; (b) chitosan; (c) physical mixture; and (d) kneaded product (ECH-4).

Sl. No.	Wavenumber (cm^{-1})			
	TDF	**Chitosan**	**Physical Mixture**	**Microparticle (ECH-4)**
1	3219.58	3430.74	3204.15	3625.52
2	3049.84	2868.59	3066.26	3343
3	2985.27	1655.59	2986.23	3201.26
4	2938.98	1504.2	1752.01	2926.45
5	1760.69	1378.85	1682.59	2850.27
6	1678.73	1159.01	1502.28	1657.52
7	1619.91	-	1418.39	1545.67
8	1506.13	-	1259.29	1377.89
9	1421.28	-	1198.54	1461.78
10	1267.97	-	-	1209.15
11	1186.97	-	-	-

4.4.5. DSC Analysis

The DSC thermogram of TDF gave a sharp exothermic peak at 115.4°C; the peak onset at 112.04°C, corresponding to the drug's melting point as displayed in Figure 20.

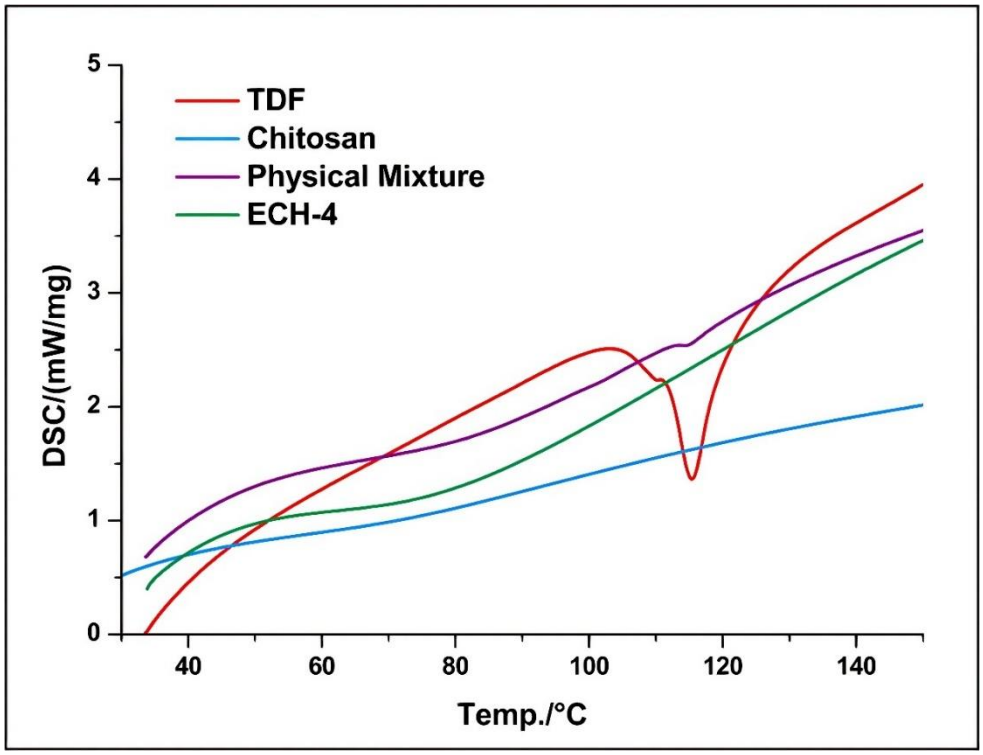

Figure 20: DSC thermogram of TDF, chitosan, physical mixture, and kneaded product (ECH-4).

4.4.6. P-XRD Analysis

An overlay of the P-XRD pattern of TDF, chitosan, physical mixture, and the kneaded product (ECH-4) is displayed in Figure 21, where the crystalline nature of TDF was clearly demonstrated.

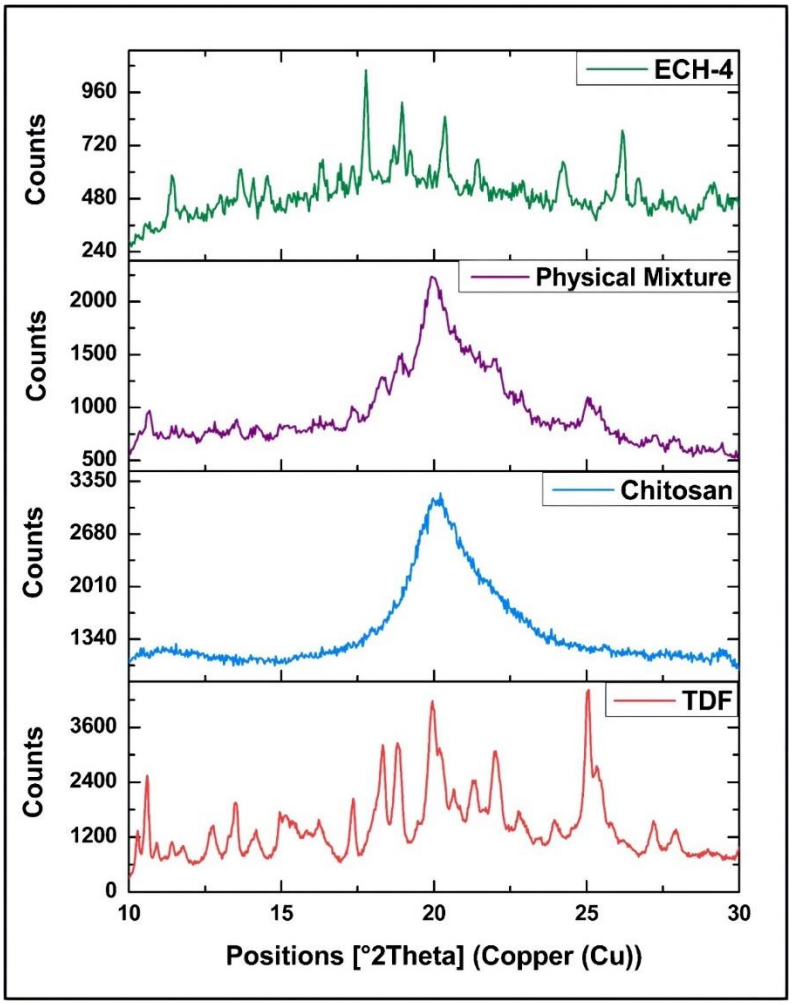

Figure 21: P-XRD diffractogram of TDF, chitosan, physical mixture, and kneaded product (ECH-4).

4.4.7. *In-vitro* Drug Release

The comparative IVDR dissolution profiles of T-CM are represented in Figure 22. Formulations EC-1 to EC-4 exhibited nearly 100% rapid release of TDF by the end of 6 hours. In contrast, formulations ECH-1 to ECH-4 released 99.07 ± 0.41%, 99.23 ± 0.59%, 98.96 ± 1.18%, and 88.05 ± 0.38% of TDF by the end of 6, 8, 12, and 24 h, respectively.

The results of the curve fitting into different mathematical models are summarized in Table 11.

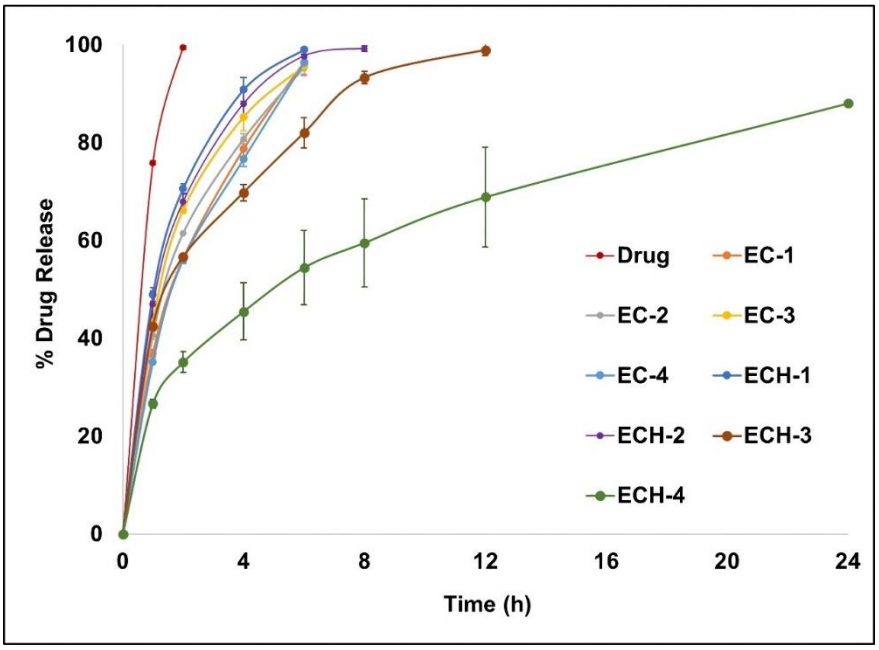

Figure 22: Cumulative IVDR profile of T-CM in SVF for a period of 24 h.

Table 11: Results of curve fitting of the dissolution data for the microparticles.

FC	Zero Order Kinetic Model		First Order Kinetic Model		Higuchi Release Model		Korsmeyer-Peppas Release Model		
	R^2	K	R^2	K	R^2	K	R^2	K	n
ECH-2	0.85± 0.03	49.83 ± 1.09	0.79 ± 0.03	0.29 ± 0.01	0.93 ± 0.02	23.96 ± 2.40	-	-	-
ECH-3	0.90 ± 0.01	46.04 ± 1.91	0.83 ± 0.01	0.32 ± 0.01	0.97 ± 0.007	22.23 ± 2.81	1.00 ± 0.00	0.37 ± 0.02	0.41 ± 0.07
ECH-4	0.93 ± 0.05	27.78 ± 2.04	0.86 ± 0.07	0.53 ± 0.02	0.98 ± 0.01	10.62 ± 3.58	0.99 ± 0.007	0.57 ± 0.008	0.38 ± 0.07

4.4.8. *Ex-vivo* Mucoadhesion Study

Figure 23a shows representative images of the bio-adhesion of T-CM (ECH-4) on the vaginal mucosa, while Figure 23b demonstrates the correlation of *ex-vivo* bio-adhesion of T-CM (ECH-4) on vaginal mucosa with its IVDR.

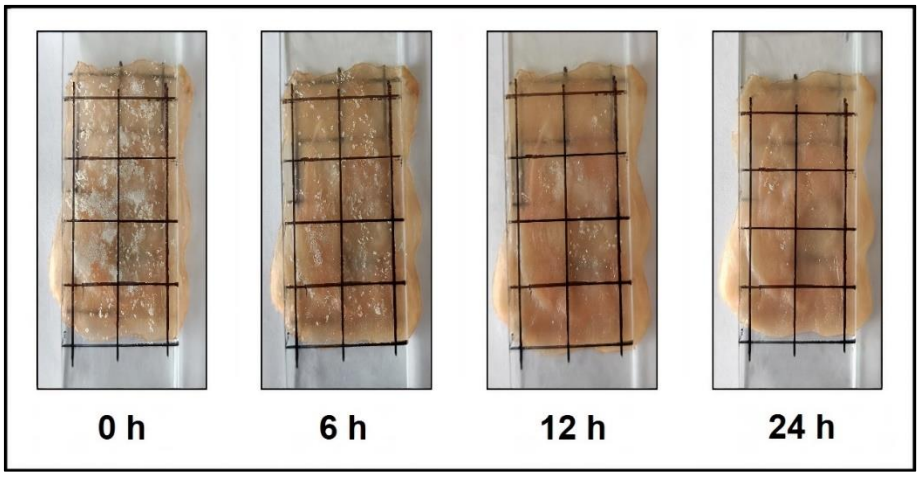

Figure 23a: Representative images of bio-adhesion of T-CM (ECH-4) on rabbit vaginal mucosa.

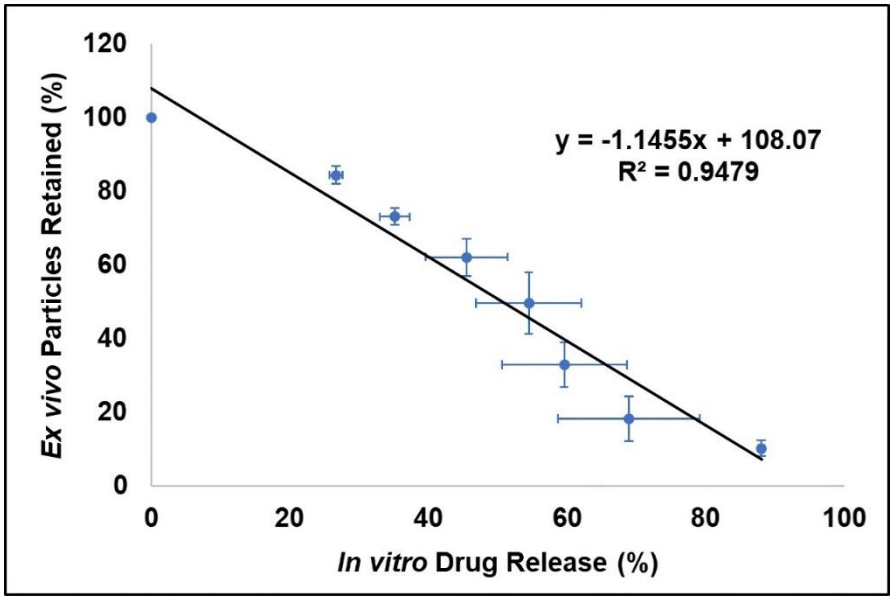

Figure 23b. Correlation between the percentage of microparticles retained on the vaginal mucosa (*ex-vivo*) and the IVDR from T-CM (ECH-4).

4.5. Preparation of Vaginal Tablets

Figure 24 represents the images of the formulated DT-T-CM composed of ECH-4 (T-CM) for intra-vaginal delivery.

Figure 24: DT of T-CM for intra-vaginal delivery.

4.6. Evaluation of Vaginal Tablets

4.6.1. Physical Characterization of Vaginal Tablets

Table 12 summarizes the results of various quality control tests conducted on batches of tablets labeled F1 to F4, including weight variation, thickness, diameter, hardness, friability, content uniformity, and *in-vitro* disintegration.

Table 12: Physical characterization of DT.

Parameters	F1	F2	F3	F4
Weight Uniformity (mg) (n=20)	298.82 ± 3.17	301.80 ± 1.03	301.67 ± 0.82	100.62 ± 0.11
Thickness (mm) (n=10)	4.30 ± 0.01	4.29 ± 0.01	4.31 ± 0.01	3.01 ± 0.01
Diameter (mm) (n=10)	8.00 ± 0.00	8.01 ± 0.01	8.01 ± 0.01	6.01 ± 0.01

Hardness (kg/cm^2) (n=10)	3.19 ± 0.41	3.08 ± 0.41	3.50 ± 0.16	3.05 ± 0.28
Friability (%) (n=22)	0.43 ± 0.17	0.90 ± 0.04	0.37 ± 0.08	0.32 ± 0.04
Content Uniformity (%) (n=10)	90.75 ± 3.37	88.43 ± 3.03	95.06 ± 3.97	99.08 ± 1.36
Disintegration Time (s) (n=6)	34.33 ± 3.14	27.33 ± 1.51	31.33 ± 4.63	60.83 ± 4.17

4.6.2. *In-vitro* Dissolution Study

Comparing the IVDR profiles of TDF microparticles (ECH-4), DT-T-CM (F3), and DT (F4) as illustrated in Figure 25, it was observed that both released about ~70% of the drug by the end of 12 h.

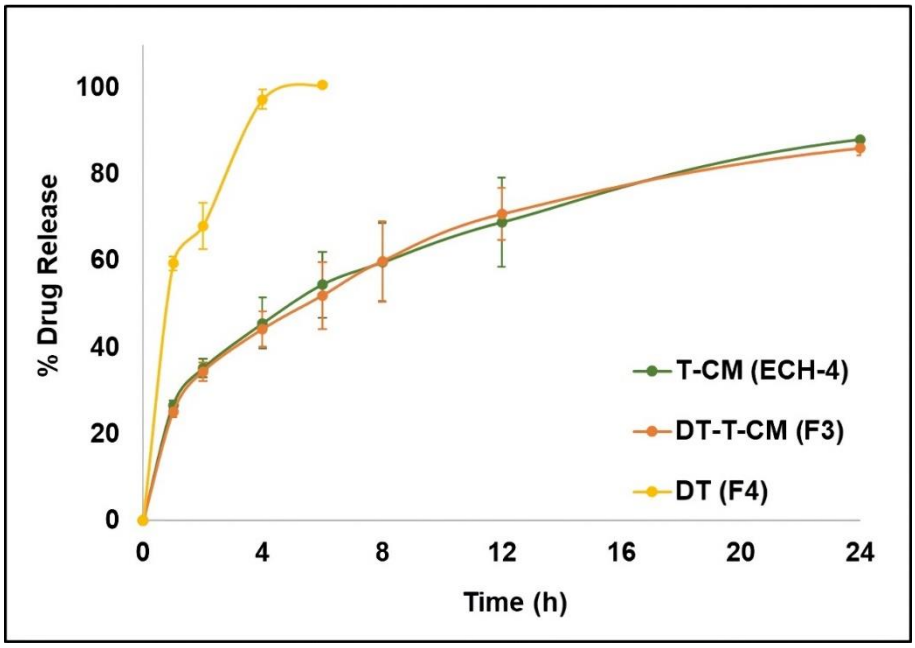

Figure 25: Comparative IVDR profile of T-CM (ECH-4), DT-T-CM (F3), and DT (F4).

4.7. Preparation of T-AM

The formulated T-AM is represented in Figure 26.

Figure 26: T-AM.

4.8. Evaluation of T-AM

4.8.1. Practical Yield and Drug Entrapment Efficiency

The %yield of T-AM showed a significant increase from 53.44 ± 5.32% to 90.95 ± 3.06% as the amount of polymer increased from EH-1 to EH-12, as illustrated in Figure 27. Among the formulations tested, EH-8 exhibited the highest yield (97.47 ± 1.9%).

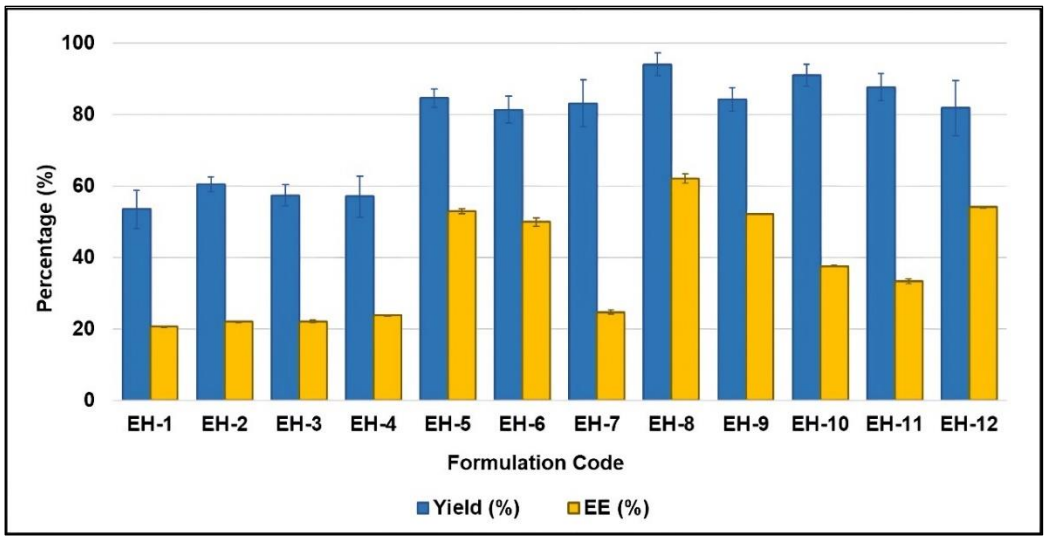

Figure 27: The % yield and %EE of T-AM.

As the drug-to-polymer ratio increased from 1:2 to 1:9, a considerable increase in the encapsulation efficiency, ranging from 20.61 ± 0.16% to 62.09 ± 1.34% was observed as represented in Figure 27.

4.8.2. Surface Morphology

The photomicrograph of ECH-4 (T-CM) under a magnification of 20k× and 40k× is represented in Figure 28.

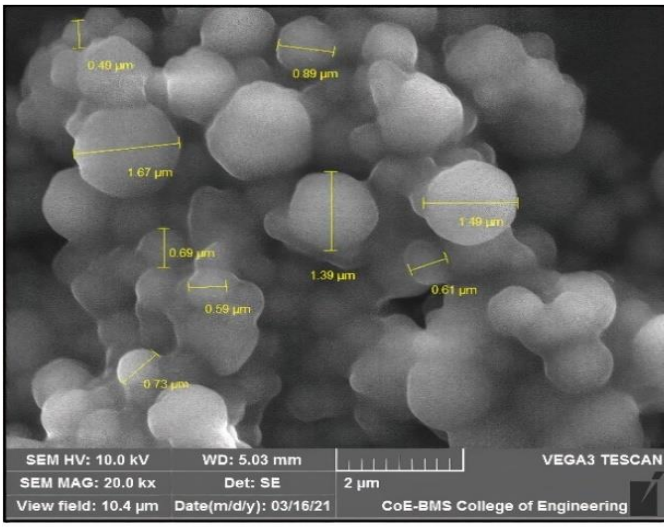

A

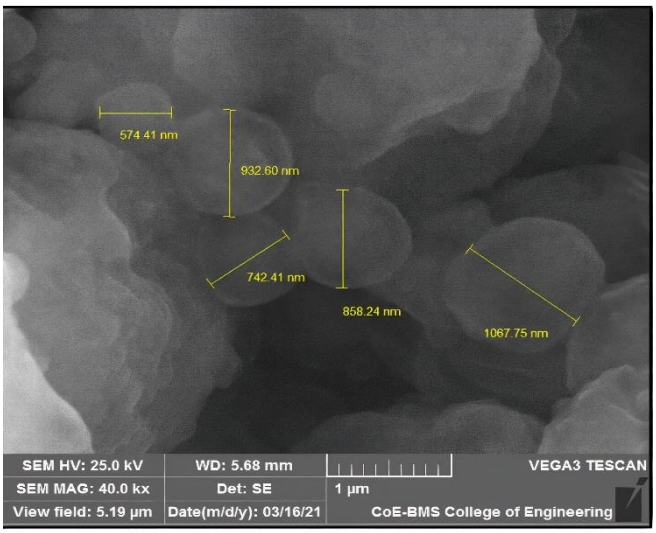

B

Figure 28: Photomicrographs of T-AM of formulation EH-8 on a SEM under a magnification of (A) 20 k× and (B) 40 k×, respectively.

4.8.3. Particle Size Analysis

The surface-mean-diameter and volume-mean-diameter of formulation EH-8 were found to be 11.06 ± 0.18 µm and 33.23 ± 0.46 µm, respectively (Figure 29). About 50% of the microparticles in EH-8 were 28.94 ± 0.73 µm in size whereas 90% of the particles were 68.69 ± 0.90 µm in size.

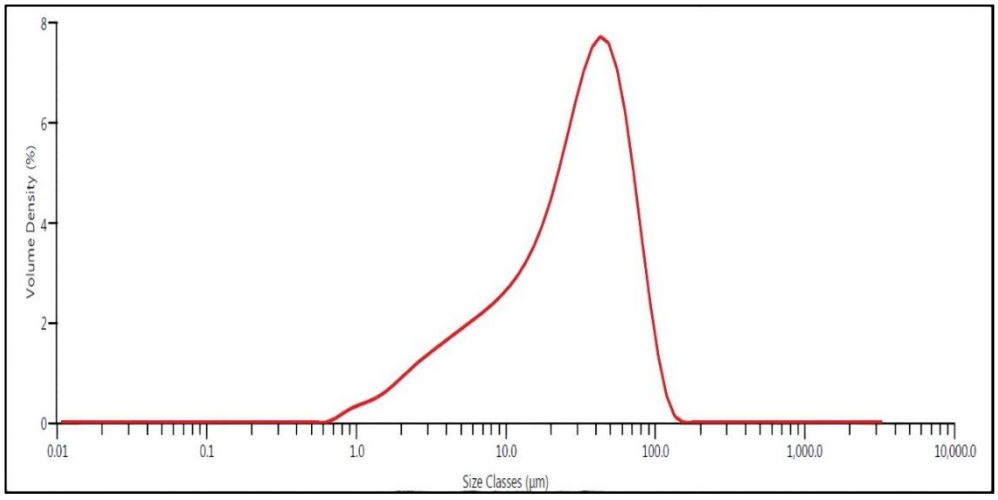

Figure 29: Particle size distribution curve of the optimized formulation (EH-8).

4.8.4. FTIR Spectroscopic Analysis

An overlay of the FTIR spectra of TDF, polymers, physical mixture, and the kneaded product (EH-8) is represented in Figure 30.

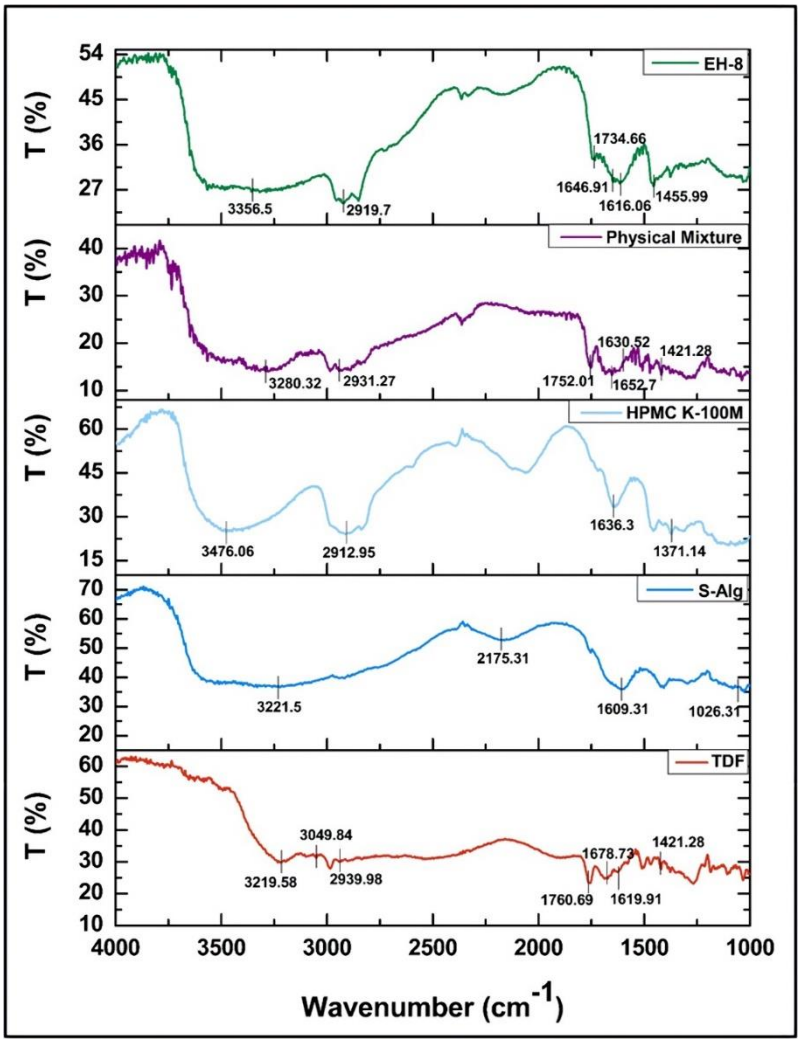

Figure 30: FTIR spectra of TDF, S-Alg, HPMC K100M, physical mixture, and optimized formulation (EH-8).

4.8.5. DSC Analysis

The DSC thermogram (Figure 31) displayed a sharp endothermic peak of TDF at 115.4°C with the peak onset at 112.04°C indicating the crystallinity of TDF.

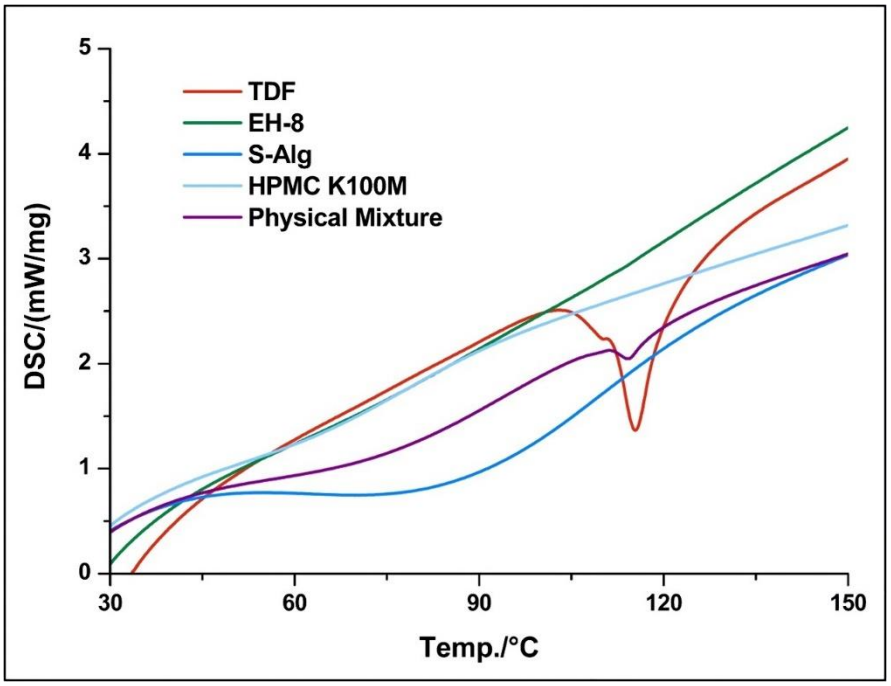

Figure 31: DSC thermograms of TDF, S-Alg, HPMC K100M, physical mixture, and optimized formulation (EH-8).

4.8.6. P-XRD Analysis

The P-XRD patterns of TDF, polymers, physical mixture, and formulation EH-8 are displayed in Figure 32 and its corresponding interpretation of 2θ values and peak intensities is given in Table 13.

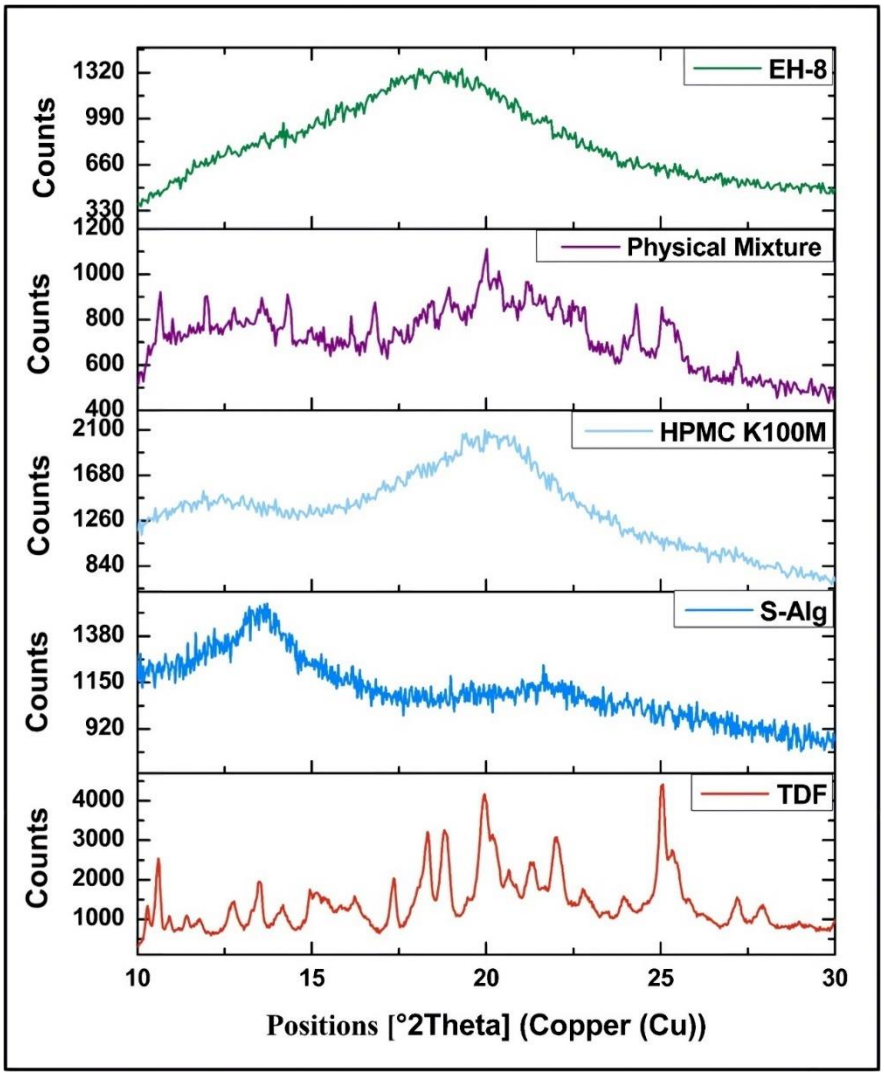

Figure 32: P-XRD diffractogram of TDF, S-Alg, HPMC K100M, physical mixture, and optimized formulation (EH-8).

Table 13: Interpretation of P-XRD pattern of TDF, physical mixture of EH-8, and formulation EH-8.

Sl. No.	Angle (2θ ± 2)	Peak Intensity (Counts)		
		Drug (TDF)	Physical Mixture of Formulation EH-8	Formulation EH-8
1	10.29	1339	651	312
2	10.59	2540	842	304

3	13.48	1954	1161	487
4	14.17	1361	1000	535
5	18.32	3212	1049	657
6	18.80	3258	967	680
7	19.95	4172	1195	576
8	21.36	2438	1114	574
9	22.02	3077	1075	579
10	25.07	4419	1086	503

4.8.7. *In-vitro* Drug Release

The comparative IVDR dissolution profiles of T-AM over a period of 12 h is represented in Figure 33 and the results of curve fitting into different mathematical models are summarized in Table 14.

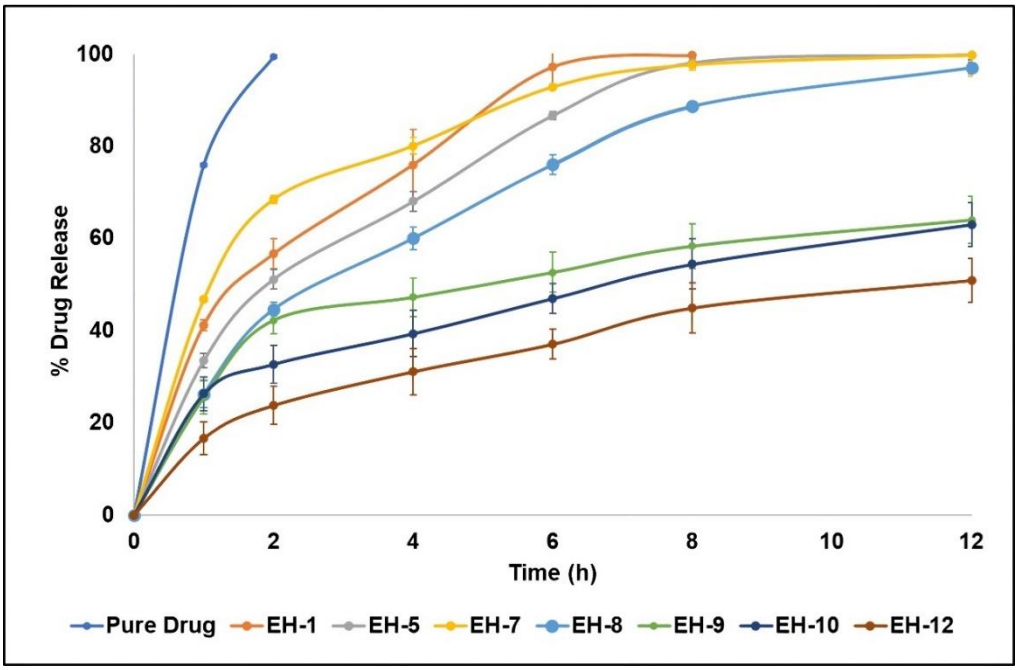

Figure 33: Cumulative IVDR profile of T-AM in SVF for 12 h.

Table 14: Results of curve-fitting of the dissolution data of T-AM.

FC	Zero-Order Kinetic Model		First Order Kinetic Model		Higuchi Release Model		Korsmeyer-Peppas Release Model		
	R^2	K	R^2	K	R^2	K	R^2	K	n
EH-1	0.936 ± 0.007	38.005 ± 0.962	0.892 ± 0.017	0.380 ± 0.007	0.974 ± 0.001	8.669 ± 1.145	1.000 ± 0.000	0.3748 ± 0.000	0.3114 ± 0.000
EH-5	0.843 ± 0.043	39.559 ± 3.437	0.769 ± 0.054	0.389 ± 0.025	0.933 ± 0.021	10.216 ± 3.978	1.000 ± 0.000	0.479 ± 0.015	0.610 ± 0.066
EH-7	0.774 ± 0.017	56.675 ± 1.897	0.701 ± 0.021	0.248 ± 0.013	0.892 ± 0.012	23.586 ± 19.799	-	-	-
EH-8	0.905 ± 0.031	30.813 ± 1.728	0.794 ± 0.032	0.479 ± 0.010	0.974 ± 0.014	2.731 ± 0.626	0.976 ± 0.021	0.567 ± 0.004	0.631 ± 0.069
EH-9	0.836 ± 0.078	31.562 ± 0.470	0.728 ± 0.099	0.498 ± 0.012	0.918 ± 0.051	16.896 ± 0.789	0.911 ± 0.040	0.552 ± 0.029	0.3664 ± 0.054
EH-10	0.967 ± 0.038	25.521 ± 4.442	0.923 ± 0.042	0.563 ± 0.056	0.984 ± 0.009	10.855 ± 6.106	0.981 ± 0.015	0.593 ± 0.054	0.3496 ± 0.050

4.8.8. *Ex-vivo* Mucoadhesion Studies

Formulation EH-8 demonstrated an excellent bio-adhesive ability over a 12 h period, where, approximately 7.17 ± 2.02% of the microparticles remained adhered to the mucosa, while 92.83 ± 2.02% of the microparticles were washed off by the SVF. Approximately 50% of the particles were washed off from the mucosa by the end of 4 h, corresponding to a 60.04 ± 1.72% IVDR.

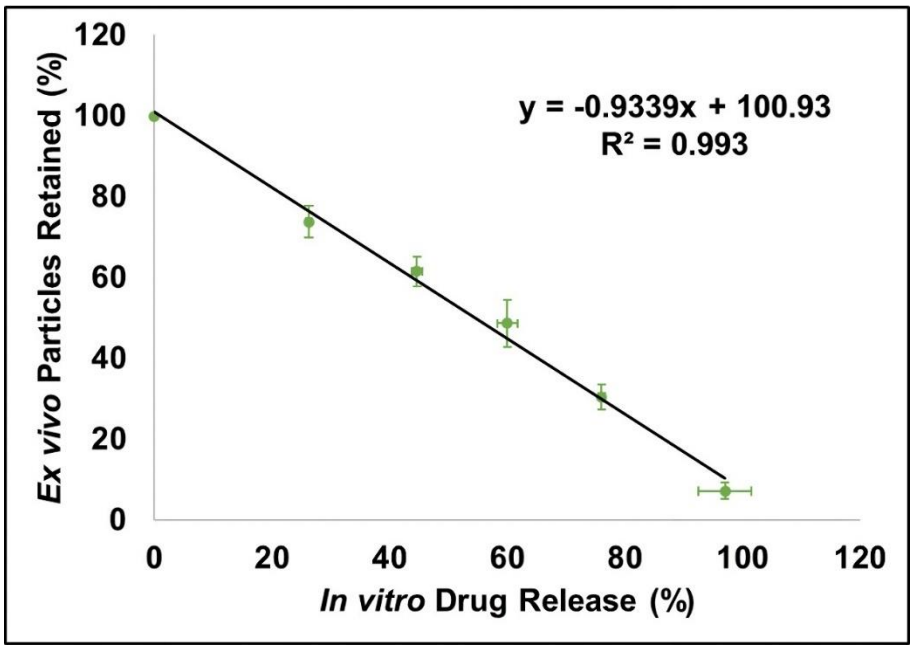

Figure 34: Correlation between *ex-vivo* particles retained (%) on the mucosa and the IVDR (%) from T-AM (EH-8).

On comparing the *ex-vivo* adhesion with the IVDR, an excellent correlation was observed between the percentage of microparticles retained on the mucosa and the IVDR, with a correlation coefficient value of 0.996 as indicated in Figure 34.

4.9. Preparation of Pessaries

Figure 35 represents the images of the formulated pessaries composed of EH-8 (T-AM) for intra-vaginal delivery. The prepared pessaries were in the shape of a bullet having a smooth surface.

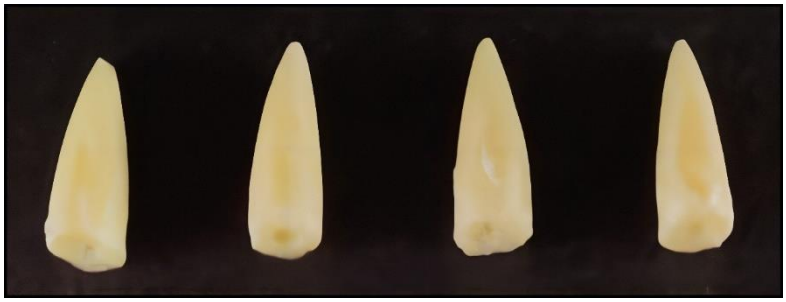

Figure 35: Pessaries of EH-8 for intra-vaginal delivery.

4.10. Evaluation of Pessaries

4.10.1. Physical Characterization of Pessaries

Table 15 enlists the results of the physical evaluation of the pessaries of batches F1 to F3.

Table 15: Physical characterization of pessaries.

Parameters	F1	F2	F3
Weight Uniformity (mg) (n=20)	901.27 ± 0.26	901.50 ± 0.10	901.37 ± 0.10
Melting Point (°C) (n=3)	30.33 ± 2.52	35.33 ± 0.58	42.33 ± 2.08
Content Uniformity (%) (n=10)	97.42 ± 0.86	99.09 ± 1.42	96.88 ± 1.30
Disintegration Time (s) (n=6)	2.33 ± 0.31	3.63 ± 0.15	4.00 ± 0.20

4.10.2. *In-vitro* Dissolution Study

Comparing the IVDR profiles (Figure 36) of T-AM with pessaries, both formulations released a similar amount of TDF within 12 h.

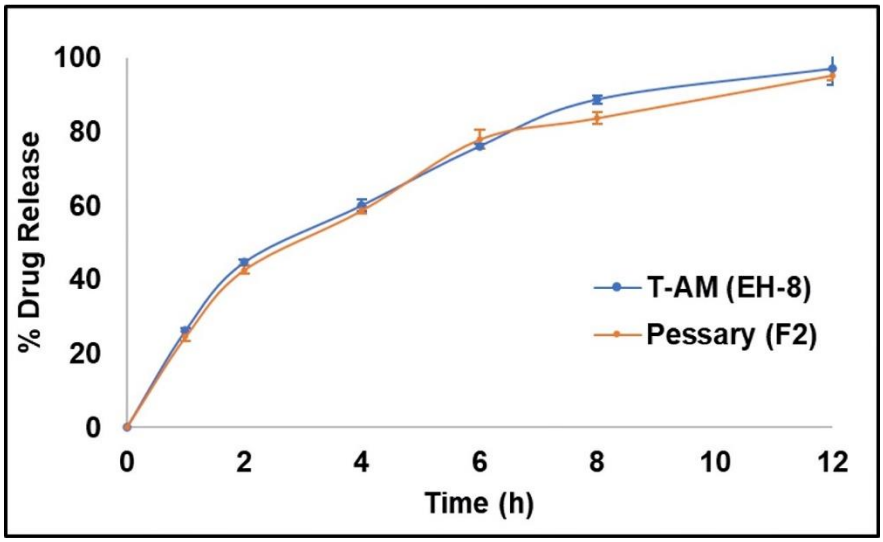

Figure 36: Comparative dissolution profile of T-AM and pessaries.

4.11. *In-vivo* Studies

Pharmacokinetic Studies: Comparative pharmacokinetic parameters of the three treatment groups are tabulated in Table 16. Figure 37 demonstrates that the vaginal administration of pessaries resulted in a higher concentration of TDF in the vagina compared to oral dosing of the marketed formulation and intra-vaginal dosing of the formulated DT.

Table 16: Comparative pharmacokinetic parameters of the three treatment groups.

Parameters	MT	TT	PT	Inference
C_{max}	6.05 ± 0.39 ng/mL	8.18 ± 1.17 ng/mL	41.18 ± 3.57 ng/mL	Pessaries elicit a significantly (P<0.005) higher local concentration compared to conventional oral MT in the **crucial initial hours of insertion**.
T_{max}	6.00 ± 0.02 h	4.00 ± 0.01 h	1.00 ± 0.01 h	Quicker T_{max} (P<0.0001) observed with the pessaries is likely to arrest the viral transmission during intercourse and ensure adequate protection against the transmission of HIV.
$AUC_{0\text{-}24h}$	91.05 ±13.53 ng/mL*h	58.56 ±7.06 ng/mL*h	88.37 ±8.90 ng/mL*h	Comparable AUC.

Tissue Concentration Studies: After the 24 h study, mean TDF concentrations in the cranial vagina from pessaries were approximately 1.55 ± 0.41 ng/g, with lower concentrations in the caudal vagina but still within a comparable range to those in the cranial vagina. Mean TDF concentrations from tablets in the cranial vagina were ~4.68 ± 6.02 ng/g.

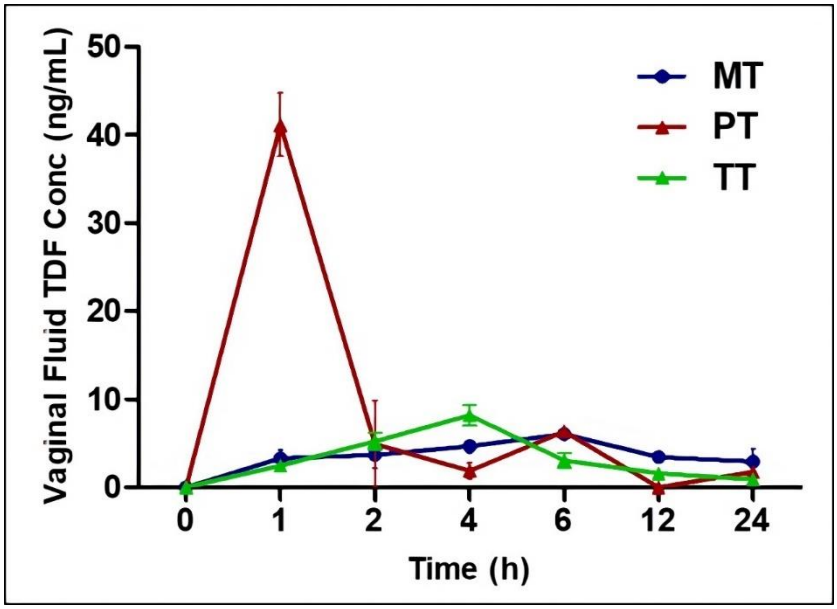

Figure 37: VF concentration of TDF over time following oral administration of marketed formulation and vaginal administration of DT and pessaries.

Histopathology: The histopathological evaluation of vaginal tissue observed at 10× and 40× magnification is represented in Figure 38.

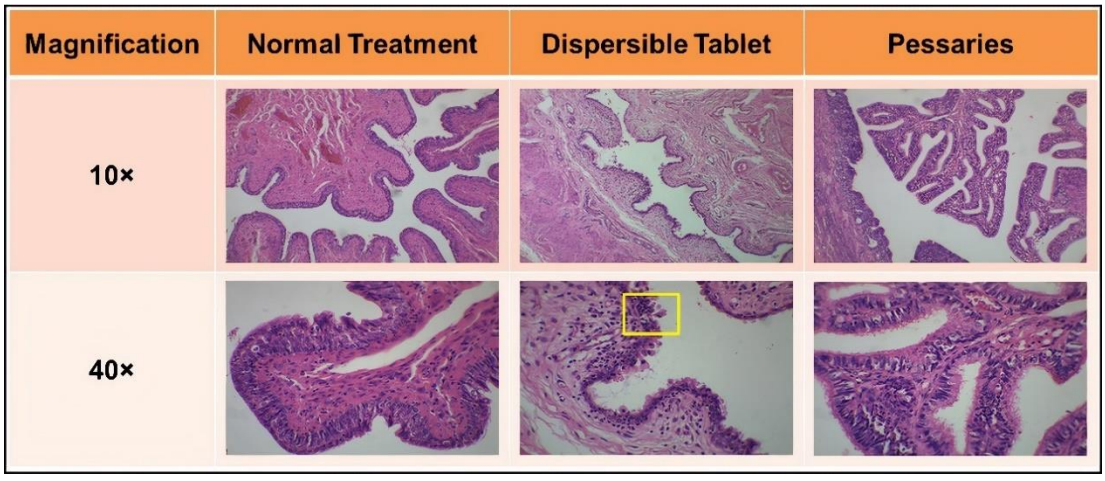

Figure 38: Histopathological evaluation of the vaginal tissue observed at 10× and 40× magnification.

DISCUSSION

5. DISCUSSION

5.1. Authentication of Drug

5.1.1. Melting Point

The DSC curve of TDF shows a sharp endothermic peak that corresponds to drug melting (T_{onset} = 112.04 °C; ΔH_{fus} = 4.054 J/g). The second sharp endothermic peak is observed at 116.74 °C.[51,69]

5.1.2. Mass Spectroscopy

The calculated molecular weight of TDF is 635.5 g/mol. The observed molecular weight of TDF from the spectra is 635.3 m/z [M] and 636.30 m/z [M+1].[53,54]

5.1.3. FTIR Spectroscopy

The FTIR spectra of TDF revealed the major functional groups, i.e., –NH_2 stretching, –OH stretching, aromatic and aliphatic –CH stretching, –C=O, –C=C– stretching, NH_2 scissoring band, aromatic –C=N and aliphatic –CN stretching, and P=O stretching. The FTIR spectra of TDF and its physical mixture with polymers revealed that the peaks of the major functional group of the TDF were retained. Hence there was no probable interaction between TDF and polymers.[69]

5.1.4. UV-VIS Spectrophotometry

The linear regression data obtained from the calibration curve showed a linear relationship over the concentration range of 5-40 µg/mL. Based on the average absorbance at 259 nm, the equation for the best line fit was generated (y = 0.0233x; R^2 = 0.999).[56,57]

5.2. Pre-formulation Studies

5.2.1. Solubility Studies

The solubility of TDF in water, 0.1 (N)HCl (pH1.2) SVF, and phosphate buffer (pH7.4) was found to be 13.0 ± 0.02 mg/mL, 34 ± 0.04 mg/mL, 30 ± 0.02mg/mL and 21 ± 0.03 mg/mL respectively.

5.2.2. Drug-Excipient Compatibility Studies

The FTIR spectra of TDF and its physical mixture with polymers like S-Alg, S-CMC, HPMCK4Mand HPMCK100M revealed that the peaks of the major functional groups of the drug were retained. Hence there was no probable interaction between drug and polymers.[97,98]

5.3. Preparation of Chitosan Microparticles

The emulsification internal gelation technique was utilized to create TDF microparticles, capitalizing on the drug's good aqueous solubility (13.4 mg/mL) and its classification as a BCS Class III compound.[99] Chitosan, a bio-adhesive polymer, was employed in this process. The technique involved forming a w/o emulsion stabilized with Span 80, a w/o surfactant. The emulsion was stirred at 500 rpm for 1 hour until globules formed, reaching a steady state. TPP was used as a cross-linking agent, reacting with compounds containing primary amine groups to create covalently cross-linked networks.[100] The addition of TPP solution to the drug-chitosan emulsion required a 30-minute curing time to ensure uniform distribution in the continuous oil phase, resulting in a more uniformly cross-linked product. During crosslinking, -OH ions competed with tri-polyphosphate ions to react with the amino group of chitosan immediately through ionic interaction. Once diffused into chitosan microparticles, the

tri-polyphosphate ions interacted with the amine groups of chitosan.[101] A double washing process with petroleum ether followed by distilled water was then implemented to remove excess oil, salts, and free TPP.[102]

5.4. Evaluation of Chitosan Microparticles

5.4.1. Practical Yield and Drug Entrapment Efficiency

The yield refers to the total quantity of microparticles produced, and optimizing the formulation aims to achieve a high yield of the product. Increasing the polymer concentration can enhance drug entrapment, reduce drug loss, and improve process yield.[51] This effect is evident in Figure 16.

Incorporating therapeutically active molecules into microparticles can be influenced by several factors, including the method of preparation, drug-to-polymer ratio, and TPP concentration. The entrapment of the drug was found to increase with higher polymer amounts. Increasing the polymer concentration (from 1% to 4%) leads to the formation of stabilized microparticles, preventing drug leakage during the hardening process. Previous studies have reported an increase in %EE with an increase in the drug-to-polymer ratio.[103-105] As indicated in Figure 16, an increase in TPP concentration enhances crosslinking with chitosan, resulting in a denser matrix that reduces drug leakage during stirring and improves encapsulation efficiency.[106,107]

5.4.2. Surface Morphology

The SEM images of formulation ECH-4 showed that the microparticles were spherical and had a smooth surface. Under 20,000x magnification (20k×), the particles appeared to be sticking together, indicating their bio-adhesive nature. The surface roughness and abrasions on the microspheres could be attributed to polymer deposits.[100,101]

5.4.3. Particle Size Analysis

Particle size is a crucial parameter in targeted drug delivery, impacting stability, %EE, IVDR profile, bio-distribution, mucoadhesion, and cellular uptake.[108] The particle size-volume distribution curve of ECH-4 (Figure 18) indicates a size range from 0.52 ± 0.00 µm to 284.79 ±21.41µm. The curve does not exhibit a typical bell-shaped pattern, suggesting a broad particle size distribution due to the tendency of bio-adhesive microparticles to adhere to each other.[68] Approximately 50% of microparticles in ECH-4 were around58.014 ± 1.037 µm in size, while 90% were ~193.42 ± 3.70 µm. The predominance of large particles is likely due to the adherence of bio-adhesive microparticles to each other. These results align well with the SEM photomicrographic images.[109,110]

5.4.4. FTIR Spectroscopic Analysis

FTIR spectroscopy is valuable for determining molecular interactions between a drug and its carrier. The FTIR spectra of TDF exhibited distinct peaks at 3219.58cm^{-1} (strong -OH stretching bond), 3049.84cm^{-1} (aromatic -CH stretching) 2985.27cm^{-1} and 2938.98cm^{-1} (aliphatic -CH stretching bond), 1760.69cm^{-1} (C=O group), 1678.73cm^{-1} (P=O stretching), 1619.91cm^{-1} (-C=C- stretching bond) and 1421.28cm^{-1} (aromatic C=N stretching bond), 1267.97cm^{-1} (aliphatic C-N stretching) and 1186.97cm^{-1} (C-O stretching) confirming the earlier report.[69] Chitosan, the polymer used in the formulation, exhibited characteristic peaks such as the N-H stretching vibration at 3430.74 cm-1 and the C=O bond of amide I at 1655.59 cm-1.[20,111] The FTIR spectra of the physical mixture retained principal peaks of both TDF and chitosan, suggesting weak interaction between them. In the formulation ECH-4, peaks corresponding to N-H stretching vibration, aliphatic -CH stretching vibration, and

C=O stretching vibration were observed. The characteristic peaks of TDF as represented in Figure 19 were also present but with decreased intensity, indicating no interaction between the drug and excipients.[112] Overall, these studies suggested that there was no incompatibility between TDF and other excipients used in the microparticle preparation, maintaining the chemical integrity of the drug.[113]

5.4.5. DSC Analysis

The formation of microparticles includes dispersing the drug in either crystalline or amorphous form or dissolving it in the polymer matrix. Any sudden or significant change in the thermal behavior of the drug/polymer could indicate a potential interaction between them, as shown in Figure 20. The DSC thermogram of TDF exhibited a sharp exothermic peak at 115.4°C, with the peak-onset at 112.04°C, corresponding to the drug's melting point. Interestingly, this endothermic peak completely disappeared in the thermogram of T-CM, suggesting a change in the thermal behavior due to the drug's encapsulation in the microparticles.

The enthalpy of fusion (ΔH_f) for TDF in its pure state, as determined by DSC, was found to be 71.41 J/g. In the thermogram of the physical mixture, a very low intensity endothermic peak indicated the semicrystalline nature of the drug. The melting point of TDF in the physical mixture was broadened and shifted to 118.4°C. In the thermogram of ECH-4, the drug's characteristic peak almost disappeared, suggesting that the drug was amorphous in the chitosan matrix. This indicates complete miscibility of the drug in the polymer, forming a solid-solid solution. Therefore, based on the DSC studies, it can be inferred that TDF was dissolved in the bio-adhesive chitosan matrix in an amorphous state.[51,69,114]

5.4.6. P-XRD Analysis

The crystalline nature of TDF was clearly demonstrated in P-XRD pattern with about 10 distinct well defined high-intensity sharp peaks at 2θ values of 10.29°(1339 counts), 10.59° (2540counts), 13.48° (1954counts), 14.17° (1361counts), 18.32° (3212counts), 18.80° (3258counts), 19.95° (4172counts), 21.36° (2438counts), 22.02° (3077counts) and 25.07°(4419counts).[69,114] The diffractogram of chitosan displayed characteristic peaks at 2θ values at 20.27° (3123 counts). These peaks were attributed to the semi-crystalline nature of chitosan as per the earlier reports.[113,115] The diffractogram of the physical mixture displayed the six prominent crystalline peaks of the drug at 18.32°, 18.8°, 19.95°, 21.36°, 22.02° and 25.07° indicating TDF exists in a semi-crystalline state in the physical-mixture. The diffractogram of ECH-4 showed six characteristic low-intensity peaks of TDF at 10.59° (358counts), 18.32° (548 counts), 18.8°(643 counts), 19.95° (528counts), 22.02° (486 counts), and 25.07° (431 counts).

Comparing the peak intensities of ECH-4 to those of pure TDF, a 3-10 times decrease in peak intensity was observed, indicating the amorphization of TDF in the chitosan polymer matrix. These characteristic peaks of TDF were previously reported in the same region, confirming our findings.[69,112] Therefore, the appearance of sharp crystalline TDF peaks and the presence of broad peaks in the diffractogram of ECH-4 confirmed that the drug (TDF) underwent a solid-state-transition during the emulsification process in the presence of chitosan..[115,116] This can be interpreted as a clear indication of the drug's molecular dispersion within the chitosan matrix as a solid-solid solution.

5.4.7. *In-vitro* Drug Release

IVDR of microparticles is usually performed in three steps. During the initial burst period, the drug at the surface of the microparticles is immediately released into the medium. In the sustained release phase, the drug is released at a gradually decreasing rate. During the steady-state period, the drug is released at a constant and slow rate.[106]

When comparing the IVDR dissolution profiles of T-CM, formulations EC-1 to EC-4 exhibited nearly 100% rapid release of TDF by the end of 6 h. In contrast, formulations ECH-1 to ECH-4 released 99.07 ± 0.41%, 99.23 ± 0.59%, 98.96 ± 1.18%, and 88.05% ± 0.38% of TDF by the end of 6, 8, 12, and 24 h, respectively. Formulations EC-1 to EC-4, produced with 5% TPP, showed a biphasic mode of drug release, with an initial burst effect followed by a slow-release phase. This initial release was likely due to the smaller particle size and surface drug content, leading to rapid release followed by slower diffusion from the core of the microparticles.[106,100]

Formulations ECH-2, ECH-3, and ECH-4, produced with 10% TPP, exhibited minimal burst release, followed by progressively slower drug release until a steady state was reached. Approximately 50% of TDF was released within the first 2 h from ECH-2 and ECH-3, whereas from ECH-4, 50% of the drug was released within 6 h. The concentration of chitosan in the formulation played a significant role in microparticle formation and subsequent drug release. Higher chitosan concentrations resulted in stronger microparticle walls, reduced swelling potential, and a sustained release of TDF.[101] Additionally, TPP concentration also influenced drug release, with formulations ECH-2 to ECH-4, produced with 10% TPP, displaying a more sustained release compared to EC-1 to EC-4, produced with 5% TPP. This sustained release

pattern was attributed to the higher cross-linking density of chitosan with increased TPP concentration.[106,101]

Drug release from hydrophilic polymer-based controlled-release dosage forms is primarily governed by the hydration of the polymer chains. This process typically involves three steps: first, the penetration of the medium into the matrix (hydration); second, swelling with subsequent dissolution or erosion of the matrix; and third, the transport of the dissolved drug either through the hydrated matrix or from the eroded parts into the surrounding medium.

To understand the kinetics and mechanism of TDF release from CM, the dissolution profiles of various batches of T-CM were compared statistically or using model-dependent approaches. The higher R2 values indicated that the drug release from all formulations was not concentration-dependent, and the mechanism of drug release was found to be swelling and diffusion controlled by the disentanglement rate of the polymer at the swollen front. This suggests that all formulations followed zero-order kinetics and the Higuchi model. This was further confirmed by the Korsmeyer-Peppas model, where $n<0.50$, indicating an approximation to a Fickian diffusion release mechanism.[61,64,74,9] Among all formulations, ECH-4 exhibited a better-sustained release of TDF from the chitosan matrix.

5.4.8. *Ex-vivo* Mucoadhesion Study

Depending on the %yield, %EE, and IVDR, formulation ECH-4 was considered for further studies. The bio-adhesive ability of formulation ECH-4 was found to be excellent over a 24 h period. By the end of 12 h, 18.33 ± 6.11% of the T-CM were adhered and retained on the mucosa, while 81.67 ± 6.11% of the microparticles were

washed off by the SVF. A higher retention of microparticles on the mucosa indicates minimal dissipation of the drug from the vagina due to vaginal secretion.

When correlating the *ex-vivo* adhesion with the IVDR (Figure 9), it was observed that the cumulative drug release decreased as the percentage of particles on the mucosa decreased. By the end of 6 h, 50% of the particles were washed off from the mucosa, which corresponds to 54.48 ± 7.59% IVDR. By the end of 24 h, only about 10.33 ± 2.08% of the particles were adhered to the mucosa, corresponding to 88.05 ± 0.38% of IVDR of TDF from the CM.[66,64]

The CM exhibited good initial adhesion to rabbit vaginal mucosa, with a residence time of 24 h, ensuring near-complete drug release. The percentage of drug release linearly declined as the percentage of particles adhered reduced with time. An excellent correlation (correlation coefficient value of 0.975) was observed between the percentage of microparticles retained on the mucosa and the IVDR, as in Figure 9b. The mucoadhesive potential of the chitosan microparticles appears to be sufficient, as TDF release occurs over a short period of time and there is no therapeutic justification to retain the formulation adhered to the patient's vaginal mucosa once the drug has been completely released.[117]

5.5. Preparation of Vaginal Tablets

For topical PrEP, vaginal inserts containing multiparticulate-based drug delivery systems offer several advantages, including targeted drug delivery, improved drug penetration in mucous and tissue, bio-adhesion, and sustained drug release after intra-vaginal administration.[4] To produce consistent batches of DT-T-CM, a direct-compression method was employed. This method involves blending the dry drug with excipients and compacting the mixture using a rotary tablet press. Direct compression

is a simple robust, and cost-effective method with minimal processing steps, resulting in less friable tablets with high mechanical strength, making them easier to handle and package.

To optimize the release of TDF from DT-T-CM intra-vaginally, various batches of tablets were prepared using ECH-4 microparticles as the API. The formulation included 40% Avicel (pH 102) as a diluent and disintegration agent, polyvinyl pyrrolidine K-30 as a binder, croscarmellose sodium as a super disintegrant, and magnesium stearate and talc as lubricants and glidants. These tablets were designed to provide a controlled release of TDF for effective topical PrEP.[4,118]

5.6. Evaluation of Vaginal Tablets

5.6.1. Physical Characterization of Vaginal Tablets

The DTs were prepared to be spherical, with a flat face, beveled edge, and a buff color. The tablets were designed to be 8 mm in diameter for easy administration into the vaginal cavity. Each tablet contained 15 mg of TDF with a total weight of 300 mg, and consistent thickness and hardness were maintained across all baches. The tablets showed minimal variation in thickness, diameter, and weight uniformity (RSD<1%), with a weight variation range within the acceptable limit of ±5% as per IP specifications. Friability tests indicated that all tablets had good mechanical strength, with friability values below the pharmacopoeial limit of 1%.[78] Drug content uniformity across all batches met official pharmacopoeial specifications, indicating the uniform distribution of T-CM within the tablet matrix.[77,78] In disintegration studies, the tablets from batches F1toF3 disintegrated rapidly in SVF within approximately 30-40 s, with no mass remaining in the apparatus. Batch F4 tablets disintegrated slightly slower, in about 60 s. The rapid disintegration of F3 tablets

suggested good hydrophilicity of chitosan, indicating its super disintegrant ability. Based on these findings, tablet batch F3 was selected for further *in-vitro* dissolution studies.[60,119]

5.6.2. *In-vitro* Dissolution Study

The dissolution profiles of the DT-T-CM were compared to the drug-loaded chitosan microparticles (ECH-4) to evaluate the impact of compaction on the microparticles. Using the USP IV Flow through cell dissolution apparatus in a closed-loop setup, allowed the disaggregation of particles, thereby enhancing the dissolution. The glass beads used ensured a laminar and more homogeneous flow of the dissolution medium from the bottom of the sample cell. Once the tablet disintegrates in a flow-through cell, the glass beads present in the lower cone of the cell prevent the particles from descending into the inlet tubing. The circulation of SVF in a closed loop helps the strain rate to be more controlled.[71,72]

Formulation F3 exhibited a slow and sustained drug release until reaching a steady state. In contrast, formulation F4 (pure TDF) showed an initial burst release within the first hour (59.42 ± 1.61%) followed by a slower release, reaching almost complete drug release within 6 h. Approximately 50% of TDF was released from F3 by the end of 6 h, with sustained release of 85.98 ± 1.61% over the duration of the study, likely due to the hydrodynamics in the dissolution apparatus.[71]

Comparing the IVDR profiles of TDF microparticles with the TDF vaginal tablets containing T-CM, it was observed that 70.77 ± 6.03% of the drug was released from the latter by the end of 12 h, which was approximately similar to that of the microparticles (68.91 ± 10.23%). This indicates that the drug release from the formulated vaginal tablets was similar to that of the chitosan microparticles,

suggesting that the complex DT-T-CM system did not alter the release profile of TDF. Thus, the microparticulate form of drug administration could potentially reduce the frequency of drug administration in the vagina, making it more patient-friendly.

The f_2 and f_1 values are widely used to compare dissolution profiles and assess bioequivalence between two formulations. An f_2 value between 50-100 indicates that the two dissolution profiles are similar, while an f_1 value close to zero indicates a high degree of similarity. In this case, the f_2 value of 78.02 and f_1 value of 1.51 suggest that the dissolution profiles of the T-CM (ECH-4) and DT-T-CM (F3) formulations are highly similar, indicating that the process of incorporating the T-CM into a tablet dosage form did not significantly alter its dissolution profile.[79]

The drug release study results were used to assess release mechanisms and kinetics. The selection of the most appropriate model for drug release was based on the linearity value, i.e., the correlation coefficient R^2. A higher R^2 value indicated that the release of TDF from the vaginal tablet was independent of its concentration. The mechanism of drug release from the DT-T-CM was found to be swelling and diffusion-controlled, indicating compliance with zero order kinetics ($R^2 = 0.95 \pm 0.02$) and the Higuchi model ($R^2 = 0.98 \pm 0.01$) due to the properties of the polymer. The diffusion coefficient value from the Korsmeyer-Peppas model was found to be $n = 0.414 \pm 0.081 < 0.50$, indicating drug diffusion out of the matrix tablet via pure Fickiandiffusion.[61,74,119] Therefore, the formulated vaginal DT-T-CM sustained drug release, making it a potential candidate for use as a vaginal insert for anti-retroviral drug delivery, considering the significance of this route in HIV transmission prevention.

5.7. Preparation of T-AM

The water solubility of TDF (13.4 mg/mL), which falls under BCS Class III,[99] justifies the selection of emulsification-internal-gelation technique to produce mucoadhesive T-AM developed using other hydrophilic bio-adhesive polymers like S-CMC, HPMC K4M and HPMC K100M as these polymers play a crucial role in swelling of the matrix and the diffusion of the drug.[24,29] To stabilize the emulsion droplets and prevent coalescence, a 1.5%v/v concentration of Span 80 surfactant was used. Span 80 effectively reduces the interfacial tension between the water and oil phases, facilitating the dispersion of a viscous aqueous solution of alginate in the oil. The properties of the microspheres produced by emulsification can be influenced by optimizing different processing parameters, such as agitation duration and solidifying/curing time.[83] In this case, the emulsion was stirred at a speed of 500 rpm for a duration of 1 h to achieve a proper dispersion and uniform dispersion of the two phases. Following the stirring, homogenization was performed for 15 mins to further reduce the size of the particles to a micron level. This additional step aids in achieving a finer and more consistent particle size distribution. By the end of the specified time period, the process reaches a steady state, indicating that the microspheres of desired physicochemical properties are formed. Calcium chloride is commonly used as a cross-linking agent in the preparation of sodium alginate microspheres. The presence of divalent cations in calcium chloride, promotes the interaction with alginates, leading to the formation of biodegradable microspheres. In the emulsification process, a curing time of 30 mins was allowed. This duration ensured uniform distribution of $CaCl_2$ within the continuous oil phase.[101] Each Na^+ cation is bonded to a single carboxyl group in the alginate chain, while the Ca^{2+} cation interacts with two carboxyl

groups from different polymer chains. When an aqueous solution of S-Alg reacts with a Ca^{2+} ion, the two Na^{+} ions are substituted with Ca^{2+} ions during the cross-linking process. The cross-linking of copolymers (polymerization) through ionic bonding between Ca^{2+} cations and alginate anions, resulted in a more consistent and evenly cross-linked product.[120,121]

5.8. Evaluation of T-AM

5.8.1. Practical Yield and Drug Entrapment Efficiency

The yield refers to the total amount of microspheres that are produced during the emulsification internal gelation process. The primary goal of optimizing the formulation is to achieve a high yield and entrapment of the desired product. By increasing the amount of polymer in the formulation, a greater amount of the drug would be encapsulated within the microspheres. This reduces the likelihood of drug loss during the production process and additionally, contributes to an improved yield.[51] Among the formulations tested, EH-8 exhibited a significantly higher ($P<0.05$) %yield (97.47 ± 1.9%). Microspheres formed using S-CMC and HPMC K4M had a tendency to form lumps and therefore were not considered for further studies. The immediate cross-linking reaction resulted in the agglomeration of microspheres and the formation of harder particles along with the microspheres specifically in formulations EH-2, EH-3, EH-4, EH-6, and EH-11.[83,122]

Various factors, including the type of polymers used, the amount of polymer used, and the concentration of the cross-linking agent, play a crucial role in determining the successful incorporation of therapeutic actives into S-Alg microspheres.[123] In our study, it was observed that a higher amount of polymer led to enhanced encapsulation efficiency. As the drug-to-polymer ratio increased from 1:2 to 1:9, the drug was better

entrapped within the polymer, effectively preventing drug leakage during the hardening process (Figure 27). The %EE for EH-8 (62.09 ± 1.34 %) was significantly higher ($P < 0.05$) compared to all other batches of T-AM produced with the ratio of 1:4. Similar results have been reported in the earlier studies.[82,110] Higher amounts of S-Alg produced a more viscous dispersion, which formed larger droplets and subsequently larger microspheres. The higher loss incurred at lower polymer amounts could be due to the formation of smaller microspheres with higher surface area reducing %EE. Formulations EH-2 and EH-3 exhibited the formation of larger and more rigid particles due to the rapid cross-linking of alginates induced by calcium ions. The immediate interaction between calcium ions and alginates led to a swift cross-linking process, resulting in the generation of particles with increased size and hardness compared to other formulations, thereby limiting the polymer chain mobility and preventing uniform dispersion.[124] Loss of the drug in the emulsification method can be accounted for in the hardening, washing, and filtering processes only.[62,125]

5.8.2. Surface Morphology

The SEM photomicrographs of EH-8 indicated the particles were spherical with smooth and dense surface topography under 20k× and 40k× magnification. The microspheres appear to be adhering to each other indicating their bio-adhesive nature. The adhesion of the microspheres to each other is also likely due to the polymer deposits.[66,110,109]

5.8.3. Particle Size Analysis

Particle size is one of the crucial parameters, which affects the stability, EE, drug release profile, drug bio-distribution, mucoadhesion, and cellular uptake.[110] The immediate cross-linking of alginates, due to the interaction of Ca^{2+} ions, causes the

formation of particles of different diameters and different porosity.[83,73] The results of particle size analysis are known to agree well with the SEM photomicrographic images.

5.8.4. FTIR Spectroscopic Analysis

The FTIR spectrum of TDF showed the presence of a strong -OH stretching bond (3219.58 cm^{-1}), aliphatic -CH stretching bond (3049.84 cm^{-1} and 2938.98 cm^{-1}), C=O group (1760.69 cm^{-1}), P=O stretching (1678.73 cm^{-1}), -C=C- stretching bond (1619.91 cm^{-1}) and an aromatic C=N stretching bond (1421.28 cm^{-1}) confirming the earlier reports.[69] In the FTIR spectrum of S-Alg, stretching vibrations of O–H bonds of alginate appeared at 3221.5 cm^{-1}, stretching vibrations of aliphatic-CH were observed at 2175.31 cm-1, and -C=C- stretching bond was observed at 1609.31 cm^{-1}. The bands at 1026.91 cm^{-1} were attributed to the C–O stretching vibration of the pyranosyl ring and the C–O stretching with contributions from C–C–Hand C–O–H deformation. In the FTIR spectrum of HPMC, the presence of the hydroxyl group was observed at 3476.06 cm^{-1}, and the presence of methyl and hydroxy propyl group was observed at 2912.95 cm^{-1}. The bands at 1636.3 cm^{-1} confirm the presence of a six-membered cyclic ring and the band at 1371.14 cm^{-1} indicates the presence of cyclic anhydrides. The characteristics peaks of the polymers, S-Alg and HPMC were similar to those as reported by Daemi et al., 2012, Helmiyati et al., 2017 and Zafar et al., 2020.[126,127,98,128,129] The characteristic peaks of TDF appeared in the spectra of EH-8 though with minor shifts ruling out any possible chemical interaction between these groups and the excipients used during the process. Thus, the FTIR studies proved the chemical integrity of TDF in the polymer matrix.

5.8.5. DSC Analysis

The process of developing microspheres includes dispersing the drug, either in its crystalline or amorphous state or dissolving it within the polymer matrix. Sudden or significant changes in the thermal characteristics of the drug or polymer during this process may indicate a possible interaction between the drug and the polymer.

The DSC thermogram (Figure 31) displayed a sharp endothermic peak of TDF at 115.4°C with the peak onset at 112.04°C indicating the crystallinity of TDF. The peak was found to correspond to the melting point of the drug.[51] The ΔH_f for TDF in a pure state by DSC was reported to be 71.41 J/g. The ΔH_f value for the physical mixture was found to be 0.49 J/g indicating the decrease in the crystallinity of TDF in the mixture. The X_c of the physical mixture was found to be 0.86% when compared to TDF as a reference. The crystallinity of TDF was found to further drop to ~ 0.1% in the formulation EH-8 indicating the drug is dispersed in an amorphous state in the polymeric matrix. The endothermic peak of TDF was broadened and shifted towards lower temperature in microsphere Formulation EH-8. This could be attributed to the uniform distribution of the drug in the polymer crust, resulting in the complete miscibility of the molten drug in the polymer to form a solid-solid solution. From the DSC studies, it can be inferred that the drug is uniformly dispersed in the microspheres in an amorphous or molecular state.[51,69]

5.8.6. P-XRD Analysis

The crystalline nature of the drug was clearly demonstrated in the P-XRD pattern with about 10 distinct well-defined high-intensity peaks as represented in Table 4. TDF is reported to display 10 characteristic peaks in between 10.29° to 25.07° 2θ region justifying the observation in the present study.[52,114] The P-XRD pattern of the physical

mixture displayed about 7 high-intensity peaks and a number of low-intensity peaks, indicating a decrease in the drug crystallinity in the mixture. The number of peaks and the peak intensities relevant to the drug were further reduced in the formulation EH-8 indicating a substantial reduction in the crystallinity of TDF in the formulation. Considering the peak of TDF at around 25.07° 2θ region with an intensity of 4419 counts as the reference peak, the intensity of the same peak in the physical mixture was found to further reduce to an intensity of 1086 counts, indicating the decrease in crystallinity to nearly 24%. The intensity of the reference peak dropped to about 11% in formulation EH-8, indicating the drug is reduced to an amorphous state in the polymer matrix. The solid-state characterization using DSC and XRD conclusively indicates that TDF is likely to be present in the amorphous molecular state as a solid-solid solution in the polymer matrix. Dispersion of polar drug in hydrophilic controlled release polymers would improve the drug miscibility in polymer and would control the drug release as well.[130]

5.8.7. *In-vitro* Drug Release

The IVDR profiles of the bio-adhesive microspheres exhibited three distinct phases: an initial rapid release resulting in a burst effect, a slower release phase as drug molecules diffuse from the core, and a steady state phase with a slow, controlled release. The initial burst effect diminishes with increasing polymer concentration, leading to longer diffusion paths for drug molecules and slower release rates. The polymers used in the study form hydrophilic swellable matrices, increasing diffusional path length over time. Additionally, higher polymer concentrations reduce the number of pores in the microsphere matrix, further impeding drug release. This sustained release mechanism enables controlled and prolonged drug delivery, enhancing treatment efficacy.[106]

Effect of Drug-to-Polymer ratio - The drug release increased with decreasing polymer amounts, as shown in Figure 33. Formulation EH-1, with a 1:2 drug-to-polymer ratio, exhibited a biphasic drug release pattern. Initially, there was a burst effect, releasing nearly 50% of the drug within 2 h, followed by a slower release phase. Similar patterns were observed for formulations EH-5 and EH-7, which had a 1:4 drug-to-polymer ratio. The initial burst release is attributed to the smaller particle size of the microspheres and the presence of surface-bound drug.[106] In contrast, Formulation EH-8, containing TDF, S-Alg, and HPMC K100M, showed minimal burst release initially, followed by a gradual release until reaching a steady state (97.03 ± 4.45% in 12 h). This formulation exhibited significantly lower ($P<0.05$) burst release at 2 h compared to other formulations with a 1:4 drug-to-polymer ratio.

In formulations EH-9, EH-10, and EH-12, which had a higher polymer concentration with a drug-to-polymer ratio of 1:9, the rate of drug release was notably slower, with approximately 22.80 ± 5.35% of the drug released after 1 h. This decelerated release can be attributed to the increased interlocking of linear polymer chains, which enhances the formation of a robust gel layer through a process termed 'virtual crosslinking.' This increased cross-linking is likely to hinder the penetration of the dissolution media, thereby slowing down the release of the drug.[83,130]

Effect of Type of polymers – The selection of polymers, in combination with sodium alginate, significantly influenced the *in-vitro* release profile of TDF, as illustrated in Fig. 10. Incorporating polymers with higher molecular weights was observed to impart controlled release properties to the microspheres. Notably, the molecular weights of HPMC K100M, HPMC K4M, sodium CMC, and S-Alg were reported as 1150, 500, 262.19, and 216.12 g/mol, respectively.[131-133]

Formulations EH-1 and EH-5, which solely comprised sodium alginate as the hydrophilic polymer, did not effectively control the drug release. Conversely, formulation EH-9, formulated with high levels of drug-to-alginate ratio (1:9), exhibited approximately 63.99 ± 1.26% TDF release over 12 h.

To achieve controlled yet complete drug release from T-AM at lower polymer levels (1:4), efforts were made to substitute 50% of S-Alg with other hydrophilic polymers. Replacing approximately 50% of S-Alg with HPMC K100M in formulations EH-4 (99.05±1.10%), EH-8 (97.03 ± 4.54%), and EH-12 (50.89 ± 4.76%) effectively controlled the release over 12 h at reduced polymer concentrations. Additionally, it was observed that the drug release from the microspheres decreased with an increase in the molecular weight of the hydrophilic polymers.[110,130]

Depending on the molecular weight of the polymers used, the amount of drug release was found to decrease in the order: HPMC K100M< HPMC K4M< S-CMC indicating the molecular weight was found to have a considerable effect on the release of drug. The IVDR dissolution studies indicated that formulations EH-9, EH-10, and EH-12 developed with the drug-to-polymer ratio of 1:9 displayed incomplete release ranging from 50.89 ± 4.76 % to 63.99 ± 5.16 % by the end of 12h. Based on the results EH-8 was considered as an ideal formulation as it was found to display minimal burst release and at the same time released most of TDF in a controlled manner in SVF in 12h that can be considered to be a realistic standard intravaginal retention time.[72,92]

The R^2 values close to 1.0 indicated that the majority of the formulations followed zero-order kinetics, wherein the concentration of the drug did not affect its release from any of the formulations. The mechanism of drug release was determined to be

primarily governed by swelling and diffusion, which is influenced by the disentanglement rate of the polymer at the swollen front. This suggests that the drug release from the formulations followed zero-order kinetics, where the release rate is independent of the drug concentration, as well as the Higuchi model, which describes the release of drugs from polymeric matrices based on diffusion. These findings indicate the release behavior of the formulations and help in understanding and optimizing their drug delivery characteristics.[43] This was further confirmed from the Korsmeyer-Peppas model, where the 'n' value is used to characterize different release mechanisms. Formulation EH-5 and EH-8 indicate anomalous or non-Fickian transport, i.e., the Fickian diffusion as well as the swelling and relaxation of the drug from the matrix are both responsible for the drug delivery. Formulation EH-9 and EH-10 ($n<0.45$) indicate hindered Fickian diffusion which means that it is characterized by a diffusive regime with hampered release.[134,61,135]

Therefore, among all the formulations studied, formulation EH-8 demonstrated a desirable drug entrapment efficiency of 62.09 ± 1.34% and a significant drug release of 97.03 ± 4.54% over a period of 12 h.[136] These results indicate that EH-8 exhibited a favorable sustained drug release profile, making it a promising candidate for further investigations and studies. The high drug entrapment efficiency suggests efficient encapsulation of the drug within the polymer matrix in the molecular state that could account for controlled drug release of TDF.

5.8.8. *Ex-vivo* Mucoadhesion Studies

Formulation EH-8 was considered for further studies based on its percentage yield, entrapment efficiency, and drug release. Formulation EH-8 demonstrated an excellent bio-adhesive ability over a 12h period, where, approximately 7.17 ± 2.02% of the

microparticles remained adhered to the mucosa, while 92.83 ± 2.02% of the microparticles were washed off by the SVF. The increased adherence of microparticles to the mucosa suggests that there is minimal drug loss from the vagina, most likely due to a decrease in vaginal secretion. Approximately 50% of the particles were washed off from the mucosa by the end of 4 h, corresponding to a 60.04 ± 1.72% IVDR.[66,74] This indicates that S-Alg and HPMC K100M microparticles demonstrated strong adhesion to rabbit vaginal mucosa by virtue of their bio-adhesive properties and ensured nearly complete TDF release by 12 h.

On comparing the *ex-vivo* adhesion with the IVDR, an excellent correlation was observed between the percentage of microparticles retained on the mucosa and the IVDR, with a correlation coefficient value of 0.996 as indicated in Figure 9. As the percentage of adhered particles decreased over time, the drug release also decreased in a linear manner. This indicates the mucoadhesive potential of the EH-8 microparticles. The *ex-vivo* study indicates the suitability of the bio-adhesive microparticles for intra-vaginal delivery of TDF.

5.9. Preparation of Pessaries

Vaginal inserts using multiparticulate-based drug delivery technologies offer several advantages for topical PrEP. These advantages include targeted drug delivery to specific sites, enhanced drug penetration in mucous and tissues, bio-adhesion for retention, and prolonged drug release after intravaginal administration. To ensure consistent and reproducible batches of pessaries, the molding method was chosen as it is a simple, robust, and cost-effective approach with minimal processing steps. This method produces less-friable inserts with high mechanical strength, making them easier to handle and package. Figure 10 represents the formulated cocoa butter pessaries.

5.10. Evaluation of Pessaries

5.10.1. Physical Characterization of Pessaries

The prepared pessaries were in the shape of a bullet having a smooth surface. They appeared to be pale yellow in color. All formulations exhibited uniform drug distribution, weight uniformity, and adequate mechanical strength for pessaries. The dimensions of the pessaries (width, 0.82 cm to 0.90 cm and length, 2.11 cm to 2.14 cm) for different formulations with good homogeneity and the impact of additional varied slightly but were generally homogeneous, with minimal impact from additional excipients. Weight variation fell within the acceptable range, indicating precise mold calibration. Disintegration time increased with higher concentrations of white wax, which acted as a stabilizer and controlled-release agent. Based on these findings, formulation F2 was selected for further IVDR dissolution studies.[87,88,137]

5.10.2. *In-vitro* Dissolution Study

The dissolution of pessaries was compared with EH-8 to assess the impact of molding on the bio-adhesive microparticles. Ideally, we expect the dissolution of the pessaries to be comparable to that of the constituent bio-adhesive microparticles. The USP IV Flow through cell dissolution apparatus was employed to perform the dissolution studies. The closed-loop technique was followed as it allows disaggregation of the particles thereby enhancing the dissolution. The glass beads used ensured a laminar and more homogeneous flow of the dissolution medium from the bottom of the sample cell. Once the pessary disintegrates in a flow-through cell, the glass beads present in the lower cone of the cell prevent the particles from descending into the inlet tubing. The circulation of SVF in a closed loop helps the strain rate to be more controlled.[71,72]

Comparing the IVDR dissolution profiles of T-AM with pessaries, the pessaries released 95.31 ± 1.38 % of TDF within 12 h similar to that of T-AM (EH-8), *i.e.*, 97.02 ± 4.54 %, indicating that the release from the pessaries was not hindered by the cocoa butter base. This suggests that the T-AM is likely to remain intact in the lipophilic base, releasing the drug upon melting in the dissolution media.

Difference and similarity factors serve as effective model-independent tools for reliably comparing dissolution profiles. The formulated pessaries were found to display a dissolution profile similar to the constituent EH-8, with an f_2 value of 72.09 and an f_1 value of 2.50.[138] The similarity factor values indicate that the dissolution profile of the T-AM was not significantly altered by incorporation into the pessary, suggesting that the formulated pessaries provide sustained drug release. This makes pessaries a potential option for vaginal drug delivery to prevent HIV transmission.

5.11. *In-vivo* Studies

Pharmacokinetic Studies: The calculated pharmacokinetic parameters of all the formulations were compared to assess their efficacy. PT exhibited a significantly higher ($P < 0.005$) C_{max} of 41.18 ± 3.57 ng/mL at 1 h post-administration compared to MT. This indicates that pessaries can achieve a higher local concentration than conventional oral MT, particularly in the critical initial hours after insertion. The increased regional concentrations exceeding the IC_{50} value of TDF (11.5 ng/mL) suggest improved distribution and retention of the microparticulate system in the vaginal mucosa.[139]

Additionally, PT showed a significantly shorter T_{max} of 1.00 ± 0.01 h compared to MT (6 ± 0.02 h). The rapid T_{max} observed with PT could help prevent viral transmission during intercourse, ensuring adequate protection against HIV. The prolonged T_{max} and

lower C_{max} observed with MT are likely due to poor drug distribution to the vaginal tissue and fluid following oral administration, leading to systemic distribution.

However, peak VF concentrations with PT quickly dropped following T_{max}, indicating rapid clearance from the vagina. This dissipation may be attributed to TDF's characteristics as a BCS class III molecule, which is prone to dissipation due to its good aqueous solubility and the rabbits' frequent urination during the study. Reports suggest that lower drug levels in the caudal vaginal fluids over longer periods may be due to dilution by urine following intravaginal insertion in rabbit models.[95,42] It is important to note that physiological differences between animal models and humans can influence drug dissipation from intra-vaginal devices. Rabbit vaginas are longer and feature an urovaginal sphincter that separates the lower urovagina from the cervicovagina. Inserting a drug-loaded pessary in the urovagina of rabbits could be challenging as it would be constantly perfused by urine, leading to a drug washout that may impact bio-distribution studies.[140]

Tissue Concentration Studies: After the 24 h study, mean TDF concentrations in the cranial vagina from PT were ~1.55 ± 0.41 ng/g, with lower concentrations in the caudal vagina but still within a comparable range to those in the cranial vagina. Mean TDF concentrations from TT in the cranial vagina were ~4.68 ± 6.02 ng/g. These results suggest that the pessary formulation containing TDF exhibits favorable pharmacokinetic properties, potentially offering effective protection against HIV transmission when administered intra-vaginally. Understanding the protective efficacy and duration of protection for both pre-exposure and post-exposure dosing is crucial for determining appropriate dosage and dosing regimens in future clinical trials.[42]

Histopathology: The histopathological evaluation of vaginal tissue (Figure 13) revealed a consistent thickness of the vaginal epithelium, indicating that the pessaries did not cause any damage or shedding of epithelial cells. This finding suggests that the pessaries can be safely incorporated into the vagina without disrupting the vaginal layer. The lack of adverse effects on the vaginal epithelium also indicates that the pessaries are likely to be well-tolerated by patients, making them a patient-compliant option for drug delivery.[77]

SUMMARY

6. SUMMARY

HIV and AIDS pose significant worldwide challenges, impacting health, society, and economies on a global scale. The progression from HIV to AIDS exemplifies the virus's insidious nature, as it systematically dismantles the body's defenses, making it increasingly susceptible to opportunistic infections. Despite advancements in healthcare, awareness, and treatment availability, HIV/AIDS is a major global health concern. The low oral bioavailability of AntiRVs hampers their effectiveness in reaching infection sites, increasing the risk of relapse. PrEP is crucial in reducing HIV transmission. Traditional vaginal inserts, such as gels, creams, suppositories, and douches containing AntiRVs, are promising dosage forms for on-demand PrEP.

Achieving effective prophylactic prevention requires ensuring that the drug reaches adequate therapeutic levels at potential infection sites. Vaginal inserts are designed to deliver the drug locally to target cells and tissues in the vaginal lumen. Bio-adhesive vaginal dosage forms, in particular, can deliver active ingredients over a prolonged period by adhering to the vaginal mucosa, ensuring controlled and sustained drug release into the cervicovaginal fluid and tissue. This sustained release is essential for maintaining effective drug concentrations at the infection site, enhancing the prophylactic treatment's effectiveness.

The project aimed to develop a novel PrEP DT composed of T-CM and pessaries constituting T-AM for intra-vaginal administration, to address the limitations of conventional oral dosage forms.

Part I: Development of dispersible vaginal tablets of TDF-loaded bioadhesive chitosan microparticles

T-CM were developed by emulsification-internal-gelation technique, adjusting the drug-to-polymer ratio and cross-linking agent quantity. The ECH-4 batch showed a high %EE (68.93 ± 1.76%) and sustained TDF release over 24 h (88.05 ± 0.38%). *Ex-vivo* studies with rabbit vaginal mucosa indicated good bio-adhesion for 24 h. SEM confirmed the spherical shape of T-CM, and DLSA showed a mean diameter of 193.42 ± 3.70 µm. FTIR analysis ruled out chemical interactions between TDF and excipients. DSC and P-XRD revealed amorphization of TDF within the chitosan matrix. ECH-4 was incorporated into DT for intra-vaginal use, that dispersed rapidly (31.33 ± 4.63 s) and releasing 89.98 ± 1.61% of TDF over 24 h in SVF.

Part II: Development of pessaries constituting TDF-loaded bioadhesive sodium alginate microparticles

T-AM was developed by emulsification-internal-gelation technique, varying the drug-to-S-Alg ratio, which influenced particle size, %EE, and IVDR. Batch EH-8, with a 1:4 drug-to-polymer ratio and equal parts S-Alg and HPMC K100M, exhibited optimal %EE (62.09 ± 1.34%) and controlled TDF release (97.02 ± 4.54%) over 12 h. EH-8 displayed good mucoadhesion on rabbit vaginal mucosa for over 12 h. SEM demonstrated the spherical shape of T-AM, and DLSA indicated a diameter of 68.68 ± 0.91 µm. FTIR analysis confirmed the chemical integrity of TDF in T-AM, while DSC and P-XRD revealed the presence of TDF in an amorphous state in the polymer matrix. EH-8-loaded meltable pessaries melted at 37°C and exhibited sustained TDF release (95.31 ± 1.37%) over 12 h in SVF.

To determine the biodistribution of TDF in the vagina, the intra-vaginal tablets and pessaries developed were compared to an oral marketed formulation in rabbits. *In-vivo* experiments revealed that pessaries displayed significantly higher C_{max} in VF with a lower T_{max} compared to oral and intra-vaginal tablets. The pessaries efficiently maintained inhibitory concentrations in the critical early hours of insertion, which is crucial for providing adequate protection against HIV transmission during intercourse.

The smaller size and higher surface-to-volume ratio of bio-adhesive microparticulate systems enhance vaginal drug delivery by improving residence time and prolonging TDF release. These properties make bio-adhesive microparticles ideal carriers for retention in the vaginal mucosa, facilitating regional concentration and biodistribution.

Timely delivery of TDF directly to the pathogen's entry portal using these pessaries offers a novel strategy to prevent HIV transmission effectively during intercourse. While long-acting systemic formulations dominate HIV prevention trends, these pessaries provide a promising on-demand PrEP option for HIV-negative women. The proposed novel pessaries are likely to bring a paradigm shift in HIV PrEP management.

CONCLUSION

7. CONCLUSION

Novel pre-exposure prophylactic bio-adhesive formulations containing TDF present a promising strategy for protecting HIV-uninfected individuals against HIV acquisition. These formulations, utilizing bio-adhesive polymers in vaginal drug delivery, enhance mucoadhesive strength, prolong drug release, and increase residence time. The small size and high surface-to-volume ratio of bio-adhesive particulate systems promote regional concentration and biodistribution, making them well-suited for retention in the vaginal mucosa. By delivering particles directly to the site of action, they effectively prevent HIV transmission during sexual intercourse. While the trend in HIV prevention is towards long-acting systemic formulations, intra-vaginal DT offers a novel on-demand option for HIV-negative men and women.

The successful production of drug-loaded S-Alg-based bio-adhesive microspheres by ionotropic gelation technique employing a mixture of cellulose polymers is a significant advancement. These microspheres not only adhere well to the mucosal surface but also display a controlled release of TDF. When loaded into meltable pessaries for intra-vaginal delivery, these microspheres maintained inhibitory concentration during the crucial initial hours of insertion, which is vital for ensuring adequate protection against HIV transmission. This novel approach with TDF pessaries presents a promising platform for protecting HIV-uninfected individuals from acquiring HIV.

Timely delivery of TDF directly to the portal of entry of the pathogen using these pessaries represents a novel strategy that would effectively prevent HIV transmission during sexual intercourse. While the trend in HIV prevention leans toward long-acting systemic formulations, these pessaries offer a novel, promising on-demand pre-

exposure prophylactic self-protective platform for HIV-negative women. The proposed novel pessaries are likely to bring about a paradigm shift in PrEP management of HIV.

Furthermore, the acceptability and desirability of new dosage forms for HIV prevention are essential factors to consider. User preferences play a role in the successful implementation and uptake of preventive measures. Therefore, considering the perspectives and preferences of potential users when developing and evaluating these novel pessary formulations is crucial for their successful adoption and widespread use as an HIV prevention strategy.

BIBLIOGRAPHY

8. BIBLIOGRAPHY

1. HIV Transmission, Centers for Disease Control and Prevention. https://www.cdc.gov/hiv/basics/index.html (Accessed as on 23 January 2023)
2. Latest HIV Estimates and Update On COVID-19 Disruptions, July 2022, World Health Organisation. https://cdn.who.int/media/docs/default-source/hq-hiv-hepatitis-and-stis-library/2022_global_summary_web_v12.pdf (Accessed as on 1 February 2023)
3. Devi K and Pai RS. Antiretrovirals: Need for an effective drug delivery. Indian J. Pharm. Sci. 2006;8:1-6.
4. Peet M, Agrahari V, Anderson S, et al. Topical inserts: A versatile delivery form for HIV prevention. Pharm. 2019;11:1-17.
5. Grande F, Ioele G, Occhiuzzi MA, et al. Reverse transcriptase inhibitors nanosystems designed for drug stability and controlled delivery. Pharm. 2019;11:1-26.
6. Vyslouzil J, Kubova K, Tkadleckova VN, et al. Clinical testing of antiretroviral drugs as future prevention against vaginal and rectal transmission of HIV infection – A review of currently available results, Acta Pharm. 2019;69:297–319.
7. Patki M, Vartak R, Jablonski J, et al. Efavirenz nanomicelles loaded vaginal film (EZ film) for preexposure prophylaxis (PrEP) of HIV. Colloids and Surfaces B: Biointerfaces. 2020. https://doi.org/10.1016/j.colsurfb.2020.111174
8. Gov H. Pre-exposure prophylaxis, https://www.hiv.gov/hiv-basics/hiv-prevention/using-hivmedication-to-reduce-risk/pre-exposure-prophylaxis. (Accessed as on 15 December 2022).

9. Arnold EAA. Qualitative study of provider thoughts on implementing pre-exposure prophylaxis (PrEP) in clinical settings to prevent HIV infection. PLoS One. 2012;e40603. https://doi.org/10.1371/journal.pone.0040603.
10. Tetteh RA. Pre-exposure prophylaxis for HIV prevention: Safety concerns. Drug Saf. 2017;40:273-283. https://doi.org/10.1007/s40264-017-0505-6.
11. USFDA. FDA approves second drug to prevent HIV infection as part of ongoing efforts to end the HIV epidemic, https://www.fda.gov/news-events/press-announcements/fda-approves-seconddrug-prevent-hiv-infection-part-ongoing-efforts-end-hiv-epidemic. 2019. (Accessed as on 4 March 2020)
12. Mesquita M, Galante J, Nunes R, et al. Pharmaceutical vehicles for vaginal and rectal administration of anti-HIV microbicide nanosystems. Pharm. 2019;11:1-20.
13. Blakney AK, Jiang Y, Woodrow KA. Application of electrospun fibers for female reproductive health. Drug Deliv. Transl. Res. 2017;7:796–804.
14. Jalalvandi E, Jafari H, Amorim CA, et al. Vaginal administration of contraceptives. Sci. Pharm. 2021;89:3. https://doi.org/10.3390/scipharm89010003
15. Veiga-Ochoa M, Ruiz-Caro R, Cazorla-Luna R, et al. Vaginal formulations for prevention of sexual transmission of HIV. Adv. HIV AIDS Control. 2018;3:227-248.
16. Celum A and Baeten JM. Tenofovir-based pre-exposure prophylaxis for HIV prevention: Evolving evidence. Curr.Opin. Infect. Dis. 2012;25:51–57.
17. Watkins ME, Wring S, Randolph R, et al. Development of a novel formulation that improves preclinical bioavailability of tenofovir disoproxil fumarate. J. Pharm. Sci. 2017;106:906-919.
18. Date A. and Destache CJ. A review of nanotechnological approaches for the prophylaxis of HIV/AIDS. Biomaterials. 2013;34:6202-6228.

19. Mesquita PMM, Rastogi R, Segarra TJ, et al. Intravaginal ring delivery of tenofovir disoproxil fumarate for prevention of HIV and herpes simplex virus infection. J. Antimicrob. Chemother. 2012;67:1730–1738.
20. Cazorla-Luna R, Notario-Perez F, Martin-Illana A, et al. Chitosan-based mucoadhesive vaginal tablets for controlled release of the anti-HIV drug tenofovir. Pharm. 2019;11:1-19.
21. Chapman TM, McGavin JK, Noble S. Tenofovir disoproxil fumarate. Drug. 2003;63:1597-1608.
22. Rahman SS, Ahmed AB. Vaginal drug delivery system a promising approach for antiretroviral drug in the prevention of HIV infection: A review. J. Pharm. Sci. & Res. 2016;8:1330-1338.
23. Mohideen M, Quijano E, Song E, et al. Degradable bioadhesive nanoparticles for prolonged intravaginal delivery and retention of elvitegravir. Biomaterials. 2017;144:144–154.
24. Dedeloudi A, Siamidi A, Pavlou P, et al. Recent advances in the excipients used in modified release vaginal formulations. Materials. 2022;15:327. https://doi.org/10.3390/ma15010327
25. Jhaveri J, Raichura Z, Khan T, et al. Chitosan nanoparticles-insight into properties, functionalization and applications in drug delivery and theranostics. Molecules. 2021;26:272. https://doi.org/10.3390/molecules26020272
26. Herdiana Y, Wathoni N, Shamsuddin S, et al. Drug release study of the chitosan-based nanoparticles. Heliyon. 2022;8. https://doi.org/10.1016/j.heliyon.2021.e08674

27. Lucio D, Martinez-Oharrix MC. Chitosan: Strategies to increase and modulate drug release rate. In J Biological Activities and App Marine Polysaccharides, 2017. https://doi.org/10.5772/65714

28. Letocha M, Miastkowska E, Sikora A. Preparation and characteristics of alginate microparticles for food, pharmaceutical and cosmetic applications, Polymers. 2022;14:3834. https://doi.org/10.3390/polym14183834.

29. Hariyadi, D.M. and Islam, N. Current Status of Alginate In Drug Delivery. Adv. Pharmacol. Pharma. Sci. 2020. https://doi.org/10.1155/2020/8886095

30. Kumar K, Dhawan N, Sharma H, Vaidya S, Vaidya B. Bioadhesive polymers: Novel tool for drug delivery, Artificial Cells, Nanomed. Biotech. 2014;42:274-283. https://doi.org/10.3109/21691401.2013.815194.

31. Das Neves J, Nunes R, Machado A, Sarmento B. Polymer-based nanocarriers for vaginal drug delivery. Adv. Drug Deliv. Rev. 2015;92:53–70.

32. Ham AS, Buckheit RW, Designing and developing suppository formulations for anti-HIV drug delivery. Ther. Deliv. 2017;9:805-817.

33. Xu S, Sun L, Liu X, Zhan P. Opportunities and challenges in new HIV therapeutic discovery: What is the next step?, Expert Opinion on Drug Discovery.2023;18:1195-1199. https://doi.org/10.1080/17460441.2023.2246872

34. Gatto GJ, Krovi A, Li L, Massud I, Holder A, Gary J, et al., Comparative pharmacokinetics and local tolerance of tenofovir alafenamide (TAF) from subcutaneous implant in rabbits, dogs, and macaques. Front Pharmacol. 2022;13:923-54.

35. Paredes A, Volpe-Zanutto F, Vora L, Tekko I, Permana A, Picco C, et al., Systemic delivery of tenofovir alafenamide using dissolving and implantable microneedle patches. Materials Today Bio. 2022;13:1-14.
36. Sankaraiah J, Sharma N, Naim J. Formulation and development of fixed-dose combination of bi-layer tablets of efavirenz, lamivudine and tenofovir disoproxil fumarate tablets 600 mg/300 mg/300 mg. Int J App Pharm. 2022;14:185-97.
37. Sneller M, Blazkova J, Justement S, Shi V, Kennedy B, Gittens K et al., Combination anti-HIV antibodies provide sustained virological suppression. Nature. 2022;606:375-95.
38. Cobb D, Smith N, Deodhar S, Bade A, Gautam N, Shetty B, et al., Transformation of tenofovir into stable ProTide nanocrystals with long-acting pharmacokinetic profiles. Nat Comm. 2021;12:1-16.
39. Godela R, Kammari V, Gummadi S and Beda D. Concurrent estimation of lamivudine, tenofovir disoproxil fumarate, and efavirenz in blended mixture and triple combination tablet formulation by a new stability indicating RP-HPLC method. Future J Pharm Sci. 2021;7: 1-12.
40. Thoueille P, Choong E, Cavassini M, Buclin T and Decosterd L. Long-acting antiretrovirals: A new era for the management and prevention of HIV infection. J Antimicrob Chemother. 2021;324:1-13.
41. Lee S, Kim E, Moon S, Jung J, Lee S and Yu K. Comparative pharmacokinetics between tenofovir disoproxil phosphate and tenofovir disoproxil fumarate in healthy subjects. Transl Clin Pharmacol. 2021;29:45-52.
42. Jhunjhunwala K, Dobard CW, Sharma S, Makarova N, Holder A, Dinh C, et al., Development, characterization and in vivo pharmacokinetic assessment of rectal

suppositories containing combination antiretroviral drugs for HIV prevention. Pharmaceutics. 2021;13:1110-27.

43. Pashayan M, Hovhannisyan H. Development of bifunctional vaginal suppositories by joint use terconazole and probiotic for treatment and prophylaxis of vulvovaginal candidiasis. Drug Development and Industrial Pharmacy 2021. https://doi.org/10.1080/03639045.2021.2001485
44. Osmałek T, Froelich A, Jadach B, Tatarek A, Gadzi´nski P, Falana A, et al., Recent advances in polymer-based vaginal drug delivery systems. Pharmaceutics. 2021;13:884-932.
45. Sailaja I, Baghel M and Shaker I, Nanotechnology based drug delivery for HIV-AIDS treatment. Intechopen. 2021. https://doi.org/10.5772/intechopen.97736
46. Patel A, Patel J. Mucoadhesive in-situ gel formulation for vaginal delivery of tenofovir disoproxil fumarate. Indian J Pharm Edu Res. 2020;54:963-70.
47. Kim YH, Kim YC, Kim JY, Byeon J, Maeng HJ, Kim ST, et al., Preparation and characterization of tenofovir disoproxil-loaded enteric microparticle. J Nanosci Nanotechnol. 2020;20:5796-9.
48. Rao R, Jayasawal P and Tangri P. Development and evaluation of tenofovir disoproxil fumarate based microsponge loaded gel. Int J Pharm Technol. 2020;12:32296-311.
49. Fernandes T, Baxi T, Sawarkar S, Sarmento B, das Neves J. Vaginal multipurpose prevention technologies: promising approaches for enhancing women's sexual and reproductive health, Expert Opinion on Drug Delivery. 2020. https://doi.org/10.1080/17425247.2020.1728251

50. Gada S, Anandkumar Y and Setty M. Preparation, evaluation and stability of lamivudine loaded alginate-tamarind mucilage microspheres. Int J App Pharma. 2019;11:365-70.
51. Elsayed M. Controlled release alginate-chitosan microspheres of tolmetin sodium prepared by internal gelation technique and characterized by response surface modeling. Braz. J. Pharm. Sci. 2020;56. https://doi.org/10.1590/s2175-97902020000118414
52. Thulluru A, Varma M, Setty C, et al. Effect of sodium alginate in combination with HPMC K 100 M in extending the release of metoprolol succinate from its gastro-retentive floating tablets. Indian J. Pharm. Edu. Res. 2015;49:293-303.
53. Kurmi M, Golla VM, Kumar S, Sahu A, Singh S. Stability behaviour of antiretroviral drugs and their combinations: Characterization of tenofovir disoproxil fumarate degradation products by mass spectrometry. RCS Adv. 2013;1-14.
54. Wiriyakosol N, Puangpetch A, Manosuthi W, Tomongkon S, Sukasem C, Pinthong D. A LC/MS/MS method for determination of tenofovir in human plasma and its application to toxicity monitoring. J Chromb. 2018; 1-25.
55. Hiorth M, Nilsen S, Tho I. Bioadhesive mini-tablets for vaginal drug delivery. Pharma. 2014;6:494-511.
56. AbdelHay H, Gazy A, Shaalan RA, Ashour HK. Simple spectrophotometric methods for determination of tenofovir fumarate and emtricitabine in bulk powder and in tablets. J Spectroscopy. 2013;1-7.
57. Venkatesan S, Kannappan N. Simultaneous spectrophotometric method for determination of emtricitabine and tenofovir disoproxil fumarate in three-

component tablet formulation containing rilpivirine hydrochloride. Int Scholarly Res Notices. 2014;1-4.

58. Bazzo GC, Mostafa D, França MT, Pezzini BR, Stulzer HK. How tenofovir disoproxil fumarate can impact on solubility and dissolution rate of efavirenz?. Int J Pharm. 2019;1-7.
59. Mandal S, Kumar S, Krishnamoorthy B, et al., Development and evaluation of calcium alginate beads prepared by sequential and simultaneous methods. Brazilian J. Pharm. 2010;46:785-793.
60. Khan A, Thakur R. Formulation and evaluation of mucoadhesive microspheres of tenofovir disoproxil fumarate for intravaginal use. Curr. Drug Del. 2014;11:112-122.
61. Nesalin J, Smith A. Preparation and evaluation of stavudine loaded chitosan nanoparticles. J. Pharm. Res. 2013;6:268-274.
62. Nagpal M, Maheshwari DK, Rakha P, et al. Formulation development and evaluation of alginate microspheres of ibuprofen. J. Young Pharm. 2012;4:13-16.
63. Shivakumar HN, Vaka SRK, Murthy SN. Albumin microspheres for oral delivery of iron. J. Drug Target. 2010;18:36-44.
64. Cazorla-Luna R, Notario-Perez F, Martin-Illana A, et al., Chitosan-based mucoadhesive vaginal tablets for controlled release of the anti-HIV drug tenofovir. Pharm. 2019;11:1-19.
65. Dahmane E, Rhazi M, Taourirte M. Chitosan nanoparticles as a new delivery system for the anti-HIV drug zidovudine. Bull. Korean Chem. Soc. 2013;34:1333. https://doi.org/10.5012/bkcs.2013.34.5.1333

66. Beg S, Rahman M, Panda SK, et al., Nasal mucoadhesive microspheres of lercanidipine with improved systemic bioavailability and antihypertensive activity. J. Pharm. Innov. 2020. https://doi.org/10.1007/s12247-020-09441-5

67. Hani U, Shivakumar HG, Gowrav MP. Formulation design and evaluation of a novel vaginal delivery system of clotrimazole. Int. J. Pharm. Sci. Res. 2014;5:220-227. https://doi.org/10.13040/IJPSR.0975-8232.5(1).220-27

68. Sinko PJ. Micromeritics. In Martin's Physical Pharmacy and Pharmaceutical Sciences, 5th ed.; Lippincott Williams & Wilkins, Philadelphia, 2006; pp 535-537.

69. Gomes E, Mussel W, Resende JM, et al., Characterization of tenofovir disoproxil fumarate and its behavior under heating. Cryst. Growth Des. 2015;15:1915-1922.

70. Deveswaran R, Bharath S, Basavaraj BV, et al., Development of mesalazine microspheres for colon targeting. Int. J. Appl. Pharm. 2017;9:1-9.

71. Goudarzi NM, Samaro A, Vervaet C, et al. Development of flow-through cell dissolution method for in situ visualization of dissolution processes in solid dosage forms using X-ray_CT. Pharm. 2022;14:2475. https://doi.org/10.3390/pharmaceutics14112475

72. Sievens-Figueroa L, Pandya N, Bhakay A, et al., Using USP I and USP IV for discriminating dissolution rates of nano- and microparticle-loaded pharmaceutical strip-films. AAPS Pharm. Sci. Tech. 2012;13:1473-1482.

73. Gao Z. *In Vitro* dissolution testing with flow-through method: A technical note. AAPS Pharm. Sci. Tech. 2009;10:1401-1405.

74. Szekalska M, Wróblewska M, Czajkowska-Ko´snik A, et al. The spray-dried alginate/gelatin microparticles with luliconazole as mucoadhesive drug delivery system. Materials. 2023;16:403. https://doi.org/10.3390/ma16010403

75. Swain S, Behera U, Beg S, et al. Design and characterization of enteric-coated controlled release mucoadhesive microcapsules of rabeprazole sodium. Drug. Dev. Ind. Pharm. 2013;39:548-460.

76. Panchagnula CS, Naware NB, Bhamre SS, et al. Formulation and development of novel and stable dosage forms of lamivudine and tenofovir disoproxil fumarate tablets by wet granulation technique. Int. J. Pharm. Sci. Res. 2018;9:3538-3542.

77. Khan AB, Thakur R. Design and evaluation of mucoadhesive vaginal tablets of tenofovir disoproxil fumarate for pre-exposure prophylaxis of HIV. Drug Dev. Indus. Pharm. 2017. https://doi.org/10.1080/03639045.2017.1399272

78. Tests for Tablets. In Indian Pharmacopoeia, Government of India, Ministry of Health and Family Welfare Department, 9th ed.; Indian Pharmacopoeia Commission: Ghaziabad, India, 2023; Vol 1 and 2 pp: 356-360 and 1342-1344.

79. Zandu SK, Kumari R, Singh I. Formulation and evaluation of fast disintegrating tablets of domperidone using chitosan-glycine conjugates as superdisintegrant. Thai J. Pharm. Sci. 2020;45:32-40.

80. Brahmankar DM, Jaiswal SB. Bioavailability and Bioequivalence. In Biopharmaceutics and Pharmacokinetics – A Treatise, 2nd ed.; Vallabh Prakashan: Delhi, India, 2009, pp: 331-332.

81. Rawat S, Bisht S, Kothiyal P. Characterization and release kinetics of microspheres and tableted microspheres of diclofenac sodium. American J. Adv. Drug Del. 2013;1:596-605.

82. Das M, Maurya D. Evaluation of diltiazem hydrochloride-loaded mucoadhesive microspheres prepared by emulsification-internal gelation technique. Acta Poloniae Pharmaceutica. Drug Res. 2008;65:249-59.

83. Letocha A, Miastkowska M, Sikora E. Preparation and characteristics of alginate microparticles for food, pharmaceutical and cosmetic applications, Polymers. 2022;14:3834. https://doi.org/10.3390/polym14183834.

84. Uyen NTT, Abdul Hamida ZA, Nurazreena A. Fabrication and characterization of alginate microspheres, Materials Today: Proceedings. 2019;17:792–797.

85. Tarani E, Arvanitidis I, Christofilos D, Bikiaris DN, Chrissafis K, Vourlias G. Calculation of the degree of crystallinity of HDPE/GNPs nanocomposites by using various experimental techniques: A comparative study, J. Mater. Sci. 2023;58:1621-1639.

86. Aleem O, Kuchekar B, Pore Y, Late S. Effect of β-cyclodextrin and hydroxypropyl β-cyclodextrin complexation on physicochemical properties and antimicrobial activity of cefdinir J. Pharm. Biomed. Anal. 2008;47:535-540.

87. Baviskar P, Jaiswal S, Sadique S, Landged A. Formulation and evaluation of lornoxicam suppositories. J. Pharm. Innov. 2013;2:20.

88. Salunkhe NH, Jadhav NR, Mali KK, Dias RJ, Ghorpade VS, Yadav AV. Mucoadhesive microsphere based suppository containing granisetron hydrochloride for management of emesis in chemotherapy, J. Pharm. Investig. 2014;44:253-263.

89. Tests for Pessaries, in Indian Pharmacopoeia, Government of India, Ministry of Health and Family Welfare Department, 9th ed,; Indian Pharmacopoeia Commission: Ghaziabad, India, 2023; Vol 1 and 2, pp. 356-360 and 1342-1344.

90. El-Majri MA, El-Basir MM. Formulation and evaluation of ibuprofen suppositories. J. Res. Pharm. Pract. 2016;7:87-90.

91. Castner CS. Cocoa butter composition and method of making the same, US Patent. https://patents.google.com/patent/US3862197A/en. 1974 (accessed 4 May 2023).

92. Goudarzi NM, Samaro A, Vervaet C, et al. Development of flow-through cell dissolution method forin situ visualization of dissolution processes in solid dosage forms using X-ray_CT. Pharm. 2022;14:2475. https://doi.org/10.3390/pharmaceutics14112475

93. Rabbit Anaesthesia. https://research.utexas.edu/wp-content/uploads/sites/7/2020/02/Rabbit_Anesthesia_guidance_ARC.pdf, 2022 (accessed January 14, 2022).

94. Ajayi A, Akhigbe RE. Staging of the estrous cycle and induction of estrus in experimental rodents: An update, Fertility Res. Pract. 2020;6:5. https://doi.org/10.1186/s40738-020-00074-3.

95. Clark M, Friend DR. Pharmacokinetics and topical vaginal effects of two tenofovir gels in rabbits. AIDS Res. Human Retrovir. 2012;1458-66.

96. Cunha-Reis C, Machado A, Barreiros L, et al., Nanoparticles-in-film for the combined vaginal delivery of anti-HIV microbicide drugs. J. Controlled Release. 2016. https://doi.org/doi:10.1016/j.jconrel.2016.09.020.

97. Helmiyati, Aprilliza M. Characterization and properties of sodium alginate from brown algae used as an ecofriendly superabsorbent, IOP Conf. Ser.: Mater. Sci. Eng. 2017;188:012019.

98. Fatmanur T, Acarturk A, Ozkul A. Preparation and characterization of bioadhesive controlled-release gels of cidofovir for vaginal delivery. J Biomaterials Sci. 2015:1-39.
99. Tenofovir Disoproxil Fumarate. Drug Bank Online. https://go.drugbank.com/salts/DBSALT000172 (Accessed as on 3 December 2019)
100. Calderon L, Harris R, Diaz M, et al. Nano and microparticulate chitosan-based systems for antiviral topical delivery. European J. Pharm. Sci. 2013;48:216-222.
101. Ko JA, Park HJ, Hwang SJ, et al. Preparation and characterization of chitosan microparticles intended for controlled drug delivery. Int. J. Phar. 2002;249:165-174.
102. Pandit K, Nanayakkara IA, Cao W, et al. capture and direct amplification of DNA on chitosan microparticles in a single PCR-optimal solution. Anal. Chem. 2015;87:11022−11029.
103. Subedi G, Shrestha A, Shakya S. Study of effect of different factors in formulation of micro and nanospheres with solvent evaporation technique. Open Pharm. Sci. J. 2016;3:182-195.
104. Akbari J, Reza E, Majid S, et al. Influence of hydroxypropyl methylcellulose molecular weight grade on water uptake, erosion and drug release properties of diclofenac sodium matrix tablets. Trop. J. Pharm. Res. 2011;5:535-541.
105. Sinha RD, Rohera BD. Comparative evaluation of rate of hydration and matrix erosion of HEC and HPC and study of drug release from their matrices. Eur. J. Pharm. Sci. 2002;16:193-199.
106. Patel K, Patel M. Preparation and evaluation of chitosan microspheres containing nicorandil. Int. J. Pharm. Inves. 2014;4:32-37.

107. Patil SB, Sawant KK. Chitosan microspheres as a delivery system for nasal insufflations. Colloids Surf. B Biointerfaces. 2011;84:384-389.

108. Danaei M, Dehghankhold M, Ataei S, et al. Impact of particle size and polydispersity index on the clinical applications of lipidic nanocarrier systems. Pharm. 2018;10:57. https://doi.org/10.3390/pharmaceutics10020057

109. Chen W, Palazzo A, Hennink W, et al. The effect of particle size on drug loading and release kinetics of gefitinib-loaded plga microspheres. Mol. Pharm. 2016. https://doi.org/10.1021/acs.molpharmaceut.6b00896

110. Bullet E, Sanli O. Novel ionically crosslinked acrylamide-grafted poly(vinyl alcohol)/sodium alginate/sodium carboxymethyl cellulose ph-sensitive microspheres for delivery of alzheimer's drug donepezil hydrochloride: Preparation and optimization of release conditions. Artificial Cells, Nanomed. Biotechnol. 2016;44:431-442. https://doi.org/10.3109/21691401.2014.962741

111. Meng J, Sturgis T, Youan B. Engineering tenofovir loaded chitosan nanoparticles to maximize microbicide mucoadhesion. European J. Pharm. Sci. 2011;44:57-67.

112. Zaman M, Butt MH, Siddique W, et al. Fabrication of PEGylated chitosan nanoparticles containing tenofovir alafenamide: Synthesis and characterization. Molecules. 2022;27:8401. https://doi.org/10.3390/molecules27238401

113. Martin A, Oliveira D, Pereira A, et al. Chitosan/TPP microparticles obtained by microemulsion method applied in controlled release of heparin. Int. J. Biological. Macromol. 2012;51:1127-1133.

114. Patil S, Kadam C, Pokharkar V. QbD based approach for optimization of tenofovir disoproxil fumarate loaded liquid crystal precursor with improved permeability. J. Adv. Res. 2017;8:607-616.

115. Safari JB, Bapolisi AM, Krause RWM. Development of pH-sensitive chitosan-g-poly(acrylamide-co-acrylic acid) hydrogel for controlled drug delivery of tenofovir disoproxil fumarate. Polymers. 2021;13:3571. https://doi.org/10.3390/polym13203571

116. Vedha H, Narayanan B, Lewandowski A, et al. Spray-dried tenofovir alafenamide-chitosan nanoparticles loaded oleogels as a long-acting injectable depot system of anti-HIV drug. Int. J. Biological Macromol. 2022;222:473-486.

117. Cazorla-Luna R, Notario-Perez F, Martin-Illana A, et al., Chitosan-based mucoadhesive vaginal tablets for controlled release of the anti-HIV drug tenofovir. Pharm. 2019;11:1-19.

118. Khar R, Vyas SP, Ahmad FJ, et al. Tablets. In Lachman/Liberman's The Theory And Practice of Industrial Pharmacy, 4th ed.; CBS Publishers & Distributors Pvt Ltd, India, 2013; pp 449-545.

119. Anraku M, Mizukai Y, Maezaki Y, et al. The preparation and validation of chitosan tablets that rapidly disperse and disintegrate as an oral adsorbent in the treatment of lifestyle-related diseases. Carb. Polymers. 2021;253. https://doi.org/10.1016/j.carbpol.2020.117246.

120. Frent OD, Vicas LG, Duteanu N, et al., Sodium alginate—Natural microencapsulation material of polymeric microparticles. Int. J. Mol. Sci. 2022;23:12108. https://doi.org/10.3390/ijms232012108.

121. Zhang C, Grossier R, Candoni N, Veesler S. Preparation of alginate hydrogel microparticles by gelation introducing cross-linkers using droplet-based microfluidics: A review of methods. Biomat. Res. 2021;25:41. https://doi.org/10.1186/s40824-021-00243-5.

122. Siddam H, Kotla NG, Maddiboyina B, et al., Formulation and evaluation of atenolol floating bioadhesive system using optimized polymer blends, Int. J. Pharm. Investig. 2016;6:116.

123. Vaka SRK, Shivakumar HN, Repka M, Murthy N. Formulation and evaluation of carnosic acid nanoparticulate system for upregulation of neutrophins in the brain. J. Drug Target. 2012;1-10.

124. Chen W, Palazzo A, Hennink W, et al., The effect of particle size on drug loading and release kinetics of gefitinib-loaded PLGA microspheres, Mol. Pharmaceutics. 2016. https://doi.org/10.1021/acs.molpharmaceut.6b00896.

125. Patel N, Lalwani D, Gollmer S, Injeti E, Sari Y, Nesamony J. Development and evaluation of a calcium alginate based oral ceftriaxone sodium formulation. Prog Biomater. 2016;5:117–133.

126. Aprilliza H. Characterization and properties of sodium alginate from brown algae used as an ecofriendly auperabsorbent, IOP Conf. Ser.: Mater. Sci. Eng. 2017;188:012019.

127. Daemi H, Barikani M. Synthesis and characterization of calcium alginate nanoparticles, sodium homopolymannuronate salt and its calcium nanoparticles. Scientia Iranica. 2012;19:2023-2028.

128. Bashir S, Zafar N, Lebaz N, Mahmood A, Elaissari A, Hydroxypropyl methylcellulose-based hydrogel copolymeric for controlled delivery of galantamine hydrobromide in dementia. Process. 2020;8:1350. https://doi.org/10.3390/pr8111350.

129. Sahoo S, Chakraborti CK, Behera PK. Spectroscopic investigations of a ciprofloxacin/HPMC mucoadhesive suspension. Int. J. App. Pharmaceutics. 2012;4:1-8.

130. Venkatesh DN, Meyyanathan SN, Kovacevic A, et al., Effect of hydrophilic polymers on the release rate and pharmacokinetics of acyclovir tablets obtained by wet granulation: *In vitro* and *in vivo* assays. Molecules. 2022;27:6490.

131. Hydroxypropyl Methyl Cellulose. https://www.chembk.com/en/chem/HPMC, 2022 (accessed 18 March 2022)

132. Sodium CMC. https://pubchem.ncbi.nlm.nih.gov/compound/Sodium-carboxymethyl-cellulose, 2022 (accessed 18 March 2022).

133. Frent OD, Vicas LG, Duteanu N, Morgovan CM, Jurca T, Pallag A, Muresan ME, Filip SM, Lucaciu R-L, Marian E. Sodium alginate—Natural microencapsulation material of polymeric microparticles. Int J Mol Sci. 2022; 23:12108. https://doi.org/10.3390/ijms232012108

134. Fernando NP, Illana AM, Cazorla-Luna R, et al., Development of mucoadhesive vaginal films based on HPMC and zein as novel formulations to prevent sexual transmission of HIV. Int. J. Pharm. 2019;570. https://doi.org/10.1016/j.ijpharm.2019.118643.

135. Raymond CR, Sheskey PJ, Weller P. Cellulose microcrystalline, chitosan, magnesium stearate, povidone, talc, In Handbook of Pharmaceutical Excipients, The Pharmaceutical Press and the American Pharmaceutical Association: London, USA, 2003, pp. 108-110, 132-134, 354-356, 508-512 and 641-643.

136. Witter FR, Barditch-Crovob UP, Roccob L, Trapnellc CB, Duration of vaginal retention and potential duration of antiviral activity for five nonoxynol-9 containing intravaginal contraceptives. Int. J. Gynecol. Obstetrics. 1999;65:165-170.

137. Katata-Seru L, Ojo BM, Okubanjo O, Soremekun R, Aremu OS. Nanoformulated eudragit lopinavir and preliminary release of its loaded suppositories. Heliyon. 2020;6:e03890. https://doi.org/10.1016%2Fj.heliyon.2020.e03890.

138. Zandu SK, Kumari R, Singh I. Formulation and evaluation of fast disintegrating tablets of domperidone using chitosan-glycine conjugates as superdisintegrant. Thai J. Pharm. Sci. 2020;45:32-40.

139. Best BM, Letendre SL, Koopmans P, et al., Low CSF concentrations of the nucleotide HIV reverse transcriptase inhibitor, tenofovir. Acquir. Immune Defic. Syndr. 2012;59:376–381. https://doi.org/10.1097/QAI.0b013e318247ec54.

140. Moss JA, Malone AM, Smith TJ, et al., Simultaneous delivery of tenofovir and acyclovir via an intravaginal ring. Antimicrobial Agents Chemother. 2011;875-882.

ANNEXURES

9. ANNEXURES

9.1. Ethical Clearance Letter

KLE ACADEMY OF HIGHER EDUCATION & RESEARCH, BELAGAVI
(Formerly known as KLE University's)
KLE College of Pharmacy
(Re-Accredited by NBA, Approved by PCI and AICTE - New Delhi)
[Declared as Deemed-to-be-University under section 3 of the UGC Act, 1956 vide Government of India Notification No F.9-19/2000U.3(A)]
[A constituent unit of the KAHER, Belagavi]
2nd Block, Rajajinagar, Bengaluru - 560 010, Karnataka, India.
☎ 080-23325611 FAX No. : 080-23425373 Web http://www.kleblrpharm.org E-mail : princpharmblr@kledeemeduniversity.edu.in

Ref No. KLE/COPBLR/ Date : ....

INSTITUTIONAL ANIMAL ETHICS COMMITTEE CERTIFICATE

This is to certify that the project proposal no 05/ HNSK /2021entitled "Formulation and Evaluation of Vaginal Drug Delivery System of Tenofovir : An Experimental Study" submitted by Ms Dhruti Avlani has been approved /recommended by the IAEC of KLE College of Pharmacy,Bengaluru in its meeting dated 12/10/2021 and has been sanctioned 24 New Zealand Rabbits under this proposal for a duration of next 12 months

Authorized by	Name	Signature	Date
Chairman:	Dr.Raman Dang		12/10/21
Member Secretary	Dr.Hariprasad M.G		12/10/21
Main Nominee of CPCSEA	Dr.Giridhar.P		12/10/21

INSTITUTIONAL ANIMAL ETHICS COMMITTEE KLE College of Pharmacy Bangalore

9.2. Presentations And Publications

PRESENTATIONS				
Sl. No.	**Date**	**Type**	**Presented At**	**Title**
1	27th - 28th August 2022	E-Oral	International conference on "Pharma Summit 2022: Drug Discovery and Community Trial" organized by Association of Pharmaceutical Research (APR)	Formulation and Evaluation of Vaginal Drug Delivery System of Tenofovir Disoproxil Fumarate
2	2nd - 4th September 2022	Poster	25th Annual National Convention of the Association of Pharmaceutical Teachers of India – 2022 (25th APTICON – 2022)	Formulation and Evaluation of Bioadhesive Microparticulate System for Intravaginal Drug Delivery of Tenofovir Disoproxil Fumarate

PUBLICATIONS			
Sl. No.	**Date**	**Name of the Journal**	**Title**
1	1st September 2023	Molecular Pharmaceutics (IF 2023-24: 5.36)	Development of Dispersible Vaginal Tablets of Tenofovir Loaded Mucoadhesive Chitosan Microparticles for Anti-HIV Pre-Exposure Prophylaxis
2	18th December 2023	International Journal of Biological Macromolecules (IF 2023-24: 8.2)	Pre-exposure prophylactic mucoadhesive sodium alginate microsphere laden pessaries for intravaginal delivery of tenofovir disoproxil fumarate

9.2.1. Oral Presentation

Pharma Summit 2022:
Drug Discovery & Community Trial
27th & 28th August, 2022_ Virtual Conference& Expo

Formulation and Evaluation of Vaginal Drug Delivery System of Tenofovir Disoproxil Fumarate

Avlani D
Department of Pharmaceutics, KLE College of Pharmacy, 2nd Block Rajajinagar, Bengaluru
Shivakumar H.N
Department of Pharmaceutics, KLE College of Pharmacy, 2nd Block Rajajinagar, Bengaluru
Prajila A
Department of Pharmaceutics, KLE College of Pharmacy, 2nd Block Rajajinagar, Bengaluru

Abstract

The present research is aimed to develop a novel pre-exposure prophylactic bioadhesive microparticulate system for vaginal drug delivery of Tenofovir Disoproxil Fumarate (TDF) to overcome the limitations of the conventional dosage forms. Emulsification-internal gelation technique was used to prepare TDF loaded bioadhesive microparticles using sodium alginate and hydroxypropyl methyl cellulose K-100 as polymers at varying drug: polymer ratios of 1:2, 1:4 and 1:9 (EH-1 to EH-6). Scanning electron microscopy of microparticles revealed that they are spherical in shape and particle size decreases with increase in drug: polymer ratio. The entrapment efficiency of TDF in microparticles (EH-4) was found to be 62.09 ± 1.34%. FTIR results ruled out the possibilities of any chemical interaction between the drug and polymers used. DSC and XRD studies indicated that the drug existed in amorphous state in the bioadhesive polymers. Ex vivo bioadhesion studies performed on rabbit vagina showed good bioadhesion. In vitro drug release of the microparticles (EH-4) in simulated vaginal fluid was found to be in a controlled manner and displayed 93.65 ± 5.87 % to 99.19 ± 1.80 % drug release by the end of 8 hours. Thus, the formulated bioadhesive microparticles can be a promising alternative to conventional route of delivery.

Keywords
Bioadhesion, microparticles, sodium alginate, HPMC K-100, tenofovir, controlled release

ISBN: 978-93-92106-05-7

Pharma Summit 2022 : Drug Discovery & Community Trial
27th & 28th August 2022

CERTIFICATE
OF PRESENTATION

ASSOCIATION OF PHARMACEUTICAL RESEARCH

PHARMA SUMMIT 2022
DRUG DISCOVERY AND COMMUNITY TRIAL

27th & 28th August 2022 | Virtual Conference & Expo

BioLEAGUES UNITED innovators

This is to certify that Mr/Mrs/Ms/Dr. **Dhruti Avlani** of KLE College of Pharmacy, Bengaluru presented his/her worthy **E-Oral** **Presentation** titled Formulation and Evaluation of Vaginal Drug Delivery System of Tenofovir Disoproxil Fumarate in the International Conference on "Pharma Summit 2022: Drug Discovery and Community Trial" organized by Association of Pharmaceutical Research (APR) on 27th & 28th August 2022.

Dr. Anil Kharia	Ms. Priyamvada Jain	Dr. Md Salahuddin	Mr. Rudra Bhanu Satpathy
Partner - Modern Laboratories Director - Nandani Medical Laboratories Pvt Ltd Chairman - Modern Group of Institutions Indore, Madhya Pradesh, India	Associate Director-Regulatory Affairs Jubilant Generics Limited Greater Noida, Uttar Pradesh India	Principal Al-Ameen College of Pharmacy Bangalore, Karnataka India	CEO & Founder Association of Pharmaceutical Research (APR), India

9.2.2. Poster Presentation

PT/ST1/00117

Formulation and Evaluation of Bioadhesive Microparticulate System for Intravaginal Drug Delivery of Tenofovir Disoproxil Fumarate

Dhruti Avlani*, H.N. Shivakumar, Prajila A.

Department of Pharmaceutics, KLE College of Pharmacy, Bengaluru – 560010. India

*Presenting Author:
dhrutiavlani@gmail.com

Abstract: TDF loaded bioadhesive chitosan microparticles intended for Pre-exposure prophylaxis (PrEP) were prepared as an intravaginal drug delivery system to overcome the limitations of conventional oral dosage forms. Chitosan microparticles of TDF were prepared using emulsification-internal gelation technique at varying drug: polymer ratios of 1:1 to 1:4 (ECH-1 to ECH-4). Scanning electron microscopy of microparticles revealed that they are spherical in shape. Differential laser scattering analysis using Malvern Zetasizer indicated that particle size decreased with increase in drug: polymer ratio. 68.93 ± 1.76% of TDF was entrapped in the chitosan microparticles (ECH-4). FTIR results suggested an electrostatic interaction between TDF and chitosan. DSC and XRD studies suggested that the drug may be present in the molecular as well as microcrystalline state in the matrix, which could also explain the sustained drug release from the microparticles. *Ex vivo* bioadhesion studies using mucosa as a substrate indicated that 49.66 ± 8.38 % particles were retained with ECH-4 at the end of 6 h. *In vitro* drug release from the optimised formulation in simulated vaginal fluid indicated TDF was released in a sustained manner as 83.07 ± 7.29 % drug released by the end of 24 h. Thus, the formulated bioadhesive microparticles for intravaginal drug delivery system for PrEP is a promising new strategy and alternative to conventional route of delivery.

Keywords: *Bioadhesive microparticles, Chitosan, Vaginal delivery, Tenofovir, Sustained release.*

FORMULATION AND EVALUATION OF BIOADHESIVE MICROPARTICULATE SYSTEM FOR INTRAVAGINAL DRUG DELIVERY OF TENOFOVIR DISOPROXIL FUMARATE

Dhruti Avlani*, H.N. Shivakumar, Prajila A.
Department of Pharmaceutics, KLE College of Pharmacy, Bengaluru - 560010. India
*Presenting Author: dhrutiavlani@gmail.com Contact: +91-9674058488

APTICON - PT/ST1/00117

INTRODUCTION

- **HIV** - Human Immunodeficiency Virus attacks and destroys the infection-fighting CD4 cells of the immune system.
- **Mode of Transmission:**
  - Blood, Semen
  - **Intercourse (vaginal, anal or oral)**
  - Needles, Surgical blades, etc.

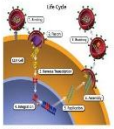

Fig 1: HIV life cycle

- **HIV Prevention:**
  - **Pre-exposure Prophylaxis (PrEP)**
  - Post-exposure Prophylaxis (PEP)
  - Mother-to-Child Transmission

NEED FOR THE STUDY

Table 1: FDA approved Anti-HIV Medicines

PRODUCT	DOSAGE FORM	MFG. BY
Viread® (TDF)	**Oral Tablets**	Gilead Sciences Inc.
Epivir® (Lamivudine)	**Oral Tablets** **Oral Solution**	ViiV Healthcare
Emtriva® (Emtricitabine)	**Oral Capsules** **Oral Solution**	Gilead Sciences Inc.
Truvada® (TDF – Emtricitabine)	**Oral Tablets**	Gilead Sciences, Inc
Descovy® (TAF – Emtricitabine)	**Oral Tablets**	Gilead Sciences, Inc

After an Anti-HIV drug is absorbed and enters the blood circulation, metabolism/elimination and transport barriers substantially ↓ the effective amount of drug reaching the target action site.

VAGINAL DRUG DELIVERY

- Increased local absorption of drug substances due to large surface area
- Enhanced bioavailability
- Minimal off-target systemic side effects
- Relatively low enzymatic activity

NOVEL TOPICAL INSERTS

- Deliver drugs to the portal of viral entry
- Low systemic exposure
- Dissolve fats, release the active drugs within minutes of insertion
- Controlled drug delivery

Fig 2: Vaginal dosage forms

OBJECTIVE: To formulate and evaluate bioadhesive chitosan microparticles for intravaginal drug delivery of Tenofovir to overcome the limitations of the conventional dosage forms.

METHODOLOGY

EMULSIFICATION - INTERNAL GELATION METHOD

Dispersed Phase (Drug Chitosan) + **Continuous Phase** (Light Liquid Paraffin + 1.5%v/v Span 80) + **Cross-Linking Agent** (Na Tripolyphosphate Solution)

Stirring @ 500 rpm
Homogenisation @ 3000 rpm, 15 mins

Emulsion

Centrifugation @ 4000 rpm, 30 mins
Decantation of Oil
Wash with Petroleum Ether
Air dry at room temperature

DRIED MICROPARTICLES

ABOUT THE DRUG: TENOFOVIR DISOPROXIL FUMARATE (TDF)

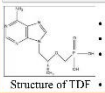

Structure of TDF

- Molecular Formula : $C_{23}H_{34}N_5O_{14}P$
- Molecular Weight : 635.5 g/mol
- Category : Antiretroviral (Nucleoside Reverse Transcriptase Inhibitor)
- Melting Point : 116.74°C

Table 2: Composition & physicochemical characterisation of chitosan microparticles

E. Code	Drug (%)	Chitosan (%)	Na-TPP (%)	Practical Yield (%)	Drug Entrapment Efficiency (%)
ECH-1	1.0	1.0	10.0	48.75	16.812 ± 0.862
ECH-2	1.0	2.0	10.0	67.50	34.859 ± 1.615
ECH-3	1.0	3.0	10.0	78.83	51.449 ± 0.905
ECH-4	1.0	4.0	10.0	90.80	68.931 ± 1.768

Fig 6: FTIR spectrum of formulation ECH-4

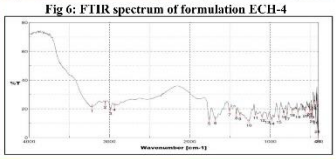

RESULTS

Fig 3: Cumulative dissolution profile of chitosan microparticles

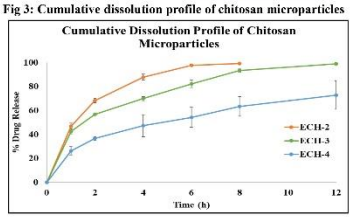

Fig 4: Comparative graph of *ex vivo* bioadhesion of particles & *in vitro* drug release of formulation ECH-4

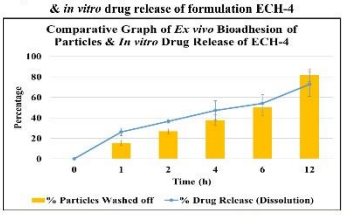

Fig 5: SEM photomicrograph & particle size analysis of formulation ECH-4

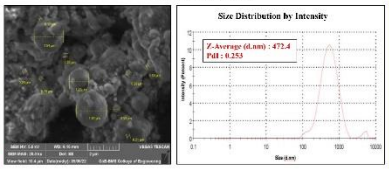

Fig 7: DSC thermogram of formulation ECH-4

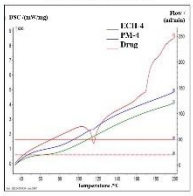

Fig 8: XRD diffractogram of formulation ECH-4

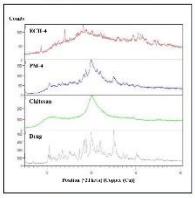

DISCUSSIONS

68.93 ± 1.76% of TDF was entrapped in the chitosan microparticles (ECH-4).

***In vitro* drug release** from ECH-4 in simulated vaginal fluid (pH 4.5) indicated TDF was released in a sustained manner as 83.07 ± 7.29 % drug released by the end of 24 h.

***Ex vivo* bioadhesion** studies using mucosa as a substrate indicated that 49.66 ± 8.38 % particles were retained with ECH-4 at the end of 6 h.

Scanning electron microscopy of microparticles revealed that they are spherical in shape.

Differential laser scattering analysis using Malvern Zetasizer indicated that particle size ↓ with ↑ in drug: polymer ratio.

FTIR results suggested an electrostatic interaction between TDF and chitosan.

DSC and XRD studies suggested that the drug may be present in the molecular as well as microcrystalline state in the matrix, which could also explain the sustained drug release from the microparticles.

Thus, the formulated bioadhesive microparticles for intravaginal drug delivery system for PrEP is a promising new strategy.

CONCLUSION

- ✓ TDF oral administration is limited by several factors leading to low bioavailability (25-30%).
- ✓ The vaginal route is usually investigated as an administration site for topically acting active ingredients as the anatomical and physiological features of the vagina make it suitable also for drug absorption.
- ✓ ↑ Surfactant concentration → Smoother and slightly porous surface of the microsphere.
- ✓ *Ex vivo* bioadhesion studies indicated that 49.66 ± 8.38 % particles were retained on the substrate at the end of 6 h and the *in vitro* drug release studies confirmed that 54.26 ± 8.224 % drug released in a sustained manner by the end of 6 h.
- ✓ Thus, the formulated bioadhesive microparticles for intravaginal delivery can be a promising alternative to conventional route of delivery and demonstrates the potential to bridge gaps in preventative sexual and reproductive health care.

ACKNOWLEDGEMENT

I am thankful to KLE College of Pharmacy, Bengaluru for providing the infrastructure and library facilities. I respect and convey my sincere thanks and a sense of gratitude to **The Principal, KLECOP** for providing me with all the necessary facilities. I owe my profound gratitude to **Dr. H.N. Shivakumar (Guide)** for taking keen interest in my topic and guiding me. I would also thank my co-authors and my parents for the unceasing encouragement & support.

REFERENCES

1. Cazorla-Luna R, Notario-Perez F, Martin-Illana A, Ruiz-Caro R, Tamayo A, Rubio J, et al. Chitosan-based mucoadhesive vaginal tablets for controlled release of the anti-HIV drug Tenofovir. Pharm 2019;11(20):1-19.
2. Nesalin A, Smith A. Preparation and evaluation of stavudine loaded chitosan nanoparticles. J Pharm Res 2013;268-74.
3. Khan A, Thakur R. Formulation and evaluation of mucoadhesive microspheres of Tenofovir Disoproxil Fumarate for intravaginal use. Curr Drug Del 2014;11:112-22.

Presented at 25th Annual National Convention of Association of Pharmaceutical Teachers of India 2022 on Empowering Academia for Advancing Pharmacy Education organized by JSS College of Pharmacy, Mysuru, Karnataka & APTI from 2nd to 4th September 2022 at JSS College of Pharmacy, Mysuru, Karnataka, India.

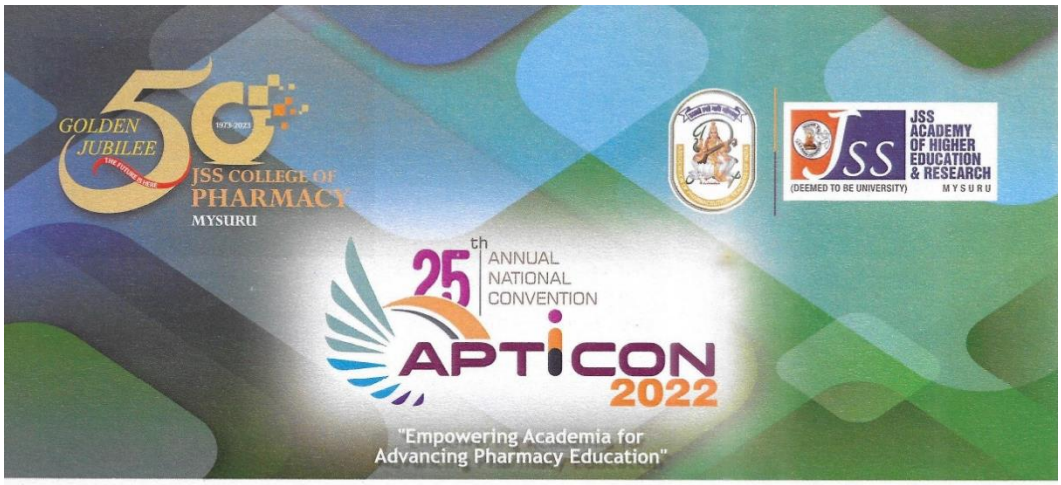

ASSOCIATION OF PHARMACEUTICAL TEACHERS OF INDIA (APTI)
AND
JSS COLLEGE OF PHARMACY, MYSURU
JSS ACADEMY OF HIGHER EDUCATION & RESEARCH, MYSURU

CERTIFICATE

OF APPRECIATION

This is to Certify that

Dr./Mr./Ms. *Dhruti Avlani*

has participated as a Delegate and Presented a Poster entitled "Formulation And Evaluation Of Bioadhesive Microparticulate System For Intravaginal Drug Delivery Of Tenofovir Disproxil Fumarate " in **25th Annual National Convention of the Association of Pharmaceutical Teachers of India- 2022** (25th APTICON- 2022) held at JSS College of Pharmacy, JSS Academy of Higher Education & Research, Mysuru, India from 2nd to 4th September 2022.

Dr. Milind J Umekar	Dr. Raman Dang	Dr. T M Pramod Kumar	Dr. Balamuralidhara V
President, APTI	Secretary, APTI	Organizing Chairman 25th APTICON 2022	Organizing Secretary 25th APTICON 2022

9.2.3. Publication: Dispersible Vaginal Tablets

molecular pharmaceutics

pubs.acs.org/molecularpharmaceutics Article

Development of Dispersible Vaginal Tablets of Tenofovir Loaded Mucoadhesive Chitosan Microparticles for Anti-HIV Pre-Exposure Prophylaxis

Published as part of the Molecular Pharmaceutics virtual special issue "Advances in Molecular Pharmaceutical Research from Asia".

Dhruti Avlani, Avichal Kumar, and Shivakumar H.N*

Cite This: *Mol. Pharmaceutics* 2023, 20, 5006−5018 Read Online

ACCESS | Metrics & More | Article Recommendations

ABSTRACT: Tenofovir disoproxil fumarate (TDF)-loaded bioadhesive chitosan microparticles (CM) were developed by an emulsification internal gelation technique. Among different batches produced, ECH-4 was found to display a high % entrapment efficiency (68.93 ± 1.76%) and sustained drug release of 88.05 ± 0.38% at 24 h. Solid state characterization of ECH-4 employing DSC and PXRD indicated that the TDF existed in an amorphous state as a solid−solid solution in chitosan. Scanning electron microscopy revealed CM of ECH-4 was spherical in shape with a rough surface topography. Laser scattering analysis using Malvern Master sizer indicated that particle size of ECH-4 was in the range of 0.52 ± 0.10 μm to 284.79 ± 21.42 μm with a surface-mean diameter of 12.41 ± 0.06 μm. *Ex vivo* mucoadhesion studies using rabbit mucosa as a substrate indicated that 10.34 ± 2.08% of CM of ECH-4 was retained at the end of 24 h. The microparticles of ECH-4 were incorporated into dispersible tablets (DT-TCM) intended for intravaginal administration, in view to arrest the pre-exposure transmission of HIV during sexual intercourse. *In vitro* release from the dispersible tablet (F3) into simulated vaginal fluid (pH 4.5) displayed a sustained release profile of TDF as 89.98 ± 1.61% of TDF was released at 24 h. The *in vitro* dissolution profile of the DT-TCM was found to be similar to that of TDF loaded CM with the values of f_1 (difference factor) and f_2 (similarity factor) being 1.52 and 78.02, respectively. Therefore, DT-TCM would be a promising novel drug delivery platform for pre-exposure prophylaxis against HIV.

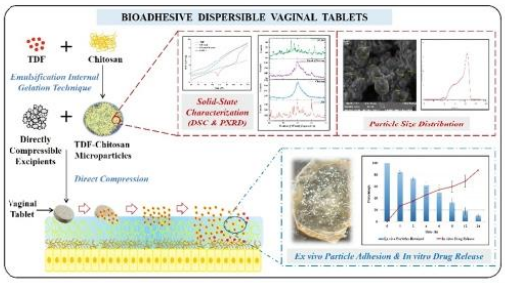

KEYWORDS: *intravaginal, chitosan, tenofovir, vaginal tablet, mucoadhesion, sustained release*

1. INTRODUCTION

For several decades, Human Immunodeficiency Virus (HIV) and Acquired Immunodeficiency Syndrome (AIDS) have remained significant health, social, and economic concerns worldwide. HIV specifically targets and damages the CD4 cells of the immune system responsible for fighting infections. In the absence of treatment, it gradually weakens and destroys the immune system, leading to the progression of AIDS.[1] According to estimates made by WHO, in 2021, there were around 38.4 million HIV-positive individuals worldwide, 1.5 million people newly contracted the virus, and 650,000 fatalities resulting from HIV-AIDS related ailments.[2]

According to the Centers for Disease Control and Prevention, the majority of individuals who contract HIV acquire it via sexual intercourse involving the anus or vagina, or by sharing needles, syringes, or other equipment used for injecting drugs.[1] The success of Highly Active Antiretroviral Therapy (HAART) in developed nations has significantly decreased morbidity and mortality rates. Nevertheless, several antiretroviral medicines are recognized for their low oral bioavailability because they either are poorly soluble or have difficulty permeating cell membranes. The primary reason for relapse is the inadequate targeting of antiretroviral drugs to latent infection sites.[3−5]

In this context, preventative measures such as pre-exposure prophylaxis (PrEP) play a crucial role in reducing HIV

Received: March 31, 2023
Revised: August 24, 2023
Accepted: August 25, 2023
Published: September 1, 2023

https://doi.org/10.1021/acs.molpharmaceut.3c00288
Mol. Pharmaceutics 2023, 20, 5006−5018

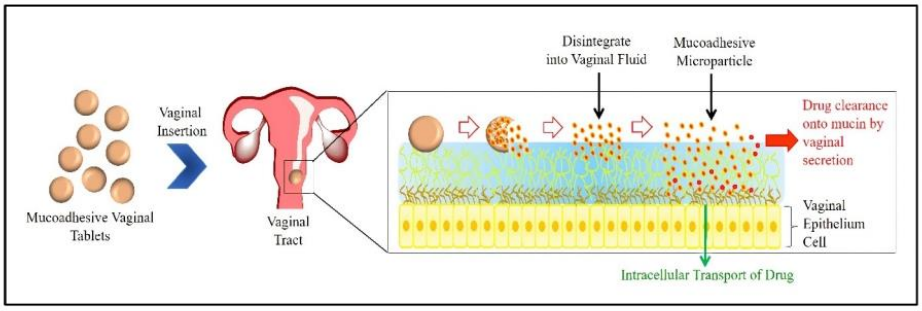

Figure 1. Fate of tenofovir delivered by dispersible tablets containing bioadhesive microparticles.

transmission involving daily intake of antiretrovirals by HIV-negative individuals to lower their risk of contracting the virus. Currently, only two antiretroviral formulations, Truvada and Descovy, have been approved by the FDA for daily oral use as PrEP. Truvada is underutilized in the US due to its high cost, kidney-related toxicity, and poor patient adherence.[6] The approval of Descovy as a second option for HIV PrEP in 2019 offered a better safety profile compared to Truvada. While the formulation's safety and efficacy are crucial, participant adherence to product use is also vital for successful outcomes, as evidenced by various research studies.[7−11]

Topical PrEP, in addition to other methods, has significant potential in combating new HIV-1 infections. This approach involves using microbicides, which are medical products designed to be administered in the vagina and/or rectum to prevent the initial stages of viral transmission during sexual intercourse. The underlying concept behind topical PrEP is to prevent HIV-1 at the mucosal level by using one or more compounds that have varying degrees of specific antiviral activity.[12,13]

In contrast to the oral route of drug delivery, topical vaginal inserts are an effective delivery platform for potent antiretrovirals, particularly when utilized as the foundation for on-demand and event-driven PrEP.[4] Drugs administered vaginally bypass the gastrointestinal and hepatic first-pass effects. This is because the vaginal route lacks cell layers with metabolic enzymes, allowing drugs to reach the systemic circulation directly, which reduces the required dosage and, in turn, the incidence of side effects.

Formulations designed for intravaginal administration enhance the absorption of drug substances in the local area by virtue of the dense network of blood vessels and the large surface area, leading to enhanced bioavailability at the site of action. Furthermore, vaginal formulations can minimize off-target systemic side effects due to the limited absorption of drug substances into the bloodstream, while also exhibiting relatively low enzymatic activity.[14,15]

Vaginal inserts like, tablets, films, gels, and suppositories appear to be a promising approach to address PrEP.[4,5] Vaginal gels have several disadvantages. First, adherence can be an issue, meaning that people may have difficulty consistently using the gel as prescribed. Vaginal gels have several disadvantages such as the difficulty in consistently using the gels as prescribed. Additionally, gels are prone to dissipation and may not be effectively retained for prolonged periods of time periods. This can limit their efficacy in delivering the intended dosage and therapeutic effects. Furthermore, the administration of vaginal gels requires the use of an applicator, which may be an inconvenience for some individuals. There is also a risk of experiencing local irritation and leakage when using these gels, which can cause discomfort or affect their overall effectiveness. Also, vaginal gels may not be particularly stable under adverse environmental conditions. Factors such as temperature, humidity, or exposure to certain substances can potentially affect the stability and efficacy of the gel, making it less reliable in these situations.[12,15] The tenofovir 1% gel, which comes in prefilled applicators, initially showed promise in the CAPRISA 004 trial. However, subsequent Phase IIb/III trials were unable to confirm its efficacy through an intention-to-treat analysis. This was likely because the gel was inconsistently and insufficiently used by young, at-risk women in both daily and pericoital dosing regimens.[4]

To achieve efficient and effective prophylactic prevention, it is crucial to reach adequate levels of the preventive agent at the possible infection location.[16] Based on the physicochemical characteristics and mechanism of action of the ingredients employed, vaginal inserts are expected to operate by delivering the drug locally to target cells and tissues within the vaginal lumen. Bioadhesive vaginal inserts can deliver the active agents for an extended period at a predictable rate into the surrounding cervicovaginal fluid and tissue.[4,17] The novel DT-TCM would readily disintegrate into the constituent bioadhesive microparticles on coming into contact with the intravaginal fluid. The bioadhesive microparticulate system by virtue of its small size and the high surface-to-volume ratio is known to positively modify biodistribution, is well retained, and exhibits better cellular uptake. They are modified to enhance the penetration through the mucus barrier layer and increase penetration into the epithelium. These microparticles are less prone to expulsion, unlike single-unit dosage forms. As these particles are directly delivered to the site of action, these formulations are known to effectively arrest the transmission of HIV during sexual intercourse.[18]

Vaginal tablets are compact, monolithic matrix systems intended for vaginal insertion, designed and formulated for immediate or sustained delivery of active ingredients. Vaginal tablets offer advantages over conventional vaginal dosage forms, such as more accurate dosing and greater stability along with low manufacturing cost.[19] They are versatile and can be modulated to obtain sustained or controlled delivery of drugs by incorporating mucoadhesive polymers like sodium alginate, hydroxy propyl methyl cellulose (HPMC), chitosan, and a few more as their primary excipients.[20−23] The mucoadhesive polymers are likely to interact with the vaginal surface through

https://doi.org/10.1021/acs.molpharmaceut.3c00288
Mol. Pharmaceutics 2023, 20, 5006−5018

specific functional groups in the polymers and biological tissues, enabling the formulation to remain adhered to the vaginal mucosa, while the drug is released. This interaction is crucial to the success of the formulation. Gelation of these polymers upon contact with aqueous media can be beneficial in controlling drug release via diffusion through the gel layer.[4,15,17,24] Dispersible tablets composed of multiparticulate systems are advantageous over single-unit vaginal dosage forms as they are known to exhibit a more reliable vaginal mucosal retention time (Figure 1). The chances of failure of such a specialized dosage form are very merger.

Tenofovir has been extensively evaluated as a prophylactic modality. Tenofovir ($C_9H_{14}N_5O_4P$) belongs to the class of Nucleoside Reverse Transcriptase Inhibitors used in the treatment of HIV infection. It belongs to the BCS Class III drug. To enhance the permeability of tenofovir, a prodrug (Tenofovir Disoproxil Fumarate, TDF) has been developed. TDF inhibits reverse transcription by causing chain termination during the extension of the DNA chain after they have been incorporated into viral DNA during the reverse transcription process which is carried out by the enzyme HIV Reverse Transcriptase.[12,25] The oral bioavailability of TDF is low (25% in the fed state) owing to the intestinal degradation and efflux transport that justifies the need to develop a vaginal dosage form of the drug.[26] TDF is known to result in a 1000-fold increase in the intracellular concentration of tenofovir diphosphate in comparison to the tenofovir base. Additionally, TDF displays a 100-fold lower IC_{50} when compared to the tenofovir base, due to better permeability.[16,27] TDF displays an extended half-life ($t_{1/2}$ = 12−15 h),[5] efficacy and safety profile making it an ideal topical microbicide for preventing the sexual transmission of HIV.[28,29]

Chitosan is a nature-derived, hydrophilic, and positively charged mucopolysaccharide, having good biodegradability and biocompatibility.[20,30] It has similar flexibility to that of natural tissue and is widely available, making it a sustainable biomaterial for the development of healthcare products and tissue engineering.[31] The ability of chitosan to adhere to mucus is due to its positively charged nature. Mucin glycoprotein makes up the mucous membrane, which contains negatively charged sialic and sulfonic acid groups. Chitosan's cationic group interacts with these anionic acids in the mucous, resulting in ionic bonding and mucoadhesive properties of chitosan. Drug release from chitosan microparticles (CM) is governed by polymer swelling, drug absorption, drug diffusion, polymer erosion or degradation, and a combination of erosion and degradation.[14,22,30]

The focus of the current project is to develop novel pre-exposure prophylactic dispersible tablets of TDF-loaded bioadhesive chitosan microparticles (DT-TCM) for intravaginal administration in view of overcoming the limitations of conventional dosage forms. The novelty of the project lies in the fact that the dispersible tablets would readily disperse into the constituent bioadhesive microparticles that adhere well to the vaginal mucosa for a considerable time period. Unlike conventional bioadhesive vaginal tablets that are single-unit dosage forms, the novel dispersible tablets are not prone to the "all or none rule" and therefore are less susceptible to expulsion or dissipation, which would be the big advantage of our present work. Thus, the novel dispersible tablets can elicit a higher therapeutic concentration at the site of transmission, that is likely to exceed the IC_{50} of TDF. As no such product is available in the Indian market, vaginal administration of TDF is a promising alternative to oral PrEP dosage forms. Considering the fact that nearly half of the HIV-infected population is female, and the majority acquire the infection through sexual intercourse, topical bioadhesive vaginal DT is expected to save the lives of several millions of people from HIV infections.

2. MATERIALS AND METHODS

2.1. Materials. Tenofovir disoproxil fumarate was received as a gift sample from Aurobindo Pharma, Hyderabad, India. Chitosan was received as a gift sample from the Central Institute of Fisheries Technology, Kochi, Kerala, India. Sodium tripolyphosphate anhydrous (TPP) (extra pure) was procured from Sisco Research Laboratories Pvt. Ltd., Maharashtra, India. Acetic acid, light liquid paraffin, span 80, and petroleum ether were purchased from SD. Fine Chemicals Ltd. (India). All other excipients and chemicals used were of analytical grade.

2.1.1. Preparation of TDF-Loaded Chitosan Microparticles (TCM). The emulsification internal gelation technique was employed to produce TDF microparticles by using chitosan as a bioadhesive polymer. Weighed amounts of TDF and chitosan at varying concentrations were dissolved in 2%v/v acetic acid to form a homogeneous solution.[32,33] About 20 mL of the resulting solution was added into 60 mL of light liquid paraffin containing 1.5%v/v Span 80 constituted the continuous phase.[34] Addition of the dispersed phase into the continuous phase under constant mechanical stirring at 500 rpm resulted in the formation of water in oil (w/o) emulsion that was homogenized at 5000 rpm for 15 min. TPP solution was added with continuous stirring to produce rigid discrete microparticles. The microparticles were finally separated by centrifugation at 4000 × *g* for 30 min, washed several times with petroleum ether to remove the traces of oil adhering to the microparticle, and dried at room temperature.[33,34] The composition of different batches of CM of TDF is indicated in Table 1.

Table 1. Composition of TDF-Loaded Microparticles

formulation code (FC)	drug (% w/v)	chitosan (% w/v)	TPP (% w/v)
EC-1	1.0	1.0	5.0
EC-2	1.0	2.0	5.0
EC-3	1.0	3.0	5.0
EC-4	1.0	4.0	5.0
ECH-1	1.0	1.0	10.0
ECH-2	1.0	2.0	10.0
ECH-3	1.0	3.0	10.0
ECH-4	1.0	4.0	10.0

2.2. Characterization of Microparticles. *2.2.1. Practical Yield and Drug Encapsulation Efficiency (EE).* The percent yield of each batch of microparticles was calculated from the proportions of the total raw materials used in the preparation of the microparticles to assess the mass balance using equation 1. To determine the %EE, an accurately weighed quantity of TCM were pulverized and digested in 5 mL of simulated vaginal fluid (pH 4.5) (SVF)[35] in a screw cap vial on a bath sonicator to extract the entrapped drug. The resulting dispersion was centrifuged at 10,000 × *g* for 5 min. The amount of TDF in the supernatant was assayed after appropriate dilution using a UV−visible spectrophotometer at 259 nm. The EE (%) was determined in triplicate for all batches using eqs 2−4.[33,36,37]

https://doi.org/10.1021/acs.molpharmaceut.3c00288
Mol. Pharmaceutics 2023, 20, 5006−5018

$$\% \text{ Practical Yield} = \frac{\text{Weight of microparticles}}{\text{Weight of drug} + \text{Weight of polymers}} \times 100 \quad (1)$$

$$\% \text{ Theoretical Drug Loading (DL)} = \frac{\text{Weight of drug taken}}{\text{Weight of drug taken} + \text{Weight of polymers taken}} \times 100 \quad (2)$$

$$\% \text{ Practical Drug Loading (DL)} = \frac{\text{Weight of drug-loaded into microparticles}}{\text{Weight of microparticles}} \times 100 \quad (3)$$

$$\%EE = \frac{\%\text{Practical DL}}{\%\text{Theoretical DL}} \times 100 \quad (4)$$

2.2.2. Surface Morphology. The surface morphology and topography of TCM were examined by scanning electron microscope (SEM) (TESCAN-VEGA3 LMU). The microparticles were affixed to a SEM sample holder with adhesive tape and coated with a layer of gold (~200 nm) through ion sputtering at reduced pressure for a duration of 5 min. This gold coating helps to improve the resolution and contrast of the SEM images by increasing the conductivity of the microparticles. The gold coated samples were scanned to obtain photomicrographs of suitable magnification.[23,38]

2.2.3. Particle Size Analysis. Laser scattering technique was employed to determine the size of the microspheres on Malvern Mastersizer (v3.62, Malvern Instruments, Ltd.). The microparticles were dispersed in propanol and subjected to sonication with a 600 W probe for 10 min before measurement in order to deaggregate the microparticles to enable clear detection. The volume-surface mean diameter was calculated using eq 5.[39−42]

$$\text{Volume} - \text{Surface Mean Diameter } (d_{vs}) = \frac{\Sigma nd^3}{\Sigma nd^2} \quad (5)$$

where n is the number of particles in each size range and d is the mean of the size range in μm.

2.2.4. Fourier Transform Infrared (FTIR) Spectroscopic Analysis. FTIR spectrometry is an appropriate analytical technique to characterize TDF, polymers, physical mixture, and formulation. The samples were prepared by finely grinding in a glass mortar and pestle with potassium bromide to minimize IR scattering on the particle surface. The prepared sample was placed in the sample holder and observed in the FTIR spectrometer (Jasco 460 Plus) in the range of 4000−1000 cm^{-1}.[39,43,44]

2.2.5. Differential Scanning Calorimetry (DSC) Analysis. DSC has been an extensively used calorimetric technique to characterize the solid state of the drug in polymer. The thermal response of TDF, polymers, physical mixture, and the formulation were recorded using DSC NETZSCH's STA 449 F5 Jupiter thermal analyzer system. Samples were analyzed at a heating rate of 30 °C/10.0 K/min over a temperature range of 20−300 °C to enable data acquisition.[39,43,45]

2.2.6. Powder X-ray Diffraction (PXRD) Analysis. PXRD techniques have been one of the widely used techniques to characterize the solid state of the drug in polymer. The diffraction studies of TDF, polymers, physical mixture, and the formulations were recorded using Bruker D8 ADVANCE X-ray Diffractometer. The operation data were: 2.2 kW X-ray source of Cu anode with fine focus ceramic X-ray tube operated at 40 kV voltage and 40 mA current at 1.6 kW power. Data was recorded between 5 and 40° 2θ values and collected using LYNXEYE high speed SSD160−2 detector with 500 μm sensor.[39,46]

2.2.7. In Vitro Drug Release. The *in vitro* dissolution studies were performed in triplicate for all batches using USP IV flow through cell dissolution apparatus (Electrolab, Model No. EFT-01). About 150 mg of TCM was confined in the sample holder. Glass beads were loaded into the flow-through cell to ensure that a laminar flow of the media (SVF maintained at 37 ± 0.5 °C) is maintained throughout the studies. A flow rate of 16 mL/min was maintained in a closed loop to allow the disaggregation of the particles, which in turn helps in enhancing the dissolution. Tenofovir disoproxil fumarated has good aqueous solubility, and therefore, the medium (900 mL) was easily able to maintain sink conditions. Therefore, the study was conducted in a closed loop configuration, which indicated recirculation of the fixed volume of media similar to USP Apparatus I and II.[47−49] Aliquots were withdrawn at predetermined time intervals up to 24 h and analyzed spectrophotometrically at 259 nm to measure the released API.

The obtained *in vitro* release data were fitted to four different kinetic mathematical model-dependent methods: zero-order, first-order, Higuchi, and Korsmeyer−Peppas; the release equations as presented in Table 2.[50,51,33]

Table 2. Mathematical Models Used to Describe Drug Release Curves[a]

model	equation
zero-order	$Q_t = Q_0 + K_0 t$
first-order	$\text{Log } Q_t = \text{Log } Q_0 + K_1 t$
Higuchi model	$Q = K_H * \sqrt{t}$
Korsmeyer−Peppas	$F = (Q_t/Q) = K_K * t^n$

[a] t = time in hours, Q_0 = initial amount of drug, Q_t = cumulative amount of drug release at time (t), K_0, K_1, K_H, K_K = zero-order, first-order, Higuchi, and Korsmeyer−Peppas release constant respectively, F = fraction of drug released at time (t), Q_t = amount of drug released at time (t), Q = total amount of drug in dosage form, n = diffusion or release exponent which explains different mechanisms of drug transport from polymeric drug delivery systems

2.2.8. Ex Vivo Mucoadhesion Studies/Wash-Off Test. The mucoadhesive properties of microparticles were evaluated using a modified USP disintegration apparatus. Freshly excised piece of rabbit vagina (5 × 1 cm) was used as a substrate and mounted on a glass slide using a glue. About 200 microparticles were sprinkled uniformly over the substrate, and the glass slide was hung onto the arm of the disintegration apparatus with a suitable support. When the disintegrating apparatus was operated, the tissue specimen was subjected to a slow, regular up and down movement in the SVF at 37 ± 0.5 °C for a period of 24 h. At predetermined time intervals, the apparatus was stopped and the number of particles adhering to the mucosal tissue were counted using a microscope in triplicates and percentage mucoadhesion was calculated using eq 6.[23,52]

https://doi.org/10.1021/acs.molpharmaceut.3c00288
Mol. Pharmaceutics 2023, 20, 5006−5018

$$\% \text{ Mucoadhesion} = \frac{\text{No. of microparticles adhered}}{\text{Initial no. of microparticles}} \times 100 \quad (6)$$

2.2.9. Preparation of Vaginal Tablets. The optimized TCM formulation ECH-4 was incorporated into dispersible tablets (DT-TCM) employing the conventional direct compression technique. TCM (ECH-4) containing 15 mg of TDF was geometrically dry blended with croscarmellose sodium, polyvinyl pyrrolidine K-30 and microcrystalline cellulose (pH 102) in varying ratios and passed through a 120 μm sieve. The sieved blend was lubricated with magnesium stearate and talc for a few mins. The lubricated blend was compressed into flat-faced bevel-edge tablets weighing 300 mg on rotary tablet press (Model RSB-4, Rimek mini press) using tablet B tooling of 8.75 mm diameter. The batch size of each tablet composition was 30 tablets. Three different batches of dispersible tablets containing ECH-4 (coded as F1–F3) and one batch of dispersible tablet containing TDF (coded as F4) were produced by varying the blend composition as represented in Table 3.[53,54]

Table 3. Composition of Vaginal Tablets

ingredients	quantity (mg)			
	F1	F2	F3	F4
TDF				15
ECH-4[a]	150	150	150	
Avicel (PH 102)	120	120	120	75
polyvinyl pyrrolidine K-30	9	12	15	5
croscarmellose sodium	15	12	9	3
magnesium stearate	3	3	3	1
talc	3	3	3	1
weight of each tablet	300 mg			100 mg

[a]150 mg ECH-4 contains 15 mg of TDF

2.2.10. Physical Characterization of Vaginal Tablets. The prepared tablets were evaluated for quality control tests like organoleptic properties, tablet thickness, diameter, weight variation, hardness, friability, and content uniformity tests following the official procedures.[55]

i. Organoleptic properties: The tablets were inspected visually for shape and color.
ii. Weight variation: Twenty tablets were randomly selected and weighed individually. The average weight and percentage deviation from the average weight was calculated.
iii. Tablet thickness and diameter: Uniformity in tablet thickness and diameter of tablets ensures uniformity of tablet size which is essential during packaging. Ten tablets were examined for their thickness and diameter using vernier callipers, and the mean thickness and diameter value along with standard deviation were calculated.
iv. Hardness: The resistance of tablet to shipping or breakage, under conditions of storage, transportation, and handling, before usage, depends on its hardness. Ten tablets were randomly selected, and the hardness of each tablet was measured using Pfizer hardness tester.
v. Friability: Friability is the measure of tablet strength. Twenty-two tablets were accurately weighed and placed in the Roche friabilator chamber that revolves at 25 rpm for 4 min dropping the tablets through a distance of six inches with each revolution. After 100 revolutions the tablets were reweighed and the percentage loss in tablet weight was determined following eq 7.

$$\% \text{ Friability} = \frac{\text{Initial weight of tablets} - \text{Final weight of tablets}}{\text{Initial weight of tablets}} \times 100 \quad (7)$$

vi. Content uniformity: The TDF content in 10 randomly selected tablets from each batch were determined spectrophotometrically at 259 nm.
vii. *In vitro* disintegration test: Disintegration time for six dispersible tablets was determined using Electrolab Disintegration test apparatus in SVF maintained at 37 ± 0.5 °C. The time point at which the tablets completely disintegrated was recorded as the disintegration time.

2.2.11. In Vitro Dissolution Study. The *in vitro* release of TDF from the DT-TCM tablets for all batches was performed in triplicate using USP IV flow through cell dissolution apparatus (Electrolab, Model No. EFT-01). The USP apparatus IV addresses various issues encountered in the USP apparatus 1 and 2, such as tablet sticking, floating, coning, dead zones, as well as problems related to sampling and sample introduction effects. By using the USP apparatus IV, these challenges are likely to be eliminated, ensuring more accurate and reliable dissolution testing. TDF has no solubility issues. The study was performed in a closed-loop flow-through method in SVF maintained at 37 ± 0.5 °C for a period of 24 h. The tablet was placed in the sample holder in a manner such that the medium flow is always perpendicular to the disintegrated particles of the tablet. A flow rate of 16 mL/min was maintained for a period of 24 h. Aliquots were withdrawn at predetermined time intervals, filtered and analyzed at 259 nm using double beam UV–vis spectrophotometer to measure the released API.[47,49]

A model-dependent method was followed to compare the dissolution profile of TDF tablets and TCM tablet by determining the difference factor (f_1) and similarity factor (f_2) using eqs 8 and 9.

$$\text{Difference Factor } (f_1) = \frac{\sum_{t=1}^{n} (R_t - T_t)}{\sum_{t=1}^{n} R_t} \times 100 \quad (8)$$

$$\text{Similarity Factor } (f_2) = 50 \times 100 \log\left\{\sqrt{\left[1 + \frac{1}{n}\sum_{t=1}^{n} (R_t - T_t)^2\right]} \times 100\right\} \quad (9)$$

where n is the number of dissolution time points; R_t is the dissolution value of the reference drug product at time t; and T_t is the dissolution value of the test drug product at time t.

In the range of 0–100, the dissolution profile of the test sample is considered to be identical to that of the reference sample if f_2 ranges from $50 \leq 100$ and f_1 ranges from $0 \leq 15$.[56,57]

The obtained *in vitro* release data from DT-TCM were subjected to fitting to four different kinetic mathematical model-dependent methods; the zero-order, first-order, Higu-

https://doi.org/10.1021/acs.molpharmaceut.3c00288
Mol. Pharmaceutics 2023, 20, 5006–5018

chi, and Korsmeyer−Peppas release equations are presented in Table 2.[32,50,58]

3. RESULTS AND DISCUSSION

Considering the good aqueous solubility of TDF (13.4 mg/mL) that belongs to BCS Class III,[59] w/o emulsification internal gelation technique was employed to prepare TDF microparticles using chitosan as a bioadhesive polymer. The w/o emulsion formed was stabilized using Span 80 (w/o surfactant). The emulsion was stirred at 500 rpm for a period of 1 h to form globules that reach a steady state by the end of the time period. TPP is one of the common cross-linking agents for the preparation of CM as it reacts with compounds containing primary amine groups to form covalently cross-linked networks.[60] When the TPP solution was added to drug−chitosan emulsion, 30 min of curing time was allowed to obtain uniform distribution in the continuous oil phase resulting in a more uniformly cross-linked product. During the cross-linking, the −OH ions compete with tripolyphosphoric ions to react with amino group of chitosan immediately by ionic interaction, and then the tripolyphosphoric ions once diffused into chitosan microparticles, interact with amine groups of chitosan.[61] A double-washing process with petroleum ether followed by distilled water was implemented to remove excess oil, salts, and free TPP.[62]

3.1. Practical Yield and Entrapment Efficiency. The yield is the total quantity of microparticles produced. The main objective behind optimizing the formulation is to produce a good yield of the product. An increase in the polymer would improve the drug entrapment, minimize drug loss, and improve the process yield.[39] This was clearly visible in Figure 2, where

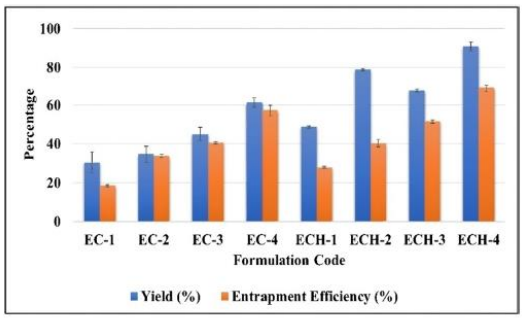

Figure 2. Yield and EE of TCM.

the percentage yield of TCM increased from 30.50 ± 5.32% to 61.23 ± 2.61% from EC-1 to EC-4 and from 48.75 ± 0.50% to 90.80 ± 2.31% from ECH-1 to ECH-4 with the increase in the chitosan concentration.

The incorporation of therapeutically active molecules into microparticles can be governed by various factors like method of preparation, drug to polymer ratio and TPP concentration.[63] Entrapment of drug was found to increase with an increase in the amount of polymer used. With the increase in polymer concentration (1% to 4%), the drug-polymer dispersion forms stabilized microparticles and prevents the leakage of drug during the hardening process. An increase in the %EE with increase in the drug to polymer ratio has been reported in the earlier studies.[64−66] The %EE of EC-1 to EC-4 produced with 5% TPP ranged from 18.55 ± 0.41% to 57.24 ± 2.73%. On increasing the TPP concentration was increased to 10% for ECH-1 to ECH-4, an increase in the %EE was observed that ranged from 27.97 ± 0.60% to 68.93 ± 1.76% as indicated in Figure 2. Therefore, increase in TPP concentration, increased the cross-linking with chitosan that resulted in a significantly denser matrix, which lowers drug leakage during stirring, thereby improving encapsulation efficiency.[34,67]

3.2. Surface Morphology and Particle Size Analysis. The SEM photomicrographs of the formulation ECH-4 revealed that the microparticles were spherical with a smooth surface. In Figure 3, the particles appeared to be adhering to

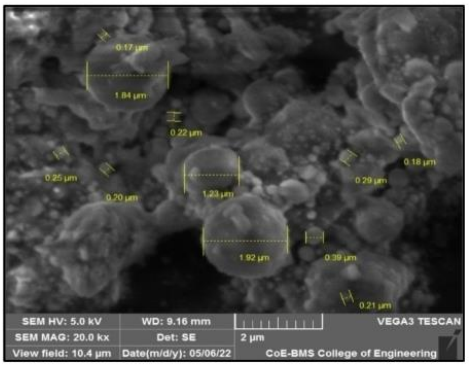

Figure 3. Photomicrographs of TCM of formulation ECH-4 on a scanning electron microscope under a magnification of 20000×

each other under 20000× magnification that indicates their bioadhesive nature. The surface roughness and abrasions on the microspheres could be possible due to polymer deposits.[60,61]

Particle size is one of the crucial parameters of targeted drug delivery, which affects the stability, EE, drug release profile, drug biodistribution, mucoadhesion, and cellular uptake.[68] The particle size−volume distribution curve of ECH-4 is represented in Figure 4, which indicates the particle size

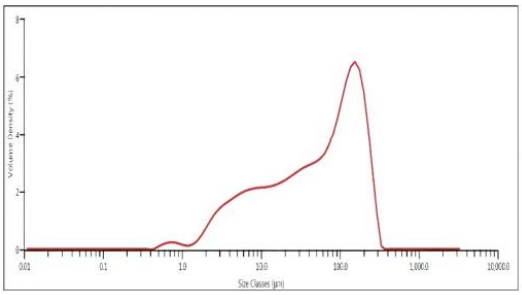

Figure 4. Particle size distribution curve of formulation ECH-4.

range to be from 0.52 ± 0.00 μm to 284.79 ± 21.41 μm. The particle size distribution curve obtained is not typical as it does not have a bell-shaped pattern. This can be attributed to a broad particle size distribution, as the bioadhesive microparticles tend to adhere to each other. The volume−surface mean diameter of formulation ECH-4 was calculated to be 204.42 ± 0.13 μm.[42] About 50% of the microparticles in ECH-

https://doi.org/10.1021/acs.molpharmaceut.3c00288
Mol. Pharmaceutics 2023, 20, 5006−5018

4 were of 58.014 ± 1.037 μm in size whereas 90% of the particles were of 193.42 ± 3.70 μm in size.[69,70] A major fraction of the particles being in the higher size range is likely due to adherence of the bioadhesive microparticles to each other. The results of particle size analysis were known to agree well with the SEM photomicrographic images.

3.3. FTIR Analysis. An overlay of the FTIR spectra of TDF, chitosan, physical mixture, and the kneaded product (ECH-4) are displayed in Figure 5 and Table 4.

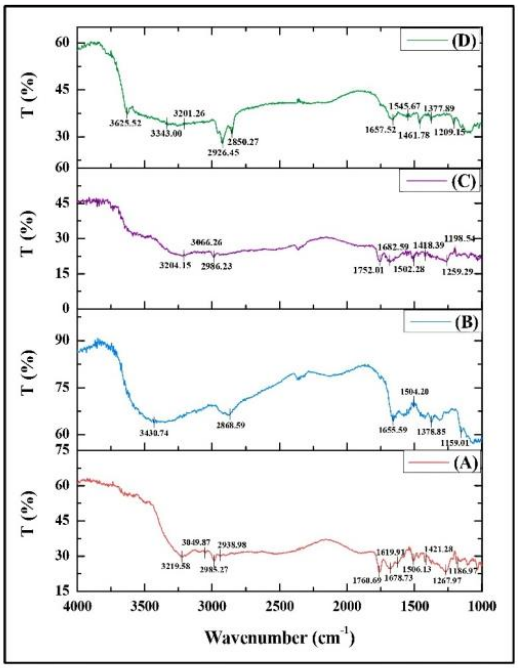

Figure 5. FTIR spectra of (A) TDF; (B) chitosan; (C) physical mixture; and (D) kneaded product (ECH-4).

Table 4. Peaks Observed in FTIR Spectra[a]

	wavenumber (cm^{-1})			
sample	TDF	chitosan	physical mixture	microparticle (ECH-4)
1	3219.58	3430.74	3204.15	3625.52
2	3049.84	2868.59	3066.26	3343
3	2985.27	1655.59	2986.23	3201.26
4	2938.98	1504.2	1752.01	2926.45
5	1760.69	1378.85	1682.59	2850.27
6	1678.73	1159.01	1502.28	1657.52
7	1619.91		1418.39	1545.67
8	1506.13		1259.29	1377.89
9	1421.28		1198.54	1461.78
10	1267.97			1209.15
11	1186.97			

[a]TDF; chitosan; physical mixture; and kneaded product (ECH-4).

The FTIR spectroscopy aids in determining the molecular interactions between the drug and its carrier. The FTIR spectra of TDF exhibited distinct peaks at 3219.58 cm^{-1} (strong −OH stretching bond), 3049.84 cm^{-1} (aromatic −CH stretching) 2985.27 and 2938.98 cm^{-1} (aliphatic −CH stretching bond), 1760.69 cm^{-1} (C═O group), 1678.73 cm^{-1} (P═O stretching), 1619.91 cm^{-1} (−C═C− stretching bond) and 1421.28 cm^{-1} (aromatic C═N stretching bond), 1267.97 cm^{-1} (aliphatic C−N stretching), and 1186.97 cm^{-1} (C−O stretching) confirming the earlier report.[45] The FTIR spectra of the polymer chitosan was characterized by a broad band at 3430.74 cm^{-1}corresponding to the N−H stretching vibration, a −CH stretching vibration at 2868.59 cm^{-1}, the presence of C═O bond of amide I at 1655.59 cm^{-1}, N−H bond of amide II at 1504.2 cm^{-1} and N−H bond of amide III at 1378.85 cm^{-1}and C−O stretching at 1159.01 cm^{-1}.[28,71] The FTIR spectra of the physical mixture, retained the principal peaks of TDF and chitosan at 3204.15 cm^{-1} (strong −OH stretching bond), 3066.26 and 2986.23 cm^{-1} (aliphatic −CH stretching bond), 1752.01 cm^{-1} (C═O group), 1682.59 cm^{-1} (P═O stretching), 1502.28 cm^{-1} (N−H bond of amide II), 1418.39 cm^{-1} (aromatic C═N stretching bond), 1259.29 cm^{-1} (aliphatic C−N stretching), and 1198.54 cm^{-1} (C−O stretching), suggesting a weak interaction between the drug and polymer used in the formulation.[72] The FTIR spectra of formulation ECH-4, depicted a very sharp peak of N−H stretching vibration at 3625.52 cm^{-1}, aliphatic −CH stretching vibration at 2926.45 and 2850.27 cm^{-1}, C═O stretching vibration at 1657.52 cm^{-1}, N−H bond of amide III at 1377.89, and 1209.15 cm^{-1}C−O stretching.. The characteristic peaks of the TDF appeared in the FTIR spectra of the formulation ECH-4 with a decreased intensity at 3201.26 cm^{-1} (−OH stretching vibration), 1461.78 cm^{-1} (aromatic C═N stretching vibration), and 1545.67 cm^{-1} (N−H bond of amide II). The presence of only a few characteristic peaks of TDF in the FTIR spectra of formulation, ECH-4, infers that the drug characteristic peaks retained in the optimized formulation which indicates that there is no interaction between drug and excipients.[73] Therefore, the studies indicated that there was no incompatibility between TDF and other excipients used to prepare the microparticles. Thus, it can be inferred that the chemical integrity of the drug was maintained and there was no chemical interaction between the drug and the excipients during the process of preparation employed.[74]

3.4. DSC Analysis. The formation of microparticles involves dispersion of the drug in the crystalline or amorphous form or dissolution of the drug in the polymer matrix. Any rapid or extreme change in the drug's or the polymer's thermal behavior could point to a potential drug−polymer interaction as represented in Figure 6. The DSC thermogram of TDF displayed a sharp exothermic peak at 115.4 °C with a peak onset at 112.04 °C that corresponds to the melting point of the drug. The endothermic peak was found to completely disappear in the thermogram of TCM.

The enthalpy of fusion (ΔH_f) for TDF in the pure state by DSC was found to be 71.41 J/g. The presence of a very low intensity endothermic peak in the thermogram of the physical mixture indicating the semicrystalline nature of the drug in the physical mixture. The corresponding to the melting point of TDF was broadened and shifted to 118.4 °C in the thermogram of the physical mixture of TDF and chitosan. The drug characteristic thermogram almost disappeared indicating the amorphization of the drug in chitosan matrix in ECH-4. This would have resulted in complete miscibility of drug in the polymer to form a solid−solid solution. Therefore, from the DSC studies it can be inferred that the TDF was dissolved in the bioadhesive CM in the amorphous state.[39,45,75]

https://doi.org/10.1021/acs.molpharmaceut.3c00288
Mol. Pharmaceutics 2023, 20, 5006−5018

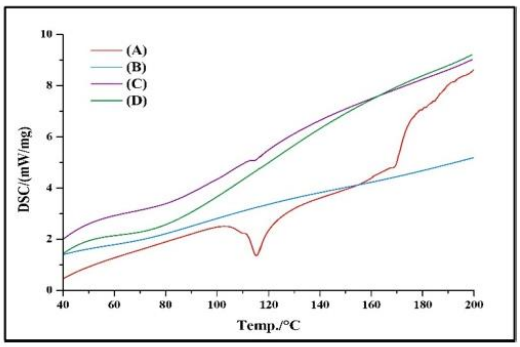

Figure 6. DSC thermograms of (A) TDF; (B) chitosan; (C) physical mixture; and (D) kneaded product ECH-4.

3.5. Powder XRD Analysis. The PXRD of TDF, chitosan, physical mixture, and formulation ECH-4 were performed to investigate the crystallinity of TDF upon its transformation into microparticle, and their corresponding PXRD patterns are displayed in Figure 7.

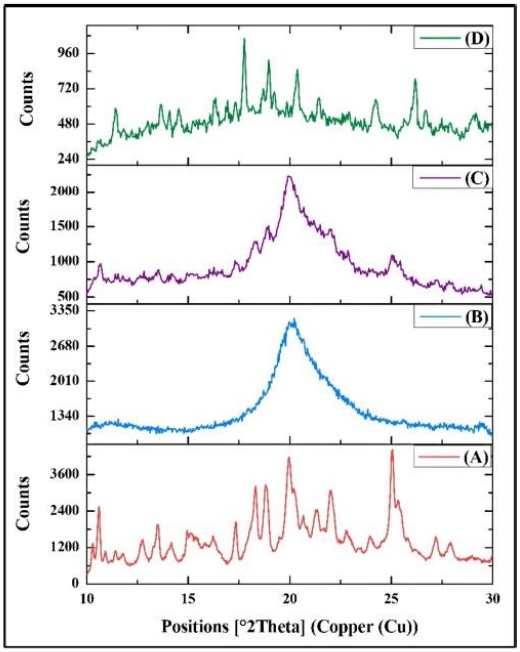

Figure 7. PXRD diffractogram of (A) TDF; (B) chitosan; (C) physical mixture; and (D) kneaded product (ECH-4).

The crystalline nature of TDF was clearly demonstrated in the PXRD pattern with about 10 distinct well-defined high intensity sharp peaks at 2θ values of 10.29° (1339 counts), 10.59° (2540 counts), 13.48° (1954 counts), 14.17° (1361 counts), 18.32° (3212 counts), 18.80° (3258 counts), 19.95° (4172 counts), 21.36° (2438 counts), 22.02° (3077 counts), and 25.07° (4419 counts). 10 similar high intensity peaks in the same region were reported earlier indicating the crystalline nature of the drug.[45,76] The diffractogram of chitosan displayed characteristic peaks at 2θ values of 20.27° (3123 counts). These peaks were attributed to the semicrystalline nature of chitosan as per the earlier reports.[74,77] The diffractogram of the physical mixture displayed the six prominent crystalline peaks of the drug at 18.32°, 18.8°, 19.95°, 21.36°, 22.02°, and 25.07°, indicating TDF exists in a semicrystalline state in the physical mixture. The diffractogram of ECH-4 indicated a total of 6 characteristic low intensity peaks of TDF at 10.59° (358 counts), 18.32° (548 counts), 18.8° (643 counts), 19.95° (528 counts), 22.02° (486 counts), and 25.07° (431 counts). On comparing the peak intensities of formulation ECH-4 were compared to those of TDF, a 3- to 10-fold decrease in the peak intensity was observed. This is a clear indication of the drug amorphization of TDF in the chitosan polymer matrix. The characteristics peaks of TDF were reported in the same region earlier by Zaman et al. justifying our findings.[73,45] Therefore, the disappearance of sharp crystalline TDF peaks and the presence of broad and broad peaks as observed in the diffractogram of formulation ECH-4, confirmed that drug (TDF) had undergone solid-state transition during the emulsification process in the presence of chitosan.[77,78] This can be interpreted as a clear indication of the drug's molecular dispersion within the chitosan matrix as a solid−solid solution.

3.6. *In Vitro* Drug Release. The *in vitro* drug release from microparticles usually takes place into 3 phases: the initial burst period, where the drug at the surface of the microparticles is immediately released into the medium; the slow-release phase period, where the drug is released at a progressively decreasing pace; and the steady state period, where the drug is released at a steady slow rate.[34]

On comparing the *in vitro* drug dissolution profiles of TCM, formulations EC-1−EC-4 displayed nearly 100% rapid release of TDF by the end of 6 h, whereas 99.07 ± 0.41%, 99.23 ± 0.59%, 98.96 ± 1.18%, and 88.05% ± 0.38% of TDF was released from formulations ECH-1−ECH-4 by the end of 6, 8, 12, and 24 h, respectively, as represented in Figure 8.

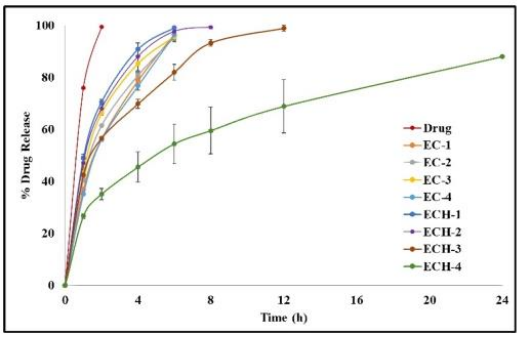

Figure 8. Cumulative *in vitro* release profile of TCM in SVF (pH 4.5) for 24 h. The data represent the mean ± SD of three determinations.

Formulations EC-1−EC-4 produced with 5% TPP exhibited a biphasic mode of drug release, namely, the burst effect followed by a slow-release phase. The smaller particle size of the microparticles and the surface drug were likely attributed to initial burst release of TDF from the microparticles, followed by slow diffusion of TDF from the core of the

https://doi.org/10.1021/acs.molpharmaceut.3c00288
Mol. Pharmaceutics 2023, 20, 5006−5018

Table 5. Results of Curve Fitting of the Dissolution Data for the Microparticles

	zero-order kinetic model		first-order kinetic model		Higuchi release model		Korsmeyer–Peppas release model		
FC	R^2	K	R^2	K	R^2	K	R^2	K	n
ECH-2	0.85 ± 0.03	49.83 ± 1.09	0.79 ± 0.03	0.29 ± 0.01	0.93 ± 0.02	23.96 ± 2.40			
ECH-3	0.90 ± 0.01	46.04 ± 1.91	0.83 ± 0.01	0.32 ± 0.01	0.97 ± 0.007	22.23 ± 2.81	1.00 ± 0.00	0.37 ± 0.02	0.41 ± 0.07
ECH-4	0.93 ± 0.05	27.78 ± 2.04	0.86 ± 0.07	0.53 ± 0.02	0.98 ± 0.01	10.62 ± 3.58	0.99 ± 0.007	0.57 ± 0.008	0.38 ± 0.07

CM.[34,60] Formulations ECH-2–ECH-4 that were produced with 10% TPP displayed minimal burst release followed by a progressively slower drug release until a steady state is attained, as observed in Figure 8. From ECH-2 and ECH-3, 50% of TDF was released within first 2 h, whereas from ECH-4, 50% of drug was released within 6 h which could be related to the hydrodynamics in the flow through dissolution apparatus.[47,48] The concentration of the chitosan solution plays a vital role in microparticle formulation and subsequent drug release. Increase in the chitosan concentration, resulted in significantly stronger microparticle walls, reduced swelling potential, and a sustained release of the TDF.[61] Therefore, the amount of TDF release was found to be inversely proportional to the chitosan concentration. Along with chitosan, the TPP concentration also determines the drug release. Formulations ECH-2–ECH-4 produced with 10% TPP displayed a sustained release of TDF when compared to EC-1–EC-4 produced with 5% TPP. The drug release profile supports the fact that higher level of TPP favored better cross-linking that in turn sustained the drug release. This could be explained by the increased cross liking density of chitosan with increased amount of TPP.[34,61]

Drug release is primarily governed by the hydration of the polymer chains. The drug release kinetics of hydrophilic polymer based controlled release dosage forms should follow three steps: The first step is the penetration of the medium in the matrix (hydration). The second step is swelling with subsequent dissolution or erosion of the matrix. The third step is the transport of the dissolved drug either through the hydrated matrix or from the eroded parts into the surrounding medium. The dissolution profiles of various batches of TCM were compared statistically or model-dependent approaches in order to understand the kinetic and mechanism of the TDF release from CM. The results of curve fitting into different mathematical models are tabulated in Table 5.

The higher R^2 values indicated that the drug release from all the formulations was not concentration-dependent and the mechanism of drug release was found to be swelling and diffusion controlled by the disentanglement rate of the polymer at the swollen front, indicating that all the formulations were in accordance with the zero-order kinetics and Higuchi model. This was further confirmed from the Korsmeyer-Peppas model, where n < 0.50and approximates to Fickian diffusion release mechanism.[33,50,51,79] Therefore, among all the formulations, formulation ECH-4 approximates better sustained release of TDF from the CM matrix.

3.6.1. Ex Vivo Mucoadhesion Studies/Wash-Out Test. Depending on the %yield, %EE and drug release, the formulation ECH-4 was considered for further studies. Figure 9A depicts the representative images of bioadhesion of TCM (ECH-4)on vaginal mucosa, and Figure 9B represents the correlation of *ex vivo* bioadhesion of TCM (ECH-4) on vaginal mucosa and its *in vitro* drug release.

The bioadhesive ability of formulation ECH-4 was found to be excellent for a period of 24 h. By the end of 12 h, 18.33 ± 6.11% of the microparticles were adhered and retained to the

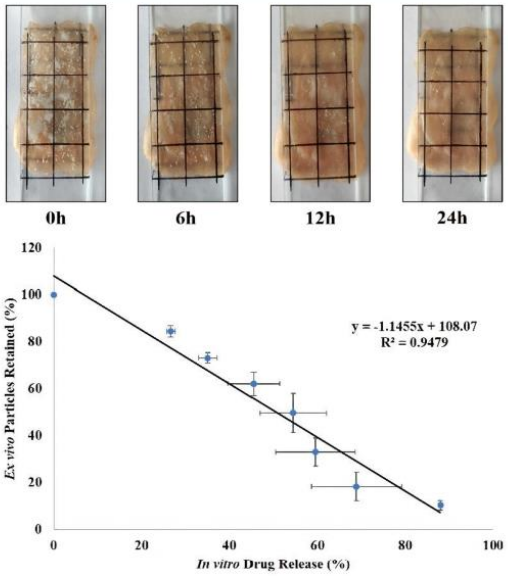

Figure 9. (A) Representative images of bioadhesion of TCM (ECH-4) on rabbit vaginal mucosa. (B) Correlation between the percentage microparticles retained on the mucosa (*ex vivo*) and the *in vitro* drug release from ECH-4.

mucosa while 81.67 ± 6.11% of the microparticles were washed off by the SVF. Higher retention of microparticles on the mucosa indicates minimal dissipation of drug from the vagina due to vaginal secretion. On correlating the *ex vivo* adhesion was correlating with the *in vitro* drug release (Figure 9) it was observed that the cumulative drug release was found to drop as the percentage particles on the mucosa decreased. It was observed that by the end of 6 h, 50% of the particles were washed off from the mucosa, which corresponds to 54.48 ± 7.59% *in vitro* drug release. It was also observed that by the end of 24 h, only about 10.33 ± 2.08% of the particles were adhered to the mucosa corresponding to 88.05 ± 0.38% of *in vitro* release of TDF from the CM.[40,50] Thus, chitosan microparticles not only displayed good initial adhesion to rabbit vaginal mucosa (residence time of 24 h) but ensured near complete drug release. The percentage of drug release was found to linearly decline as the percentage of particles adhered decreased with time. An excellent correlation between the percentage microparticles retained on the mucosa and the *in vitro* drug release with a correlation coefficient value of 0.975 was observed as indicated in Figure 9B.The mucoadhesive potential of the chitosan microparticles appears to be sufficient because TDF release occurs over a short period of time and there is no therapeutic justification to retain the formulation

https://doi.org/10.1021/acs.molpharmaceut.3c00288
Mol. Pharmaceutics 2023, 20, 5006–5018

Table 6. Physical Characterization of Vaginal Tablets

parameters	F1	F2	F3	F4
weight uniformity (mg) (n = 20)	298.82 ± 3.17	301.80 ± 1.03	301.67 ± 0.82	100.62 ± 0.11
thickness (mm) (n = 10)	4.30 ± 0.01	4.29 ± 0.01	4.31 ± 0.01	3.01 ± 0.01
diameter (mm) (n = 10)	8.00 ± 0.00	8.01 ± 0.01	8.01 ± 0.01	6.01 ± 0.01
hardness (kg/cm^2) (n = 10)	3.19 ± 0.41	3.08 ± 0.41	3.50 ± 0.16	3.05 ± 0.28
friability (%) (n = 22)	0.43 ± 0.17	0.90 ± 0.04	0.37 ± 0.08	0.32 ± 0.04
content uniformity (%) (n = 10)	90.75 ± 3.37	88.43 ± 3.03	95.06 ± 3.97	99.08 ± 1.36
disintegration time (s) (n = 6)	34.33 ± 3.14	27.33 ± 1.51	31.33 ± 4.63	60.83 ± 4.17

adhered to the patient's vaginal mucosa once the drug has been completely released.[23]

For topical PrEP, vaginal inserts consisting of multiparticulate-based drug delivery technologies have the potential to accomplish a number of desirable features, including specific site-targeted drug delivery, increased drug penetration in the mucous and tissue, bioadhesion, and retention, and prolonged drug release after intravaginal administration.[4] In order to produce good reproducible batches of DT-TCM, the direct compression method involving dry drug−excipient blending was employed, followed by compaction using a rotary tablet press. The direct compression method of tablet preparation is the simplest, robust, and cost-effective method with minimum processing steps, producing less-friable insert with high mechanical strength for better handling and packaging feasibility.[4,19]

A set of preliminary steps were undertaken to fabricate different batches of tablets employing ECH-4 microparticles as the API with the aim to optimize the release of TDF from the chitosan matrix dispersible tablet for intravaginal delivery. 40% Avicel (pH 102) incorporated in the tablets functions as a unique diluent by producing cohesive compacts and also acts as a disintegration agent. Polyvinyl pyrrolidine K-30 was used as a binder. Croscarmellose sodium played the role of a superdisintegrant, and magnesium stearate and talc are the commonly used lubricants and glidants in the tablet manufacturing process.[19,80]

3.7. Evaluation of Dispersible Vaginal Tablets. The prepared dispersible tablets were spherical in shape, flat-faced, bevel-edged, and buff colored in appearance. Table 6 enlists the results of weight variation, thickness, diameter, hardness, friability, content uniformity tests, and *in vitro* disintegration of tablet batches of F1−F4 and Figure 10 displays a comparative dissolution profile of TDF microparticles (ECH-4) and dispersible vaginal tablets (F3 and F4).

A spherical tablet punch of 8 mm diameter was chosen considering easy administration into the vaginal cavity. The API content per tablet (15 mg), tablet weight of 300 mg, tablet thickness, and hardness were maintained constant throughout the tablet manufacturing process. Minimum variation existed among the tablet batches with respect to thickness, diameter, and weight variation as reported in Table 6. The percent variation in weight was in the range of −0.404 ± 1.070% to 0.596 ± 0.340%, i.e., within the range of ±5% complying with the IP specifications. The tablets exhibited a good weight uniformity as indicated by the low values of relative standard deviation (RSD < 1%).[55] All the tablets passed the friability test, as the percent friability was reported to be within the pharmacopeial limit (F < 1%), indicating good mechanical properties. The drug content uniformity of all the batches of tablets were found to comply with the official pharmacopeial specifications, as the assay values were calculated to be 90.75 ± 3.37%, 88.43 ± 3.03%, 95.06 ± 3.97%, and 99.08 ± 1.36% for F1, F2, F3, and F4 respectively. This reflects good TCM distribution and homogeneity in the matrix of the dispersible tablet.[54,55] The dimensional stability of F1−F3 tablets was maintained for a few seconds after dropping it in SVF, following which complete disintegration was observed within approximately 30−40 s of time with no mass remaining in the apparatus. The tablets from batch F4 were found to disintegrate in approximately 60 s. The rapid disintegration of F3 tablet within 31.34 ± 4.63 s, indicates faster penetration of water into the interparticle space and good hydrophilicity of chitosan, thereby reflecting the superdisintegrant ability of chitosan polymer.[32,81] From the results of the physical characterization of the tablets, it was concluded that tablet F3 should be considered for further *in vitro* dissolution studies.

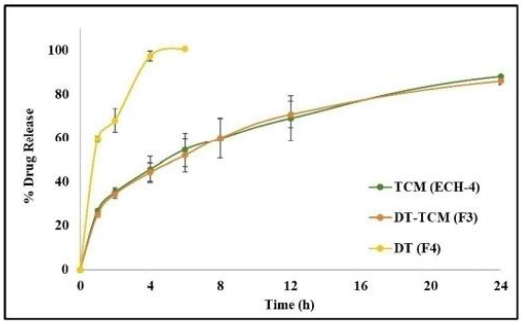

Figure 10. Comparative dissolution profiles of TDF microparticles (ECH-4) and dispersible vaginal tablets (F3 and F4).

The dissolution of DT-TCM was compared with ECH 4 to assess the impact of compaction on the bioadhesive microparticles. Ideally, we expect the dissolution of the dispersible tablets to be comparable to that of the constituent bioadhesive microparticles. The USP IV Flow through cell dissolution apparatus was employed to perform the dissolution studies. The closed-loop technique was followed as it allows disaggregation of the particles, thereby enhancing the dissolution. The glass beads used ensured laminar and more homogeneous flow of the dissolution medium from the bottom of the sample cell. Once the tablet disintegrates in a flow through cell, the glass beads present in the lower cone of the cell prevent the particles from descending into the inlet tubing. The circulation of SVF in a closed loop helps the strain rate to be more controlled.[47,48] Formulation F3 produced with TCM (ECH-4) displayed a progressively slower drug release until a steady state was attained. Formulation F4 produced with pure TDF displayed a burst release of drug within the first hour (59.42 ± 1.61%) followed by a slow release in the second hour and finally a burst release of approximately 100% drug within 6

https://doi.org/10.1021/acs.molpharmaceut.3c00288
Mol. Pharmaceutics 2023, 20, 5006−5018

h. It was observed that about 50% of TDF was released from F3 by the end of 6 h. The sustained drug release of 85.98 ± 1.61% from F3 could be related to the hydrodynamics presented in the flow through dissolution apparatus.[47] On comparing the dissolution profiles of the TDF microparticles were compared with those of the TDF vaginal tablets containing chitosan microparticles (Figure 10), it was observed that 70.77 ± 6.03% of the drug was released from the latter by the end of 12 h, which was approximately similar to that of the microparticles (68.91 ± 10.23%). The graph depicts that the drug released in a controlled manner from the formulated vaginal tablets similar to that of the constituent chitosan microparticles, which indicates that DT-TCM being a more complex system than TCM does not alter the release profile of TDF when incorporated into a rapidly dispersible tablet. Therefore, it can be inferred that administration of drug in microparticulate form retarded the drug release up to a period of 24 h, indicating it to be patient-compliant with reduced frequency of drug administration in the vagina.

Difference and similarity factors are efficient model-independent tools for reliable comparison of dissolution profiles. The dissolution profiles of TCM (ECH-4) and DT-TCM (F3) were compared to check the bioequivalence of the prepared TCM after being incorporated into a tablet dosage form, which could aid in understanding and comparing the effect of administration of a dispersible tablet in the vagina from that of the microparticulate system. The formulated tablets were considered to be bioequivalent to the microparticles with f_2 value of 78.02 and f_1 value of 1.51.[56] Therefore, the similarity value indicates that the preparation process does not affect the dissolution profile of the TCM.

The data obtained from the drug release study were used to evaluate release mechanisms and kinetics. The criteria for selecting the most appropriate model for drug release was based on the linearity value, i.e., the value of correlation coefficient, R^2. The higher R^2 value indicated that the release of TDF from the vaginal tablet was independent of its concentration. By virtue of the polymer properties, the mechanism of drug release from the tablets containing bioadhesive microparticles was found to be swelling and diffusion controlled, thereby indicating that the formulation was in accordance with the zero-order kinetics (R^2 = 0.95 ± 0.02) and Higuchi model (R^2 = 0.98 ± 0.01). From the Korsmeyer−Peppas model, the diffusion coefficient value was found to be n = 0.414 ± 0.081 < 0.50, indicating drug diffusion out of the matrix tablet via pure Fickian diffusion.[33,50,81] Therefore, the formulated vaginal tablet inherently exhibited a sustained drug release. From the commercial perspective, tablets can be considered as vaginal inserts for antiretroviral drug delivery, as it is one of the major source regions for HIV transmission.

4. CONCLUSION

Novel pre-exposure prophylactic bioadhesive formulations containing TDF offer a promising new strategy for protecting HIV-uninfected individuals against HIV acquisition. The use of bioadhesive polymers in vaginal drug delivery enhances mucoadhesive strength, prolongs drug release, and increases the residence time. The small size and high surface-to-volume ratio of bioadhesive particulate systems promote regional concentration and biodistribution, making them well-suited for retention on the vaginal mucosa. As these particles are delivered directly to the site of action, they are effective in preventing HIV transmission during sexual intercourse. While the trend in HIV prevention is toward the development of long-acting systemic formulations, intravaginal dispersible tablets offer a novel on-demand option for HIV-negative men and women.

AUTHOR INFORMATION

Corresponding Author

Shivakumar H.N − *Department of Pharmaceutics, Dr. Prabhakar B Kore Basic Science Research Center, Off-campus, KLE College of Pharmacy (A constituent unit of KAHER-Belagavi), Bengaluru 560010 Karnataka, India;* orcid.org/0000-0003-1596-9941; Phone: +91-9448241420; Email: shivakumarhn@gmail.com

Authors

Dhruti Avlani − *Department of Pharmaceutics, Dr. Prabhakar B Kore Basic Science Research Center, Off-campus, KLE College of Pharmacy (A constituent unit of KAHER-Belagavi), Bengaluru 560010 Karnataka, India;* orcid.org/0000-0001-5030-4801

Avichal Kumar − *Department of Pharmaceutics, Dr. Prabhakar B Kore Basic Science Research Center, Off-campus, KLE College of Pharmacy (A constituent unit of KAHER-Belagavi), Bengaluru 560010 Karnataka, India*

Complete contact information is available at: https://pubs.acs.org/10.1021/acs.molpharmaceut.3c00288

Notes

The authors declare no competing financial interest.

ACKNOWLEDGMENTS

The authors are grateful to Sri Prabhakar Kore, Chancellor, KLE Academy of Higher Education and Research, Deemed University, Belgaum, for providing facilities to carry out the research work. They are grateful to the Department of Pharmaceutics, KLE College of Pharmacy, Bengaluru, for providing all the necessary instruments, facilities and support for carrying out the research work. The authors are grateful to Vision Group on Science and Technology, Bengaluru, Karnataka, India, for funding (GRD No. 747 of CISEE) to procure the necessary equipment needed to undertake the project. They are thankful to Aurobindo Pharma, Hyderabad, India, for providing the gift sample of tenofovir disoproxil fumarate and Central Institute of Fisheries Technology, Kochi, Kerala, India, for providing the gift sample of chitosan. The authors acknowledge Malvern Instruments Inc., Bengaluru, Karnataka, India, for measurement of particle size. The authors also thank the BMS College of Engineering, Bengaluru, Karnataka, India, for the scanning electron microscopic images; Centre for Advanced Materials Technology, MS Ramaiah Institute of Technology, Bengaluru, Karnataka, India for performing the DSC and PXRD studies.

REFERENCES

(1) HIV Transmission, *Centers for Disease Control and Prevention*. https://www.cdc.gov/hiv/basics/transmission.html (Accessed as on 23 January 2023).

(2) Latest HIV Estimates and Update On COVID-19 Disruptions, July 2022, *World Health Organisation*. https://cdn.who.int/media/docs/default-source/hq-hiv-hepatitis-and-stis-library/2022_global_summary_web_v12.pdf (Accessed on 1 February 2023).

(3) Devi, K.; Pai, R. S. Antiretrovirals: Need For An Effective Drug Delivery. *Indian J. Pharm. Sci.* **2006**, *68*, 1−6.
(4) Peet, M. M.; Agrahari, V.; Anderson, S. M.; Hanif, H.; Singh, O. N.; Thurman, A. R.; Doncel, G. F.; Clark, M. R. Topical Inserts: A Versatile Delivery Form For HIV Prevention. *Pharmaceutics* **2019**, *11*, 374.
(5) Grande, F.; Ioele, G.; Occhiuzzi, M. A.; De Luca, M.; Mazzotta, E.; Ragno, G.; Garofalo, A.; Muzzalupo, R. Reverse Transcriptase Inhibitors Nanosystems Designed For Drug Stability And Controlled Delivery. *Pharmaceutics* **2019**, *11*, 197.
(6) Vyslouzil, J.; Kubova, K.; Tkadleckova, V. N.; et al. Clinical Testing of Antiretroviral Drugs As Future Prevention Against Vaginal And Rectal Transmission of HIV Infection − A Review Of Currently Available Results. *Acta Pharm.* **2019**, *69*, 297−319.
(7) Patki, M.; Vartak, R.; Jablonski, J.; et al. Efavirenz Nanomicelles Loaded Vaginal Film (EZFilm) For Preexposure Prophylaxis (PrEP) of HIV. *Colloids Surf., B* **2020**, *194*, 111174.
(8) Pre-Exposure Prophylaxis. https://www.hiv.gov/hiv-basics/hiv-prevention/using-hivmedication-to-reduce-risk/pre-exposure-prophylaxis (Accessed on 15 December 2022).
(9) Arnold, E. A. A Qualitative Study of Provider Thoughts On Implementing Pre-Exposure Prophylaxis (Prep) In Clinical Settings To Prevent HIV Infection. *PLoS One* **2012**, *7*, No. e40603.
(10) Tetteh, R. A.; Yankey, B. A.; Nartey, E. T.; Lartey, M.; Leufkens, H. G. M.; Dodoo, A. N. O. Pre-Exposure Prophylaxis For HIV Prevention: Safety Concerns. *Drug Saf.* **2017**, *40*, 273−283.
(11) FDA Approves Second Drug to Prevent HIV Infection As Part of Ongoing Efforts To End The HIV Epidemic, 2019. https://www.fda.gov/news-events/press-announcements/fda-approves-seconddrug-prevent-hiv-infection-part-ongoing-efforts-end-hiv-epidemic (Accessed on 4 March 2020).
(12) Mesquita, L.; Galante, J.; Nunes, R.; Sarmento, B.; das Neves, J. Pharmaceutical Vehicles For Vaginal And Rectal Administration of Anti-HIV Microbicide Nanosystems. *Pharmaceutics* **2019**, *11*, 145.
(13) Blakney, A. K.; Jiang, Y.; Woodrow, K. A. Application of Electrospun Fibers For Female Reproductive Health. *Drug Delivery Transl. Res.* **2017**, *7*, 796−804.
(14) Jalalvandi, E.; Jafari, H.; Amorim, C. A.; et al. Vaginal Administration of Contraceptives. *Sci. Pharm.* **2021**, *89*, 3.
(15) Veiga-Ochoa, M.-D.; Ruiz-Caro, R.; Cazorla-Luna, R.; Martin-Illana, A.; Notario-Perez, F. Vaginal Formulations For Prevention of Sexual Transmission of HIV. *Adv. HIV AIDS Control* **2018**, *3*, 227−248.
(16) Date, A.; Destache, C. J. A Review of Nanotechnological Approaches For The Prophylaxis of HIV/AIDS. *Biomaterials.* **2013**, *34*, 6202−6228.
(17) Rahman, S. S.; Ahmed, A. B. Vaginal Drug Delivery System A Promising Approach For Antiretroviral Drug In The Prevention Of HIV Infection: A Review. *J. Pharm. Sci. Res.* **2016**, *8*, 1330−1338.
(18) Mohideen, M.; Quijano, E.; Song, E.; et al. Degradable Bioadhesive Nanoparticles For Prolonged Intravaginal Delivery And Retention Of Elvitegravir. *Biomaterials.* **2017**, *144*, 144−154.
(19) Khar, R.; Vyas, S. P.; Ahmad, F. J.; et al. Tablets. In *Lachman/Liberman's The Theory And Practice of Industrial Pharmacy*, 4th ed.; CBS Publishers & Distributors Pvt Ltd.: India, 2013; pp 449−545.
(20) Dedeloudi, A.; Siamidi, A.; Pavlou, P.; et al. RecentAdvances In The Excipients Used In Modified Release VaginalFormulations. *Materials* **2022**, *15*, 327.
(21) Hariyadi, D. M.; Islam, N. Current Status of Alginate In Drug Delivery. *Adv. Pharmacol. Pharma. Sci.* **2020**, *2020*, 1.
(22) Lucio, D.; Martínez-Ohárriz, M. C. Chitosan: Strategies To Increase snd Modulate Drug Release Rate. In *Biological Activities and Application of Marine Polysaccharides*; Intech Open, 2017.
(23) Notario-Perez, F.; Martin-Illana, A.; Cazorla-Luna, R.; Ruiz-Caro, R.; Bedoya, L.-M.; Tamayo, A.; Rubio, J.; Veiga, M.-D. Influence of Chitosan Swelling Behaviour On Controlled Release Of Tenofovir From Mucoadhesive Vaginal Systems For Prevention of Sexual Transmission of HIV. *Mar. Drugs* **2017**, *15*, 50.
(24) das Neves, J.; Nunes, R.; Machado, A.; Sarmento, B. Polymer-based Nanocarriers For Vaginal Drug Delivery. *Adv. Drug Delivery Rev.* **2015**, *92*, 53−70.
(25) Celum, A.; Baeten, J. M. Tenofovir-based Pre-Exposure Prophylaxis For HIV Prevention: Evolving Evidence. *Curr.Opin. Infect. Dis.* **2012**, *25*, 51−57.
(26) Watkins, M. E.; Wring, S.; Randolph, R.; et al. Development of A Novel Formulation That Improves Preclinical Bioavailability Of Tenofovir Disoproxil Fumarate. *J. Pharm. Sci.* **2017**, *106*, 906−919.
(27) Mesquita, P. M. M.; Rastogi, R.; Segarra, T. J.; et al. Intravaginal Ring Delivery Of Tenofovir Disoproxil Fumarate For Prevention Of HIV And Herpes Simplex Virus Infection. *J. Antimicrob. Chemother.* **2012**, *67*, 1730−1738.
(28) Cazorla-Luna, R.; Notario-Perez, F.; Martin-Illana, A.; Ruiz-Caro, R.; Tamayo, A.; Rubio, J.; Veiga, M. D. Chitosan-based Mucoadhesive Vaginal Tablets For Controlled Release of The Anti-HIV Drug Tenofovir. *Pharmaceutics* **2019**, *11*, 20.
(29) Chapman, T. M.; McGavin, J. K.; Noble, S. Tenofovir Disoproxil Fumarate. *Drug.* **2003**, *63*, 1597−1608.
(30) Jhaveri, J.; Raichura, Z.; Khan, T.; et al. Chitosan Nanoparticles-Insight Into Properties, Functionalization And Applications In Drug Delivery And Theranostics. *Molecules.* **2021**, *26*, 272.
(31) Herdiana, Y.; Wathoni, N.; Shamsuddin, S.; Muchtaridi, M. Drug Release Study of The Chitosan-Based Nanoparticles. *Heliyon* **2022**, *8*, e08674.
(32) Khan, A.; Thakur, R. Formulation And Evaluation Of Mucoadhesive Microspheres of Tenofovir Disoproxil Fumarate For Intravaginal Use. *Curr. Drug Del.* **2014**, *11*, 112−122.
(33) Adlin Jino Nesalin, J.; Anton Smith, A. Preparation And Evaluation of Stavudine Loaded Chitosan Nanoparticles. *J. Pharm. Res.* **2013**, *6*, 268−274.
(34) Patel, K.; Patel, M. Preparation And Evaluation of Chitosan Microspheres Containing Nicorandil. *Int. J. Pharm. Inves.* **2014**, *4*, 32−37.
(35) Hiorth, M.; Nilsen, S.; Tho, I. Bioadhesive Mini-Tablets For Vaginal Drug Delivery. *Pharma.* **2014**, *6*, 494−511.
(36) Nagpal, M.; Maheshwari, D. K.; Rakha, P.; et al. Formulation Development And Evaluation of Alginate Microspheres Of Ibuprofen. *J. Young Pharm.* **2012**, *4*, 13−16.
(37) Shivakumar, H. N.; Vaka, S. R. K.; Murthy, S. N. Albumin Microspheres For Oral Delivery Of Iron. *J. Drug Target.* **2010**, *18*, 36−44.
(38) Dahmane, E.; Rhazi, M.; Taourirte, M. Chitosan Nanoparticles As A New Delivery System For The Anti-HIV Drug Zidovudine. *Bull. Korean Chem. Soc.* **2013**, *34*, 1333.
(39) Elsayed, M. Controlled Release Alginate-Chitosan Microspheres of Tolmetin Sodium Prepared By Internal Gelation Technique and Characterized By Response Surface Modeling. *Braz. J. Pharm. Sci.***2020**, *56*, DOI: 10.1590/s2175-97902020000118414.
(40) Beg, S.; Rahman, M.; Panda, S. K.; et al. Nasal Mucoadhesive Microspheres of Lercanidipine With Improved Systemic Bioavailability And Antihypertensive Activity. *J. Pharm. Innov.* **2021**, *16*, 237.
(41) Hani, U.; Shivakumar, H. G.; Gowrav, M. P. Formulation Design And Evaluation of A Novel Vaginal Delivery System of Clotrimazole. *Int. J. Pharm. Sci. Res.* **2014**, *5*, 220−227.
(42) Sinko, P. J. Micromeritics. In *Martin's Physical Pharmacy and Pharmaceutical Sciences*, 5th ed.; Lippincott Williams & Wilkins: Philadelphia, 2006; pp 535−537.
(43) Thulluru, A.; Varma, M.; Setty, C.; et al. Effect of *Sodium alginate* in Combination With HPMC K 100 M in Extending the Release of Metoprolol Succinate from its Gastro-Retentive Floating Tablets. *Indian J. Pharm. Edu. Res.* **2015**, *49*, 293−303.
(44) Mandal, S.; Kumar, S. S.; Krishnamoorthy, B.; Basu, S. K. Development And Evaluation Of Calcium Alginate Beads Prepared By Sequential And Simultaneous Methods. *Braz. J. Pharm. Sci.* **2010**, *46*, 785−793.
(45) Gomes, E.; Mussel, W.; Resende, J. M.; et al. Characterization Of Tenofovir Disoproxil Fumarate And Its Behavior Under Heating. *Cryst. Growth Des.* **2015**, *15*, 1915−1922.

(46) Deveswaran, R.; Bharath, S.; Basavaraj, B. V.; et al. Development of Mesalazine Microspheres For Colon Targeting. *Int. J. Appl. Pharm.* **2017**, *9*, 1−9.
(47) Moazami Goudarzi, N.; Samaro, A.; Vervaet, C.; Boone, M. N. Development of Flow-Through Cell Dissolution Method For*In Situ* Visualization of Dissolution Processes In Solid Dosage Forms Using X-ray _CT. *Pharmaceutics* **2022**, *14*, 2475.
(48) Sievens-Figueroa, L.; Pandya, N.; Bhakay, A.; et al. Using USP I And USP IV For Discriminating Dissolution Rates of Nano- And Microparticle-Loaded Pharmaceutical Strip-Films. *AAPS Pharm. Sci. Technol.* **2012**, *13*, 1473−1482.
(49) Gao, Z. *In Vitro* Dissolution Testing With Flow-Through Method: A Technical Note. *AAPS PharmSciTech* **2009**, *10*, 1401−1405.
(50) Szekalska, M.; Wroblewska, M.; Czajkowska-Kosnik, A.; Sosnowska, K.; Misiak, P.ł; Wilczewska, A. Z.; Winnicka, K. The Spray-Dried Alginate/Gelatin Microparticles With Luliconazole As Mucoadhesive Drug Delivery System. *Materials* **2023**, *16*, 403.
(51) Notario-Perez, F.; Martin-Illana, A.; Cazorla-Luna, R.; Ruiz-Caro, R.; Bedoya, L.-M.; Pena, J.; Veiga, M.-D. Development of Mucoadhesive Vaginal Films Based On HPMC And Zein As Novel Formulations To Prevent Sexual Transmission Of HIV. *Int. J. Pharm.* **2019**, *570*, 118643.
(52) Swain, S.; Behera, U.; Beg, S.; et al. Design And Characterization of Enteric-Coated Controlled Release Mucoadhesive Microcapsules of Rabeprazole Sodium. *Drug. Dev. Ind. Pharm.* **2013**, *39*, 548−460.
(53) Panchagnula, C. S.; Naware, N. B.; Bhamre, S. S.; Deo, K. D.; Meenakshisunderam, S. Formulation And Development of Novel And Stable Dosage Forms of Lamivudine And Tenofovir Disoproxil Fumarate Tablets By Wet Granulation Technique. *Int. J. Pharm. Sci. Res.* **2018**, *9*, 3538−3542.
(54) Khan, A. B.; Thakur, R. Design And Evaluation of Mucoadhesive Vaginal Tablets of Tenofovir Disoproxil Fumarate For Pre-Exposure Prophylaxis of HIV. *Drug Dev. Ind. Pharm.* **2018**, *44*, 472.
(55) Tests for Tablets. In *Indian Pharmacopoeia, Government of India, Ministry of Health and Family Welfare Department*, 9th ed.; Indian Pharmacopoeia Commission: Ghaziabad, India, 2023; Vol. *1* and *2* pp: 356−360 and 1342−1344.
(56) Singh, I.; Zandu, S. K.; Kumari, R. Formulation and Evaluation of Fast Disintegrating Tablets of Domperidone Using Chitosan-Glycine Conjugates as Superdisintegrant. *Thai J. Pharm. Sci.* **2020**, *45*, 32−40.
(57) Brahmankar, D. M.; Jaiswal, S. B. Bioavailability and Bioequivalence. In *Biopharmaceutics and Pharmacokinetics − A Treatise*, 2nd ed.; Vallabh Prakashan: Delhi, India, 2009; pp: 331−332.
(58) Rawat, S.; Bisht, S.; Kothiyal, P. Characterization and Release Kinetics of Microspheres and Tableted Microspheres of Diclofenac Sodium. *Am. J. Adv. Drug Del.* **2013**, *1*, 596−605.
(59) Tenofovir Disoproxil Fumarate, *Drug Bank Online*. https://go.drugbank.com/salts/DBSALT000172 (Accessed on 3 December 2019).
(60) Calderon, L.; Harris, R.; Cordoba-Diaz, M.; Elorza, M.; Elorza, B.; Lenoir, J.; Adriaens, E.; Remon, J.P.; Heras, A.; Cordoba-Diaz, D. Nano And Microparticulate Chitosan-Based Systems For Antiviral Topical Delivery. *Eur. J. Pharm. Sci.* **2013**, *48*, 216−222.
(61) Ko, J. A.; Park, H. J.; Hwang, S. J.; et al. Preparation And Characterization of Chitosan Microparticles Intended For Controlled Drug Delivery. *Int. J. Phar.* **2002**, *249*, 165−174.
(62) Pandit, K.; Nanayakkara, I. A.; Cao, W.; et al. Capture And Direct Amplification Of DNA On Chitosan Microparticles In A Single PCR-Optimal Solution. *Anal. Chem.* **2015**, *87*, 11022−11029.
(63) Vaka, S.; Shivakumar, H. N.; Repka, M.; et al. Formulation And Evaluation Of Carnosic Acid Nanoparticulate System For Upregulation of Neurotrophins In The Brain Upon Intranasal Administration. *J. Drug. Target.* **2013**, *21*, 44.
(64) Subedi, G.; Shrestha, A.; Shakya, S. Study of Effect of Different Factors In Formulation of Micro And Nanospheres With Solvent Evaporation Technique. *Open Pharm. Sci. J.* **2016**, *3*, 182−195.
(65) Akbari, J; Enayatifard, R; Saeedi, M; Saghafi, M Influence of Hydroxypropyl Methylcellulose Molecular Weight Grade On Water Uptake, Erosion And Drug Release Properties of Diclofenac Sodium Matrix Tablets. *Trop. J. Pharm. Res.* **2011**, *10*, 535−541.
(66) Sinha Roy, D.; Rohera, B. D Comparative Evaluation Of Rate of Hydration And Matrix Erosion Of HEC And HPC And Study of Drug Release From Their Matrices. *Eur. J. Pharm. Sci.* **2002**, *16*, 193−199.
(67) Patil.; et al. 2011 − Patil, S.B. and Sawant, K.K. Chitosan Microspheres As A Delivery System For Nasal Insufflations. *Colloids Surf. B Biointerfaces* **2011**, *84*, 384−389.
(68) Danaei, M.; Dehghankhold, M.; Ataei, S.; et al. Impact of Particle Size And Polydispersity Index On The Clinical Applications of Lipidic Nanocarrier Systems. *Pharm.* **2018**, *10*, 57.
(69) Chen, W.; Palazzo, A.; Hennink, W.; et al. The Effect of Particle Size On Drug Loading And Release Kinetics of Gefitinib-Loaded PLGA Microspheres. *Mol. Pharm.* **2017**, *14*, 459.
(70) Bulut, E.; Şanlı, O. Novel Ionically Crosslinked Acrylamide-Grafted Poly(Vinyl Alcohol)/Sodium Alginate/Sodium Carboxymethyl Cellulose Ph-Sensitive Microspheres For Delivery of Alzheimer's Drug Donepezil Hydrochloride: Preparation And Optimization Of Release Conditions. *Artificial Cells, Nanomed., Biotechnol.* **2016**, *44*, 431−442.
(71) Yuan, Q.; Shah, J.; Hein, S.; et al. Controlled And Extended Drug Release Behaviorof Chitosan-Based Nanoparticle Carrier. *Acta Biomaterilia.* **2010**, *6*, 1140−1148.
(72) Meng, J.; Sturgis, T.; Youan, B. Engineering Tenofovir Loaded Chitosan Nanoparticles To Maximize Microbicide Mucoadhesion. *European J. Pharm. Sci.* **2011**, *44*, 57−67.
(73) Zaman, M.; Butt, M. H.; Siddique, W.; et al. Fabrication of PEGylated Chitosan Nanoparticles Containing Tenofovir Alafenamide: Synthesis and Characterization. *Molecules* **2022**, *27*, 8401.
(74) Martins, A. F.; de Oliveira, D. M.; Pereira, A. G.B.; Rubira, A. F.; Muniz, E. C. Chitosan/TPP Microparticles Obtained By Microemulsion Method Applied In Controlled Release of Heparin. *Int. J. Biol. Macromol.* **2012**, *51*, 1127−1133.
(75) Tong, Z.; Chen, Y.; Liu, Y.; et al. Preparation, Characterization and Properties of Alginate/Poly(g-glutamic acid) Composite Microparticles. *Mar. Drugs.* **2017**, *15*, 91.
(76) Patil, S.; Kadam, C.; Pokharkar, V. QbD Based Approach For Optimization Of Tenofovir Disoproxil Fumarate Loaded Liquid Crystal Precursor With Improved Permeability. *J. Adv. Res.* **2017**, *8*, 607−616.
(77) Safari, J. B.; Bapolisi, A. M.; Krause, R. W. M. Development of pH-Sensitive Chitosan-g-poly(acrylamide-co-acrylic acid) Hydrogel for Controlled Drug Delivery of Tenofovir Disoproxil Fumarate. *Polymers* **2021**, *13*, 3571.
(78) Narayanan, V. H. B.; Lewandowski, A.; Durai, R.; Gonciarz, W.; Wawrzyniak, P.ł; Brzezinski, M. Spray-Dried Tenofovir Alafenamide-Chitosan Nanoparticles Loaded OleogelsAsA Long-Acting Injectable Depot System Of Anti-Hiv Drug. *Int. J. Biol. Macromol.* **2022**, *222*, 473−486.
(79) Kelly, S.; Upadhyay, A.; Mitra, A.; et al. Analyzing Drug Release Kinetics From Water-Soluble Polymers. *Ind. Eng. Chem. Res.* **2019**, *58*, 7428−7437.
(80) Raymond, C. R.; Sheskey, P. J.; Weller, P. Cellulose Microcrystalline, Chitosan, Magnesium Stearate, Povidone, Talc. In *Handbook of Pharmaceutical Excipients*, 4th ed.; Pharmaceutical Press and the American Pharmaceutical Association: London, 2003; pp 108−110, 132−134, 354−356, 508−512, and 641−643.
(81) Anraku, M.; Mizukai, Y.; Maezaki, Y. The Preparation And Validation of Chitosan Tablets That Rapidly Disperse And Disintegrate As An Oral Adsorbent In The Treatment of Lifestyle-Related Diseases. *Carb. Polymers.* **2021**, *253*, 117246.

https://doi.org/10.1021/acs.molpharmaceut.3c00288
Mol. Pharmaceutics 2023, 20, 5006−5018

9.2.4. Publication: Pessaries

International Journal of Biological Macromolecules 258 (2024) 128816

Contents lists available at ScienceDirect

International Journal of Biological Macromolecules

journal homepage: www.elsevier.com/locate/ijbiomac

Pre-exposure prophylactic mucoadhesive sodium alginate microsphere laden pessaries for intravaginal delivery of tenofovir disoproxil fumarate

Dhruti Avlani [a], H.N. Shivakumar [a,*], Avichal Kumar [a], A. Prajila [a], Babiker Bashir Haroun Baraka [b], V. Bhagya [b]

[a] Department of Pharmaceutics, Dr. Prabhakar B Kore Basic Science Research Center, Off-campus, KLE College of Pharmacy (A constituent unit of KAHER-Belagavi), Rajajinagar, Bengaluru 560010, Karnataka, India
[b] Department of Pharmacology, Dr. Prabhakar B Kore Basic Science Research Center, Off-campus, KLE College of Pharmacy (A constituent unit of KAHER-Belagavi), Rajajinagar, Bengaluru 560010, Karnataka, India

ARTICLE INFO

Keywords:
Intravaginal
Sodium alginate
Tenofovir
Pessaries
Mucoadhesion
Sustained release

ABSTRACT

The research aimed to develop novel bioadhesive sodium alginate (Na-Alg) microspheres laden pessaries for intravaginal delivery of tenofovir disoproxil fumarate (TDF), to overcome limitations of conventional dosage forms. Twelve batches of microspheres formulated by emulsification gelation method indicated that drug-polymer ratios and polymer type affected particle size, drug release, and entrapment efficiency (%EE). Microspheres of batch EH-8 with drug: polymer ratio of 1:4 containing equal amounts of Na-Alg and HPMC K100M displayed optimal %EE (62.09 ± 1.34 %) and controlled drug release (97.02 ± 4.54 % in 12 h). Particle size analysis in Matersizer indicated that microspheres (EH-8) displayed a surface-mean diameter of 11.06 ± 0.18 μm. *Ex-vivo* mucoadhesion studies on rabbit mucosa indicated that microspheres (EH-8) adhered well for 12 h. Microspheres integrated into pessaries displayed a sustained release profile (95.31 ± 1.37 % in 12 h) in simulated vaginal fluid. *In vivo* studies in rabbits indicated that pessaries displayed a significantly higher C_{max} (41.18 ± 3.57 ng/mL) ($P < 0.005$) and reduced T_{max} (1.00 ± 0.01 h) ($P < 0.0001$) of TDF concentrations in vaginal fluid compared to oral tablets. The microparticulate pessaries with the ability to elicit higher vaginal fluid levels in the crucial initial hours of insertion demonstrates a potential novel platform to offer better self-protection to HIV-negative women against HIV during sexual intercourse.

1. Introduction

HIV and AIDS have been major global issues that have affected the health, society, and economies around the world [1]. The World Health Organisation (WHO) estimates indicate that around 39 million people had HIV in 2022, with 1.5 million new infections, and about 650,000 deaths due to HIV/AIDS, emphasizing its severe consequences [2]. According to Centers for Disease Control and Prevention (CDC), HIV spreads mainly through sexual intercourse involving vagina/anus. In developed countries, Highly Active Antiretroviral Therapy (HAART) has lowered HIV-related illness and death rates [3]. However, many drugs used in HAART have low oral bioavailability due to issues like poor solubility or limited permeability preventing drugs from reaching infection sites thereby raising the risk of relapse [4,5].

In this context, preventive measures like pre-exposure prophylaxis (PrEP) are vital to cut down on HIV transmission. PrEP involves the administration of antiretroviral drugs to HIV-negative individuals daily to decrease their risk of acquiring the virus. Currently, USFDA has approved two antiretroviral formulations, Truvada® and Descovy®, for daily oral use as PrEP. Truvada® is not widely used in the US due to its high cost, potential kidney toxicity, and low patient adherence [6]. In 2019, the approval of Descovy® as an alternative option for HIV PrEP provided a better safety profile compared to Truvada®. However, the safety and effectiveness of the formulation as well as participant adherence are critical for achieving positive therapeutic outcomes, as demonstrated by clinical studies [7–11].

Topical vaginal PrEP is a novel HIV prevention method for HIV-negative women, using antiretrovirals at the vaginal mucosal surfaces to block viral entry [4]. It involves applying medications like vaginal tablets, vaginal gels, pessaries, or vaginal rings to create a protective barrier against HIV exposure. Products such as gels, douches inserts, or suppositories are reported to be promising dosage forms for on-demand

* Corresponding author.
E-mail address: shivakumarhn@gmail.com (H.N. Shivakumar).

https://doi.org/10.1016/j.ijbiomac.2023.128816
Received 5 October 2023; Received in revised form 4 December 2023; Accepted 13 December 2023
Available online 18 December 2023

pre-exposure prophylaxis (PrEP) [12–16]. Topical vaginal inserts offer site-specific drug delivery and convenience over oral methods. Compared to oral administration, topical PrEP bypasses gastrointestinal and hepatic first-pass effects, reducing the required dose and incidence of side effects [4,14]. These formulations maintain effective local concentrations, limiting systemic exposure and making them preferable for avoiding viral transmission and ensuring effective treatment [15].

Conventional vaginal inserts, such as tablets, films, creams, gels, and rings, are being commonly explored as a promising approach for PrEP [4,5]. However, most of these dosage forms exhibit several limitations like poor retention, need for an applicator, potential irritation, leakage, and instability, thereby reducing the effectiveness. Thus, the effectiveness of the tenofovir 1 % gel, which initially showed promise in the CAPRISA 004 trial, was not confirmed in subsequent Phase IIb/III trials, likely due to inconsistent and insufficient use by young, at-risk women in different dosing regimens. Thus, most of the conventional formulations used for PrEP demonstrated poor adherence and compliance issues [12,15,16].

Considering the limitations of conventional intravaginal PrEP formulations our group was the first to develop an instantaneously dispersible tablet comprising of bioadhesive microspheres to improve drug retention and drug delivery [17]. In continuation, the current project aims to develop novel pessaries containing tenofovir disoproxil fumarate (TDF) loaded bioadhesive sodium alginate (Na-Alg) microspheres for intravaginal administration. Pessaries are ideal intravaginal dosage forms that can incorporate materials of diverse polarity [16]. TDF by virtue of its longer half-life (12-15 h), and lower IC_{50}, makes it a promising topical microbicide for development of prophylactic pessaries [18–20]. Sodium alginate (Na-Alg) would be employed as a bioadhesive polymer to fabricate the microspheres. Cocoa butter were specifically preferred as the base material to develop the pessaries to prevent the dissipation of water soluble TDF into pessary base. The novel, first of its kind microspheres laden pessaries unlike the conventional single unit intravaginal dosage forms are less prone to expulsion as they melt to readily disperse the constituent drug loaded bioadhesive microspheres. The dispersed bioadhesive microspheres in turn would be well retained on the vaginal mucosa and release the drug in a controlled fashion as represented in Fig. 1.

TDF inhibits reverse transcription by terminating the DNA chain by HIV Reverse Transcriptase [12,21]. TDF, which belongs to BCS Class III, exhibits low oral bioavailability (~25 %) due to intestinal and efflux transport [22]. Alginate is a natural biomacromolecule that is biocompatible, biodegradable, that is used for delivery of microencapsulated actives [23,24]. Alginate can be combined with hydrophilic polymers like chitosan, hydroxypropyl methylcellulose (HPMC), and sodium carboxymethyl cellulose (Na-CMC), to enhance drug delivery by improving absorption [24]. Na-Alg is a monovalent, water-soluble polysaccharide that hardens into a gel when exposed to divalent ions like calcium [25]. Alginate exhibits robust mucoadhesion when in a solid state, primarily by mechanisms involving hydrogen bonding, hydration, and polymer gelation [26].

2. Materials and methods

2.1. Materials

TDF was received as a gift sample from Aurobindo Pharma, Hyderabad, India. Na-Alg (Protanal LFR 5/60 USP NF; M/G = 30/70 %) was received as a gift sample from FMC BioPolymers, USA. HPMC K4M (Methocel) and K-100 M (Benecel) were received as a gift sample from The Dow Chemical Company, USA. Cocoa butter was purchased from SK Organics, Anand, Gujarat, India. Na-CMC, light liquid paraffin, span 80, calcium chloride, petroleum ether, beeswax, and tween 60 were purchased from S.D. Fine Chemicals Ltd. (India). All reagents and chemicals used were of analytical grade.

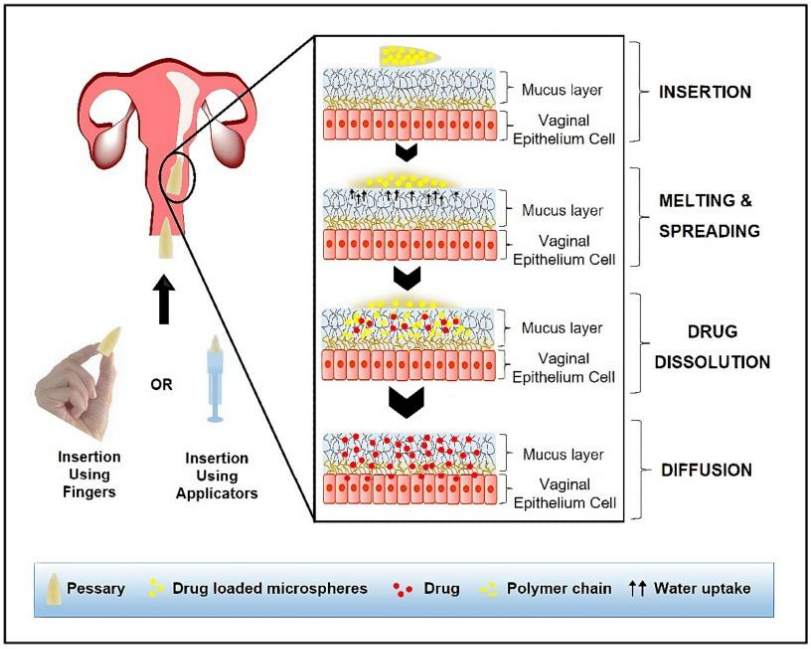

Fig. 1. Intravaginal drug delivery from pessaries containing drug loaded bioadhesive microspheres.

2.2. Preparation of TDF loaded Na-Alg microspheres

Emulsification internal gelation technique as depicted in Fig. 2 was employed for the preparation of TDF loaded Na-Alg microspheres (TAM) using Na-Alg as a bioadhesive polymer alone and in combination with various polymers (Table 1) [27]. A homogeneous aqueous dispersion (2%*w/v*) of TDF and polymers was added to the continuous phase which comprised 60 mL light liquid paraffin and 1.5%*v/v* Span 80, under constant mechanical stirring at 500 rpm [23]. The homogeneous water-in-oil emulsion was homogenized at 5000 rpm for 15 mins (T18 digital Ultra Turrax®, IKA®). Under continuous stirring, 10%*w/v* calcium chloride ($CaCl_2$) solution was added to obtain rigid discrete particles [28]. The microspheres obtained were isolated through centrifugation at 4000 ×*g* for 30 mins, rinsed multiple times with petroleum ether to eliminate any residual oil remnants in the microspheres, and air-dried at ambient room temperature [29,30].

2.3. Characterization of microspheres

2.3.1. Practical yield and drug entrapment efficiency (%EE)

The mass balance was evaluated by determining the yield of every batch of microsphere, based on the proportions of the raw materials utilized in their preparation using Eq. (1). An accurately measured amount of TAM was pulverized and digested in 5 mL of simulated vaginal fluid (pH 4.5) (SVF) [31] using an ultrasonic bath to release the entrapped drug for a period of one night. The resulting dispersion was subjected to centrifugation at a speed of 10,000 rpm for 5 mins. The quantity of TDF present in the supernatant was determined spectrophotometrically (Shimadzu UV–Vis Spectrophotometer 1900i, Shimadzu Corporation, Japan) at 259 nm after appropriate dilution. The % EE was determined in triplicate for all batches and calculated using the Eqs. (2), (3), and (4) [29,32].

$$\%\text{Practical Yield} = \frac{\text{Weight of microspheres}}{\text{Weight of drug} + \text{Weight of polymers}} \times 100 \quad (1)$$

$$\%\text{Theoretical Drug Loading (TDL)} = \frac{\text{Weight of drug taken}}{\text{Weight of drug taken} + \text{Weight of polymers taken}} \times 100 \quad (2)$$

$$\%\text{Practical Drug Loading (PDL)} = \frac{\text{Weight of drug loaded into microspheres}}{\text{Weight of microspheres}} \times 100 \quad (3)$$

$$\%EE = \frac{\%PDL}{\%TDL} \times 100 \quad (4)$$

2.3.2. Surface morphology

The surface morphology and topography of the TAM were investigated by scanning electron microscope (SEM) (Scanning Electron Microscope, TESCAN-VEGA3 LMU) The samples were mounted on SEM stab with double-sided sticking tape and gold coated (~200 μm) using an ion sputtering device under reduced pressure (0.001 Torr) for 5 min. The gold coated (~200 nm) samples were scanned under suitable magnification to acquire photomicrographs of TAM [33].

2.3.3. Particle size analysis

The size of the TAM was determined in triplicate employing the laser diffraction technique using Malvern Mastersizer -v3.62 (Malvern Instruments Ltd., UK). The microspheres were subjected to sonication in propanol using a 600 W probe for a span of 10 min. This technique helps to disperse the cluster of microspheres and de-aggregate any aggregates to achieve a uniform distribution of the microspheres, ensuring clear detection during measurement [34].

2.3.4. Fourier transform infra-red (FTIR) spectroscopic analysis

FTIR spectroscopy is a commonly employed analytical method for characterizing drugs, polymers, physical mixture, and optimized formulation. To minimize infrared (IR) scattering on the particle surface, the samples were prepared by uniformly mixing with potassium bromide. The resulting mixture was loaded into the diffuse reflectance sample holder and analyzed using an FTIR spectrometer (Jasco, 460 Plus, Jasco Inc., United States) within the wavelength range of 4000 cm^{-1} to 1000 cm^{-1} at a scanning speed of 2 mm/s [33,35,36].

2.3.5. Differential scanning calorimetry (DSC) analysis

DSC has been widely employed as a calorimetric technique to analyze the solid state of drugs in various polymers. The thermal behavior of the drug, polymers, physical mixture, and the optimized formulation was examined using a DSC system (NETZSCH, STA 449 F5 Jupiter thermal analyzer, Germany). The samples were subjected to a heating rate of 30 °C/min, covering a temperature range of 20 to 300 °C, to collect data for analysis [33,35,37]. The degree of crystallinity (X_c) of TAM was calculated using Eq. (5).

$$X_c = \frac{\Delta H_m}{(1 - w) \times \Delta H_m^0} \times 100 \quad (5)$$

where ΔH_m is the measured heat of fusion, ΔH_m^0 is the heat of fusion of 100 % crystalline sample, and w is the weight fraction of TDF in the polymer matrix [38].

2.3.6. Powder X-ray diffraction (PXRD) analysis

PXRD techniques have been extensively utilized for characterizing the solid state of the drugs in various polymers. In this study, the diffraction patterns of the drug, polymers, physical mixture, and optimized formulation were obtained using Bruker D8 ADVANCE X-ray Diffractometer, United States. The instrument was equipped with a 2.2 kW X-ray source utilizing a Cu anode and a fine focus ceramic X-ray tube operated at 40 kV voltage and 40 mA current, resulting in a power output of 1.6 kW. Data collection was performed within the 5 to 40° 2θ range using a LYNXEYE high-speed SSD160-2 detector with a 500 μm sensor [33,35,39,40]. The relative degree of crystallinity (RDC) was determined by comparing some representative peak heights in the diffraction patterns of the formulation with those of the drug, using Eq. (6) [41].

$$RDC = \frac{I_{sample}}{I_{reference}} \quad (6)$$

where, I_{sample} is the characteristic peak height of the optimized formulation and $I_{reference}$ is the characteristic peak height at the same angle for the drug with the highest intensity.

2.3.7. In vitro drug release studies

The *in vitro* dissolution studies were performed in triplicate for a period of 12 h using USP IV flow-through cell dissolution apparatus

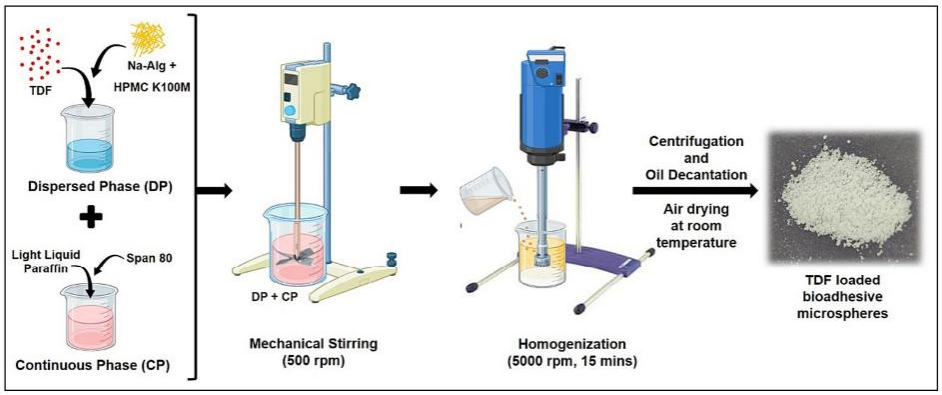

Fig. 2. Preparation of TDF loaded Na-Alg microspheres employing emulsification internal gelation technique.

(Electrolab, Model No. EFT-01) taking into account the standard intravaginal retention time as per the literature [42]. Glass beads were introduced into the flow-through cell to ensure a consistent laminar flow of SVF at a temperature of 37 ± 0.5 °C through the sample. A definite weighed amount of TAM was positioned appropriately in the sample holder. A flow rate of 16 mL/min of SVF was maintained throughout the study in a closed loop system [43–45]. At specific time points, aliquots were collected and subjected to spectrophotometric analysis at a wavelength of 259 nm to determine the extent of drug release.

The dissolution profiles of various batches of microspheres were compared on the basis of statistical methods or model-dependent approaches to understand the kinetics and mechanism of the drug release. The *in vitro* release data obtained in the present study were fitted to four different kinetic mathematical model-dependent methods – zero order, first order, Higuchi and Korsmeyer-Peppas release equations as presented in Table 2 that can explain the release behavior of TDF from the microspheres [46–48].

2.3.8. Ex vivo mucoadhesion studies

The mucoadhesive properties of optimized microspheres were assessed for a period of 12 h using a modified USP disintegration apparatus (Electrolab, ED-2 L) [17]. A freshly excised piece of rabbit vagina (5x1cm) was used as a substrate and affixed to a glass slide with glue. Around 200 microspheres were evenly distributed on the substrate, and the glass slide was attached to the disintegration apparatus. The apparatus was then operated, causing the tissue to undergo slow, regular up and down movements in SVF at 37 ± 0.5 °C. At pre-defined time intervals, the apparatus was stopped, and the microspheres adhering to the mucosal tissue were counted under an optical microscope (Labomed, LB-200). The percentage of mucoadhesion was determined in triplicate using Eq. (7) [49].

$$\%\text{Mucoadhesion} = \frac{\text{No. of microspheres adhered}}{\text{Initial no. of microspheres}} \times 100 \quad (7)$$

2.4. Preparation of pessaries

The optimized TAM formulation was incorporated into pessaries employing the conventional fusion moulding technique using pessary moulds as represented in Fig. 3. Drug loaded pessaries were produced using cocoa butter, beeswax and tween 60 employing the formula represented in Table 3. Cocoa butter was used as the pessary base and melted in a porcelain dish placed on a heated water bath (~40 °C). Beeswax, tween 60 and TAM were added to the melt in small portions to avoid the formation of aggregates. The base-microsphere mixture was thoroughly dispersed and once uniformity was achieved; the molten mass was poured into previously calibrated stainless steel pessaries moulds (0.9–1.0 g). The pessaries were allowed to cool in a refrigerator maintained at 2–8 °C until they were completely solidified [50,51].

2.5. Characterization of pessaries

The formulated pessaries of each batch were subjected to quality control checks following the official procedures as mentioned in the Indian Pharmacopoeia 2018 (IP).

Table 1
Formulation of different batches of TAM.

Formulation code (FC)	Drug (%w/v)	Na-Alg (%w/v)	Na-CMC (%w/v)	HPMC K4M (%w/v)	HPMC K100M (%w/v)	$CaCl_2$ (%w/v)
EH – 1	1.0	2.0	–	–	–	10.0
EH – 2	1.0	1.0	1.0	–	–	10.0
EH – 3	1.0	1.0	–	1.0	–	10.0
EH – 4	1.0	1.0	–	–	1.0	10.0
EH – 5	1.0	4.0	–	–	–	10.0
EH – 6	1.0	2.0	2.0	–	–	10.0
EH - 7	1.0	2.0	–	2.0	–	10.0
EH – 8	1.0	2.0	–	–	2.0	10.0
EH – 9	1.0	9.0	–	–	–	10.0
EH – 10	1.0	4.5	4.5	–	–	10.0
EH – 11	1.0	4.5	–	4.5	–	10.0
EH – 12	1.0	4.5	–	–	4.5	10.0

Table 2
Mathematical models used to describe the release behavior of TDF from the microspheres.

Model	Equation
Zero Order Kinetic Model	$Q_t = Q_0 + K_0 t$
First Order Kinetic Model	$\text{Log } Q_t = \text{Log } Q_0 + K_1 t$
Higuchi Release Model	$Q = K_H * \sqrt{t}$
Korsmeyer-Peppas Release Model	$F = (Q_t/Q) = K_K * t^n$

Where, t = Time in hours, Q_0 = Initial amount of drug, Q_t = Cumulative amount of drug release at time (t), K_0, K_1, K_H, K_K = Zero order, First order, Higuchi and Korsmeyer-Peppas release constant respectively, F = Fraction of drug released at time (t), Q_t = Amount of drug released at time (t), Q = Total amount of drug in dosage form, n = Diffusion or release exponent which explains different mechanisms of drug transport from polymeric drug delivery systems.

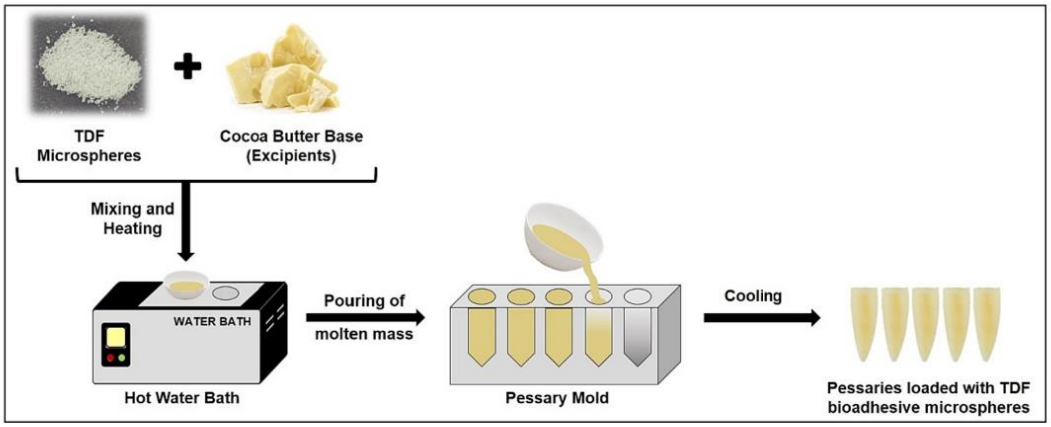

Fig. 3. Diagrammatic representation of the preparation of pessaries employing fusion moulding technique.

Table 3
Composition of pessaries.

Sl. No.	Ingredients	Quantity (%)		
		F1	F2	F3
1	Drug (TAM EH-8)	17	17	17
2	Cocoa Butter	65	62	60
3	Beeswax	10	15	17
4	Tween 60	8	6	6

2.5.1. Physical appearance

Ten randomly selected pessaries from each batch were visually inspected to examine the color and surface texture of the pessaries for possible cracks and pits that could be caused by air entrapment.

2.5.2. Weight uniformity

Twenty pessaries from each batch were randomly selected and weighed individually in an analytical balance (Shimadzu, BL-220H). The average weight and percentage deviation from the average weight were calculated to assess the weight uniformity [52].

2.5.3. Melting point

The melting points of three batches of pessaries were determined using the ascending melting point method. In this method, capillary tubes, sealed at one end and measuring 10 cm in length, were filled with the pessary formulation to a height of approximately 1 cm. This filling procedure was carried out while the capillaries were in an ice bath to prevent the pessary from melting during handling. Subsequently, these tubes were immersed in an electro-thermal thermometer with heat gradually increasing, and the temperature at which the pessaries melted was noted.

2.5.4. Content uniformity

Ten pessaries were randomly selected from each batch and tested for content uniformity. Each pessary was allowed to melt in SVF maintained at 40 °C and sonicated to extract the drug. The drug content was quantified spectrophotometrically on suitable dilution at 259 nm [52–54].

2.5.5. In vitro disintegration time

Disintegration time (DT) of six pessaries from each batch was determined using Electrolab Disintegration tester apparatus (Electrolab, Model No. ED 2 L) in SVF (500 mL) maintained to 37 ± 0.5 °C. The time point at which the fat-soluble-based pessaries melted to release the constituent TAM was recorded as the DT [52].

2.5.6. In vitro dissolution studies

The *in vitro* release of drug from the pessaries was studied using USP IV flow-through cell dissolution apparatus (Electrolab, Model No. EFT-01). The study was performed in a flow-through method in SVF maintained at 37 ± 0.5 °C for a period of 12 h, following closed loop method. The pessary was placed in the sample holder in a manner such that the medium flow is always perpendicular to the pessary. A flow rate of 16 mL/min of the SVF was maintained for a period of 12 h. Aliquots were withdrawn at predetermined time intervals, filtered and analyzed at 259 nm using double beam UV-VIS spectrophotometer to measure the released TDF [43,45].

A model-dependent method was followed to compare the dissolution profile of TAM and pessaries by determining the difference factor (f_1) and similarity factor (f_2) using Eqs. (8) and (9).

$$\text{Difference Factor } (f_1) = \frac{\sum_{t=1}^{n}(R_t - T_t)}{\sum_{t=1}^{n} R_t} \times 100 \quad (8)$$

$$\text{Similarity Factor } (f_2) = 50 \times log\left\{\sqrt{\left[1 + \frac{1}{n}\sum_{t=1}^{n}(R_t - T_t)^2\right]} \times 100\right\} \quad (9)$$

where, 'n' is the number of dissolution time points; R_t is the dissolution value of the reference drug product at time t; and T_t is the dissolution value of the test drug product at time t. In the range of 0 to 100, the dissolution profile of the test sample is considered to be identical to that of the reference sample if f_2 ranges from 50 ≤ 100 and f_1 ranges from 0 ≤ 15 [55,56].

Table 4
Experimental design of *in vivo* study.

Group No.	Treatment	Animals allotted
Group – I	Normal Control (NC)	6
Group – II	Treated with Marketed TDF Oral Tablet (MT)	6
Group – III	Treated with TDF Vaginal Pessary (P-TAM)	6

2.6. In vivo studies

The *in vivo* experimental protocol was approved by the Institutional Animal Ethical Committee (No.05/HNSK/2021) and conducted at KLE College of Pharmacy, Bengaluru. A total of three treatment groups with six animals in each group were assigned for the animal studies. A total of 18 female adult (10–12 months) New Zealand Rabbits weighing approximately 2.0 kg were selected as the *in vivo* model for the pharmacokinetic studies and grouped as mentioned in Table 4.

To begin with the studies, the rabbits were anesthetized with Isoflurane (0.1–0.2 mL/kg) [57] prior to drug administration. Animals of group I were treated with intravaginal dispersion of 1 mL of placebo microspheres that served as the control. A dose of 7.5 mg/kg body weight was administered orally to group II animals while group III was treated intravaginally with the help of a catheter. The vaginal secretion/fluids measuring 4–5 mL were withdrawn at pre-determined time intervals of 1, 2, 4, 6, 12, and 24 h with the help of a catheter and syringe using the flush technique in addition to the sample drawn at time zero which was considered as the baseline value [58,59]. The samples were subjected to cold centrifugation (10,000 rpm, 10 mins) and analyzed chromatographically using Liquid Chromatography Mass spectroscopy/Mass spectroscopy (LC-MS/MS) (Sciex, API-4000, Shimadzhu) [59–61].

2.6.1. Analytical method

The preparation of the extraction solution involved combining 200 mL of acetonitrile, 200 μL of 100 % formic acid, and 40 μl of Verapamil used as internal standard (250 μg/mL), followed by vortexing for 2 mins. The standard stock solution was prepared with 1 mg of TDF standard and 1 mL of Methanol (MeOH) was introduced to achieve a concentration of 1 mg/mL. The working solutions for the calibration curve were in the concentration range of 12.5–20,000 ng/mL. In the processing method, 22.5 μl of vaginal fluid was taken and placed in a centrifuge tube. Subsequently, 2.5 μL of calibrant or QC working solutions and 1 mL of internal standard extraction solutions were added to the labelled tubes. After vigorous vortexing for 10 mins at 1200 rpm, the samples were centrifuged for 15 mins at 15,000 rpm. Finally, 100 μL of the resulting supernatant was collected and subjected to analysis using LC-MS/MS.

The pharmacokinetic parameters namely maximum vaginal fluid concentration (C_{max}) and the time to reach the maximum vaginal fluid concentration (T_{max}) and the area under the curve (AUC) of TDF concentration in the vaginal fluid as a function of time; were computed for the three groups from the plot of vaginal fluid concentration *versus* time profiles. The pharmacokinetic parameters were calculated using pkSolver software.

After the 24-h study period, the animals were euthanized using an overdose of Isoflurane to collect the vaginal tissue samples from each rabbit. The cranial and caudal parts of the vagina were separated and placed into cryovials. The tissues were then rapidly frozen and stored at −80 °C until further analysis for tissue concentration studies that were performed according to the procedure reported by Clark et al. [59]. The tissues intended for histopathology study were preserved in formalin. Subsequently, these tissues were stained with hematoxylin and eosin and subjected to microscopic examination to evaluate the overall morphological state of the cervicovaginal mucosa. To assess cervicovaginal tissue damage, a scoring system was followed is mentioned in Table S1 [62].

2.6.2. Data analysis

The statistical analysis was carried out using GraphPad Prism 5.0 software. The mean values were presented with standard deviation. Paired *t*-test (two-tailed) was used to statistically compare the different groups where a *P*-value of <0.05 was considered to be statistically significant.

3. Results and discussions

3.1. Optimization of microspheres

The good aqueous solubility of TDF (13.4 mg/mL) justifies the selection of emulsification internal gelation technique using liquid paraffin as a continuous phase to produce mucoadhesive TAM [63]. The TAM was developed using other hydrophilic bioadhesive polymers like Na-Alg, Na-CMC, HPMC K4M, and HPMC K100M which play a crucial role in controlling the swelling and release kinetics of the drug [24,64]. To stabilize the emulsion droplets and prevent coalescence, Span 80 was used at a concentration of 1.5%v/v. Span 80 effectively reduces the interfacial tension between the water and oil phases, facilitating the easy dispersion of a viscous aqueous polymeric solution in liquid paraffin. The properties of the microspheres produced by emulsification can be influenced by optimizing different processing parameters, such as agitation duration and solidifying or curing time as mentioned by Letocha et al., 2022 [23]. In the present study, the w/o emulsion was stirred at 500 rpm for one hour to achieve a uniform dispersion of two immiscible phases. Following the stirring, the emulsion was homogenized for another 15 mins to further reduce the size of the particles to a micron level. This additional step aids in achieving a finer and more consistent particle size distribution. By the end of the 15 mins, the emulsification process reaches a steady state, indicating that the microspheres of desired physicochemical properties are formed. $CaCl_2$ is commonly used as a cross-linking agent in the preparation of Na-Alg microspheres. The presence of divalent calcium ions in the continuous aqueous phase, promotes interaction with alginates, leading to the formation of biodegradable microspheres with good bioadhesion and sustained release properties. In the emulsification process, generally, a curing time of 30 mins ensures uniform distribution of $CaCl_2$ within the continuous oil phase. A similar curing time was reported to ensure uniform cross-linking of Na-Alg using $CaCl_2$ by emulsification method [65]. Each Na^+ cation in sodium alginate is bonded to a single carboxyl group in the alginate chain, while the Ca^{2+} cation interacts with two carboxyl groups from different polymer chains. When sodium alginate reacts with a calcium ion in aqueous media, the two Na^+ ions of sodium alginate are substituted with Ca^{2+} ions during the cross-linking process. The cross-linking of copolymers (polymerization) through ionic bonding between Ca^{2+} cations and alginate anions as depicted in Fig. 4, results in an evenly cross-linked product by the end of the curing period [66,67].

3.2. Characterization of microspheres

3.2.1. Practical yield and percentage entrapment efficiency

The primary goal of optimizing the formulation is to obtain a high yield and entrapment of the desired product. By increasing the polymer amount in the formulation, a greater amount of the drug was found to get entrapped within the microspheres. This enhancement at higher polymer levels cuts down on drug loss during production and boosts overall yield [33]. The yield (%) of TAM was found to considerably increase as the proportion of polymer increased (Fig. 5). Among the formulations produced with the optimal ratio of 1:4, EH-8 exhibited the significantly higher ($P < 0.05$) yield of microsphere (94.00 ± 3.21 %) compared to other batches. Microspheres formulated with Na CMC and HPMC K4M, on rapid cross-linking with $CaCl_2$ resulted in the agglomeration of microspheres and formation of larger spheres (EH-2, EH-3, EH-4, EH-6, and EH-11) [23,68].

Various factors, including the type/amount of polymers used, and the concentration of the cross-linking agent, play a crucial role in determining the successful incorporation of therapeutic actives into alginate microspheres [69]. As the drug-to-polymer ratio increased from 1:2 to 1:9, the drug was better entrapped within the polymer, effectively preventing drug leakage during the hardening process (Fig. 5). The %EE for EH-8 (62.09 ± 1.34 %) was significantly higher ($P < 0.05$) compared to all other batches of TAM produced with the ratio of 1:4. Reports in the

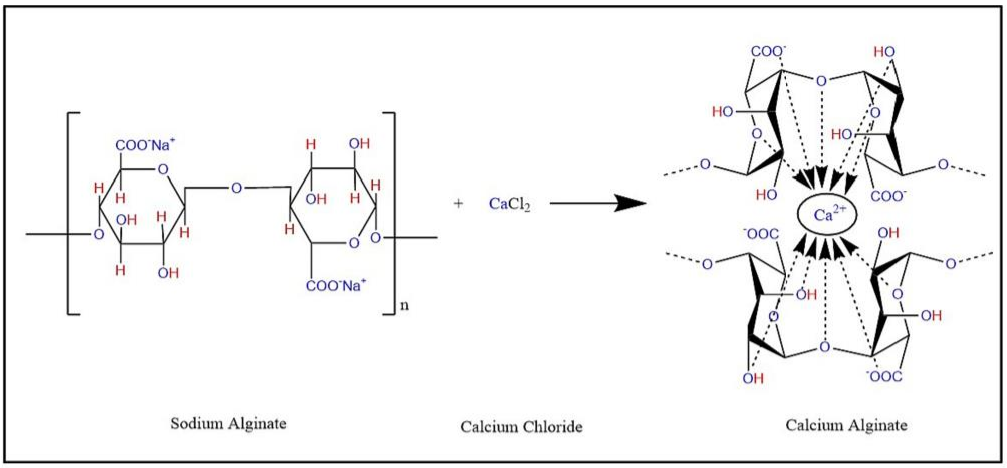

Fig. 4. Cross-linking of Na-Alg with calcium ions.

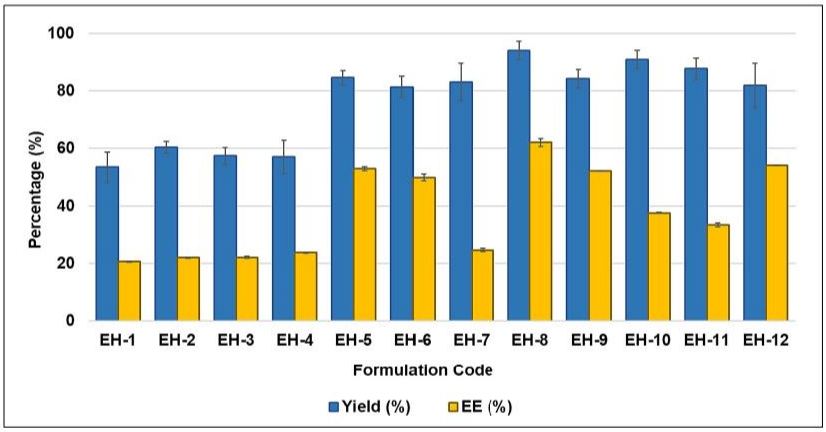

Fig. 5. Percentage yield and %EE of bioadhesive microspheres.

past indicate that the highest %EE was achieved with Na-Alg in combination with HPMC [27,70]. The higher loss incurred at lower polymer amounts could be due to the formation of smaller microspheres with higher surface area resulting in more surface drug and eventually reducing % EE. As the drug-to-polymer ratio increased, %EE increased as represented in Table S2. As size increases, drug diffusion from these microspheres is reported to slow down, leading to a higher %EE [71]. Loss of the drug in the emulsification method can be accounted by several steps involved that including hardening, washing, and filtering [29,32].

3.2.2. Surface morphology and particle size analysis

The SEM photomicrographs (Fig. 6(a) and (b)) of TAM (EH-8) indicated the particles were spherical with smooth and dense surface topography under 20 k× and 40 k× magnification. The larger microspheres appeared to adhere to smaller microspheres indicating their bioadhesive nature. The adhesion of the microspheres to each other is also likely due to the polymer deposits [34,70,72]. Particle size is one of the crucial parameters, which affects the stability, %EE, drug release profile, drug bio-distribution, mucoadhesion, and cellular uptake [70]. The surface mean diameter and volume mean diameter of formulation EH-8 (Fig. 6(c)) were found to be 11.06 ± 0.18 μm and 33.23 ± 0.46 μm, respectively [45]. About 50 % of the microspheres in EH-8 were of 28.94 ± 0.73 μm in size whereas 90 % of the microspheres were 68.69 ± 0.90 μm in size. The rapid cross-linking of alginates, due to the interaction of calcium ions, is likely to result in the formation of microspheres of different diameters and varied porosity [23]. The results of particle size analysis are known to agree well with the SEM photomicrographic images indicating the reproducibility of the technique involved to produce the TAM.

3.2.3. FTIR spectroscopic analysis

An overlay of the FTIR spectra of TDF, polymers, physical mixture, and the kneaded product (EH-8) are displayed in Fig. 7. The FTIR spectrum of TDF displayed the presence of a strong -OH stretching bond (3219.58 cm^{-1}), aliphatic -CH stretching bond (3049.84 cm^{-1} and

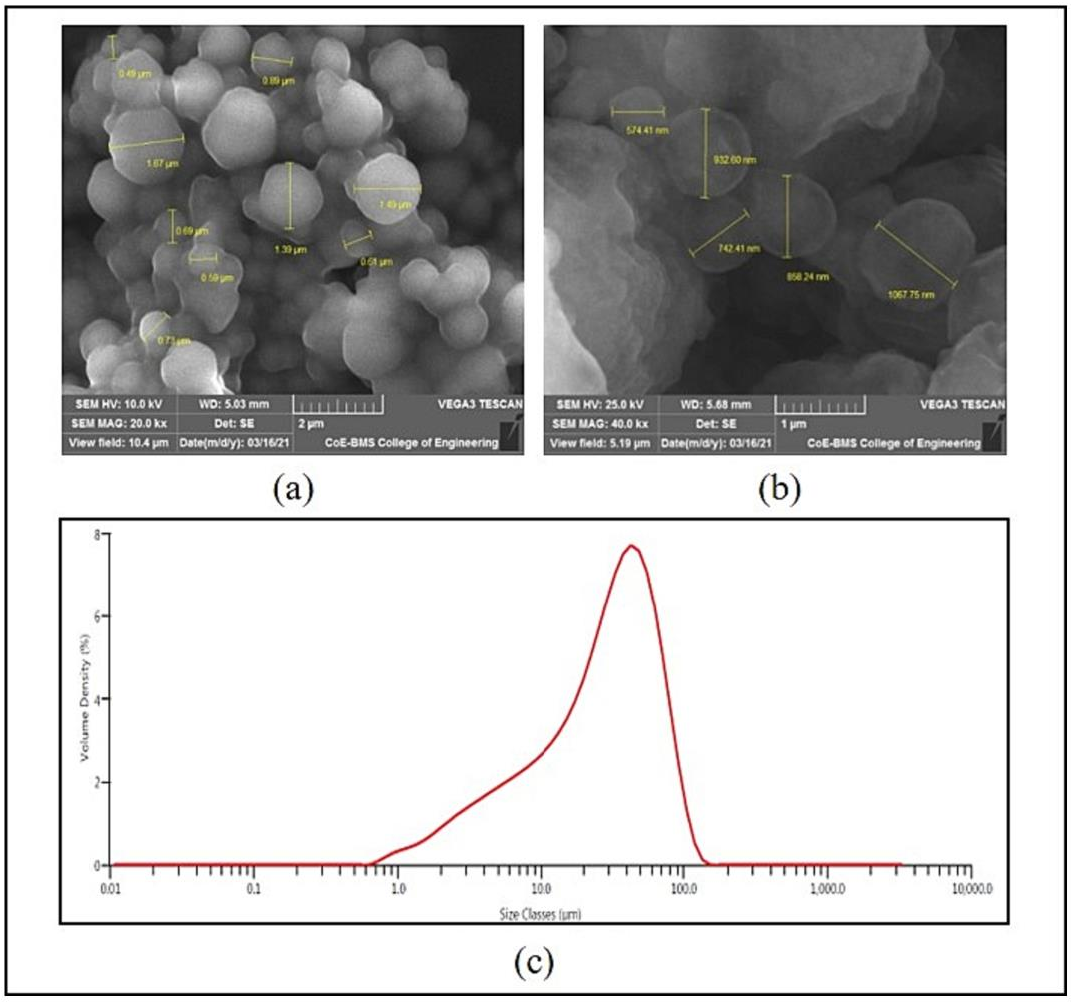

Fig. 6. Photomicrographs of the optimized formulation under a magnification of (a) 20 k×, and (b) 40 k×, respectively, (c) Particle size distribution curve of the optimized formulation (EH-8).

2938.98 cm^{-1}), C═O group (1760.69 cm^{-1}), P═O stretching (1678.73 cm^{-1}), -C=C- stretching bond (1619.91 cm^{-1}) and an aromatic C═N stretching bond (1421.28 cm^{-1}) confirming the earlier reports [37]. In the FTIR spectrum of Na-Alg, stretching vibrations of O—H bonds of alginate appeared at 3221.5 cm^{-1}, stretching vibrations of aliphatic -CH was observed at 2175.31 cm-1, and -C=C- stretching bond was observed at 1609.31 cm^{-1}. The bands at 1026.91 cm^{-1}were attributed to the C—O stretching vibration of pyranosyl ring and the C—O stretching with contributions from C–C–Hand C–O–H deformation. Similar characteristic peaks of the Na-Alg reported by Helmiyati et al., 2017, Daemi et al., 2012 [73,74]. In the FTIR spectrum of HPMC, the presence of hydroxyl group was observed at 3476.06 cm^{-1}, and the presence of methyl and hydroxypropyl group was observed at 2912.95 cm^{-1}. The bands at 1636.3 cm^{-1} confirm the presence of six membered cyclic ring and the band at 1371.14 cm^{-1} indicates the presence of cyclic anhydrides. The characteristic peaks of HPMC were similar to those as reported by Zafar et al., 2020, and Sahoo et al., 2012 [75–77]. The characteristic peaks of TDF appeared in the spectra of EH-8 though with minor shifts ruling out any possible chemical interaction between these groups and the excipients used during the process. Thus, the FTIR studies proved the chemical integrity of TDF in the polymer matrix.

3.2.4. DSC analysis

The process of developing microspheres includes dispersing the drug, either in its crystalline or amorphous state or dissolving it within the polymer matrix. Substantial changes in the thermal characteristics of the drug or polymer during this process may indicate a possible interaction between the drug and the polymer.

The DSC thermogram (Fig. 8) displayed a sharp endothermic peak of TDF at 115.4 °C with the peak onset at 112.04 °C indicating the crystallinity of TDF. The peak was found to correspond to the melting point of the drug as reported by Gomes and co-workers [37]. The enthalpy of

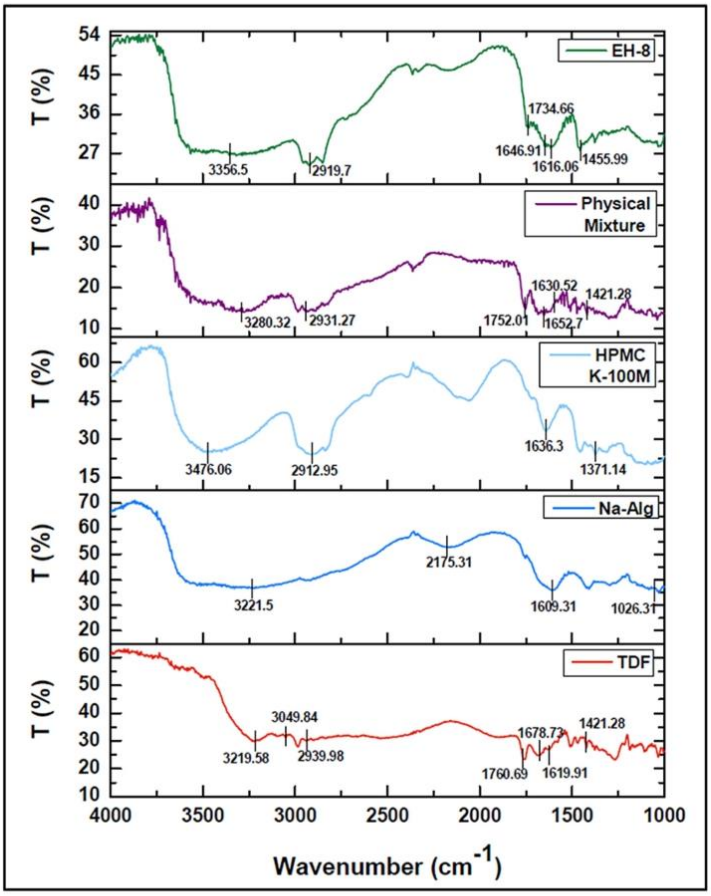

Fig. 7. FTIR spectra of TDF, Na-Alg, HPMC K100M, physical mixture, and optimized formulation (EH-8).

fusion (ΔH_f) for TDF in pure state by DSC was reported to be 71.41 J/g. The ΔH_f value for the physical mixture was found to be 0.49 J/g indicating the decrease in the crystallinity of TDF in the mixture. The X_c of the physical mixture was found to be 0.86 % when compared to TDF as a reference. The X_c of TDF was found to further drop to ~0.1 % in the formulation EH-8 indicating the drug is dispersed in an amorphous state in the polymeric matrix. The endothermic peak of TDF was broadened and shifted toward lower temperature in microsphere Formulation EH-8. This could be attributed to the uniform distribution of the drug in the polymer crust, resulting in the complete miscibility of the molten drug in the polymer to form a solid-solid solution [33,37].

3.2.5. PXRD analysis

The Powder X-ray diffractogram of TDF, polymers, physical mixture, and formulation EH-8 are displayed in Fig. 9 and its corresponding interpretation of 2θ values and peak intensities is portrayed in Table S3. The crystalline nature of the drug was clearly demonstrated in the PXRD pattern with about 10 distinct well-defined high-intensity peaks as represented in Table S3. TDF is reported to display 10 characteristic peaks in between 10.29° to 25.07° 2θ region justifying the observation in the present study [35]. Same number of peaks were reported in the same region for TDF authenticating the crystalline nature of TDF by Patil et al., 2017 [78]. The polymers including sodium alginate were found to display diffractograms that were devoid of any characteristic peaks indicating the amorphous nature. The PXRD pattern of the physical mixture displayed about 7 high-intensity peaks and a number of low-intensity peaks, indicating a substantial decrease in the drug crystallinity in the mixture. The number of peaks and the peak intensities relevant to the drug were further reduced in the formulation EH-8 indicating a substantial reduction in the crystallinity of TDF in the formulation. Considering the peak of TDF at 25.07° 2θ with an intensity of 4419 counts as the reference peak, the intensity of the same peak in the physical mixture was found to further reduce to an intensity of 1086 counts, indicating the decrease in crystallinity to nearly 24 %. The intensity of the reference peak dropped to about 11 % in formulation EH-8, indicating the drug is reduced to nearly amorphous state in the polymer matrix. The solid-state characterization using DSC and XRD conclusively indicates that TDF is likely to be present in the amorphous or molecular state as a solid-solid solution in the polymer matrix. Dispersion of polar drug in hydrophilic controlled release polymers would improve the drug miscibility in polymer and would control the drug release as well [79].

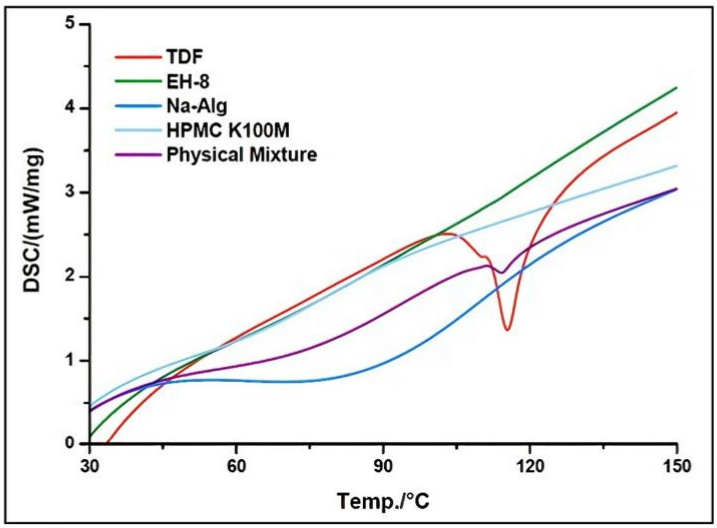

Fig. 8. DSC thermograms of TDF, Na-Alg, HPMC K100M, physical mixture, and optimized formulation (EH-8).

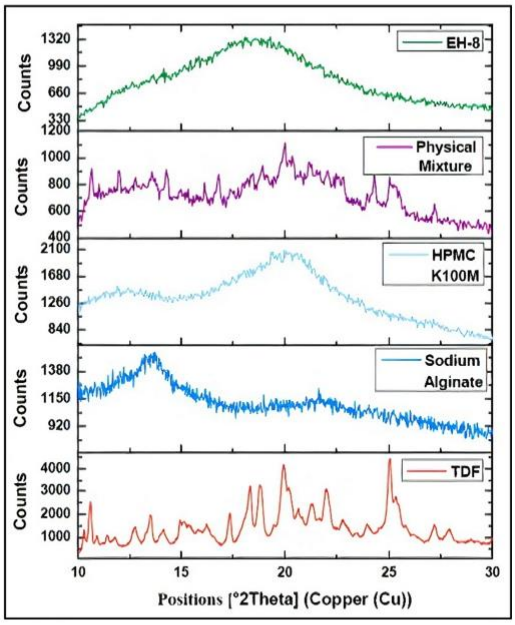

Fig. 9. PXRD diffractogram of TDF, Na-Alg, HPMC K100M, physical mixture, and optimized formulation (EH-8).

3.2.6. In vitro drug release

All the studies were performed for duration of 12 h, in line with the commonly observed vaginal retention time documented in literature. According to Witter et al. 1998, it was that a single intravaginal application of any product did not seem to result in cervical vaginal irritation or ulceration for a period of 12 to 24 h. Consequently, such an application would not only ensure protection from HIV and at the same time does not disrupt the epithelial barrier [42]. The closed-loop technique was followed as TDF demonstrated no solubility issues in dissolving in SVF. Generally, the drug release from the microspheres was found to depend on two factors namely the drug to polymer ratio and the type of polymer used. The data indicates that TDF was found to dissolve completely by the end of 2 h that can be attributed to its good aqueous solubility. Generally, the drug release profiles of bioadhesive microspheres displayed three distinct phases. There was an initial rapid release resulting in a burst effect, which is attributed to the quick dissolution of TDF on the surface of the microspheres. Following the burst effect, a slower release phase was found to occur, during which drug molecules located within the matrix of the microspheres that gradually diffuse out, and lastly, the steady state phase, where the drug is released at a steady slow rate. Notably, the intensity of the initial burst effect diminishes as the polymer amounts used in the formulation increases indicating that the burst effect can be substantially reduced using higher polymer proportions. The good aqueous solubility of TDF is known to responsible to certain extent for the initial burst release. Subsequently, the longer diffusion path the drug molecules need to traverse was found to slow down the drug release in the slow release phase. It has to be noted that the polymers used in the present study tend to form hydrophilic swellable matrices that tend to form torturous pathway increasing the diffusional path length with time. Additionally, the higher polymer concentration reduces the number of pores in the microsphere matrix, further impeding the entry of the dissolution media and the drug release. This sustained release mechanism enables controlled and prolonged drug delivery, enhancing treatment efficacy [80].

3.2.6.1. Effect of drug-to-polymer ratio. The amount of drug released was found to increase with a decrease in the polymer amounts as depicted in Fig. 10. The formulation EH-1, which had a drug-to-polymer ratio of 1:2, demonstrated a biphasic mode of drug release, namely the initial burst effect where nearly 50 % of the drug was released within 2 h. The burst phase was followed by a slow-release phase. Similar results were observed for formulation EH-5 and EH-7, which had a drug-to-polymer ratio of 1:4. The initial burst release of TDF from the

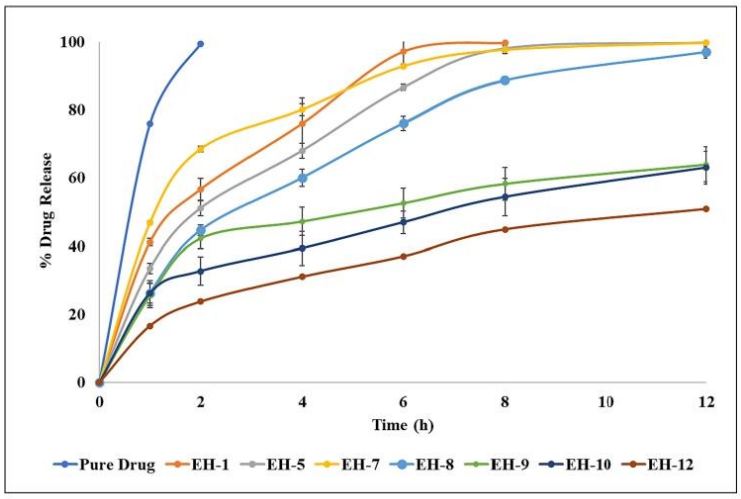

Fig. 10. Cumulative *in vitro* drug release profile of TAM in SVF (pH 4.5) for 12 h. The data represent the mean ± SD of three determinations.

microspheres was followed by the gradual diffusion of TDF from the inner polymeric matrix. The initial burst release can be attributed to the smaller particle size of the microspheres and the presence of surface-bound drug [80]. On the contrary, the Formulation EH-8, composed of TDF, Na-Alg and HPMC K100M, displayed minimal burst release initially, followed by a decelerated drug release until a steady state condition was attained (97.03 ± 4.45 % in 12 h). The formulation was found to display significantly lower 9P < 0.05) burst release at 2 h compared to other formulations produced with drug to polymer ratio of 1:4.

At higher polymer concentrations (specifically, in formulations EH-9, EH-10, and EH-12 with a drug-to-polymer ratio of 1:9), the rate of drug release was progressively slower, with ~22.80 ± 5.35 % drug release after 1 h. This phenomenon can be attributed to the increased interlocking of linear polymer chains, leading to the formation of a stronger gel layer through a process known as 'virtual crosslinking'. The increased cross linking is likely to impede the entry of the dissolution media and thereby slowing down the drug release [23,79].

3.2.6.2. Effect of type of polymers. The type of polymers used along with sodium alginate affected the *in vitro* release of TDF as depicted in Fig. 10. The incorporation of polymers with higher molecular weight was found to impart controlled release properties to the microspheres. It has to be noted that the molecular weight of HPMC K100M, HPMC K4M, sodium CMC, and Na-Alg were reported to be 1150, 500, 262.19, and 216.12 g/mol, respectively [81–83]. The formulations, EH-1 and EH-5 composed of sodium alginate alone as a hydrophilic polymer, failed to control the drug release. On the contrary, about 63.99 ± 1.26 % of TDF was released in 12 h from EH-9 that was formulated at high drug: alginate levels (1:9). In order to ensure a controlled but complete drug release from TAM at nominal polymer levels (1: 4), attempts were made to replace 50 % of sodium alginate with other hydrophilic polymers. Replacing about 50 % of sodium alginate with HPMC K100M in formulation EH-4 (99.05 ± 1.10 %), EH-8 97.03 ± 4.54 %), and EH-12 (50.89 ± 4.76 %) effectively controlled the release at lower polymer levels for 12 h. The drug release from microspheres was found to decrease with increase in the molecular weight of hydrophilic polymers. [70,79].

Depending on the molecular weight of the polymers used, the amount of drug release was found decrease in the order: HPMC K100M < HPMC K4M < sodium CMC indicating the molecular weight was found to have a considerable effect on the release of drug. The *in vitro* drug dissolution studies indicated that, formulations EH-9, EH-10, and EH-12 developed with the drug to polymer ratio of 1:9 displayed incomplete release ranging from 50.89 ± 4.76 % to 63.99 ± 5.16 % by the end of 12 h. Based on the results EH-8 was considered as an ideal formulation as it was found to display minimal burst release and at the same time releases most of TDF in a controlled manner in SVF in 12 h that can be considered to be a realistic standard intra vaginal retention time [43,44].

The release of drug is predominantly regulated by hydration process of the polymer chains. For hydrophilic polymer-based controlled release formulations, the drug release kinetics typically involves a three-stage process; firstly, the medium should penetrate the matrix (hydration), secondly, the matrix should swell with ensuring dissolution or erosion, and thirdly, the dissolved drug should be transported either through the hydrated matrix or from the eroded sections, eventually being released into the surrounding medium [56]. The mathematical modelling of dissolution profiles of different batches of TAM was carried out in order to comprehend the kinetics and mechanism of TDF release from microspheres, using model-dependent approaches. The results of curve fitting into different mathematical models are tabulated in Table S4.

The R^2 values close to 1.0 indicated that majority of the formulation followed zero order kinetics wherein the drug release was not influenced by the amount of drug present in the microspheres. The mechanism of drug release was found to be primarily governed by swelling and diffusion, which is based on the disentanglement rate of the polymer at the swollen front. This suggests that the drug release from the formulations followed the Higuchi model, which describes the release of drugs from polymeric matrices based on diffusion. These findings indicate the release behavior of the formulations and help in understanding and optimizing their drug delivery characteristics [46]. The drug release mechanism was further confirmed from the Korsmeyer-Peppas model, where the 'n' value is used to characterize different release mechanisms. Formulation EH-5 and EH-8 indicate anomalous or non-Fickian transport that involves diffusion as well as the swelling and relaxation of the drug from the matrix are both responsible for the drug delivery. On the contrary, Formulation EH-9 and EH-10 (n < 0.45) indicated hindered Fickian diffusion which infers that it is characterised by diffusive regimen with hampered release [47,48,84].

Therefore, among all the formulations studied, formulation EH-8

demonstrated a desirable drug entrapment efficiency of 62.09 ± 1.34 % and a controlled and complete drug release of 97.03 ± 4.54 % over a period of 12 h [42]. These results indicate that EH-8 exhibited a favourable sustained drug release profile, making it a promising candidate for further investigations and studies.

3.2.7. *Ex vivo* mucoadhesion studies

Formulation EH-8 was considered for further studies based on its good percentage yield, %EE and drug release. Formulation EH-8 demonstrated good bioadhesivity where, approximately 7.17 ± 2.02 % of the microspheres remained still adhered to the mucosa after 12 h, while 92.83 ± 2.02 % of the microspheres were washed off by the SVF. The *ex vivo* studies with the mucosal tissue substrate suggests that the microspheres are likely to be well retained *in vivo* too. Approximately 50 % of the microspheres were washed off from the mucosa by the end of 4 h, corresponding to a 60.04 ± 1.72 % *in vitro* drug release [34,46]. This indicates that microspheres of the batch EH-8 demonstrated both strong adhesion to rabbit vaginal mucosa by virtue of their bioadhesive properties and ensured nearly complete drug release by 12 h.

On comparing the *ex vivo* adhesion with the *in vitro* drug release, an excellent correlation was observed between the percentage of microspheres retained on the mucosa and the *in vitro* drug release, with a correlation coefficient value of 0.996 as indicated in Fig. 11. The drug release was found to decrease linearly as the percentage of adhered microspheres decreased over time. The *ex vivo* studies clearly indicates the mucoadhesive potential of the EH-8 microspheres and therefore the suitability of the bioadhesive microspheres for intravaginal delivery of TDF.

Vaginal inserts using microparticulate-based drug delivery technologies offer several advantages for topical PrEP. These advantages include regional drug delivery to specific sites, enhanced drug penetration in mucous and tissues, better retention, low chances of expulsion and prolonged drug delivery following intravaginal administration.

3.3. Characterization of pessaries

To ensure consistent and reproducible batches of pessaries, the moulding method was chosen as it is a simple, robust, and cost-effective approach with minimal processing steps. This method produces less-friable inserts with high mechanical strength, making them easier to handle and package [4]. The prepared pessaries were in the shape of a bullet having a smooth surface. They appeared to be pale yellow in color. Table 5 enlists the results of the physical evaluation of the pessaries of batches F1 to F3.

All the formulations were found to demonstrate good content uniformity, weight uniformity and sufficient mechanical strength to withstand abrasives forces which causes disintegration of prepared pessaries. The width and length of randomly selected pessaries were found to vary from 0.82 cm to 0.90 cm and 2.11 to 2.14 cm for different formulation with good homogeneity and the impact of additional excipients was minimal. The weight uniformity test indicated that for all pessaries were within the acceptable range of <5 %, indicating precision of the moulding technique. Disintegration time increased with higher concentrations of beeswax, which served both as a stabilizer and a controlled-release agent. The melting point of the pessaries was also found to be within the acceptable limit of 37 ± 0.5 °C that corresponded to the body temperature. From the results of the physical characterization of the pessaries, formulation F2 was ideal to be considered for further *in vitro* dissolution studies [50,51,85].

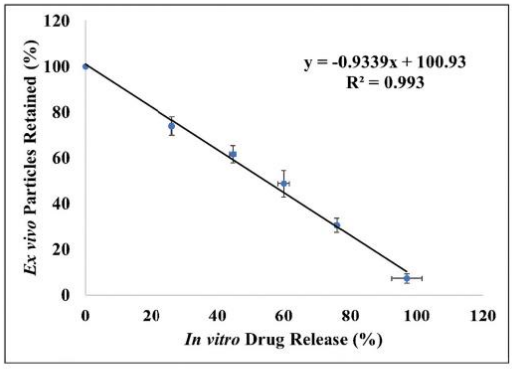

Fig. 11. Correlation between *ex vivo* microspheres retained (%) on the mucosa and the *in vitro* drug release (%) from the optimized formulation (EH-8).

Table 5
Physical characterization of pessaries.

Parameters	F1	F2	F3
Weight uniformity (mg) (n = 20)	901.27 ± 0.26	901.50 ± 0.10	901.37 ± 0.10
Melting point (°C) (n = 3)	30.33 ± 2.52	35.33 ± 0.58	42.33 ± 2.08
Content uniformity (%) (n = 10)	97.42 ± 0.86	99.09 ± 1.42	96.88 ± 1.30
Disintegration time (s) (n = 6)	2.33 ± 0.31	3.63 ± 0.15	4.00 ± 0.20

The dissolution of F2 was compared with the constituent batch of TAM (EH-8) to assess the impact of moulding on the dissolution of bioadhesive microspheres. Ideally, we expect the dissolution of the pessaries to be comparable to that of the constituent bioadhesive microspheres.

On comparing the dissolution profiles of TAM with P-TAM (Fig. 12), the pessaries released 95.31 ± 1.38 % of TDF within 12 h similar to that of TAM (EH-8), *i.e.*, 97.02 ± 4.54 %. From the graph it was clear that the drug released in a controlled manner from the formulated pessaries similar to that of EH-8. The results indicate that the release from the P-TAM is no way hampered on incorporation into the cocoa butter base [50]. This confirmed that the TAM are most likely to remain intact in the lipophilic base that would readily melt to release the constituent TAM on contact with the dissolution media maintained at 37 ± 0.4 °C [85]. The graph depicts that TDF released in a controlled manner from the formulated vaginal pessaries similar to that of the constituent microspheres, which indicates that P-TAM being a more complex system than TAM does not alter the release profile of EH-8 when incorporated into a pessary.

Difference and similarity factors serve as effective model-independent tools for reliably comparing dissolution profiles. In this study, the dissolution profiles of TAM (EH-8) and P-TAM (F2) were compared to assess the similarity in dissolution profiles of the TAM after being incorporated into a pessary dosage form. The formulated pessaries were found to display a dissolution profile similar to the constituent EH-8, with an f_2 value of 72.09 and an f_1 value of 2.50 [55]. These similarity values indicate that the moulding technique employed for the production of pessaries did not affect the dissolution profile of the TAM. From a commercial standpoint, pessaries can be considered as ideal platform of vaginal inserts for delivery of antiretrovirals, given that the vagina is a major portal for HIV transmission during sexual intercourse.

3.4. In vivo studies

The intravaginal concentrations elicited by P-TAM were compared to that elicited by an oral marketed formulation in rabbits to determine the bio-distribution of TDF in the vagina which is the latent site of infection of HIV. The vaginal fluid concentration *versus* profiles for the marketed formulation and intravaginal P-TAM are represented in Fig. 13.

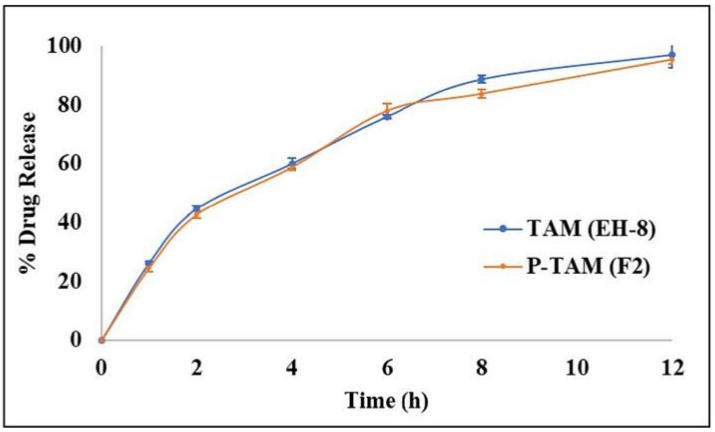

Fig. 12. Comparative dissolution profile of TDF bioadhesive microspheres and pessaries.

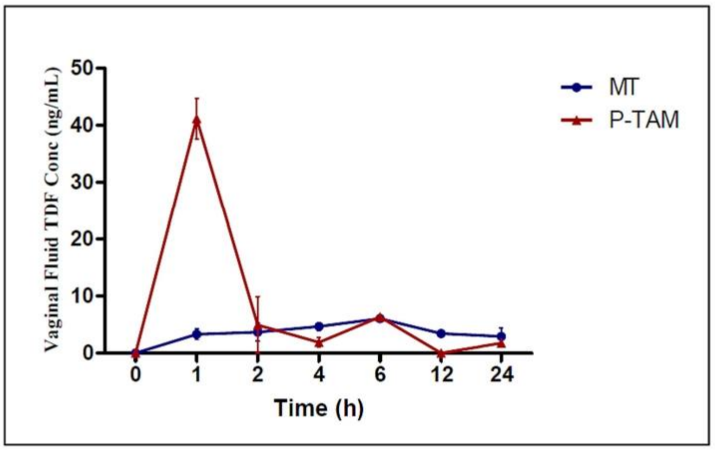

Fig. 13. Vaginal fluid concentration of TDF over time following oral administration of marketed formulation and vaginal administration of pessaries.

The calculated pharmacokinetic parameters of two formulations, P-TAM and MT, were compared. The novel P-TAM displayed a significantly higher ($P < 0.005$) C_{max} of 41.18 ± 3.57 ng/mL at 1 h after administration when compared to the MT group. These findings demonstrated the potential of P-TAM to elicit a higher local concentration compared to conventional oral MT in the crucial initial hours of insertion. The higher regional concentrations that exceeded the IC_{50} value of TDF can be ascribed to the better distribution and retention of the microparticulate system in the vaginal mucosa. An IC_{50} of 11.5 ng/mL of TDF has been reported against HIV in the reports available in the literature [86]. Likewise, the T_{max} observed with the P-TAM (1.00 ± 0.01 h) was found to be significantly short ($P < 0.0001$) compared to that observed with the conventional MT (6 ± 0.02 h). The quicker T_{max} observed with the P-TAM is likely to arrest the viral transmission during intercourse and ensure adequate protection against the transmission of HIV. The prolonged T_{max} and lower C_{max} with the MT can be attributed to poor drug distribution to the vaginal tissue and the fluid following oral administration and systemic distribution. However, the peak vaginal fluid concentrations with the P-TAM group were found to quickly drop following T_{max} indicating the rapid clearance from the vagina. The likely reason would be drug dissipation due to frequent urination of the animals during our study. It has to be noted that TDF is BCS class III molecule and therefore is prone to dissipation due to good aqueous solubility and frequent urination of the rabbits during the experiments. The drainage of urine is known to usually occur through the caudal vagina. Good number of reports have also attributed the lower drug levels in the caudal vaginal fluids at longer time periods to the dilution by urine in the rabbit model following intravaginal insertion [59,87]. There are notable physiological differences between animal models and humans that can influence drug dissipation from intravaginal devices. Unlike humans, rabbit vagina is longer and feature an urovaginal sphincter that separates the lower urovagina from the upper two-thirds, known as the cervicovagina. Furthermore, insertion of a drug-loaded pessary in the urovagina would be quite challenging in rabbits because it would be constantly perfused by urine, leading to drug washout that is likely to impact bio-distribution studies [88].

However, after 24-h study the mean TDF concentrations elicited in the cranial vagina were approximately 1.55 ± 0.41 ng/g that failed to

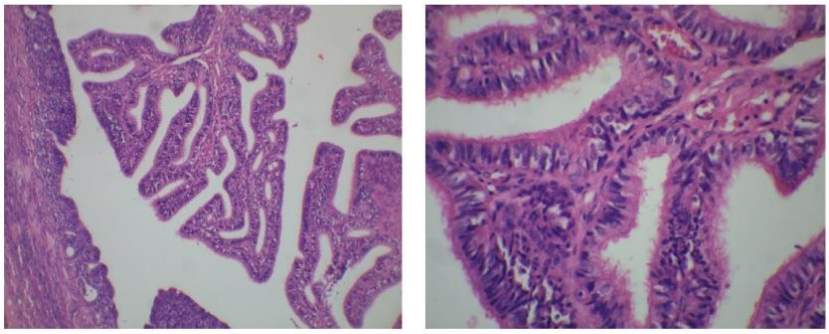

(a) (b)

Fig. 14. Histopathological evaluation of the vaginal tissue at (a) 10× and (b) 40× magnification.

exceed the IC_{50} of TDF. The animal results conclusively indicate that the novel P-TAM exhibited favourable biodistribution, which could potentially offer effective protection in the initial hours following intravaginal administration against HIV transmission. Understanding the protective efficacy and duration of protection for both pre-exposure and post-exposure dosing is crucial for determining appropriate dosage and dosing regimens in future clinical trials [87].

The histopathological evaluation of the vaginal tissue is depicted in Fig. 14. The consistent thickness of the vaginal epithelium suggests that the pessaries did not cause any damage or shedding of epithelial cells in the vaginal tissue. On insertion, the pessaries are likely to melt instantaneously dispersing into the constituent microspheres that are likely to adhere to the vaginal mucosa for prolonged time periods. This finding indicates that the P-TAM can be smoothly and safely incorporated into the vagina without causing any damage to the vaginal layer. The lack of adverse effects on the vaginal epithelium also suggests that the pessaries are likely to be well-tolerated by patients, making them a patient-compliant option for drug delivery [62].

4. Conclusion

Drug loaded Na-Alg based bioadhesive microspheres were successfully produced by ionotropic gelation technique employing a mixture of cellulose polymers. The microspheres produced not only adhered well to the mucosal surface but displayed a controlled release of TDF. These microspheres were successfully loaded into meltable pessaries for intravaginal delivery of TDF. The pessaries constituted of Na-Alg bioadhesive microsphere were able to successfully maintain inhibitory concentration during the crucial initial hours of insertion that could prove to be vital for ensuring adequate protection against HIV transmission. The novel pessaries of TDF present a promising platform for protecting HIV-uninfected individuals, from acquiring HIV. Timely delivery of TDF directly to the portal of entry of the pathogen using P-TAM represents a novel strategy that would effectively prevent HIV transmission during sexual intercourse. While the trend in HIV prevention leans toward long-acting systemic formulations, pessaries are likely to provide a novel promising on-demand pre-exposure prophylactic self-protective platform for HIV-negative women. The proposed novel pessaries are likely to bring about paradigm shift in PrEP management of HIV. Furthermore, the acceptability and desirability of new dosage forms for HIV prevention are essential factors to consider. User preferences play a significant role in the successful implementation and uptake of preventive measures. Therefore, considering the perspectives and preferences of potential users when developing and evaluating these novel pessary formulations is crucial for their successful adoption and widespread use as an HIV prevention strategy.

CRediT authorship contribution statement

Dhruti Avlani: Data curation, Investigation, Methodology, Software, Validation, Visualization, Writing – original draft. **H.N. Shivakumar:** Conceptualization, Funding acquisition, Project administration, Supervision, Validation, Visualization, Writing – review & editing. **Avichal Kumar:** Software. **A. Prajila:** Data curation, Investigation, Methodology. **Babiker Bashir Haroun Baraka:** Data curation, Investigation. **V. Bhagya:** Investigation, Supervision.

Declaration of competing interest

There are no conflicts of interest related to the work undertaken.

Acknowledgement

The authors are grateful to Sri Prabhakar Kore, Chancellor, KLE Academy of Higher Education and Research, Deemed University, Belgaum for providing facilities to carry out the research work. They are grateful to the Department of Pharmaceutics, KLE College of Pharmacy, Bengaluru for providing all the necessary instruments, facilities and support for carrying out the research work.

The authors are grateful to Vision Group on Science and Technology, Bengaluru, Karnataka, India for funding (GRD No. 747 of CISEE) to procure the necessary equipments needed to undertake the project.

They are thankful to Aurobindo Pharma, Hyderabad, India for providing the gift sample of tenofovir disoproxil fumarate and Central Institute of Fisheries Technology, Kochi, Kerala, India for providing the gift sample of chitosan.

The authors would acknowledge Malvern Instruments Inc., Bengaluru, Karnataka, India for measurement of particle size. The authors would also like to thank BMS College of Engineering, Bengaluru, Karnataka, India for the scanning electron microscopic images; Centre for Advanced Materials Technology, MS Ramaiah Institute of Technology, Bengaluru, Karnataka, India for performing the DSC and PXRD studies. The authors would acknowledge Skanda Life Sciences Pvt. Ltd., Bengaluru for performing the LCMS/MS analysis.

Appendix A. Supplementary data

Supplementary data to this article can be found online at https://doi.org/10.1016/j.ijbiomac.2023.128816.

References

[1] HIV Transmission, Centers for Disease Control and Prevention. https://www.cdc.gov/hiv/basics/index.html, 2023 (accessed 23 January 2023).
[2] Latest HIV Estimates and Update on COVID-19 Disruptions, World Health Organisation. https://cdn.who.int/media/docs/default-source/hq-hiv-hepatitis-and-stis-library/2022_global_summary_web_v12.pdf, 2022 (accessed 1 February 2023).
[3] K. Devi, R.S. Pai, Antiretrovirals: need for an effective drug delivery, Indian J. Pharm. Sci. 8 (2006) 1–6.
[4] M. Peet, V. Agrahari, S. Anderson, et al., Topical inserts: a versatile delivery form for HIV prevention, Pharm 11 (2019) 1–17.
[5] F. Grande, G. Ioele, M.A. Occhiuzzi, et al., Reverse transcriptase inhibitors nanosystems designed for drug stability and controlled delivery, Pharm 11 (2019) 1–26.
[6] J. Vyslouzil, K. Kubova, V.N. Tkadleckova, et al., Clinical testing of antiretroviral drugs as future prevention against vaginal and rectal transmission of HIV infection – a review of currently available results, Acta Pharm. 69 (2019) 297–319.
[7] M. Patki, R. Vartak, J. Jablonski, et al., Efavirenz nanomicelles loaded vaginal film (ezfilm) for preexposure prophylaxis (PrEP) of HIV, Colloids Surfaces B: Biointerfaces. (2020), https://doi.org/10.1016/j.colsurfb.2020.111174.
[8] H. Gov, Pre-exposure Prophylaxis. https://www.hiv.gov/hiv-basics/hiv-prevention/using-hivmedication-to-reduce-risk/pre-exposure-prophylaxis, 2022 (accessed 15 December 2022).
[9] E.A.A. Arnold, Qualitative study of provider thoughts on implementing pre-exposure prophylaxis (Prep) in clinical settings to prevent HIV infection, PloS One 7 (2012), e40603, https://doi.org/10.1371/journal.pone.0040603.
[10] R.A. Tetteh, Pre-exposure prophylaxis for HIV prevention: safety concerns, Drug Saf. 40 (2017) 273–283, https://doi.org/10.1007/s40264-017-0505-6.
[11] FDA Approves Second Drug to Prevent HIV Infection As Part of Ongoing Efforts To End the HIV Epidemic, USFDA, 2019 https://www.fda.gov/news-events/press-announcements/fda-approves-seconddrug-prevent-hiv-infection-part-ongoing-efforts-end-hiv-epidemic, (accessed 4 March 2020).
[12] M. Mesquita, J. Galante, R. Nunes, et al., Pharmaceutical vehicles for vaginal and rectal administration of anti-HIV microbicide nanosystems, Pharm 11 (2019) 1–20.
[13] A.K. Blakney, Y. Jiang, K.A. Woodrow, Application of electrospun fibers for female reproductive health, Drug Deliv. Transl. Res. 7 (2017) 796–804.
[14] E. Jalalvandi, H. Jafari, C.A. Amorim, et al., Vaginal administration of contraceptives, Sci. Pharm. 89 (2021) 1–18, https://doi.org/10.3390/scipharm89010003.
[15] M. Veiga-Ochoa, R. Ruiz-Caro, R. Cazorla-Luna, et al., Vaginal formulations for prevention of sexual transmission of HIV, Adv. HIV AIDS Control. 3 (2018) 227–248.
[16] A.S. Ham Jr., R.W. Buckheit, Designing and developing suppository formulations for anti-HIV drug delivery, Ther. Deliv. 9 (2017) 805–817.
[17] D. Avlani, H.N. Shivakumar, A. Kumar, Development of dispersible vaginal tablets of tenofovir loaded mucoadhesive chitosan microparticles for anti-HIV pre-exposure prophylaxis, Mol. Pharm. 20 (2023) 5006–5018, https://doi.org/10.1021/acs.molpharmaceut.3c00288.
[18] P.M.M. Mesquita, R. Rastogi, T.J. Segarra, T. J., et al., Intravaginal ring delivery of tenofovir disoproxil fumarate for prevention of HIV and herpes simplex virus infection, J. Antimicrob. Chemother. 67 (2012) 1730–1738.
[19] R. Cazorla-Luna, F. Notario-Perez, A. Martin-Illana, et al., Chitosan-based mucoadhesive vaginal tablets for controlled release of the anti-HIV drug tenofovir, Pharm 11 (2019) 1–19.
[20] T.M. Chapman, J.K. McGavin, S. Noble, Tenofovir disoproxil fumarate, Drug 63 (2003) 1597–1608.
[21] A. Celum, J.M. Baeten, Tenofovir-based pre-exposure prophylaxis for HIV prevention: evolving evidence, Curr. Opin. Infect. Dis. 25 (2012) 51–57.
[22] M.E. Watkins, S. Wring, R. Randolph, et al., Development of a novel formulation that improves preclinical bioavailability of tenofovir disoproxil fumarate, J. Pharm. Sci. 106 (2017) 906–919.
[23] A. Letocha, M. Miastkowska, E. Sikora, Preparation and characteristics of alginate microparticles for food, pharmaceutical and cosmetic applications, Polymers 14 (2022) 3834, https://doi.org/10.3390/polym14183834.
[24] D.M. Hariyadi, N. Islam, Current status of alginates in drug delivery, Adv. Pharmacol. Pharm. Sci. (2020), https://doi.org/10.1155/2020/8886095, 8886095.
[25] K. Kumar, N. Dhawan, H. Sharma, S. Vaidya, B. Vaidya, Bioadhesive polymers: novel tool for drug delivery, artificial cells, Nanomed. Biotech. 42 (2014) 274–283, https://doi.org/10.3109/21691401.2013.815194.
[26] K. Netsomboon, A. Bernkop-Schnurch, Mucoadhesive vs. mucopenetrating particulate drug delivery, European J. Pharmaceutics Biopharm. 98 (2016) 76–89.
[27] M. Das, D. Maurya, Evaluation of diltiazem hydrochloride-loaded mucoadhesive microspheres prepared by emulsification-internal gelation technique, Acta Poloniae Pharmaceutica. Drug Res. 65 (2008) 249–259.
[28] N.T.T. Uyen, Z.A. Abdul Hamida, A. Nurazreena, Fabrication and characterization of alginate microspheres, Materials Today: Proceedings. 17 (2019) 792–797.
[29] M. Nagpal, D.K. Maheshwari, P. Rakha, et al., Formulation development and evaluation of alginate microspheres of ibuprofen, J. Young Pharm. 4 (2012) 13–16.
[30] H.N. Shivakumar, S.R.K. Vaka, S.N. Murthy, Albumin microspheres for oral delivery of iron, J. Drug Target. 18 (2010) 36–44.
[31] M. Hiorth, S. Nilsen, I. Tho, Bioadhesive mini-tablets for vaginal drug delivery, Pharma 6 (2014) 494–511.
[32] N. Patel, D. Lalwani, S. Gollmer, E. Injeti, Y. Sari, J. Nesamony, Development and evaluation of a calcium alginate based oral ceftriaxone sodium formulation, Prog Biomater. 5 (2016) 117–133.
[33] M. Elsayed, Controlled release alginate-chitosan microspheres of tolmetin sodium prepared by internal gelation technique and characterized by response surface modelling, Braz. J. Pharm. Sci. 56 (2020), https://doi.org/10.1590/s2175-97902020000118414.
[34] S. Beg, M. Rahman, S.K. Panda, et al., Nasal mucoadhesive microspheres of lercanidipine with improved systemic bioavailability and antihypertensive activity, J. Pharm. Innov. (2020), https://doi.org/10.1007/s12247-020-09441-5.
[35] A. Thulluru, M. Varma, C. Setty, et al., Effect of sodium alginate in combination with HPMC K 100 M in extending the release of metoprolol succinate from its gastro-retentive floating tablets, Indian J. Pharm. Edu. Res. 49 (2015) 293–303.
[36] S. Mandal, S. Senthil Kumar, B. Krishnamoorthy, et al., Development and evaluation of calcium alginate beads prepared by sequential and simultaneous methods, Brazilian J. Pharm. 46 (2010) 785–793.
[37] E. Gomes, W. Mussel, J.M. Resende, et al., Characterization of tenofovir disoproxil fumarate and its behavior under heating, Cryst. Growth Des. 15 (2015) 1915–1922.
[38] E. Tarani, I. Arvanitidis, D. Christofilos, D.N. Bikiaris, K. Chrissafis, G. Vourlias, Calculation of the degree of crystallinity of HDPE/GNPs nanocomposites by using various experimental techniques: a comparative study, J. Mater. Sci. 58 (2023) 1621–1639.
[39] R. Deveswaran, S. Bharath, B.V. Basavaraj, et al., Development of mesalazine microspheres for colon targeting, Int. J. Appl. Pharm. 9 (2017) 1–9.
[40] Z. Tong, Y. Chen, Y. Liu, et al., Preparation, characterization and properties of alginate/poly(g-glutamic acid) composite microparticles, Mar. Drugs 15 (2017) 91, https://doi.org/10.3390/md15040091.
[41] O. Aleem, B. Kuchekar, Y. Pore, S. Late, Effect of β-cyclodextrin and hydroxypropyl β-cyclodextrin complexation on physicochemical properties and antimicrobial activity of cefdinir, J. Pharm. Biomed. Anal. 47 (2008) 535–540.
[42] F.R. Witter, U.P. Barditch-Crovob, L. Roccob, C.B. Trapnellc, Duration of vaginal retention and potential duration of antiviral activity for five nonoxynol-9 containing intravaginal contraceptives, Int. J. Gynecol. Obstet. 65 (1999) 165–170.
[43] N.M. Goudarzi, A. Samaro, C. Vervaet, et al., Development of flow-through cell dissolution method for *in situ* visualization of dissolution processes in solid dosage forms using X-ray_CT, Pharm 14 (2022) 2475, https://doi.org/10.3390/pharmaceutics14112475.
[44] L. Sievens-Figueroa, N. Pandya, A. Bhakay, et al., Using USP I and USP IV for discriminating dissolution rates of nano- and microparticle-loaded pharmaceutical strip-films, AAPS Pharm. Sci. Tech. 13 (2012) 1473–1482.
[45] Z. Gao, *In vitro* dissolution testing with flow-through method: a technical note, AAPS Pharm. Sci. Tech. 10 (2009) 1401–1405.
[46] M. Szekalska, M. Wróblewska, A. Czajkowska-Ko'snik, et al., The spray-dried alginate/gelatin microparticles with luliconazole as mucoadhesive drug delivery system, Materials 16 (2023) 403, https://doi.org/10.3390/ma16010403.
[47] N.P. Fernando, A.M. Illana, R. Cazorla-Luna, et al., Development of mucoadhesive vaginal films based on hpmc and zein as novel formulations to prevent sexual transmission of HIV, Int. J. Pharm. (2019) 570, https://doi.org/10.1016/j.ijpharm.2019.118643.
[48] J. Nesalin, A. Smith, Preparation and evaluation of stavudine loaded chitosan nanoparticles, J. Pharm. Res. 6 (2013) 268–274.
[49] S. Swain, U. Behera, S. Beg, et al., Design and characterization of enteric-coated controlled release mucoadhesive microcapsules of rabeprazole sodium, Drug Dev. Ind. Pharm. 39 (2013), 548-460.
[50] P. Baviskar, S. Jaiswal, S. Sadique, A. Landged, Formulation and evaluation of lornoxicam suppositories, J. Pharm. Innov. 2 (2013) 20.
[51] N.H. Salunkhe, N.R. Jadhav, K.K. Mali, R.J. Dias, V.S. Ghorpade, A.V. Yadav, Mucoadhesive microsphere based suppository containing granisetron hydrochloride for management of emesis in chemotherapy, J. Pharm. Investig. 44 (2014) 253–263.
[52] Tests for pessaries, in Indian pharmacopoeia, government of India, Ministry of Health and Family Welfare Department 9th ed, Vol 1 and 2, Indian Pharmacopoeia Commission, Ghaziabad, India, 2023, pp. 356–360, 1342-1344.
[53] M.A. El-Majri, M.M. El-Basir, Formulation and evaluation of ibuprofen suppositories, J. Res. Pharm. Pract. 7 (2016) 87–90.
[54] C.S. Castner, Cocoa Butter Composition and Method of Making the Same, US Patent. https://patents.google.com/patent/US3862197A/en. 1974 (accessed 4 May 2023).
[55] S.K. Zandu, R. Kumari, I. Singh, Formulation and evaluation of fast disintegrating tablets of domperidone using chitosan-glycine conjugates as superdisintegrant, Thai J. Pharm. Sci. 45 (2020) 32–40.
[56] D.M. Brahmankar, S.B. Jaiswal, Bioavailability and bioequivalence, in: Biopharmaceutics and Pharmacokinetics – A Treatise, Vallabh Prakashan, Delhi, India, 2009, pp. 331–332.
[57] Rabbit Anaesthesia, 2022 https://research.utexas.edu/wp-content/uploads/sites/7/2020/02/Rabbit_Anesthesia_guidance_ARC.pdf, (accessed January 14, 2022).
[58] A.F. Ajayi, R.E. Akhigbe, Staging of the estrous cycle and induction of estrus in experimental rodents: an update, Frtility Res. Pract. 6 (2020) 5, https://doi.org/10.1186/s40738-020-00074-3.
[59] M.R. Clark, D.R. Friend, Pharmacokinetics and topical vaginal effects of two tenofovir gels in rabbits, AIDS Res. Human Retrovir (2012) 1458–1466.
[60] C. Cunha-Reis, A. Machado, L. Barreiros, et al., Nanoparticles-in-film for the combined vaginal delivery of anti-HIV microbicide drugs, J. Control. Release (2016), https://doi.org/10.1016/j.jconrel.2016.09.020.
[61] A. Blankey, Y. Jiang, D. Whittington, K. Woodrow, Simultaneous measurement of etravirine, maraviroc and raltegravir in pigtail macaque plasma, vaginal secretions

and vaginal tissue using a LC-MS/MS assay, J. Chromatogr. B Analyt. Technol. Biomed. Life Sci. (2016) 110–118.
[62] A. Khan, R. Thakur, Design and evaluation of mucoadhesive vaginal tablets of tenofovir disoproxil fumarate for pre-exposure prophylaxis of HIV, Drug Dev. Industrial Pharm. (2017), https://doi.org/10.1080/03639045.2017.1399272.
[63] Tenofovir Disoproxil Fumarate, Drug Bank Online, 2019 https://go.drugbank.com/salts/DBSALT000172, (accessed 3 December 2019).
[64] A. Dedeloudi, A. Siamidi, P. Pavlou, et al., Recent advances in the excipients used in modified release vaginal formulations, Materials 15 (2022) 327, https://doi.org/10.3390/ma15010327.
[65] J.A. Ko, H.J. Park, S.J. Hwang, et al., Preparation and characterization of chitosan microparticles intended for controlled drug delivery, Int. J. Phar. 294 (2002) 165–174.
[66] O.D. Frent, L.G. Vicas, N. Duteanu, et al., Sodium alginate—natural microencapsulation material of polymeric microparticles, Int. J. Mol. Sci. 23 (2022) 12108, https://doi.org/10.3390/ijms232012108.
[67] C. Zhang, R. Grossier, N. Candoni, S. Veesler, Preparation of alginate hydrogel microparticles by gelation introducing cross-linkers using droplet-based microfluidics: a review of methods, Biomat. Res. 25 (2021) 41, https://doi.org/10.1186/s40824-021-00243-5.
[68] H. Siddam, N.G. Kotla, B. Maddiboyina, et al., Formulation and evaluation of atenolol floating bioadhesive system using optimized polymer blends, Int. J. Pharm. Investig. 6 (2016) 116.
[69] S.R.K. Vaka, H.N. Shivakumar, M. Repka, N. Murthy, Formulation and evaluation of carnosic acid nanoparticulate system for upregulation of neutrophins in the brain, J. Drug Target. (2012) 1–10.
[70] E. Bullet, O. Sanlı, Novel ionically crosslinked acrylamide-grafted poly(vinyl alcohol)/sodium alginate/sodium carboxymethyl cellulose ph-sensitive microspheres for delivery of alzheimer's drug donepezil hydrochloride: preparation and optimization of release conditions, Artificial Cells, Nanomed. Biotechnol. 44 (2016) 431–442, https://doi.org/10.3109/21691401.2014.962741.
[71] S. Dey, S. Pramanik, A. Malgope, Formulation and optimization of sustained release stavudine microspheres using response surface methodology, ISRN Pharmaceutics. (2011), https://doi.org/10.5402/2011/627623, 627623.
[72] W. Chen, A. Palazzo, W. Hennink, et al., The effect of particle size on drug loading and release kinetics of gefitinib-loaded PLGA microspheres, Mol. Pharm. (2016), https://doi.org/10.1021/acs.molpharmaceut.6b00896.
[73] M. Aprilliza Helmiyati, Characterization and properties of sodium alginate from brown algae used as an ecofriendly auperabsorbent, IOP Conf. Ser.: Mater. Sci. Eng. 188 (2017), 012019.
[74] H. Daemi, M. Barikani, Synthesis and characterization of calcium alginate nanoparticles, sodium homopolymannuronate salt and its calcium nanoparticles, Scientia Iranica. 19 (2012) 2023–2028.
[75] T. Fatmanur, A. Acarturk, A. Ozkul, Preparation and characterization of bioadhesive controlled-release gels of cidofovir for vaginal delivery, Aust. J. Biol. Sci. (2015) 1–39.
[76] S. Bashir, N. Zafar, N. Lebaz, A. Mahmood, A. Elaissari, Hydroxypropyl methylcellulose-based hydrogel copolymeric for controlled delivery of galantamine hydrobromide in dementia, Process 8 (2020) 1350, https://doi.org/10.3390/pr8111350.
[77] S. Sahoo, C.K. Chakraborti, P.K. Behera, Spectroscopic investigations of a ciprofloxacin/HPMC mucoadhesive suspension, Int. J. App. Phatmaceutics. 4 (2012) 1–8.
[78] S. Patil, C. Kadam, V. Pokharkar, QbD based approach for optimization of tenofovir disoproxil fumarate loaded liquid crystal precursor with improved permeability, J. Adv. Res. 8 (2017) 607–616.
[79] D.N. Venkatesh, S.N. Meyyanathan, A. Kovacevic, et al., Effect of hydrophilic polymers on the release rate and pharmacokinetics of acyclovir tablets obtained by wet granulation: *in vitro* and *in vivo* assays, Molecules 27 (2022) 6490.
[80] K. Patel, M. Patel, Preparation and evaluation of chitosan microspheres containing nicorandil, Int. J. Pharm. Inves. 4 (2014) 32–37.
[81] Hydroxypropyl Methyl Cellulose, 2022 https://www.chembk.com/en/chem/HPMC, (accessed 18 March 2022).
[82] Sodium CMC. https://pubchem.ncbi.nlm.nih.gov/compound/Sodium-carboxymethyl-cellulose, 2022 (accessed 18 March 2022).
[83] Sodium Alginate. https://encyclopedia.pub/entry/29966#:~:text=It%20has%20the%20chemical%20formula,weight%20of%20216.121%20g%2Fmol, 2022 (accessed 18 March 2022).
[84] C.R. Raymond, P.J. Sheskey, P. Weller, Cellulose Microcrystalline, Chitosan, Magnesium Stearate, Povidone, Talc, Handbook of Pharmaceutical Excipients, The Pharmaceutical Press and the American Pharmaceutical Association, London, USA, 2003, pp. 108-110, 132-134, 354-356, 508-512 and 641-643.
[85] L. Katata-Seru, B.M. Ojo, O. Okubanjo, R. Soremekun, O.S. Aremu, Nanoformulated Eudragit lopinavir and preliminary release of its loaded suppositories, Heliyon 6 (2020), e03890 doi:10.1016%2Fj.heliyon.2020.e03890.
[86] B.M. Best, S.L. Letendre, P. Koopmans, et al., LOW CSF concentrations of the nucleotide HIV reverse transcriptase inhibitor, tenofovir, Acquir. Immune Defic. Syndr. 59 (2012) 376–381, https://doi.org/10.1097/QAI.0b013e318247ec54.
[87] K. Jhunjhunwala, C.W. Dobard, S. Sharma, N. Makarova, A. Holder, C. Dinh, et al., Development, characterization and in vivo pharmacokinetic assessment of rectal suppositories containing combination antiretroviral drugs for HIV prevention, Pharmaceutics 13 (2021) 1–17.
[88] J.A. Moss, A.M. Malone, T.J. Smith, et al., Simultaneous delivery of tenofovir and acyclovir via an intravaginal ring, Antimicrobial Agents Chemother. (2011) 875–882.

SUPPLEMENTARY DOCUMENT

Table S1.

Scoring system for assessing cervicovaginal epithelial tissue damage

Score	Description of epithelial damage
0	No epithelial disturbances or sloughing of epithelial cells.
1	Light epithelial damage and disruption: localized loss of tissue integrity and epithelial sloughing over less than 5% of the epithelial surface, which is otherwise contiguous and intact.
2	Moderate epithelial damage and disruption: Multiple areas of epithelial disturbance representing 5-25% of the total epithelial surface and small regions of sloughing that expose the basal cell layer.
3	Severe epithelial damage and disruption: Sloughing over large sections of the epithelial surface (>25%) that exposes the basal cell layer.

Table S2.

Entrapment efficiency of all batches of TAM

Formulation Code	Drug Content (mg/20mg)	Practical Drug Content (%)	Entrapment Efficiency (%)
EH-1	1.85 ± 0.01	9.27 ± 0.07	20.61 ± 0.16
EH-2	1.98 ± 0.02	9.89 ± 0.09	21.99 ± 0.19
EH-3	1.99 ± 0.03	9.96 ± 0.15	22.13 ± 0.33
EH-4	2.13 ± 0.02	10.69 ± 0.08	23.77 ± 0.17
EH-5	2.12 ± 0.02	10.59 ± 0.13	52.95 ± 0.67
EH-6	1.99 ± 0.04	9.98 ± 0.25	49.91 ± 1.23
EH-7	0.98 ± 0.02	4.93 ± 0.12	24.69 ± 0.61
EH-8	2.48 ± 0.05	12.41 ± 0.27	62.09 ± 1.34
EH-9	1.04 ± 0.002	5.22 ± 0.03	52.15 ± 0.08
EH-10	0.75 ± 0.005	3.75 ± 0.03	37.57 ± 0.26
EH-11	0.67 ± 0.01	3.34 ± 0.07	33.39 ± 0.73
EH-12	1.08 ± 0.002	5.40 ± 0.01	54.04 ± 0.08

2

Table S3.

Interpretation of PXRD pattern of TDF, physical mixture of EH-8, and formulation EH-8.

Sl. No.	Angle (2θ ± 2)	Peak Intensity (Counts)		
		Drug (TDF)	Physical Mixture of Formulation EH-8	Formulation EH-8
1	10.29	1339	651	312
2	10.59	2540	842	304
3	13.48	1954	1161	487
4	14.17	1361	1000	535
5	18.32	3212	1049	657
6	18.80	3258	967	680
7	19.95	4172	1195	576
8	21.36	2438	1114	574
9	22.02	3077	1075	579
10	25.07	4419	1086	503

3

Table S4.

Results of curve fitting of the dissolution data for the microspheres.

Formulation Code	Zero Order Kinetic Model		First Order Kinetic Model		Higuchi Release Model		Korsmeyer-Peppas Release Model		
	R^2	K	R^2	K	R^2	K	R^2	K	n
EH-1	0.936 ± 0.007	38.005 ± 0.962	0.892 ± 0.017	0.380 ± 0.007	0.974 ± 0.001	8.669 ± 1.145	1.000 ± 0.000	0.3748 ± 0.000	0.3114 ± 0.000
EH-5	0.843 ± 0.043	39.559 ± 3.437	0.769 ± 0.054	0.389 ± 0.025	0.933 ± 0.021	10.216 ± 3.978	1.000 ± 0.000	0.479 ± 0.015	0.610 ± 0.066
EH-7	0.774 ± 0.017	56.675 ± 1.897	0.701 ± 0.021	0.248 ± 0.013	0.892 ± 0.012	23.586 ± 19.799	-	-	-
EH-8	0.905 ± 0.031	30.813 ± 1.728	0.794 ± 0.032	0.479 ± 0.010	0.974 ± 0.014	2.731 ± 0.626	0.976 ± 0.021	0.567 ± 0.004	0.631 ± 0.069
EH-9	0.836 ± 0.078	31.562 ± 0.470	0.728 ± 0.099	0.498 ± 0.012	0.918 ± 0.051	16.896 ± 0.789	0.911 ± 0.040	0.552 ± 0.029	0.3664 ± 0.054
EH-10	0.967 ± 0.038	25.521 ± 4.442	0.923 ± 0.042	0.563 ± 0.056	0.984 ± 0.009	10.855 ± 6.106	0.981 ± 0.015	0.593 ± 0.054	0.3496 ± 0.050